frontiers | Research Topics

Worldwide emergence of drug-resistant fungi: From basic to clinic, volume II

Edited by
Weihua Pan, Wenjie Fang and Macit Ilkit

Published in
Frontiers in Microbiology

ISSN 1664-8714
ISBN 978-2-83251-648-5
DOI 10.3389/978-2-83251-648-5

About Frontiers

Frontiers is more than just an open access publisher of scholarly articles: it is a pioneering approach to the world of academia, radically improving the way scholarly research is managed. The grand vision of Frontiers is a world where all people have an equal opportunity to seek, share and generate knowledge. Frontiers provides immediate and permanent online open access to all its publications, but this alone is not enough to realize our grand goals.

Frontiers journal series

The Frontiers journal series is a multi-tier and interdisciplinary set of open-access, online journals, promising a paradigm shift from the current review, selection and dissemination processes in academic publishing. All Frontiers journals are driven by researchers for researchers; therefore, they constitute a service to the scholarly community. At the same time, the *Frontiers journal series* operates on a revolutionary invention, the tiered publishing system, initially addressing specific communities of scholars, and gradually climbing up to broader public understanding, thus serving the interests of the lay society, too.

Dedication to quality

Each Frontiers article is a landmark of the highest quality, thanks to genuinely collaborative interactions between authors and review editors, who include some of the world's best academicians. Research must be certified by peers before entering a stream of knowledge that may eventually reach the public - and shape society; therefore, Frontiers only applies the most rigorous and unbiased reviews. Frontiers revolutionizes research publishing by freely delivering the most outstanding research, evaluated with no bias from both the academic and social point of view. By applying the most advanced information technologies, Frontiers is catapulting scholarly publishing into a new generation.

What are Frontiers Research Topics?

Frontiers Research Topics are very popular trademarks of the *Frontiers journals series*: they are collections of at least ten articles, all centered on a particular subject. With their unique mix of varied contributions from Original Research to Review Articles, Frontiers Research Topics unify the most influential researchers, the latest key findings and historical advances in a hot research area.

Find out more on how to host your own Frontiers Research Topic or contribute to one as an author by contacting the Frontiers editorial office: frontiersin.org/about/contact

Worldwide emergence of drug-resistant fungi: From basic to clinic, volume II

Topic editors
Weihua Pan — Shanghai Changzheng Hospital, China
Wenjie Fang — Shanghai Changzheng Hospital, China
Macit Ilkit — Çukurova University, Türkiye

Topic Coordinators
Lei Zhang — Shaanxi Provincial People's Hospital, China

Citation
Pan, W., Fang, W., Ilkit, M., eds. (2023). *Worldwide emergence of drug-resistant fungi: From basic to clinic, volume II*. Lausanne: Frontiers Media SA.
doi: 10.3389/978-2-83251-648-5

Table of contents

frontiers | Frontiers in Microbiology

ORIGINAL RESEARCH
published: 16 June 2022
doi: 10.3389/fmicb.2022.919677

Boric Acid Solution Inhibits *Candida albicans* Infections in Mouse Skin *via* the IL-23/Th17 Axis

Zhao Liu[1], *Qing Liu*[2], *Yanyan Xu*[1], *Zhao Han*[1], *Ling Zhang*[1] *and Xiaojing Li*[1]*

[1] Department of Dermatology, Affiliated Hospital of Hebei University of Engineering, Handan, China, [2] Department of Dermatology, Anqing Municipal Hospital, Anqing, China

The purpose of this study was to investigate the effect and mechanism of 3% boric acid solution (BAS) against *Candida albicans* (CA) infection *via* the interleukin-23 (IL-23)/T helper 17 cell (Th17) axis. 36 female mice were randomly divided into 3 groups, and 2 injection sites on the back of the mice were chosen at random. Group N was injected with sterile water for injection (SWFI), and Group M and Group B were injected with CA mycelium suspension. After successful model verification, the remaining mice entered the following treatments 5 days later. Group B was treated with 3% BAS, Group M was treated with SWFI, and Group N was not treated. Levels of interleukin-17 (IL-17), IL-22, and IL-23 in mouse blood were measured on days 1, 3, 5, and 7 of treatment. On day 7, IL-17, IL-22, and IL-23 in mouse skin were detected. Serum levels of IL-17, IL-22, and IL-23 in Group M were higher than in Group N on the first day of treatment ($p < 0.05$). Expression levels of IL-17, IL-22, and IL-23 in the epidermis of the skin lesions in Group M were higher than in Group N on day 7 ($p < 0.05$). The serum level of IL-17 in Group B was higher than in Group M on days 5 and 7 ($p < 0.05$). Serum levels of IL-22 in Group B on days 1, 5, and 7 were higher than in Group M ($p < 0.05$). Serum levels of IL-23 in Group B were higher than in Group M on days 3, 5, and 7 ($p < 0.05$). IL-17 and IL-23 in Group B reached a peak on day 5, significantly different on days 1, 3, and 7 ($p < 0.05$). The expression intensity of IL-17, IL-22, and IL-23 in the skin lesions of Group B was higher than that of Group M on day 7 ($p < 0.05$). We conclude that IL-17, IL-22, and IL-23 are involved in the anti-CA activity in mouse skin, and 3% BAS increased IL-17, IL-22, and IL-23 to mediate these effects.

Keywords: mice, *Candida albicans*, interleukin-17, interleukin-22, interleukin-23, 3% boric acid solution

OPEN ACCESS

Edited by:
Wenjie Fang,
Shanghai Changzheng Hospital, China

Reviewed by:
Xuhua Tang,
The First Affiliated Hospital of Sun Yat-sen University, China
Sha Lu,
Sun Yat-sen Memorial Hospital, China

***Correspondence:**
Xiaojing Li
zlmdsh@126.com

Specialty section:
This article was submitted to Antimicrobials, Resistance and Chemotherapy, a section of the journal Frontiers in Microbiology

Received: *13 April 2022*
Accepted: *09 May 2022*
Published: *16 June 2022*

Citation:
Liu Z, Liu Q, Xu Y, Han Z, Zhang L and Li X (2022) Boric Acid Solution Inhibits Candida albicans Infections in Mouse Skin via the IL-23/Th17 Axis. Front. Microbiol. 13:919677. doi: 10.3389/fmicb.2022.919677

INTRODUCTION

Candida albicans (CA) can cause infections on the skin or mucous membranes and invasive infections. Epidemiological studies in the United States and Europe have shown that CA is the most common *Candida* infection (Cleveland et al., 2015; Klingspor et al., 2015; Polesello et al., 2017). It can exist in the human skin, genitourinary tract, and intestines. It is a conditional pathogenic fungus, usually related to the decline of the host's immunity or the imbalance of the competitive flora (Berman, 2012). CA infection can often be caused when the superficial competition flora of the human skin is not balanced, or the body's immunity is weakened. As for immunosuppressed patients, *Candida* causes severe deep infection, with a mortality rate of 46–75% (Brown et al., 2012).

Superficial skin CA infections are usually treated with topical ointments containing azole drugs and allylamine drugs. Deep CA infection requires an oral or intravenous infusion of antifungal drugs, such as polyenes, azoles, allylamines, and echinocandins. Due to the side effects of antifungal drugs and the increased resistance of CA antifungal drugs (Xiao et al., 2018), it is necessary to find a safe and effective alternative therapy. BAS is a commonly used topical medicine in dermatology. When women have failed conventional treatment due to intravaginal Candida infection, boric acid is a safe, alternative, and economical choice for women with recurrent symptoms of chronic vaginitis, and there is no interaction with common antifungal agents (Iavazzo et al., 2011; Schmidt et al., 2018).

Human innate immunity and adaptive immune system have essential functions in resisting CA infection, among which the IL-23/Th17 axis plays an important role. Naive CD4+ T cells differentiate into various T cell subpopulations, such as Th17 cells, which secrete IL-17 and IL-22. IL-17 promotes the secretion of chemokines by epithelial cells and eliminates fungi by attracting and activating neutrophils (Yang et al., 2015). IL-22 combats fungi in keratinocytes by assisting the production of antibacterial peptides and inflammatory factors (Yang et al., 2015). Active dendritic cells and macrophages secrete IL-23, which promotes the increase in the number of Th17 cells and promotes the production of IL-17 and IL-22 (Ge et al., 2019). Our previous studies showed that 3% boric acid solution (BAS) treats CA infections in mouse skin (Liu et al., 2021); however, the specific mechanism of action has not been thoroughly studied. Therefore, we hypothesized whether BAS increased IL-17, IL-22, and IL-23 in mice, helping the host resist CA infection.

Therefore, we established a mouse skin CA infection model using 3%BAS, based on the IL-23/Th17 axis, to study its mechanism of action against CA infections in mouse skin.

MATERIALS AND METHODS

Laboratory Animals and Strains

Healthy female ICR mice aged 6–8 weeks, weighing 22–24 g, were purchased from the Beijing Weitong Lihua Experimental Animal Technology Co., Ltd. CA standard strain SC 5314 was purchased from the American Type Culture Collection.

Instruments

BAS the Affiliated Hospital of Hebei Engineering University provided the 3% BAS. IL-17, IL-22, IL-23 Enzyme-linked immunosorbent assay (ELISA) kits were purchased from Jiangsu Meimian Industrial Co., Ltd. IL-17, IL-22, and IL-23 rabbit anti-mouse polyclonal antibodies were purchased from Beijing Biosynthesis Biotechnology Co., Ltd.

Model Construction and Group Intervention

The mice were randomly divided into N ($n = 12$), M ($n = 12$), and B groups ($n = 12$). The 2 injection sites were randomly selected on the back of each mouse. Groups M and B were injected with CA mycelium suspension and Group N was injected with SWFI. From each group, we randomly selected 6 animals for model verification. Please refer to our published articles for details about the CA mycelium suspension configuration, model establishment, and verification method (Liu et al., 2021).

On day 5 after inoculation, anesthetized mice underwent an intramuscular injection of 0.2 ml chlorpromazine solution. Each mouse in Group B was hydropathic compressed with 6 layers of sterile gauze and 3% BAS for 30 min, once every 12 h. Group M was treated with SWFI, and Group N was fed normally without treatment.

Sample Collection

On days 1, 3, 5, and 7 of treatment, about 100–120 μL of tail vein blood was collected from each mouse, centrifuged at 1,000 r/min for 10 min, and the upper serum was collected and placed in a refrigerator at −70°C for later use.

After blood samples were collected on day 7, the mice were sacrificed, and tissues were cut from the skin lesions on the back of each mouse, soaked and fixed in formalin solution, and made into wax blocks.

ELISA

Expression levels of IL-17, IL-22, and IL-23 in mouse serum were measured using ELISA kits. Briefly, serum was brought to room temperature, and we performed the assay strictly according to the manufacturer's instructions to measure the expression levels of IL-17, IL-22, and IL-23 in mouse serum. Data were expressed as pg/mL.

Immunohistochemistry

First, specimens were cut into 4-μm sections, placed on anti-dropping glass slides, and treated with xylene dewaxing, ethanol hydration, and 1% methanol hydrogen peroxide solution in a microwave oven. Second, we added normal goat serum blocking solution and removed excess liquid after 20 min. Third, we added IL-17 rabbit anti-mouse polyclonal antibody drop wise, placed it in a humidification box overnight at 4°C, and then washed it with phosphate-buffered saline (PBS). Fourth, we added an appropriate amount of biotinylated secondary antibody, placed samples in a 37°C incubator for 20 min, and washed them with PBS. Fifth, we added streptavidin-horseradish peroxidase, placed it in a 37°C incubator for 20 min, and washed it with PBS. Finally, after hematoxylin counterstaining, we used a DAB kit to develop the color, 1% hydrochloric acid ethanol differentiation, 1% amine water inverse blue, ethanol dehydration, and xylene clarification. We used neutral resin to mount the slides and observe using a microscope.

The epidermis of mouse skin is the subject of our study. The criterion is to score the percentage of positive cells under the microscope and the staining intensity (Ren, 2020). Colorless gets 0 points, light yellow gets 1 point, yellowish-brown gets 2 points, and brown gets 3 points. The number of positive staining cells was calculated as follows. We randomly observed 5 high-power microscope fields (400×) for each slice and calculated the percentage of positive cells. Positive cells <5% was 0 points, 5–25% was 1 point, 26–50% was 2 points, 51–75% was 3 points, and 76–100% was

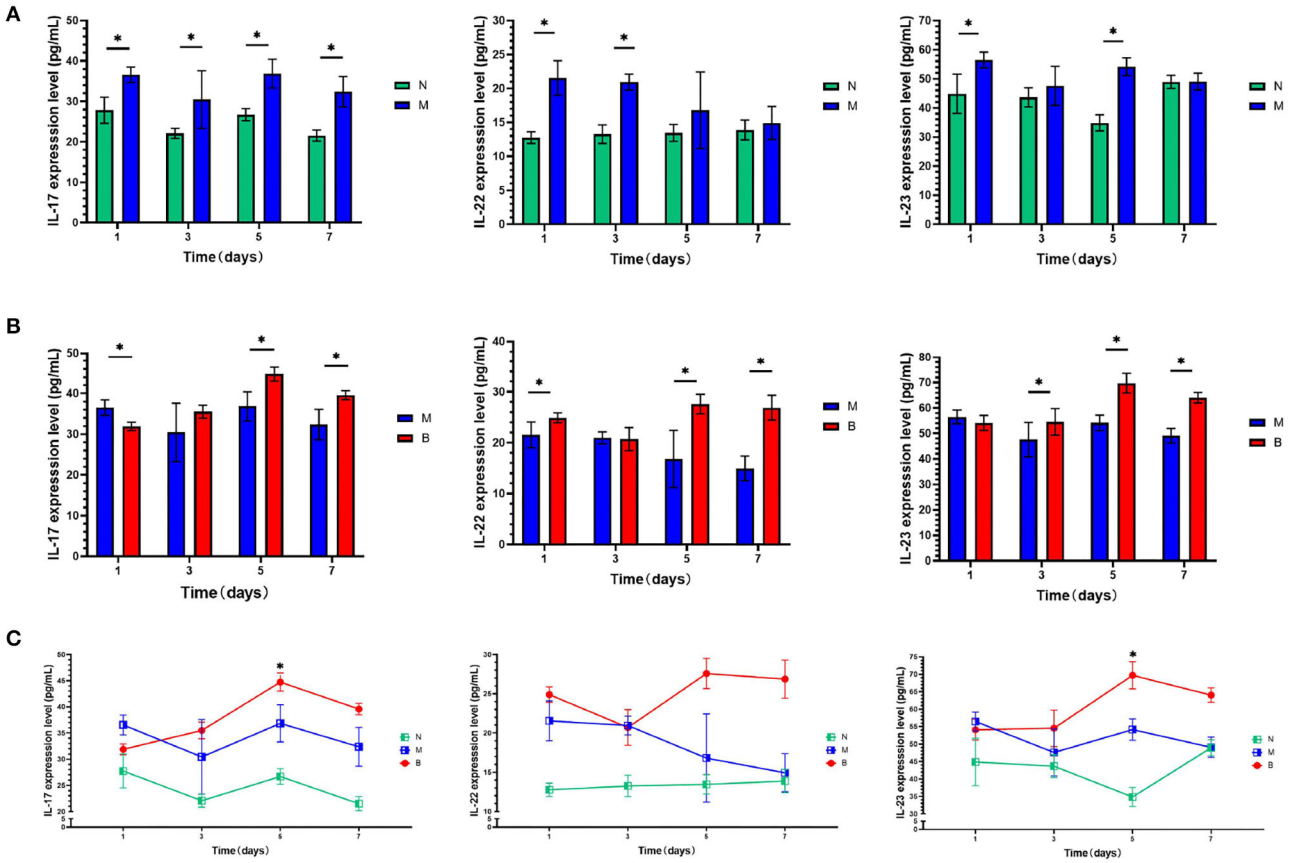

FIGURE 1 | (A) On days 1,3, 5, and 7, serum levels of cytokines of the blank group (N) and control group (M) were compared. **(B)** On days 1, 3, 5, and 7, serum levels of cytokines of the control group (M) and the experimental group (B) were compared. **(C)** On days 1,3, 5, and 7, serum levels of cytokines in the same group were compared.*$P < 0.05$.

TABLE 1 | Comparison of IL-17 expression in three groups of mice epidermis.

Group	Negative	Weakly positive	Positive	Strongly positive	*Z*	*p*
N (a)	10	2	0	0	31.627	<0.001
M (b)	0	4	8	0		
B (c)	0	0	1	11		

Different lowercase letters between groups represent statistically significant differences. $p < 0.05$.

TABLE 2 | Comparison of IL-22 expression in three groups of mice epidermis.

Group	Negative	Weakly positive	Positive	Strongly positive	*Z*	*p*
N (a)	11	1	0	0	31.46	<0.001
M (b)	0	3	9	0		
B (c)	0	0	2	10		

Different lowercase letters between groups represent statistically significant differences. $p < 0.05$.

4 points. The scores of the 2 were multiplied to provide the positivity grade: 0 was negative (–), 1–4 as weakly positive (+), 5–8 was positive (++), and 9–12 was strongly positive (+++).

Statistical Analysis

We used SPSS24.0 statistical software to analyze the data. The measurement data of the ELISA results were expressed as the mean ± standard deviation. Repeated measures analysis of

TABLE 3 | Comparison of IL-23 expression in three groups of mice epidermis.

Group	Negative	Weakly positive	Positive	Strongly positive	*Z*	*p*
N (a)	10	2	0	0	31.876	<0.001
M (b)	0	3	9	0		
B (c)	0	0	1	11		

Different lowercase letters between groups represent statistically significant differences. P < 0.05.

variance were used for overall comparison, analysis of variance was used for overall comparisons between 3 groups at the same time point, the least-squares difference was used for pair wise comparison between groups, and a *post-hoc* least-squares difference *t*-test was used for pair-wise comparison of the same group at different time points. The immunohistochemistry results were compared with the overall difference between groups using the independent sample rank-sum test.

RESULTS

CA Infection Increases Expression Levels of IL-17, IL-22, and IL-23 in Mice

To determine whether CA infection increases expression levels of IL-17, IL-22, and IL-23 in the blood and skin of mice, we compared the M and N groups. On the first day of treatment with a 3% BAS, we performed an ELISA test and found that, as shown in **Figure 1A**, the expression of IL-17, IL-22, and IL-23 in the blood of mice injected with CA suspension was significantly higher than that of mice injected with SWFI. To avoid the pathological biopsy interfering with the experiment, we did not perform immunohistochemistry on the first day of treatment. On day 7, we performed immunohistochemical testing. The results are shown in **Tables 1**–**3**, and **Figure 2**. IL-17 was negative in ten cases, weakly positive in two cases in the N group, weakly positive in four cases, and positive in eight cases in the M group. IL-22 was negative in 11 cases, weakly positive in one case in Group N, weakly positive in three cases, and positive in nine cases in Group M. IL-23 was negative in 11 cases, weakly positive in one case in Group N, weakly positive in three cases, and positive in nine cases in Group M. These differences are statistically significant. This result confirmed that to resist the infection of CA, the mice secreted more IL-17, IL-22, and IL-23 in blood and skin.

3% BAS Increases Expression Levels of IL-17, IL-22, and IL-23 in Mice

To compare whether treatment with 3% BAS would increase the expression levels of IL-17, IL-22, and IL-23 in the blood and skin of mice infected with CA, Groups B and M were compared. As shown in **Figure 1B**, on day 1, IL-17 expression in the blood of 3% boric acid-treated mice was lower than that of SWFI-treated mice, while on days 5 and 7, IL-17 expression in 3% boric acid-treated mice was significantly higher than in SWFI-treated mice. On days 1, 5, and 7, the expression of IL-22 in the blood of mice treated with 3% boric acid was significantly higher than that of mice treated with SWFI. On days 3, 5, and 7, the expression of IL-23 in the blood of mice treated with 3% boric acid was significantly higher than that of mice treated with SWFI. The results are in **Tables 1**–**3** and **Figure 2**. IL-17 was positive in one case and strongly positive in 11 cases in Group B, weakly positive in four cases and positive in eight cases in Group M. IL-22 was positive in two cases and strongly positive in ten cases in Group B, and weakly positive in three cases and positive in nine cases in Group M. IL-23 was positive in one case and strongly positive in 11 cases in Group B, and weakly positive in three cases and positive in nine cases in Group M. The expression of these three cytokines in Group B was significantly higher than in Group M. Levels of IL-17, IL-22, and IL-23 in blood and skin were significantly increased after 3% BAS application, which cause may be the result of the breakdown of CA by 3% BAS inhibition of glycolysis and mitochondrial activity (Schmidt et al., 2018), suggesting that the agent helps combat CA infections. Mice treated with 3% BAS were compared at different time points. As shown in **Figure 1C**, we found that serum levels of IL-17 and IL-23 in mice treated with 3% boric acid on day 5 were significantly higher than at other time points, reaching a peak. However, this phenomenon was not observed in the IL-22 and control groups. These findings suggest that on day 5, IL-17 and IL-23 reached peak levels, and the anti-CA effect was the strongest.

DISCUSSION

CA is a common conditional pathogenic fungus in humans. It invades tissues, skin, and mucous membranes to cause disease, and then triggers systemic or local inflammatory reactions. Among *Candida* species, CA is the most common disease-causing species, accounting for 75% of *Candida* infections; it is also the most pathogenic (Netea et al., 2015; Dadar et al., 2018).

The host's innate immune response and adaptive immune response are critical for combating CA infections, and the IL-23/Th17 axis plays a vital role. Activated dendritic cells are the primary cells that secrete IL-23; however, they can also be secreted in small amounts by monocytes, macrophages, and keratinocytes (Oppmann et al., 2000; Piskin et al., 2006). IL-23 induces Th17 cells to secrete IL-17 and IL-22 (Bettelli et al., 2007), increases the number of differentiated Th17 cells, and maintains the survival of Th17 cells (Wu et al., 2012). Th17 cells are differentiated from CD4+ helper T cells, which secrete IL-17, IL-22, and other cytokines (Langrish et al., 2005; Park et al., 2005; Fujimura et al., 2013) and play an essential role in the host's resistance to *Candida* infection (Park et al., 2018; Gaffen and Moutsopoulos, 2020). Many studies showed that the secretion of IL-17, IL-22, and IL-23 can help the host

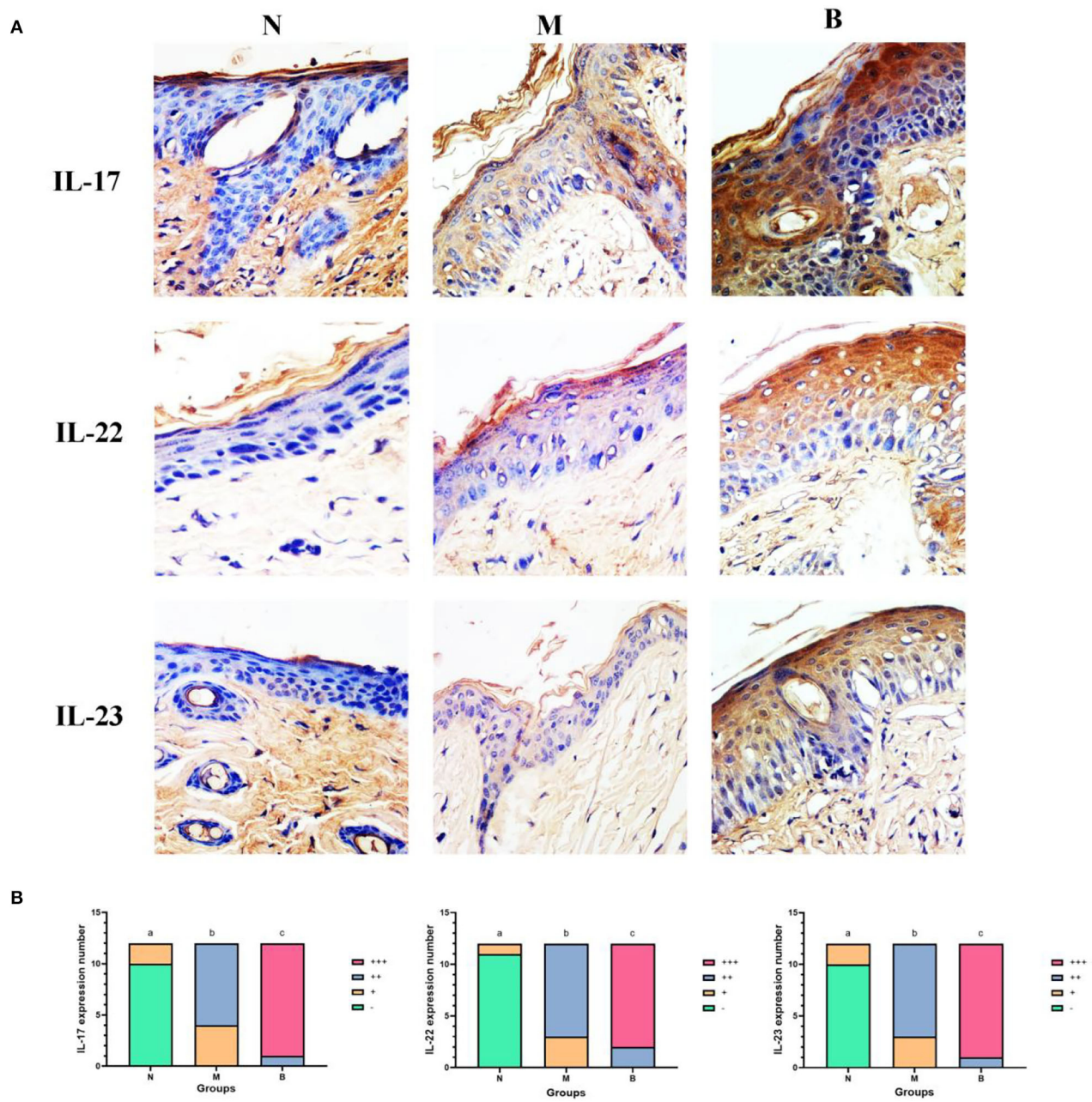

FIGURE 2 | (A) The expression of IL-17, IL-22, and IL-23 in the epidermis of each group. The positive color of these 3 cytokines is the coloring of the cytoplasm (light yellow to brown). Negative means no color development. These 3 factors are expressed in different degrees in keratinocytes, especially in spinous cells (400×). **(B)** The expression level of IL-17, IL-22, and IL-23 in the epidermis of each group of mice on day 7. Different lowercase letters between groups represent statistically significant differences. $p < 0.05$.

resist *Candida* infections, and their absence can cause severe candidiasis (Eyerich et al., 2008; Conti et al., 2009; Kagami et al., 2010). In superficial CA disease, the epidermis is the first barrier to CA infection. Keratinocytes play many roles in resisting CA infection, 1 of which is to secrete antimicrobial peptides. Increased IL-17 and IL-22 secretion promotes the secretion of antimicrobial peptides by keratinocytes, thereby helping the host resist CA infection. We injected CA mycelium suspension and SWFI into the skin of mice and found that serum IL-17, IL-22, and IL-23 in serum were significantly increased on day 1 after CA infection. On day 7, IL-17, IL-22, and IL-23 in mouse skin with CA solution were higher than those injected with SWFI. IL-17 levels increased only in serum. We hypothesized that this phenomenon might be related to decreased cytokine secretion

as the infection of CA in the skin is controlled; however, the inflammatory response in the local skin remains strong.

BAS is commonly used in dermatology. Studies showed that boric acid has the same efficacy as fluconazole for treating vaginal candidiasis (Khameneie et al., 2013). Boric acid is a broad-spectrum agent that specifically inhibits CA hyphal growth (Pointer and Schmidt, 2016), and it is more available and less expensive. Our previous study showed that skin CA infection in mice significantly improved after 3% BAS treatment, and there was evident wound healing without exudate. The effective rate of 3% BAS was 83%, and that of SWFI was 25%, which may be caused by discrepancies in drug treatment, operation during treatment, or other factors. Compared with SWFI, 3% BAS had a therapeutic effect and was statistically significant (Liu et al., 2021). However, the mechanism is not entirely clear. Investigators found that BAS destroys the cytoskeleton involving actin and leads to abnormal mycelia development (Pointer et al., 2015). Some investigators found that BAS inhibits glycolysis in CA and critical enzymes of mitochondrial activity (Schmidt et al., 2018). To determine whether 3% BAS stimulates the secretion of IL-17, IL-22, and IL-23, we used 3% BAS and SWFI to treat mice infected with CA by skin injection and found that 3% BAS increased levels of IL-17, IL-22, and IL-23. The expression level of IL-22 in blood was higher than that of the control group on the first day, and the expression level of IL-23 was higher than that of the control group on the third day, while the expression level of IL-17 was higher than that of the control group until the application of 3% BAS on the fifth day. With the application of 3% BAS, the secretion of all 3 cytokines increased in mice.

On day 7, we compared the immunohistochemical tests of 3% BAS and SWFI-treated mice and found that the results were consistent with serum levels of IL-17, IL-22, and IL-23. The expression intensity of IL-17, IL-22, and IL-23 in mice treated with 3% BAS was higher than that of mice treated with SWFI. Previous studies showed that IL-17, IL-22, and IL-23 could help resist *Candida* infections (Eyerich et al., 2008; Conti et al., 2009; Kagami et al., 2010). In addition to the fact that some scholars found that 3% BAS itself had an inhibitory effect on CA (Pointer et al., 2015; Schmidt et al., 2018), we found that it increased IL-17, IL-22, and IL-23 in mice, which cause may be the result of the breakdown of CA by inhibition of glycolysis and mitochondrial activity, to help the host to resist CA infection.

We compared the mice treated with 3% BAS and found that expression levels of IL-17, IL-22, and IL-23 in the blood of mice showed different changes with the extension of application time. The expression peaks of IL-17 and IL-23 appeared on day 5 after treatment with 3% BAS; however, this phenomenon was not observed in IL-22. It usually takes more than 96 h for the antigen recognition to affect the stage of the adaptive immune response, and the time of IL-17 and IL-23 secretion induced by 3% BAS in mice is consistent. Therefore, we speculated that BAS might be involved in a particular stage of the adaptive immune response. The specific mechanism needs to be further explored in the future. Nevertheless, IL-17 and IL-23 secretion peaked on day 5, and its anti-CA effect was also the highest.

In summary, 3% BAS increased IL-17, IL-22, and IL-23 in mice to assist the host in fighting CA infection. To treat CA infections in the skin, the course of treatment should be applied for at least 5 days to achieve the best anti-CA effect.

DATA AVAILABILITY STATEMENT

The original contributions presented in the study are included in the article/supplementary material, further inquiries can be directed to the corresponding authors.

ETHICS STATEMENT

The animal study was reviewed and approved by The Biomedical Ethics Committee of Medical School of Hebei University of Engineering.

AUTHOR CONTRIBUTIONS

ZL wrote the manuscript. XL revised the manuscript. QL, YX, ZH, and LZ gave some helpful suggestions. All authors contributed to manuscript revision, read, and approved the submitted version.

REFERENCES

Berman, J. (2012). Candida Albicans. *Curr. Biol.* 22, R620–R622. doi: 10.1016/j.cub.2012.05.043

Bettelli, E., Oukka, M., and Kuchroo, V. K. (2007). T(H)-17 cells in the circle of immunity and autoimmunity. *Nat. Immunol.* 8, 345–350. doi: 10.1038/ni0407-345

Brown, G. D., Denning, D. W., Gow, N. A., Levitz, S. M., Netea, M. G., and White, T. C. (2012). Hidden killers: human fungal infections. *Sci. Transl. Med.* 4:165rv13. doi: 10.1126/scitranslmed.3004404

Cleveland, A. A., Harrison, L. H., Farley, M. M., Hollick, R., Stein, B., Chiller, T. M., et al. (2015). Declining incidence of candidemia and the shifting epidemiology of *Candida* resistance in two US Metropolitan Areas, 2008-2013: results from population-based surveillance. *PLoS ONE* 10:E0120452. doi: 10.1371/journal.pone.0120452

Conti, H. R., Shen, F., Nayyar, N., Stocum, E., Sun, J. N., Lindemann, M. J., et al. (2009). Th17 cells and Il-17 receptor signaling are essential for mucosal host defense against oral candidiasis. *J. Exp. Med.* 206, 299–311. doi: 10.1084/jem.20081463

Dadar, M., Tiwari, R., Karthik, K., Chakraborty, S., Shahali, Y., and Dhama, K. (2018). Candida Albicans - Biology, molecular characterization, pathogenicity, and advances in diagnosis and control - an update. *Microb. Pathog.* 117, 128–138. doi: 10.1016/j.micpath.2018.02.028

Eyerich, K., Foerster, S., Rombold, S., Seidl, H. P., Behrendt, H., Hofmann, H., et al. (2008). Patients with chronic mucocutaneous candidiasis exhibit reduced production of Th17-associated cytokines Il-17 and Il-22. *J. Invest. Dermatol.* 128, 2640–2645. doi: 10.1038/jid.2008.139

Fujimura, K., Oyamada, A., Iwamoto, Y., Yoshikai, Y., and Yamada, H. (2013). Cd4 T cell-intrinsic Il-2 signaling differentially affects Th1 and Th17 development. *J. Leukoc. Biol.* 94, 271–279. doi: 10.1189/jlb.1112581

Gaffen, S. L., and Moutsopoulos, N. M. (2020). Regulation of host-microbe interactions at oral mucosal barriers by Type 17 immunity. *Sci. Immunol.* 5:eaau4594. doi: 10.1126/sciimmunol

Ge, L. Y., Liang, G. Z., and Liu, W. D. (2019). Research progress of innate immunity against mucosal Candida Albicans infection. *Chin. J. Mycol.* 14, 249–252. doi: 10.3969/j.issn.1673-3827.2019.04.014

Iavazzo, C., Gkegkes, I. D., Zarkada, I. M., and Falagas, M. E. (2011). Boric acid for recurrent vulvovaginal candidiasis: the clinical evidence. *J. Womens Health* 20, 1245–1255. doi: 10.1089/jwh.2010.2708

Kagami, S., Rizzo, H. L., Kurtz, S. E., Miller, L. S., and Blauvelt, A. (2010). Il-23 and Il-17a, but not Il-12 and Il-22, are required for optimal skin host defense against Candida albicans. *J. Immunol.* 185, 5453–5462. doi: 10.4049/jimmunol.1001153

Khameneie, K. M., Arianpour, N., Roozegar, R., Aklamli, M., and Amiri, M. M. (2013). Fluconazole and boric acid for treatment of vaginal candidiasis–New words about old issue. *East Afr. Med. J.* 90, 117–123.

Klingspor, L., Tortorano, A. M., Peman, J., Willinger, B., Hamal, P., Sendid, B., et al. (2015). Invasive Candida infections in surgical patients in intensive care units: a prospective, multicentre survey initiated by the European Confederation Of Medical Mycology (Ecmm) (2006-2008). *Clin. Microbiol. Infect.* 21, 87.E1-87.E10. doi: 10.1016/j.cmi.2014.08.011

Langrish, C. L., Chen, Y., Blumenschein, W. M., Mattson, J., Basham, B., Sedgwick, J. D., et al. (2005). Il-23 drives a pathogenic T cell population that induces autoimmune inflammation. *J. Exp. Med.* 201, 233–240. doi: 10.1084/jem.20041257

Liu, Q., Liu, Z., Zhang, C., Xu, Y., Li, X., and Gao, H. (2021). Effects of 3% boric acid solution on cutaneous *Candida albicans* infection and microecological flora mice. *Front. Microbiol.* 12:709880. doi: 10.3389/fmicb.2021.709880

Netea, M. G., Joosten, L. A., Van Der Meer, J. W., Kullberg, B. J., and Van De Veerdonk, F. L. (2015). Immune defence against Candida fungal infections. *Nat. Rev. Immunol.* 15, 630–642. doi: 10.1038/nri3897

Oppmann, B., Lesley, R., Blom, B., Timans, J. C., Xu, Y., Hunte, B., et al. (2000). Novel P19 protein engages Il-12p40 to form a cytokine, Il-23, with biological activities similar as well as distinct from Il-12. *Immunity* 13, 715–725. doi: 10.1016/S1074-7613(00)00070-4

Park, C. O., Fu, X., Jiang, X., Pan, Y., Teague, J. E., Collins, N., et al. (2018). Staged development of long-lived T-cell receptor? β T(H)17 resident memory T-cell population to Candida albicans after skin infection. *J. Allergy Clin. Immunol.* 142, 647–662. doi: 10.1016/j.jaci.2017.09.042

Park, H., Li, Z., Yang, X. O., Chang, S. H., Nurieva, R., Wang, Y. H., et al. (2005). A distinct lineage Of Cd4 T cells regulates tissue inflammation by producing interleukin 17. *Nat. Immunol.* 6, 1133–1141. doi: 10.1038/ni1261

Piskin, G., Sylva-Steenland, R. M., Bos, J. D., and Teunissen, M. B. (2006). *In Vitro* and *In Situ* expression of Il-23 by keratinocytes in healthy skin and psoriasis lesions: enhanced expression in psoriatic skin. *J. Immunol.* 176, 1908–1915. doi: 10.4049/jimmunol.176.3.1908

Pointer, B. R., Boyer, M. P., and Schmidt, M. (2015). Boric acid destabilizes the hyphal cytoskeleton and inhibits invasive growth of Candida albicans. *Yeast* 32, 389–398. doi: 10.1002/yea.3066

Pointer, B. R., and Schmidt, M. (2016). Boric acid-dependent decrease in regulatory histone H3 acetylation is not mutagenic in yeast. *FEMS Microbiol. Lett.* 363:fnw124. doi: 10.1093/femsle/fnw124

Polesello, V., Segat, L., Crovella, S., and Zupin, L. (2017). Candida infections and human defensins. *Protein Pept. Lett.* 24, 747–756. doi: 10.2174/0929866524666170807125245

Ren, X. H. (2020). *Study on the Levels of Il-4, Il-17 and Tnf-? in Cervical Tissues of Patients With Cervical Lesions*. [Master's Thesis]. [Yanan (Cn)]: University Of Yanan.

Schmidt, M., Tran-Nguyen, D., and Chizek, P. (2018). Influence of boric acid on energy metabolism and stress tolerance of *Candida albicans*. *J. Trace Elem. Med. Biol.* 49, 140–145. doi: 10.1016/j.jtemb.2018.05.011

Wu, Q., Wu, K., and Jiang, Y. Q. (2012). Interleukin-23/T helper 17 Cell/Interleukin-17 pathway and skin diseases. *Int. J. Dermatol. Venereol.* 38, 393–396. doi: 10.3389/fimmu.2020.594735

Xiao, M., Sun, Z. Y., Kang, M., Guo, D. W., Liao, K., Chen, S. C., et al. (2018). Five-year national surveillance of invasive Candidiasis: species distribution and azole susceptibility from the China Hospital Invasive Fungal Surveillance Net (CHIF-NET) Study. *J. Clin. Microbiol.* 56, e00577–18. doi: 10.1128/JCM.00577-18

Yang, L., Jia, X. M., and Jiang, Y. Y. (2015). Innate immune mechanisms for recognition *Candida albicans*. *Chin. J. Mycol.* 10, 236–240. doi: 10.3969/j.issn.1673-3827.2015.04.012

Conflict of Interest: The authors declare that the research was conducted in the absence of any commercial or financial relationships that could be construed as a potential conflict of interest.

Publisher's Note: All claims expressed in this article are solely those of the authors and do not necessarily represent those of their affiliated organizations, or those of the publisher, the editors and the reviewers. Any product that may be evaluated in this article, or claim that may be made by its manufacturer, is not guaranteed or endorsed by the publisher.

frontiers | Frontiers in Microbiology

ORIGINAL RESEARCH
published: 05 July 2022
doi: 10.3389/fmicb.2022.942940

Molecular Epidemiology and Antifungal Resistance of *Cryptococcus neoformans* From Human Immunodeficiency Virus-Negative and Human Immunodeficiency Virus-Positive Patients in Eastern China

Ziyi Zhou[1†], Chendi Zhu[2†], Margaret Ip[2], Manjiao Liu[3], Zhaoqin Zhu[4], Ryon Liu[3], Xiaomin Li[3], Lingbing Zeng[5], and Wenjuan Wu[1]* on behalf of the East China Invasive Fungal Infection Group (ECIFIG)*

[1] Department of Laboratory Medicine, Shanghai East Hospital, Tongji University School of Medicine, Shanghai, China, [2] Department of Microbiology, The Chinese University of Hong Kong, Hong Kong, Hong Kong SAR, China, [3] State Key Laboratory of Translational Medicine and Innovative Drug Development, Jiangsu Simcere Diagnostics Co., Ltd., Nanjing, China, [4] Shanghai Public Health Clinical Center, Shanghai, China, [5] Department of Laboratory Medicine, The First Affiliated Hospital of Nanchang University, Nanchang, China

OPEN ACCESS

Edited by:
Weihua Pan,
Shanghai Changzheng Hospital, China

Reviewed by:
Min Chen,
Shanghai Changzheng Hospital, China
Min Zhu,
Fudan University, China

***Correspondence:**
Lingbing Zeng
lingbing_zeng@163.com
Wenjuan Wu
wwj1210@126.com

[†] These authors have contributed equally to this work

Specialty section:
This article was submitted to Antimicrobials, Resistance and Chemotherapy, a section of the journal Frontiers in Microbiology

Received: 13 May 2022
Accepted: 13 June 2022
Published: 05 July 2022

Citation:
Zhou Z, Zhu C, Ip M, Liu M, Zhu Z, Liu R, Li X, Zeng L and Wu W (2022) Molecular Epidemiology and Antifungal Resistance of Cryptococcus neoformans From Human Immunodeficiency Virus-Negative and Human Immunodeficiency Virus-Positive Patients in Eastern China. Front. Microbiol. 13:942940. doi: 10.3389/fmicb.2022.942940

Cryptococcosis is an opportunistic and potentially lethal infection caused by *Cryptococcus neoformans* and *Cryptococcus gattii* complex, which affects both immunocompromised and immunocompetent people, and it has become a major public health concern worldwide. In this study, we characterized the molecular epidemiology and antifungal susceptibility of 133 *C. neoformans* isolates from East China Invasive Fungal Infection Group (ECIFIG), 2017–2020. Isolates were identified to species level by matrix-assisted laser desorption ionization-time of flight mass spectrometry and confirmed by *IGS1* sequencing. Whole-genome sequencing (WGS) was conducted on three multidrug-resistant isolates. Among the 133 strains, 61 (45.86%) were isolated from HIV-positive patients and 72 (54.16%) were isolated from HIV-negative patients. In total, *C. neoformans* var. *grubii* accounted for 97.74% (130/133), while *C. neoformans* var. *neoformans* was rare (2.06%, 3/133). The strains were further classified into nine sequence types (STs) dominated by ST5 (90.23%, 120/133) with low genetic diversity. No association was observed between STs and HIV status. All strains were wild type to voriconazole, while high antifungal minimal inhibitory concentrations (MICs) above the epidemiological cutoff values (ECVs) were observed in *C. neoformans* strains, and more than half of isolates were non-wild-type to amphotericin B (89.15%, 109/133). Eight isolates were resistant to fluconazole, and eight isolates were non-wild type to 5-fluorocytosine. Furthermore, WGS has verified the novel mutations of *FUR1* in 5-fluorocytosine-resistant strains. In one isolate, aneuploidy of chromosome 1 with G484S mutation of *ERG11* was observed, inducing high-level resistance (MIC: 32 μg/ml)

to fluconazole. In general, our data showed that there was no significant difference between HIV-positive and HIV-negative patients on STs, and we elucidate the resistant mechanisms of *C. neoformans* from different perspectives. It is important for clinical therapy and drug usage in the future.

Keywords: *Cryptococcus neoformans*, molecular epidemiology, antifungal susceptibility testing, resistance characteristics, whole genome sequencing

INTRODUCTION

Cryptococcosis is one of the most common fungal diseases in the world, with an estimated 223,000 new cases and 181,100 deaths worldwide each year, primarily in southern Africa and Asia (Rajasingham et al., 2017). Cryptococcosis is an opportunistic and invasive fungal infection that not only has high rates of mortality and morbidity in immunocompromised or immunosuppression patients, like acquired immune deficiency syndrome (AIDS), but also infects immunocompetent individuals (Pyrgos et al., 2013; Sloan and Parris, 2014; Beardsley et al., 2019). There are mainly two species, namely, *Cryptococcus neoformans* and *Cryptococcus gattii*, with significant differences in ecology, molecular epidemiology, and antifungal sensitivity (Cogliati, 2013; Hagen et al., 2015; Firacative et al., 2021). In recent two decades, phylogenetic analysis based on genotypes and phenotypes has revealed two subtypes of *C. neoformans* and five subtypes of *C. gattii.* The major molecular types of *C. neoformans* have most commonly been designated molecular types VNI (AFLP1), VNII (AFLP1A/IB), and VNIII (AFLP3) for *C. neoformans* var. *grubii* and molecular types VNIV (AFLP2) for *C. neoformans* var. *neoformans* (Hagen et al., 2015, 2017; Kwon-Chung et al., 2017). Cryptococcosis is a more frequently observed fungal disease in AIDS patients in Europe, United States, and Africa (Dromer et al., 2007; Park et al., 2009; Pyrgos et al., 2013). The situation, however, is quite different in China. Previous studies showed that *C. neoformans* mainly originated from human immunodeficiency virus (HIV)-negative population without any risk factors reported in other countries (Feng et al., 2008; Khayhan et al., 2013).

The treatment strategies for cryptococcal meningitis recommended by the Infectious Diseases Society of America (IDSA) were amphotericin B plus 5-fluorocytosine for induction therapy and fluconazole used for consolidation therapy (Baddley and Forrest, 2019). However, it is easy to induce drug resistance for treating cryptococcosis due to the long-term and single therapeutic drug use (Bermas and Geddes-McAlister, 2020). According to a recent report by the China Invasive Fungi Surveillance Network, the cryptococcal resistance rate to fluconazole has increased more than threefold (10.5% in 2010 to 34% in 2014) (Xiao et al., 2018). In another multicenter study in China, the resistance rate of *C. neoformans* to fluconazole has dramatically risen, and non-wild-type isolates to 5-fluorocytosine have also been found (Fan et al., 2016).

So far, the resistance mechanisms of *C. neoformans* were understudied. According to previous studies, cryptococcal resistance to fluconazole could be caused by point mutations of *ERG11* (G1785C, G1855A, and G1855T) (Rodero et al., 2003; Bosco-Borgeat et al., 2016; Gago et al., 2017; Selb et al., 2019), overexpression of *ERG11*, overexpression of *AFR1,* and aneuploidy formation. Acquisition of aneuploidies in *C. neoformans* can mediate increased MIC values to fluconazole and further enable cross-adaptation to other antifungal drugs (Yang F. et al., 2021). Mutations of *FCY1*, *FCY2*, and *FUR1* were the most common 5-fluorocytosine resistance mechanism of cryptococcus (Vu et al., 2018). Recent studies have demonstrated that mutations of *UXS1* are also involved with 5-fluorocytosine resistance (Billmyre et al., 2020; Chang et al., 2021). Indeed, comprehensive genomic characterization of *C. neoformans* is limited in China. Notably, antifungal susceptibility, particularly to fluconazole and 5-fluorocytosine, has been noted to vary in correlation not only with molecular types but also with HIV status (Espinel-Ingroff et al., 2012; Li et al., 2012; Arsic Arsenijevic et al., 2014). To investigate the molecular epidemiology of local cryptococcal isolates, several molecular typing methods have been developed, for example, PCR-fingerprinting, randomly amplified polymorphic DNA (RAPD), PCR-restriction fragment length polymorphism (PCR-RFLP), amplified fragment length polymorphism (AFLP), microsatellite typing, multilocus microsatellite typing (MLMT), multilocus sequence typing (MLST), and whole-genome sequencing (WGS) (Bovers et al., 2008; Meyer et al., 2009; Li et al., 2013; Hong et al., 2021). Extensive studies have recommended MLST as the preferred method among these molecular techniques because of its excellent discrimination ability and reproducibility between different laboratories. A normative MLST scheme of the *C. neoformans*/*C. gattii* has been established by the International Society of Human and Animal Mycoses (ISHAM) working group (Meyer et al., 2009). Seven housekeeping genes (*CAP59*, *GPD1*, *IGS1*, *LAC1*, *PLB1*, *SOD1*, and *URA5*) were selected for MLST analysis of the *C. neoformans*/*C. gattii*[1,2], and WGS exhibited high reproducibility, specificity, and discriminating power. Therefore, in this study, we explore the prevalence and antifungal drug resistance mechanism of *C. neoformans* in HIV-positive and HIV-negative patients in China by using high-precision MLST and WGS.

MATERIALS AND METHODS

Clinical Isolates Information

Exactly 133 cryptococcal isolates were collected from East China Invasive Fungal Infection Group (ECIFIG) between 2017 and

[1]http://www.mlst.net/

[2]http://mlst.mycologylab.org

2020. Sixty-one isolates derived from HIV-infected patients who had HIV antibody screening test and confirmatory tests positive were classified as HIV-positive group, while others were classified as HIV-negative group. All isolates were identified to species level by matrix-assisted laser desorption/ionization time-of-flight mass-spectrometry (Zybio, China) and confirmed by *IGS1* sequencing. Ethics approval (2021-061) for this study was obtained from the Health Research Ethics Board of Shanghai East Hospital.

Antifungal Susceptibility Testing

We conducted the antifungal susceptibility testing of 133 isolates against amphotericin B (AMB), 5-fluorocytosine (5FC), fluconazole (FCZ), and voriconazole (VCZ) by using the broth microdilution method (BMD) according to the CLSI M27-A4 guidelines (CLSI, 2017). In brief, isolates were sub-cultured on Sabouraud's dextrose agar (SDA) (Oxoid, United Kingdom) at 35°C for 48 h, the suspension was adjusted by McFarland in a sterile solution, and then, antifungal susceptibility tests were performed. *Candida krusei* ATCC 6258 and *Candida parapsilosis* ATCC 22019 were used as quality control. Epidemiological cutoff values (ECVs) were used to determine wild-type and non-wild-type strains of some antifungals due to lack of breakpoint. ECVs were recommended by CLSI M59: AMB, 0.5 μg/ml (VNI); 5FC, 8 μg/ml (VNI); FCZ, 8 μg/ml (VNI); and VCZ, 0.25 μg/ml (VNI) (CLSI, 2018).

DNA Extraction

DNA extraction of isolates was performed by the method described by Xu et al. (2000) with some modifications. Briefly, all the isolates were sub-cultured on SDA at 30°C for 48–72 h. Monoclonal colonies were collected in the sterile Eppendorf (EP) tubes containing 50 mg glass beads (BioSpec, United States), 200 μl lysis buffer, 200 μl phenol-chloroform, and broken for 10 min, and then centrifuged at high speed for 5 min. Supernatants were transported to new EP tubes. DNAs were extracted by phenol-chloroform alcohol and stored at −20°C.

Intergenic Spacer 1 Sequencing and Multilocus Sequence Typing Analysis

Identification of *Cryptococcus* spp. through amplification of the intergenic spacer 1 (*IGS1*) region was amplified using primers, *IGS1*F (5′-TAAGCCCTTGTT-3′) and *IGS1*R (5′-AAAGATTTATTG-3′), from ISHAM (see text footnote 2). Polymerase chain reaction (PCR) of the *IGS1* gene was performed in a 30 μl final volume. The PCR mixture contains 1 μl of DNA, 15 μl of PCR enzyme mix, and 1 μl of each primer. For PCR amplification, the PCR mixture was denatured for 5 min at 94°C followed by 35 cycles of 30 s at 94°C, 30 s at 53°C, and 1 min at 72°C, followed by one final step of 10 min at 72°C. For MLST analysis, PCR was performed on seven housekeeping genes (*CAP59*, *GPD1*, *IGS1*, *LAC1*, *PLB1*, *SOD1*, and *URA5*) according to the International Fungal Multi Locus Sequence Typing Database (IFMLST) (see text footnote 2). Each PCR system was amplified in a 30 μl final volume as described before, the reaction procedure was described in the IFMLST profile, and all the primers were listed in the IFMLST. Then, all PCR products were purified with Gel Extraction Kit 200 (Omega Bio-Tek, United States) according to the manufacturer's instructions and were sequenced by an ABI 3730XL DNA analyzer (Shanghai, China). Sequences were assigned to the IFMLST consensus MLST scheme database to obtain sequence types (STs).

Whole-Genome Sequencing

Three multidrug resistance isolates with MIC ≥16 μg/ml to FCZ and 5-FC were selected for whole-genome sequencing (WGS) in this study. Among them, one isolate was separated from the HIV-positive group (YQJ185), and the other two isolates were separated from the HIV-negative group (YQJ68 and YQJ247). All isolates were sub-cultured on SDA at 35°C for 48 h according to the CLSI M27-A4, and then, DNA was extracted using Zymo Quick-DNA/RNA Viral Kit (D7020), followed by library preparation using Vazyme transposase-based approach (TD502). WGS was performed using Illumina NovaSeq 6000 platform.

Bioinformatics

Raw reads were quality-controlled and trimmed with Trimmomatic (Bolger et al., 2014). SPAdes were applied for short-read assembly (Bankevich et al., 2012). The YMAP pipeline was used for mapping with reference genome H99 and computing depth to estimate the variation of copy numbers and ploidy across chromosomes (Abbey et al., 2014). To determine the MAT type, short-read sequences were aligned to MATa locus (AF542528) and MAT α (alpha) locus (AF542529).

Reads were aligned to the H99 reference genome (Janbon et al., 2014) using BWA-MEM (Li and Durbin, 2009). Alignments were further processed with SAMtools (Li et al., 2009) and Genome Analysis Toolkit (GATK) (McKenna et al., 2010). SNP and indel calling were performed using the HaplotypeCaller Component of the GATK with default settings. Variants were further filtered with filter expression "QUAL < 30.0 || QD < 2.0 || FS > 60.0 || SOR > 4.0" using VariantFiltration Component of GATK. Variants were annotated using SnpEff (Cingolani et al., 2012) and FungiDB (Stajich et al., 2012). Candidate fungi resistance-related variants were collected from publications [*ERG11* (CNAG_00040), *UXS1* (CNAG_03322), *FUR1* (CNAG_02337), *FCY1* (CNAG_00613), *FCY2* (CNAG_01681), and MSH2 (CNAG_00770)]. All candidate resistance-related variant calls were visually examined using the Integrated Genome Viewer (IGV) to remove calls resulting from poor read mapping (Thorvaldsdóttir et al., 2013). Global ST5 isolates from previous studies were retrieved from National Center for Biotechnology Information (NCBI) (Rhodes et al., 2017; Ashton et al., 2019). Core SNP phylogenetic tree was generated using IQTREE with H99 as outgroup and 10000 Ultrafast Bootstrap to support branch (Nguyen et al., 2015).

Statistical Analysis

Categorized variables were analyzed by Fisher's exact test by IBM SPSS software (version 26.0). Continuous variables were calculated by Mann–Whitney *U* test. A $p < 0.05$ was considered significant.

RESULTS

Antifungal Susceptibility Test

In vitro antifungal susceptibility testing of total isolates was performed against four agents. In brief, the majority exhibited high sensitivity to fluconazole, 5-fluorocytosine, and voriconazole, ranging from 93.98 to 100%. However, 89.15% (109/133) of isolates were non-wild type to amphotericin B. Eight isolates were resistant to fluconazole, and eight isolates were non-wild type against 5-fluorocytosine; compared with the recommended ECVs of fluconazole and 5-fluorocytosine, high MICs of cryptococcal isolates against 5-fluorocytosine (64 μg/ml) or fluconazole (32 μg/ml) were observed. Interestingly, we found three multidrug isolates (1 isolate from HIV-positive group and 2 isolates from HIV-negative group) (**Table 1** and **Supplementary Table 1**). For isolates from HIV-positive and HIV-negative groups, the MIC distribution was similar in fluconazole ($p = 0.290$) but significantly different in 5-fluorocytosine ($p < 0.001$), with higher MIC values in HIV-negative group (**Figure 1**).

Identification and Correlation Between ST5 and Human Immunodeficiency Virus Status

According to MALDI-TOF MS and *IGS1* sequencing outcomes, the 133 *C. neoformans* clinical isolates included 130 *C. neoformans* var. *grubii* and 3 *C. neoformans* var. *neoformans*. Among the 3 *C. neoformans* var. *neoformans* isolates, two isolates were from the HIV-positive group (ST77 and ST93), and the remaining isolate was from the HIV-negative group (ST185). As for MLST analysis, in this study, all isolates were classified into nine STs, and the majority of isolates belonged to ST5, VNI (90.23%, 120/133). For HIV-positive group, ST5 accounted for 86.88% (53/61), and five isolates with other STs included ST43 (1.64%), ST63 (1.64%), ST77 (1.64%), ST93 (1.64%), and ST230 (1.64%). In the other group, there were four STs, containing

TABLE 1 | *In vitro* susceptibilities of *Cryptococcus neoformans* in HIV-positive and HIV-negative cryptococcosis patients.

HIV status	Species (No. of isolates)	Antifungal drugs	MIC (μg/mL)						
			Range	MIC_{50}	MIC_{90}	GM	Mode MIC	WT%	Non-WT%
HIV-positive	*Cryptococcus neoformans* (*n* = 61)	Fluconazole	1–32	4	8	4.43	4	95.08	4.92
		Voriconazole	0.03125–0.25	0.0625	0.125	0.08	0.0625	100	0
		Amphotericin B	0.25–2	1	2	1.23	1	9.84	90.16
		Flucytosine	1–16	4	8	4.19	4	98.36	1.64
HIV-negative	*Cryptococcus neoformans* (*n* = 72)	Fluconazole	1–16	4	8	4.94	4	93.06	6.94
		Voriconazole	0.015–0.25	0.0625	0.125	0.08	0.0625	100	0
		Amphotericin B	0.0125–2	1	2	1.01	1	25	75
		Flucytosine	2–64	8	16	6.59	8	90.28	9.72

MIC, minimum inhibitory concentration; MIC50 and MIC90, MICs at which 50 and 90% of isolates were inhibited; GM, geometric mean; WT, wild type; NWT, non-wild type.

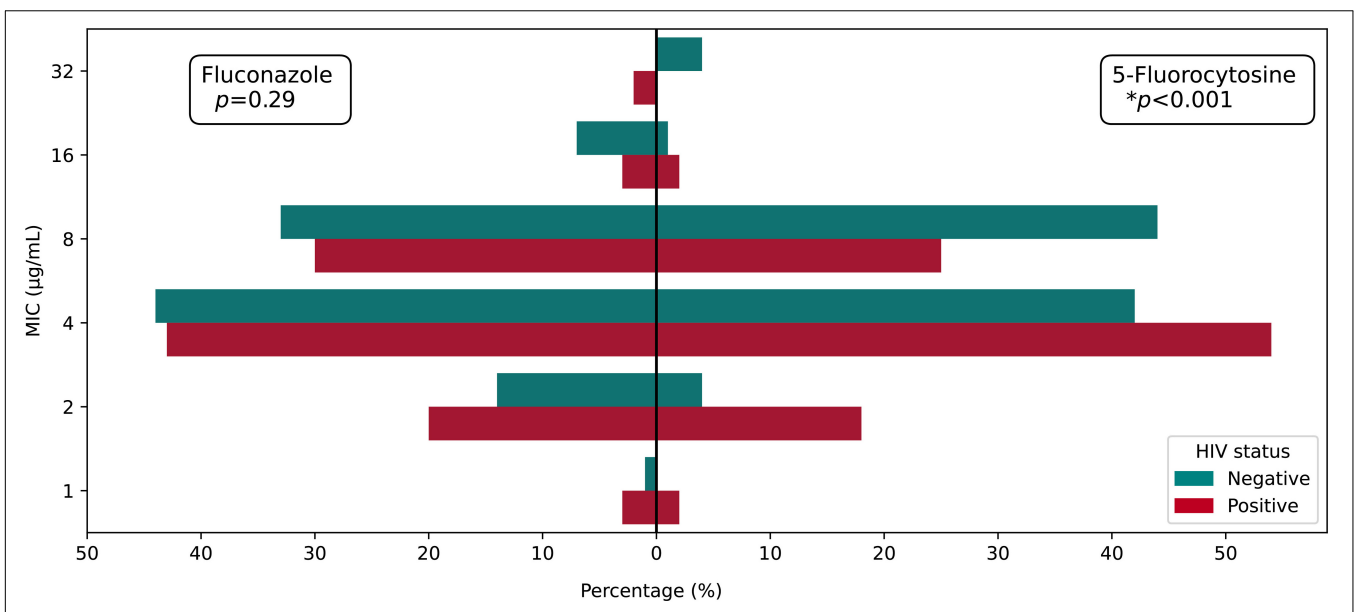

FIGURE 1 | MIC distribution of fluconazole and 5-fluorocytosine among HIV-positive and HIV-negative groups.

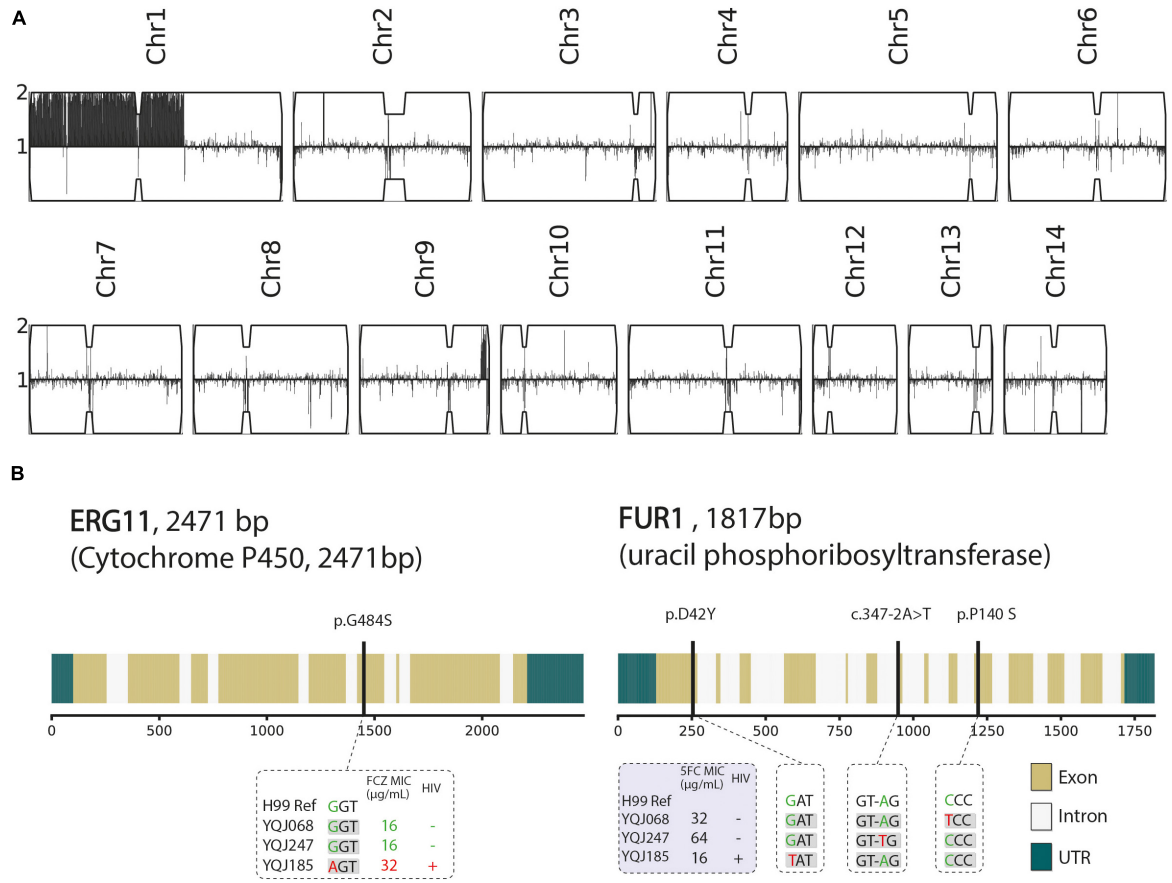

FIGURE 2 | Genetic characteristics of three resistant strains. **(A)** Karyotype of multidrug-resistant strain (YQJ185). Copy number is labeled in *y*-axis compared with haploid H99 reference using YMAP, with 1 copy number as baseline. Position of reads of each chromosome is on *x*-axis. **(B)** Non-synonymous mutation and splice site mutation of *ERG11* and *FUR1* genes.

ST5 (93.05%, 67/72), ST31 (1.39%), ST185 (1.39%), and ST653 (2.78%). In comparison with the HIV-negative group, STs of the HIV-positive group exhibited more diversity. There were four isolates unknown to STs due to failure of sequencing or identifying. In addition, compared with the HIV-positive group, there was no correlation between HIV status and STs ($p = 0.256$). More details are provided in **Supplementary Tables 2, 3**. In general, our study revealed that *C. neoformans* var. *grubii* (ST5, VNI) was the most representative and predominant species in East China.

Whole-Genome Sequencing

In this study, we analyzed the mating type and resistant mechanisms from three multidrug-resistant strains by WGS. The detailed information about WGS, including total reads, base quality, depth, and coverage, is shown in **Supplementary Table 4**. All multidrug-resistant strains belonged to MAT α. For an isolate (YQJ185) from the HIV-positive group, aneuploidy occurred in chromosome 1, but not in other chromosomes (**Figure 2A**). G484S mutation was found in *ERG11* gene of YQJ185 with a high-level MIC (32 μg/ml) to FCZ, located in the conserved heme-binding domain. Copy number variant (CNV) and *ERG11* mutation, however, were not observed in the other two resistant isolates from the HIV-negative group. The non-synonymous mutation was also observed in *FUR1* in different positions. For the HIV-positive group, D42Y mutation was found in the *FUR1* gene of YQJ185 with MIC (16 μg/ml) to 5FC. For the HIV-negative group, P140S mutation was found in the *FUR1* gene of YQJ68 with a high MIC (32 μg/ml) to 5FC, while YQJ247 has an A-T transition in an intron splice site (**Figure 2B**).

The ST5 isolates were located in the subclade of VNIa. As mentioned above, ST5 is the major genotype in China, but whole-genome sequences were rarely published. Phylogenetic relationships including ST5 isolates from other countries were generated in this study. Two isolates from HIV-negative patients were clustered into the same subclade with CHC-193 isolated from an HIV-negative patient in 1998 in China (**Figure 3**).

DISCUSSION

Cryptococcus neoformans is widely distributed in the world, and usually, it infects HIV-positive patients, particularly in South Africa and Asia (Rajasingham et al., 2017). However, the

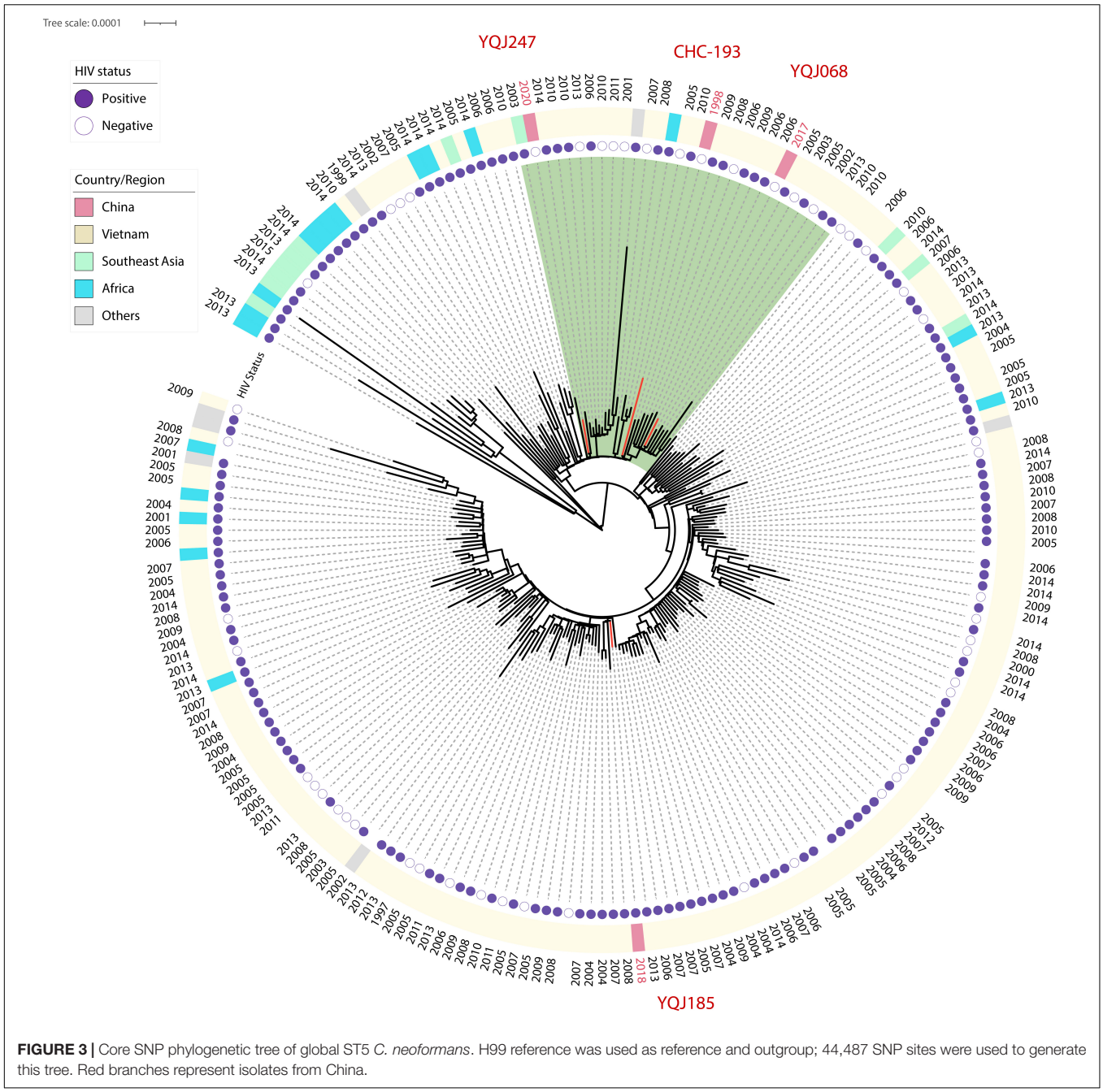

FIGURE 3 | Core SNP phylogenetic tree of global ST5 *C. neoformans*. H99 reference was used as reference and outgroup; 44,487 SNP sites were used to generate this tree. Red branches represent isolates from China.

condition appears to be extremely different in China (Chen et al., 2018). Previous studies showed that cryptococcosis was likely to occur in immunocompetent individuals or in individuals with other underlying diseases (Fang et al., 2020; Li et al., 2020). Indeed, *C. neoformans* exhibited lower genetic diversity in China than that in South Asia, and ST5 was the predominant genotype (Khayhan et al., 2013; Dou et al., 2015; Thanh et al., 2018).

The MLST was one of the most common technologies to analyze the genotypic diversity of *C. neoformans*. In this study, our results showed that there was lower genetic diversity of *C. neoformans*, and ST5 is the dominant ST in China, accounting for 90.23% (120/133) in total. The same results were observed in previous Chinese studies (Chen et al., 2018; Yang C. et al., 2021). Indeed, our research revealed no significant difference between HIV-positive and HIV-negative patients on STs ($p = 0.256$). This is consistent with southwest China (Wu et al., 2021). However, the situation is different in South Korea, where there were significant differences between HIV status and genetic types (Choi et al., 2010). In another study from Asia, it was affirmed that most isolates from HIV-negative patients were ST5 (Khayhan et al., 2013). Furthermore, in this study we identified five new STs in China, namely, ST230, ST43, ST77, ST185, and ST653, and all

of the STs haven't been reported yet in East China (Yang C. et al., 2021). Most importantly, ST31 was the most common ST for environmental *C. neoformans* in China, which mainly originated from pigeon droppings (Dou et al., 2017; Chen et al., 2021), and ST31 was also the main ST of *C. neoformans* in India (Xess et al., 2021). This suggests that attention is paid to the clinical isolates of *C. neoformans* but environmental isolates of *C. neoformans* need to be investigated more deeply and more extensively in the future.

Fluconazole and amphotericin B are the most frequent therapeutic drugs in cryptococcosis treatment. High MICs of amphotericin B above ECVs are concerned in this study, while all isolates were sensitive to voriconazole. This is consistent with a 6-year retrospective study from Hunan, China (Li et al., 2020). Interestingly, the MIC distribution of 5-fluorocytosine in the HIV-negative group was higher than that of the HIV-positive group, and there were no significant differences in other drugs. This is opposite to the study in Southeast China and is consistent with the study in Serbia (Li et al., 2012; Arsic Arsenijevic et al., 2014). Moreover, in a study from southeast China, the results exhibited no significant differences in antifungal susceptibility to fluconazole and 5-fluorocytosine between HIV-positive and HIV-negative patients (Wu et al., 2021). However, the association between STs and antifungal susceptibility was not observed. In this study, three multidrug isolates were found. Therefore, in this study, we investigated the resistance mechanisms through WGS. Aneuploidy of Chromosome 1 of an isolate (YQJ185) from an HIV-infected patient was tested. Previous studies proved the correlation between the formation of aneuploidy of Chromosome 1 and excessive doses of fluconazole (Stone et al., 2019; Yang F. et al., 2021). In addition, we also revealed a point mutation of *ERG11* (G484S) (Rodero et al., 2003; Gago et al., 2017). CNV and *ERG11* mutation would accelerate the speed of the cryptococcal resistance to fluconazole. However, the same resistance mechanisms were not observed in the other two isolates (HIV-negative group) against fluconazole (16 μg/ml). What'more, there was no available literature that described the resistance mechanisms of 5-fluorocytosine in China. In this study, we addressed point mutations of *FUR1* in different mutation sites and splice site mutation with different MICs, and it exhibited unique resistance mechanisms of 5-fluorocytosine in China. Previous studies reported that genes *FCY1*, *FCY2,* and *UXS1* were associated with resistance to 5-fluorocytosine (Vu et al., 2018; Billmyre et al., 2020); however, we didn't find it in our study. ST5 or VNIa-5 is an important phylogenetic group in Southeast Asia, characterized by its ability to infect HIV-negative patients (Ashton et al., 2019). Despite all three genomes in this study were closely related to Vietnam strains, they are assigned to two subclades, indicating the unique evolution progress of the strain from the HIV-positive group.

CONCLUSION

Cryptococcus in China exhibited a low extent of genetic diversity, whether HIV-positive or HIV-negative patients were not linked to STs. VNI is the dominant molecular type in *C. neoformans* and ST5 is the predominant ST. Phylogenetic relationship and resistance mechanisms have evolved among the subclades of ST5 isolates with certain particularity in China. However, there are limitations in this study. First, the geographical representativeness of epidemiological characteristics and resistance mechanisms in this study is limited, only representing East China. Second, only three clinical isolates were performed by WGS in our study, and the correlation among clinical isolates, standard isolates, and environmental isolates should be involved in the future. Finally, the isolates should be inoculated on the medium with FCZ, which would contribute to finding a resistance mechanism on the genomic level. WGS can be used to discover more than just about evolutionary relationships. Hence, we are taking steps to establish a database of cryptococcal genomes using WGS in East China.

DATA AVAILABILITY STATEMENT

The datasets presented in this study can be found in online repositories. The names of the repository/repositories and accession number(s) can be found below: https://ngdc.cncb.ac.cn/bioproject/browse/PRJCA009353, PRJCA009353.

AUTHOR CONTRIBUTIONS

WW designed the experiments and supervised the data analysis. ZYZ and CZ wrote the manuscript. CZ, ML, RL, and XL performed and interpreted the whole-genome sequencing data. WW, LZ, ZQZ, and ZYZ collected the strains. All authors contributed to the collection and assembly of data, manuscript writing, and final approval of the manuscript.

FUNDING

This study was supported by the National Natural Science Foundation of China (Grant Nos. 81971990 and 82172326), Key Discipline of Public Health in Shanghai (Grant No. GWV-10.1-XK04), and Excellent Technology Leader in Shanghai (Grant No. 20XD1434500).

ACKNOWLEDGMENTS

We thank the East China Invasive Fungal Infection Group (ECIFIG) members for their helpful collection of clinical strains.

SUPPLEMENTARY MATERIAL

The Supplementary Material for this article can be found online at: https://www.frontiersin.org/articles/10.3389/fmicb.2022.942940/full#supplementary-material

REFERENCES

Abbey, D. A., Funt, J., Lurie-Weinberger, M. N., Thompson, D. A., Regev, A., Myers, C. L., et al. (2014). YMAP: a pipeline for visualization of copy number variation and loss of heterozygosity in eukaryotic pathogens. *Genome Med.* 6:100. doi: 10.1186/s13073-014-0100-8

Arsic Arsenijevic, V., Pekmezovic, M. G., Meis, J. F., and Hagen, F. (2014). Molecular epidemiology and antifungal susceptibility of Serbian Cryptococcus neoformans isolates. *Mycoses* 57, 380–387. doi: 10.1111/myc.12171

Ashton, P. M., Thanh, L. T., Trieu, P. H., Van Anh, D., Trinh, N. M., Beardsley, J., et al. (2019). Three phylogenetic groups have driven the recent population expansion of Cryptococcus neoformans. *Nat. Commun.* 10:2035. doi: 10.1038/s41467-019-10092-5

Baddley, J. W., and Forrest, G. N. (2019). Cryptococcosis in solid organ transplantation-Guidelines from the American Society of Transplantation Infectious Diseases Community of Practice. *Clin. Trans.* 33:e13543. doi: 10.1111/ctr.13543

Bankevich, A., Nurk, S., Antipov, D., Gurevich, A. A., Dvorkin, M., Kulikov, A. S., et al. (2012). SPAdes: a new genome assembly algorithm and its applications to single-cell sequencing. *J. Comput. Biol.* 19, 455–477. doi: 10.1089/cmb.2012.0021

Beardsley, J., Sorrell, T. C., and Chen, S. C. (2019). Central Nervous System Cryptococcal Infections in Non-HIV Infected Patients. *J. Fungi* 5:71. doi: 10.3390/jof5030071

Bermas, A., and Geddes-McAlister, J. (2020). Combatting the evolution of antifungal resistance in Cryptococcus neoformans. *Mol. Microbiol.* 114, 721–734. doi: 10.1111/mmi.14565

Billmyre, R. B., Applen Clancey, S., Li, L. X., Doering, T. L., and Heitman, J. (2020). 5-fluorocytosine resistance is associated with hypermutation and alterations in capsule biosynthesis in Cryptococcus. *Nat. Commun.* 11:127. doi: 10.1038/s41467-019-13890-z

Bolger, A. M., Lohse, M., and Usadel, B. (2014). Trimmomatic: a flexible trimmer for Illumina sequence data. *Bioinformatics* 30, 2114–2120. doi: 10.1093/bioinformatics/btu170

Bosco-Borgeat, M. E., Mazza, M., Taverna, C. G., Córdoba, S., Murisengo, O. A., Vivot, W., et al. (2016). Amino acid substitution in Cryptococcus neoformans lanosterol 14-α-demethylase involved in fluconazole resistance in clinical isolates. *Rev. Argent. Microbiol.* 48, 137–142. doi: 10.1016/j.ram.2016.03.003

Bovers, M., Hagen, F., Kuramae, E. E., and Boekhout, T. (2008). Six monophyletic lineages identified within Cryptococcus neoformans and Cryptococcus gattii by multi-locus sequence typing. *Fungal Genet. Biol.* 45, 400–421. doi: 10.1016/j.fgb.2007.12.004

Chang, Y. C., Lamichhane, A. K., Cai, H., Walter, P. J., Bennett, J. E., and Kwon-Chung, K. J. (2021). Moderate levels of 5-fluorocytosine cause the emergence of high frequency resistance in cryptococci. *Nat. Commun.* 12:3418. doi: 10.1038/s41467-021-23745-1

Chen, M., Wang, Y., Li, Y., Hong, N., Zhu, X., Pan, W., et al. (2021). Genotypic diversity and antifungal susceptibility of environmental isolates of Cryptococcus neoformans from the Yangtze River Delta region of East China. *Med. Mycol.* 59, 653–663. doi: 10.1093/mmy/myaa096

Chen, M., Xu, Y., Hong, N., Yang, Y., Lei, W., Du, L., et al. (2018). Epidemiology of fungal infections in China. *Front. Med.* 12, 58–75. doi: 10.1007/s11684-017-0601-0

Choi, Y. H., Ngamskulrungroj, P., Varma, A., Sionov, E., Hwang, S. M., Carriconde, F., et al. (2010). Prevalence of the VNIc genotype of Cryptococcus neoformans in non-HIV-associated cryptococcosis in the Republic of Korea. *FEMS Yeast Res.* 10, 769–778. doi: 10.1111/j.1567-1364.2010.00648.x

Cingolani, P., Platts, A., Wang le, L., Coon, M., Nguyen, T., Wang, L., et al. (2012). A program for annotating and predicting the effects of single nucleotide polymorphisms, SnpEff: SNPs in the genome of Drosophila melanogaster strain w1118; iso-2; iso-3. *Fly.* 6, 80–92. doi: 10.4161/fly.19695

CLSI (2017). *Clinical and Laboratory Standards Institute (2017. b). Reference Method for Broth Dilution Antifungal Susceptibility Testing of Yeasts, 4th Ed.* Wayne, PA: CLSI.

CLSI (2018). *Epidemiological Cutoff Values for Antifungal Susceptibility Testing, 2nd Edn.* Wayne, PA: CLSI.

Cogliati, M. (2013). Global Molecular Epidemiology of Cryptococcus neoformans and Cryptococcus gattii: An Atlas of the Molecular Types. *Scientifica* 2013:675213. doi: 10.1155/2013/675213

Dou, H., Wang, H., Xie, S., Chen, X., Xu, Z., and Xu, Y. (2017). Molecular characterization of Cryptococcus neoformans isolated from the environment in Beijing. *China. Med. Mycol.* 55, 737–747. doi: 10.1093/mmy/myx026

Dou, H. T., Xu, Y. C., Wang, H. Z., and Li, T. S. (2015). Molecular epidemiology of Cryptococcus neoformans and Cryptococcus gattii in China between 2007 and 2013 using multilocus sequence typing and the DiversiLab system. *Eur. J. Clin. Microbiol. Infect. Dis.* 34, 753–762. doi: 10.1007/s10096-014-2289-2

Dromer, F., Mathoulin-Pélissier, S., Launay, O., and Lortholary, O. (2007). Determinants of disease presentation and outcome during cryptococcosis: the CryptoA/D study. *PLoS Med.* 4:e21. doi: 10.1371/journal.pmed.0040021

Espinel-Ingroff, A., Aller, A. I., Canton, E., Castañón-Olivares, L. R., Chowdhary, A., Cordoba, S., et al. (2012). Cryptococcus neoformans-Cryptococcus gattii species complex: an international study of wild-type susceptibility endpoint distributions and epidemiological cutoff values for fluconazole, itraconazole, posaconazole, and voriconazole. *Antimicrob. Agents Chemother.* 56, 5898–5906. doi: 10.1128/aac.01115-12

Fan, X., Xiao, M., Chen, S., Kong, F., Dou, H. T., Wang, H., et al. (2016). Predominance of Cryptococcus neoformans var. grubii multilocus sequence type 5 and emergence of isolates with non-wild-type minimum inhibitory concentrations to fluconazole: a multi-centre study in China. *Clin. Microbiol. Infect.* 22:887.e1-887.e9. doi: 10.1016/j.cmi.2016.07.008

Fang, L. F., Zhang, P. P., Wang, J., Yang, Q., and Qu, T. T. (2020). Clinical and microbiological characteristics of cryptococcosis at an university hospital in China from 2013 to 2017. *Braz. J. Infect. Dis.* 24, 7–12. doi: 10.1016/j.bjid.2019.11.004

Feng, X., Yao, Z., Ren, D., Liao, W., and Wu, J. (2008). Genotype and mating type analysis of Cryptococcus neoformans and Cryptococcus gattii isolates from China that mainly originated from non-HIV-infected patients. *FEMS Yeast Res.* 8, 930–938. doi: 10.1111/j.1567-1364.2008.00422.x

Firacative, C., Meyer, W., and Castañeda, E. (2021). Cryptococcus neoformans and Cryptococcus gattii Species Complexes in Latin America: A Map of Molecular Types, Genotypic Diversity, and Antifungal Susceptibility as Reported by the Latin American Cryptococcal Study Group. *J. Fungi.* 7:282. doi: 10.3390/jof7040282

Gago, S., Serrano, C., Alastruey-Izquierdo, A., Cuesta, I., Martin-Mazuelos, E., Aller, A. I., et al. (2017). Molecular identification, antifungal resistance and virulence of Cryptococcus neoformans and Cryptococcus deneoformans isolated in Seville. *Spain. Mycoses* 60, 40–50. doi: 10.1111/myc.12543

Hagen, F., Khayhan, K., Theelen, B., Kolecka, A., Polacheck, I., Sionov, E., et al. (2015). Recognition of seven species in the Cryptococcus gattii/Cryptococcus neoformans species complex. *Fungal. Genet. Biol.* 78, 16–48. doi: 10.1016/j.fgb.2015.02.009

Hagen, F., Lumbsch, H. T., Arsic Arsenijevic, V., Badali, H., Bertout, S., Billmyre, R. B., et al. (2017). Importance of Resolving Fungal Nomenclature: the Case of Multiple Pathogenic Species in the Cryptococcus Genus. *mSphere* 2:e00238-17. doi: 10.1128/mSphere.00238-17

Hong, N., Chen, M., and Xu, J. (2021). Molecular Markers Reveal Epidemiological Patterns and Evolutionary Histories of the Human Pathogenic Cryptococcus. *Front. Cell. Infect. Microbiol.* 11:683670. doi: 10.3389/fcimb.2021.683670

Janbon, G., Ormerod, K. L., Paulet, D., Byrnes, E. J. III, Yadav, V., Chatterjee, G., et al. (2014). Analysis of the Genome and Transcriptome of Cryptococcus neoformans var. grubii Reveals Complex RNA Expression and Microevolution Leading to Virulence Attenuation. *PLoS Genet.* 10:e1004261. doi: 10.1371/journal.pgen.1004261

Khayhan, K., Hagen, F., Pan, W., Simwami, S., Fisher, M. C., Wahyuningsih, R., et al. (2013). Geographically structured populations of Cryptococcus neoformans Variety grubii in Asia correlate with HIV status and show a clonal population structure. *PLoS One* 8:e72222. doi: 10.1371/journal.pone.0072222

Kwon-Chung, K. J., Bennett, J. E., Wickes, B. L., Meyer, W., Cuomo, C. A., Wollenburg, K. R., et al. (2017). The Case for Adopting the "Species Complex" Nomenclature for the Etiologic Agents of Cryptococcosis. *mSphere* 2:e00357-16. doi: 10.1128/mSphere.00357-16

Li, H., and Durbin, R. (2009). Fast and accurate short read alignment with Burrows–Wheeler transform. *Bioinformatics* 25, 1754–1760. doi: 10.1093/bioinformatics/btp324

Li, H., Handsaker, B., Wysoker, A., Fennell, T., Ruan, J., Homer, N., et al. (2009). The Sequence Alignment/Map format and SAMtools. *Bioinformatics* 25, 2078–2079. doi: 10.1093/bioinformatics/btp352

Li, M., Chen, M., and Pan, W. (2013). Approaches on genetic polymorphism of Cryptococcus species complex. *Front. Biosci.* 18:1227–1236. doi: 10.2741/4174

Li, M., Liao, Y., Chen, M., Pan, W., and Weng, L. (2012). Antifungal susceptibilities of Cryptococcus species complex isolates from AIDS and non-AIDS patients in Southeast China. *Braz. J. Infect. Dis.* 16, 175–179. doi: 10.1016/s1413-8670(12)70301-x

Li, Y., Zou, M., Yin, J., Liu, Z., and Lu, B. (2020). Microbiological, Epidemiological, and Clinical Characteristics of Patients With Cryptococcal Meningitis at a Tertiary Hospital in China: A 6-Year Retrospective Analysis. *Front. Microbiol.* 11:1837. doi: 10.3389/fmicb.2020.01837

McKenna, A., Hanna, M., Banks, E., Sivachenko, A., Cibulskis, K., Kernytsky, A., et al. (2010). The Genome Analysis Toolkit: a MapReduce framework for analyzing next-generation DNA sequencing data. *Genome Res.* 20, 1297–1303. doi: 10.1101/gr.107524.110

Meyer, W., Aanensen, D. M., Boekhout, T., Cogliati, M., Diaz, M. R., Esposto, M. C., et al. (2009). Consensus multi-locus sequence typing scheme for Cryptococcus neoformans and Cryptococcus gattii. *Med. Mycol.* 47, 561–570. doi: 10.1080/13693780902953886

Nguyen, L. T., Schmidt, H. A., von Haeseler, A., and Minh, B. Q. (2015). IQ-TREE: a fast and effective stochastic algorithm for estimating maximum-likelihood phylogenies. *Mol. Biol. Evol.* 32, 268–274. doi: 10.1093/molbev/msu300

Park, B. J., Wannemuehler, K. A., Marston, B. J., Govender, N., Pappas, P. G., and Chiller, T. M. (2009). Estimation of the current global burden of cryptococcal meningitis among persons living with HIV/AIDS. *Aids* 23, 525–530. doi: 10.1097/QAD.0b013e328322ffac

Pyrgos, V., Seitz, A. E., Steiner, C. A., Prevots, D. R., and Williamson, P. R. (2013). Epidemiology of cryptococcal meningitis in the US: 1997-2009. *PLoS One* 8:e56269. doi: 10.1371/journal.pone.0056269

Rajasingham, R., Smith, R. M., Park, B. J., Jarvis, J. N., Govender, N. P., Chiller, T. M., et al. (2017). Global burden of disease of HIV-associated cryptococcal meningitis: an updated analysis. *Lancet Infect. Dis.* 17, 873–881. doi: 10.1016/s1473-3099(17)30243-8

Rhodes, J., Desjardins, C. A., Sykes, S. M., Beale, M. A., Vanhove, M., Sakthikumar, S., et al. (2017). Tracing Genetic Exchange and Biogeography of Cryptococcus neoformans var. grubii at the Global Population Level. *Genetics* 207, 327–346. doi: 10.1534/genetics.117.203836

Rodero, L., Mellado, E., Rodriguez, A. C., Salve, A., Guelfand, L., Cahn, P., et al. (2003). G484S amino acid substitution in lanosterol 14-alpha demethylase (ERG11) is related to fluconazole resistance in a recurrent Cryptococcus neoformans clinical isolate. *Antimicrob. Agents Chemother.* 47, 3653–3656. doi: 10.1128/aac.47.11.3653-3656.2003

Selb, R., Fuchs, V., Graf, B., Hamprecht, A., Hogardt, M., Sedlacek, L., et al. (2019). Molecular typing and *in vitro* resistance of Cryptococcus neoformans clinical isolates obtained in Germany between 2011 and 2017. *Int. J. Med. Microbiol.* 309:151336. doi: 10.1016/j.ijmm.2019.151336

Sloan, D. J., and Parris, V. (2014). Cryptococcal meningitis: epidemiology and therapeutic options. *Clin. Epidemiol.* 6, 169–182. doi: 10.2147/clep.S38850

Stajich, J. E., Harris, T., Brunk, B. P., Brestelli, J., Fischer, S., Harb, O. S., et al. (2012). FungiDB: an integrated functional genomics database for fungi. *Nucleic Acids Res.* 40:D675–D681. doi: 10.1093/nar/gkr918

Stone, N. R., Rhodes, J., Fisher, M. C., Mfinanga, S., Kivuyo, S., Rugemalila, J., et al. (2019). Dynamic ploidy changes drive fluconazole resistance in human cryptococcal meningitis. *J. Clin. Invest.* 129, 999–1014. doi: 10.1172/jci124516

Thanh, L. T., Phan, T. H., Rattanavong, S., Nguyen, T. M., Duong, A. V., Dacon, C., et al. (2018). Multilocus sequence typing of Cryptococcus neoformans var. grubii from Laos in a regional and global context. *Med. Mycol.* 57, 557–565. doi: 10.1093/mmy/myy105

Thorvaldsdóttir, H., Robinson, J. T., and Mesirov, J. P. (2013). Integrative Genomics Viewer (IGV): high-performance genomics data visualization and exploration. *Brief. Bioinformatics* 14, 178–192. doi: 10.1093/bib/bbs017

Vu, K., Thompson, G. R. III, Roe, C. C., Sykes, J. E., Dreibe, E. M., Lockhart, S. R., et al. (2018). Flucytosine resistance in Cryptococcus gattii is indirectly mediated by the FCY2-FCY1-FUR1 pathway. *Med. Mycol.* 56, 857–867. doi: 10.1093/mmy/myx135

Wu, S. Y., Kang, M., Liu, Y., Chen, Z. X., Xiao, Y. L., He, C., et al. (2021). Molecular epidemiology and antifungal susceptibilities of Cryptococcus species isolates from HIV and non-HIV patients in Southwest China. *Eur. J. Clin. Microbiol. Infect. Dis.* 40, 287–295. doi: 10.1007/s10096-020-04013-4

Xess, I., Pandey, M., Dabas, Y., Agarwal, R., Das, S., Srivastava, P. M. V., et al. (2021). Multilocus Sequence Typing of Clinical Isolates of Cryptococcus from India. *Mycopathologia* 186, 199–211. doi: 10.1007/s11046-020-00500-6

Xiao, M., Chen, S. C., Kong, F., Fan, X., Cheng, J. W., Hou, X., et al. (2018). Five-year China Hospital Invasive Fungal Surveillance Net (CHIF-NET) study of invasive fungal infections caused by noncandidal yeasts: species distribution and azole susceptibility. *Infect. Drug. Resist.* 11, 1659–1667. doi: 10.2147/idr.S173805

Xu, J., Ramos, A. R., Vilgalys, R., and Mitchell, T. G. (2000). Clonal and spontaneous origins of fluconazole resistance in Candida albicans. *J. Clin. Microbiol.* 38, 1214–1220. doi: 10.1128/jcm.38.3.1214-1220.2000

Yang, C., Bian, Z., Blechert, O., Deng, F., Chen, H., Li, Y., et al. (2021). High Prevalence of HIV-Related Cryptococcosis and Increased Resistance to Fluconazole of the Cryptococcus neoformans Complex in Jiangxi Province. South Central China. *Front. Cell. Infect. Microbiol.* 11:723251. doi: 10.3389/fcimb.2021.723251

Yang, F., Gritsenko, V., Lu, H., Zhen, C., Gao, L., Berman, J., et al. (2021). Adaptation to Fluconazole via Aneuploidy Enables Cross-Adaptation to Amphotericin B and Flucytosine in Cryptococcus neoformans. *Microbiol. Spectr.* 9:e0072321. doi: 10.1128/Spectrum.00723-21

Conflict of Interest: ML, RL, and XL were employed by the Jiangsu Simcere Diagnostics Co., Ltd.

The remaining authors declare that the research was conducted in the absence of any commercial or financial relationships that could be construed as a potential conflict of interest.

Publisher's Note: All claims expressed in this article are solely those of the authors and do not necessarily represent those of their affiliated organizations, or those of the publisher, the editors and the reviewers. Any product that may be evaluated in this article, or claim that may be made by its manufacturer, is not guaranteed or endorsed by the publisher.

frontiers | Frontiers in Microbiology

ORIGINAL RESEARCH
published: 18 July 2022
doi: 10.3389/fmicb.2022.934786

Intestinal Flora-Derived Kynurenic Acid Protects Against Intestinal Damage Caused by *Candida albicans* Infection *via* Activation of Aryl Hydrocarbon Receptor

Zetian Wang[1†], Liping Yin[1†], Yue Qi[1], Jiali Zhang[2], Haiyan Zhu[3] and Jianguo Tang[1*]*

[1] Department of Trauma-Emergency & Critical Care Medicine, Shanghai Fifth People's Hospital, Fudan University, Shanghai, China, [2] Department of Central Laboratory, Shanghai Fifth People's Hospital, Fudan University, Shanghai, China, [3] Department of Biological Medicines & Shanghai Engineering Research Center of Immunotherapeutics, Fudan University School of Pharmacy, Shanghai, China

OPEN ACCESS

Edited by:
Weihua Pan,
Shanghai Changzheng Hospital, China

Reviewed by:
Michael Sigal,
Charité Universitätsmedizin Berlin, Germany
Zhen Wu,
Ningbo University, China

***Correspondence:**
Jianguo Tang
tangjianguo@5thhospital.com
Haiyan Zhu
haiyanzhu@fudan.edu.cn

[†] These authors have contributed equally to this work

Specialty section:
This article was submitted to Antimicrobials, Resistance and Chemotherapy, a section of the journal Frontiers in Microbiology

Received: 03 May 2022
Accepted: 20 June 2022
Published: 18 July 2022

Citation:
Wang Z, Yin L, Qi Y, Zhang J, Zhu H and Tang J (2022) Intestinal Flora-Derived Kynurenic Acid Protects Against Intestinal Damage Caused by Candida albicans Infection via Activation of Aryl Hydrocarbon Receptor. Front. Microbiol. 13:934786. doi: 10.3389/fmicb.2022.934786

Colonization of the intestinal tract by *Candida albicans* (*C. albicans*) can lead to invasive candidiasis. Therefore, a functional intestinal epithelial barrier is critical for protecting against invasive *C. albicans* infections. We collected fecal samples from patients with *Candida albicans* bloodstream infection and healthy people. Through intestinal flora 16sRNA sequencing and intestinal metabolomic analysis, we found that *C. albicans* infection resulted in a significant decrease in the expression of the metabolite kynurenic acid (KynA). We used a repeated *C. albicans* intestinal infection mouse model, established following intake of 3% dextran sulfate sodium salt (DSS) for 9 days, and found that KynA, a tryptophan metabolite, inhibited inflammation, promoted expression of intestinal tight junction proteins, and protected from intestinal barrier damage caused by invasive Candida infections. We also demonstrated that KynA activated aryl hydrocarbon receptor (AHR) repressor *in vivo* and *in vitro*. Using Caco-2 cells co-cultured with *C. albicans*, we showed that KynA activated AHR, inhibited the myosin light chain kinase-phospho-myosin light chain (MLCK-pMLC) signaling pathway, and promoted tristetraprolin (TTP) expression to alleviate intestinal inflammation. Our findings suggest that the metabolite KynA which is differently expressed in patients with C. *albicans* infection and has a protective effect on the intestinal epithelium, *via* activating AHR, could be explored to provide new potential therapeutic strategies for invasive C. *albicans* infections.

Keywords: intestinal flora, invasive *C. albicans* infections, aryl hydrocarbon receptor, kynurenic acid, intestinal barrier function

INTRODUCTION

As a severe systemic inflammatory response syndrome, sepsis is one of the leading causes of multiple organ dysfunction (Kuang et al., 2021). During the development of sepsis, the functions of intestinal barriers are altered. Impaired intestinal barriers allow for the invasion of intestinal bacteria and entry of endotoxins into the blood and lymph circulation, eventually causing a "second attack" and secondary pancreatic infection and sepsis (Li H. Y. et al., 2021). *Candida albicans*

(*C. albicans*) is a member of the intestinal commensal microbiota that colonizes on the mucosal surfaces of the gastrointestinal tract (Jenull et al., 2021; Li H. Y. et al., 2021). This yeast can translocate into the bloodstream through impaired gut barriers in susceptible individuals, such as patients with sepsis, resulting in opportunistic infections (Hirao et al., 2014).

The intestinal microbiota is critical for human health. An accumulating body of evidence points out the key role of intestinal flora in maintaining intestinal homeostasis (He et al., 2020). Furthermore, numerous studies have shown that the intestinal flora can also regulate intestinal movement and secretion, decompose macromolecular complex polysaccharides in food, digest and absorb nutrients, maintain the integrity of the intestinal epithelial barrier, and promote and maintain the development and functions of the immune system (Dinan and Cryan, 2017; Li X. J. et al., 2021; Tian et al., 2021). Invasive *Candida* infections have been shown to alter the microecology of gut bacteria and aggravate intestinal damage. Studies using mice demonstrated that diallyl disulfide (DADS) can modulate gut microbiota and metabolites, as well as provide intestinal protection and alleviate *C. albicans* infections (Hu et al., 2021). The increase in intestinal microflora and their metabolites may represent potential strategies for the prevention and treatment of invasive *C. albicans* infections.

The aryl hydrocarbon receptor (AHR) resides in the cytosol and participates in multiple biological processes, such as cell proliferation, differentiation, and immune cell function (Parent et al., 2011; Liu et al., 2018). As a ligand-activated transcription factor, AHR exerts an anti-inflammatory effect on gut barrier damage (Liu et al., 2018). In the presence of ligands, such as 6-formylindolo(3,2-b)carbazole (FICZ), AHR translocates to the nucleus and dimerizes with the AHR nuclear translocator (ARNY) to initiate the transcription of target genes, including cytochrome P450 (CYP1A1), which contains functional AHR responsive elements (AhRES) (Liu et al., 2018; Gasaly et al., 2021). Although previous studies reported activation of AHR by MG132 to alleviate liver injury in *in vivo* and *in vitro* models of intestinal ischemia/reperfusion, the mechanisms underlying the effect of AHR activation on intestinal barrier damage following invasive *C. albicans* infection remain unknown (Arda-Pirincci and Bolkent, 2014).

Tristetraprolin (TTP) is an mRNA-binding and decaying protein that can control inflammation response through a decrease of TNF-αtranscription (Patil et al., 2008). Furthermore, the mitogen-activated protein kinase-2/phosphorylated mitogen-activated protein kinase-2 (MK2/p-MK2) pathway can regulate TTP stability, expression, and function (Wang W. et al., 2018). Recent research has shown that the MK2/p-MK2 signaling cascade regulates TTP-mediated mRNA stability of IL-6 and TNF-α (Sun et al., 2011). Another study suggested that AHR reduces inflammation in experimental colitis *via* the downregulation of the MK2/p-MK2/TTP pathway (Ghiboub et al., 2020).

The interaction between multiple tight junctions contributes to the integrity of the intestinal epithelial barrier (Serlin et al., 2015). Tight junction regulation is mediated by myosin light chain kinase (MLCK), which phosphorylates the myosin II regulatory light chain (MLC) (Meng et al., 2013). Myosin light chain kinase (MLCK) controls the permeability of the endothelial cell (IEC) barrier by directly phosphorylating the myosin light chain (MLC) (Cheng et al., 2015). It can induce the activation of the MLCK-pMLC phosphorylation signaling pathway under various pathological conditions [such as hypoxia, lipopolysaccharide (LPS) stimulation, burn injuries, and inflammatory bowel disease (IBD), among others], leading to a decrease in the expression of the tight junction protein Zonula occludens protein 1 (ZO-1), disruption of intestinal mucosal barrier continuous distribution, and increase in the permeability of the intestinal mucosal barrier and damage of intestinal mucosal barrier function (Song et al., 2019). AHR can affect the expression and location of tight junctions in models of intestinal obstruction by regulating the MLCK-pMLC signal pathway, thereby improving the dysfunction of the intestinal mucosal barrier (Yu et al., 2018). In this study, based on differential metabolite analysis in patients with *C. albicans* infection, we hypothesized that metabolites of intestinal flora could activate AHR to protect against intestinal damage induced by *C. albicans* infection.

MATERIALS AND METHODS

Human Samples

On the day of admission, samples of human feces were collected from healthy subjects and from patients with candidemia (six cases per group) at Shanghai Fifth People's Hospital, Shanghai, China. The study protocol was approved by the Human Research Ethics Committee of Shanghai Fifth People's Hospital, School of Medicine, Shanghai, China (Reference No. 2019-118). Participants or their guardians provided informed consent. Samples were frozen and stored in aliquots at 80°C in polyethylene tubes until use. The diagnostic criteria of candidemia were based on the guidelines for the diagnosis and treatment of Candidiasis: the expert consensus issued by the Chinese Medical Association. These criteria were also in accordance with the European Society of Clinical Microbiology and Infectious Diseases (ESCMID)* guidelines for the diagnosis and management of Candida diseases 2012 and the Infectious Diseases Society of America (IDSA) Guidelines for the Management of Candidiasis: 2016 Update (Pappas et al., 2009). Exclusion criteria were as follows: (a) age < 18 years old, (b) pregnant women, (c) the blood culture was found to be contaminated or there was no bloodstream *Candida* infection, and (d) loss to follow-up.

16S rRNA Analysis of the Microbial Community

Fecal samples were collected from patients and healthy controls (six cases per group). Briefly, DNA was extracted from feces by means of a Standard DNA Extraction Kit (QIAGEN) and analyzed by agarose gel electrophoresis to assess DNA quality. The V3-V4 region of 16S rRNA genes was amplified and purified. The Illumina MiSeq platform was used to sequence the V3-V4 gene amplicons. Raw data were filtered, and clean tags were

removed to obtain valid tags for preparing operational taxonomic units (OTUs), which were classified using the Vsearch software (version 2.4.2) with a sequence similarity threshold of 97%. Then, the pynast (v0.1) software was used to create a phylogeny based on OTU sequence comparisons. A rarefied OTU table was used to determine the diversity and composition of the intestinal microbiota. Alpha-diversity indices for fecal samples were calculated using a normalized OTU table and a uniform depth. Based on the Bray-Curtis algorithm and unweighted UniFrac distance, beta-diversity indexes were generated to determine whether there were significant differences in the gut microbiota between groups (Chen et al., 2016). Principal component analysis (PCA) was also used to determine whether such differences existed.

Fecal Metabolome Analysis

Six fecal extract samples were prepared for each group by combining 100 mg of fecal samples with 500 mL of ice-cold water, vortexed, and centrifuged at 13,000 rpm for 15 min at 4°C. Then, the supernatant was filtered through a 0.22 μm microfilter and stored at −80°C for liquid chromatography–mass spectrometry (LC–MS) analysis. The quality control (QC) group was formed by pooling equal volumes of supernatant from each sample to assess if the system's mass spectrum platform remained stable throughout the experiment. Metabolite profiles were analyzed using an AB TripleTOF 6600 mass spectrometer (AB Sciex, United States) with Essential Science Indicator (ESI) sources in both positive and negative ion scan modes. Regarding MS TOF parameters, the fragmentor was set to 140 V and the skimmer to 65 V. All reagents used in this study were of high-performance liquid chromatography (HPLC) grade. The LC–MS data from fecal pellets were processed using Progenesis QI software (Waters Corporation, Milford, United States), and the metabolites were processed using the Progenesis QI Data Processing software. The ropls package in R was used to visualize the normalized data using principal component analysis (PCA) and orthogonal partial least squares-discriminant (OPLS-DA) analysis. With a 95% confidence interval threshold, the ellipses in PCA and OPLS-DA plots were used to characterize metabolic perturbation among groups in a Hotelling's T2 region.

Candida albicans Culture

Candida albicans (strain SC5314) was obtained from the China General Microbiological Culture Collection Center, Shanghai, China (CGMCC), and grown in a liquid medium containing yeast extract peptone dextrose (YEPD). Then, a single colony was streaked on a YEPD agar plate, incubated for 25 h at 35°C, and reidentified by mass spectrometry (Shanghai Fifth People's Hospital, Fudan University, China). For preparation, inoculum containing 1.0×10^6 cells of *C. albicans* clone was suspended in 0.3 mL of phosphate-buffered saline (PBS, pH 7.4).

Mouse Experiments

Six to eight week-old male and female C57BL/6 mice weighing 20–23 g were acquired from East China Normal University's Animal Center (Shanghai, China). All mice were kept in plastic boxes and fed food and water on a daily basis at 20–22°C with a 12-h light/dark cycle. Prior to experimentation, mice were left to acclimatize for 1 week. All animal experiments were authorized by the East China Normal University's Experimental Animal Ethical Review Committee research (Shanghai, China). Mice were randomly divided into three groups. In the control group ($n = 15$), mice drank only sterile water without 3% dextran sulfate (DSS), and then were gavaged with 0.2 mL sterile autoclaved phosphate-buffered saline (PBS) every three days. In the CA group ($n = 15$), mice drank sterile water containing 3% DSS every day, and to induce intestinal mucosal destruction, the intestines of the mice were colonized with Candida albicans (1×10^6 CFU, 0.2 mL) by oral gavage every 3 days, and mouse feces samples were collected for detecting the load of *Candida albicans*. In the CA+KynA group ($n = 15$), mice were treated as in the CA group but on the third day, KynA, at a dose of 10 mg/kg (0.2 mL), was administered at 6 h after intragastric administration of *C. albicans*.

Mice were sacrificed on 4, 7, and 10 days. About 0.1 g of mouse excrements from the CA group ($n = 5$) and the CA+KynA group ($n = 5$) were collected in sterile tubes and diluted 10-fold with PBS. Mice were sacrificed 10 days after treatment with KynA, and the desired organs including the liver, spleen, and the kidneys were collected, weighed, and transferred to 1.5 mL sterilized EP tubes. A schematic diagram of the experimental design is shown in **Figure 1A**.

The suspension containing the feces and tissues was processed for gradient elution. About 100 μL of the suspension was added to 1 mL of sterile PBS solution and mixed well. Then, 10 μL of this solution was dissolved in 1 mL of sterile PBS solution, and coated on the culture medium. Colonies were counted after 3 days of incubation in an incubator at 37°C.

Histomorphological Analysis

Colonic tissue samples from mice from all three groups were fixed in 4% neutral formalin, dehydrated with escalating concentrations of ethanol, and embedded in paraffin. Paraffin blocks were cut into 5-μm thick slices which were mounted on slides, cleaned, hydrated, and stained with hematoxylin and eosin (H&E). Two expert pathologists examined all specimens and were blind to the experimental group. Histologic alterations were evaluated using a modified grading system according to the amount of tissue damage. To establish a histopathological score, the following semi-quantitative parameters were used: (i) epithelial impairment, (ii) goblet cell decrease, (iii) inflammatory cell infiltration, and (iv) submucosal stiffness. The scores used were as follows: Score (i) included 0: normal, 2: distorted morphology of epithelial cells in one-third of total area, 4: distorted morphology of epithelial cells in more than one-third of total area and/or minor erosions, 6: occurrence of ulcers in 10% of ulcerated areas 8: 10–20% of ulcerated areas; and 10: > 20% of ulcerated regions). Scores (ii–iv) included 0: normal, 1: mild, 2: moderate, and 3: severe. The lowest possible score was 0 and the highest was 19.

Western Blot Analysis

The cells and mouse intestinal tissues were lysed using an appropriate lysis buffer, and protein levels were determined using

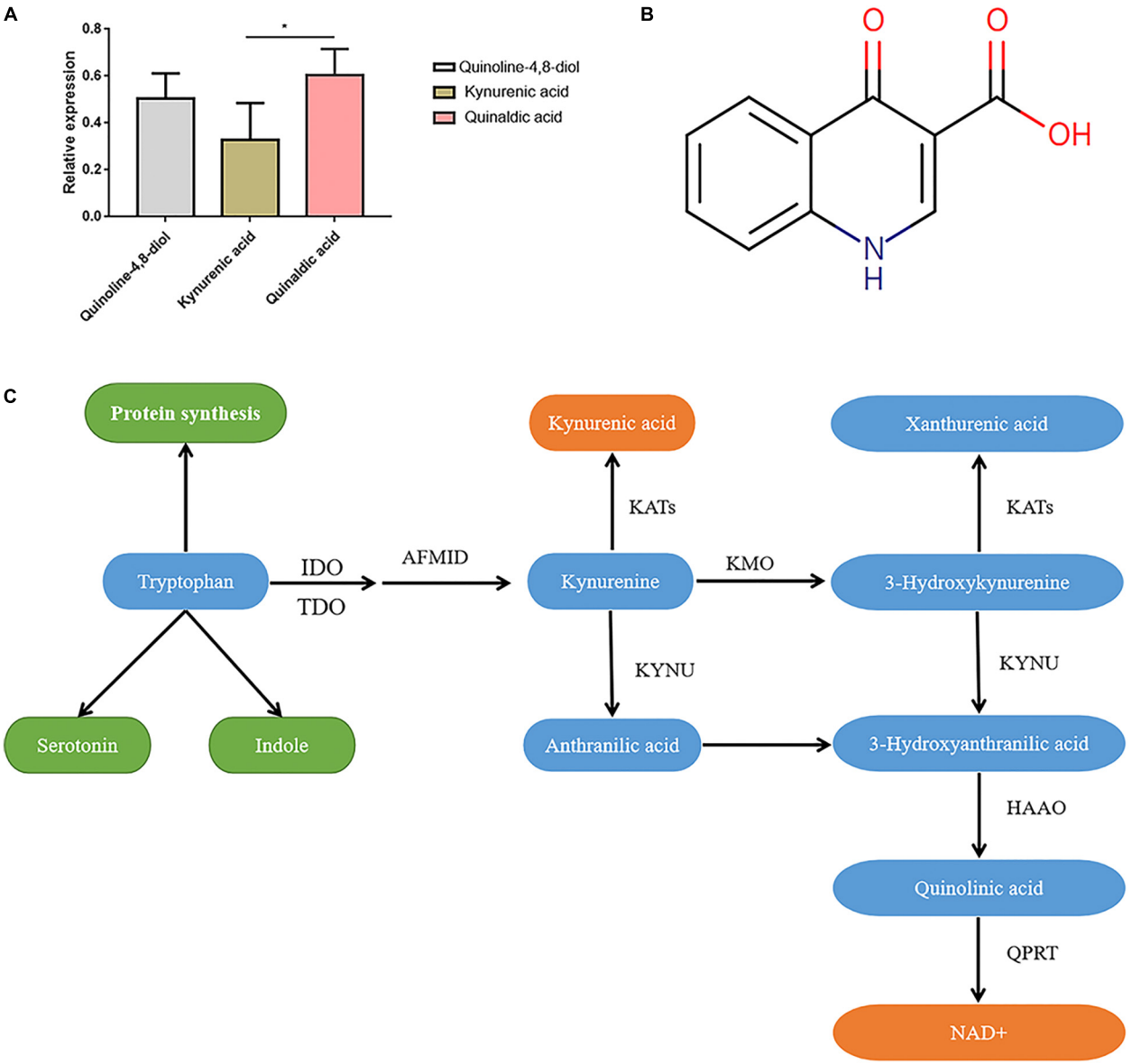

FIGURE 1 | Characteristics of kynurenic acid. **(A)** The relative expression of Kynurenic acid in the peripheral blood of patients with invasive *C. albican* infection is significantly lower than the content of other metabolites ($P < 0.05$). **(B)** Kynurenic acid (HMDB0000715) is a kind of phosphatidic acid molecule with the molecular formula of $C_{10}H_7NO_3$ and a molecular weight of 189.1675 Da. **(C)** The kynurenine pathway is the primary route for tryptophan metabolism, with one of the biologically active metabolites being kynurenic acid (KynA). T, The *Candida albicans* infection group; C, The healthy control group.

a BCA kit (Beyotime, China). Proteins were separated using SDS/PAGE in a Bio-Rad Mini-PROTEAN device before transfer to PVDF membranes (Bio-Rad, Marnes-la-Coquette, France). Membranes were then blocked for 1 h at room temperature with 5% non-fat milk (w/v), followed by overnight incubation with primary antibodies at 4°C. The following antibodies were used: anti-Occludin antibody (1:1,000, 13409-1-AP. Proteintech, United States); anti-AHR antibody (1:1,000, 67785-1-Ig; Proteintech, United States); anti-ZO-1 antibody (1:1,000, 21773-1-AP, Proteintech, United States); anti-GAPDH antibody (1:1,000, 60004-1-Ig, Proteintech, United States); anti-MK2 antibody (1:1,000, 13949-1-AP, Proteintech, United States); anti-CYP1A1 antibody (1:1,000, 13241-1-AP, Proteintech, United States); anti-TTP antibody (1:1,000, 12737-1-AP; Proteintech, United States); anti-MLCK antibody (1:1,000, 21642-1-AP; Proteintech, United States); and anti-pMLC antibody (1:2,000, CST-3671; Cell Signaling Technology, United States). The secondary antibodies used were as follows: HRP-conjugated goat anti-mouse IgG (H+L) (#115-035-003) and HRP-conjugated goat anti-rabbit IgG (H+L;#111-035-003), purchased from Jackson ImmunoResearch, United States. Protein expression was normalized to GAPDH, and densitometry

of Western blot bandings was evaluated with Image J (Version 1.50i; National institutes of Health, Bethesda, MD, United States).

Immunohistochemistry Staining

The tissues were fixed with 4% paraformaldehyde at 4℃overnight, embedded in paraffin, and sliced into 5-μm sections. Sections were dehydrated in an ethanol gradient at room temperature for 5 min, and treated with 0.3% hydrogen peroxide in methanol at room temperature for 20 min. Sections were then incubated in citrate buffer (pH 6.0) and microwaved for 20 min for antigen retrieval. Sections were incubated at 4℃ overnight with an anti-AHR antibody (1:200, 67785-1-Ig; Proteintech, United States) and then blocked with 5% bovine serum albumin (9048-46-8, Merck) at room temperature for 20 min. For incubation with the secondary antibodies, sections were then incubated at 37°C for 20 min with biotinylated goat anti-mouse and rabbit secondary antibodies (Sa1020, ready to use) and avidin-biotin complex (Sa1020, ready to use), purchased from Wuhan Boster Biological technology ltd., China. Peroxidase activity was determined by staining with diaminobenzidine (0.5 mg/mL) at room temperature for 20 s. Histological evaluation was performed under a light microscope (magnification, x400; Nikon Corporation), after counterstaining with hematoxylin (1 g/L) at room temperature for 1 min.

Enzyme-Linked Immunosorbent Assays

Five samples of peripheral blood were collected from each group and centrifuged at 3,000 rpm at 4°C for 10 min for serum collection. Serum was stored at -80 °C until use. Murine ELISA kits (DEIA1348, Creative Diagnostics, United States; DEIA-BJ2494, Creative Diagnostics, United States; Creative Diagnostics, United States) were used to measure the levels of IL-6, IFN, and D-lactic acid.

Cell Culture

Human colorectal adenocarcinomas (Caco-2) cells obtained from the American Type Culture Collection (Invitrogen, Manassas, VA, United States) were cultured in Eagle's Minimum Essential Medium supplemented with 10% heat-inactivated fetal bovine serum (Gemini Bioproducts, Calabasas, CA, United States) and 1% non-essential amino acids. Caco-2 cells were seeded on six-well plates at a density of 1×10^6 cells/well. Once the monolayers reached 70–80% confluence, they were cultured with serum-free MEM basic media overnight and then co-cultured with 1×10^5 CFU/mL concentration of *C. albicans* for 24 h, with or without 10 μM KynA (Selleck, United States), 100 nM FICZ (CAS No:172922-91-7, MeChemExpress, United States), and 10 μM CH223191 (CAS No:301326-22-7, MedChemExpress, United States), to examine the expression of AHR, CYP1A1, MLCK-pMLC, MK2-p-MK2, ZO-1, and occludin proteins.

Statistical Analysis

Data were expressed as mean and standard deviation (SD). Group differences were assessed using a one-way analysis of variance with the Student–Newman–Keuls test and the SPSS statistical software package (version 13.0; SPSS, Inc., Chicago, IL, United States). A statistically significant difference was defined as $P < 0.05$. Survival statistics were performed using Kaplan–Meier curve and log-rank test.

RESULTS

Invasive *Candida albicans* Infection Disrupts Fecal Microbiota Diversity and Metabolites in Humans

Fecal samples were collected from patients with candidemia ($n = 6$) and healthy subjects ($n = 6$) aged 55–65 years. To investigate the bacterial composition and intestinal metabolites, we used 16S rRNA gene amplicon sequencing and metabolomic analysis. A total of 3,423 OTUs were obtained from 12 samples. As shown in **Figure 2A**, in a petal diagram of OTU distribution, the number 24 in the core represents the number of OTUs shared by the two groups. According to the analysis of similarities (ANOSIM), there was a significant difference between the two groups of sampling units (**Figure 2B**). PCA analysis of OTU abundance in each group showed significant differences between the two groups (**Figure 2C**). Alpha-diversity analysis was used to estimate the microbial diversity of each individual sample. There was a significant difference in Shannon, Simpson, and Invsimpson in the candidemia group compared to the control group ($P < 0.05$). As shown in **Figure 2D**, invasive *C. albicans* infection decreases the diversity of flora. As expected, cluster analysis of species abundance based on the genus levels showed significant changes in the composition of gut microbiota between groups (**Figure 2E**). At the genus level, the relative abundances of *Lachnoclostridium*, *Bacteroides*, and *Lactococcus* were decreased in the candidemia group, whereas the relative abundances of *Bacillus, Enterobacter,* and *Caulobacter* were increased ($P < 0.05$).

The metabolic changes are closely related to alterations in the gut microbiota, which are also regarded as a key feature of intestinal inflammation. We used LC–MS to identify differentially expressed metabolites and key metabolic pathways in the two groups. A total of 962 metabolites were identified among the 12 fecal samples. The PCA scatter plots revealed clustered QC samples, indicating the high quality of metabolomic analysis (**Figure 3A**). To identify key metabolites, metabolites were visualized on a heatmap. Nineteen metabolic pathways were found to differ significantly between the two groups. We identified differentially expressed metabolites with statistical significance between groups by volcano plot filtering (**Figure 3B**). KEGG pathway enrichment analysis of differentially expressed metabolites using the Fisher precise test revealed significant changes in important pathways, such as linoleic acid metabolism, tryptophan metabolism, bile secretion, and arachidonic acid metabolism, between the groups (**Figure 3C**). When the top 50 metabolites were visualized in a heatmap, differential metabolites were found to be clustered (**Figure 3D**). Metabolites involved in tryptophan metabolism, such as quinoline-4,8-diol, kynurenic acid, and quinaldic acid, were significantly decreased in the candidemia group compared with the control group.

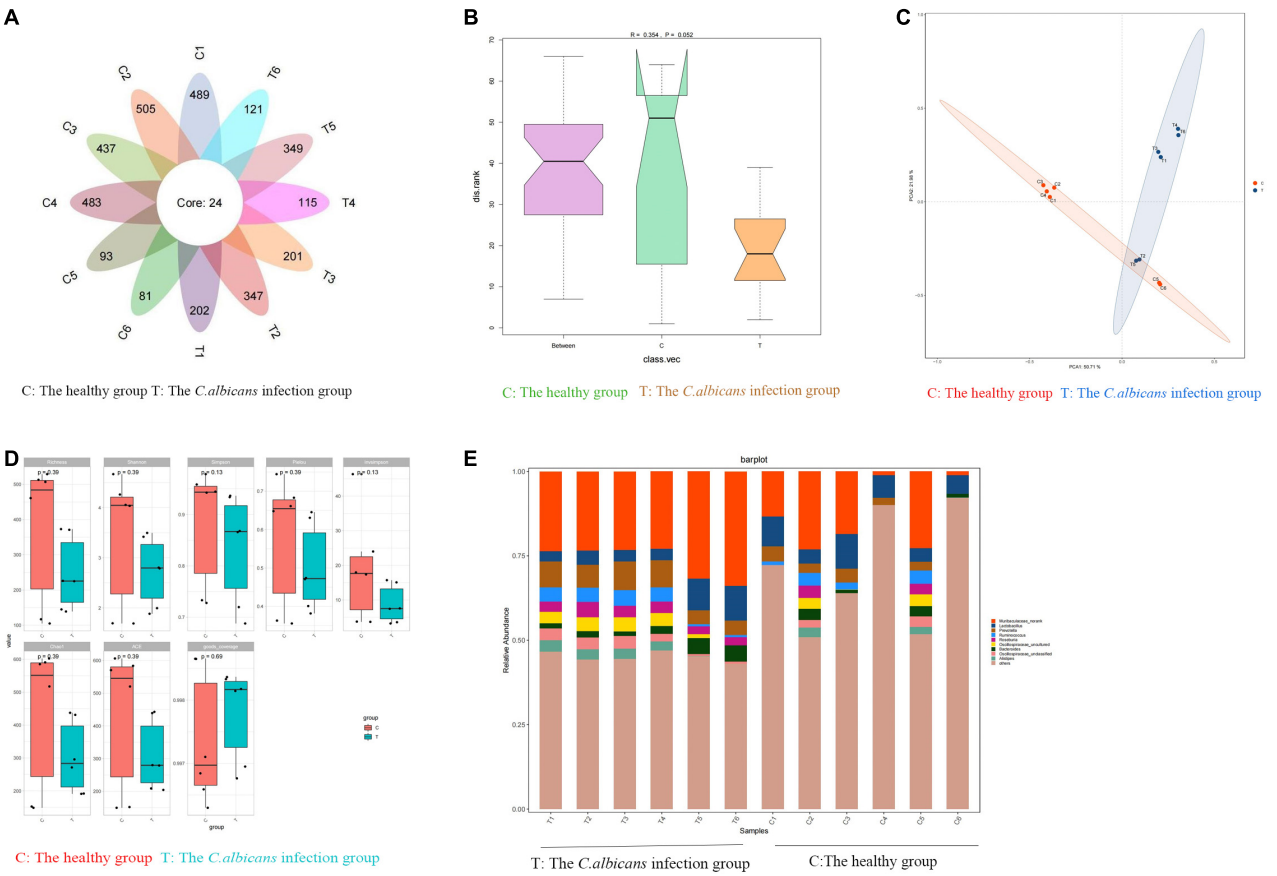

FIGURE 2 | Invasive *C. albicans* infection disrupts fecal microbiota in humans. Human fecal samples were collected from healthy people (n = 6) and patients with candidemia (n = 6). 16S rRNA gene amplicon sequencing and metabolomic analysis were done to investigate the bacterial composition and intestinal metabolites. **(A)** The petal diagram of OTU distribution. **(B)** Analysis of similarities (ANOSIM). **(C)** The PCA analysis of OTU abundance. **(D)** Alpha-diversity analysis. **(E)** At the genus level, invasive C. albicans infection disrupts fecal microbiota diversity. T, The *Candida albicans* infection group; C, The healthy control group.

Spearman correlation analysis was used to identify possible relationships between altered gut microbiota composition and fecal co-metabolites. As shown in **Figure 3E**, linoleic acid metabolism, tryptophan metabolism, bile secretion, and arachidonic acid metabolism are associated with beneficial bacteria, such as *Lactococcus, Acidibacter, and Sphingomonas*. Thus, gut microbiota dysbiosis may be associated with fecal metabolites.

The Characteristics of Kynurenic Acid

We screened three differentially expressed metabolites, quinoline-4,8-diol, kynurenic acid, and quinaldic acid (**Table 1**), and analyzed their contents in the peripheral blood of patients with invasive *C. albicans* infection and healthy controls by targeted mass spectrometry. There was a significant difference in the content of kynurenic acid in the peripheral blood of patients with invasive *C. albicans* infection compared with healthy controls. The production of kynurenic acid is closely related to *Clostridium sporogenes*, and its relative expression in the peripheral blood of patients with invasive *C. albicans* infection is significantly lower than other contents ($P < 0.05$) (**Figure 1A**). Further analysis of the physical and chemical characteristics using the HMDB metabolic database showed that kynurenic acid (HMDB0000715) is a kind of phosphatidic acid molecule with a molecular formula of $C_{10}H_7NO_3$ and a molecular weight of 189.1675 Da (**Figure 1B**). Furthermore, the metabolic pathway of kynurenic acid was associated with the metabolism of tryptophan (**Figure 1C**).

Kynurenic Acid Ameliorates Intestinal Injury Caused by Invasive *Candida albicans* Infection

Mice infected with *C. albicans* experience higher mortality than mice treated with KynA [P = 0.01, HR 2.22 (95% CI: 1.06–4.64)], and no deaths occurred in the control group (**Figure 4B**). The colonization and proliferation of *C. albicans* in the intestinal tract of mice were measured quantitatively by culturing *C. albicans* in the feces of mice on days 4, 7, and 10 in both groups. On the first day after infection, there was no significant difference in the content of *C. albicans* between the groups. The *C. albicans* load in the CA+KynA group was significantly lower than that in the CA group on days 7 and 10 after infection ($P < 0.01$),

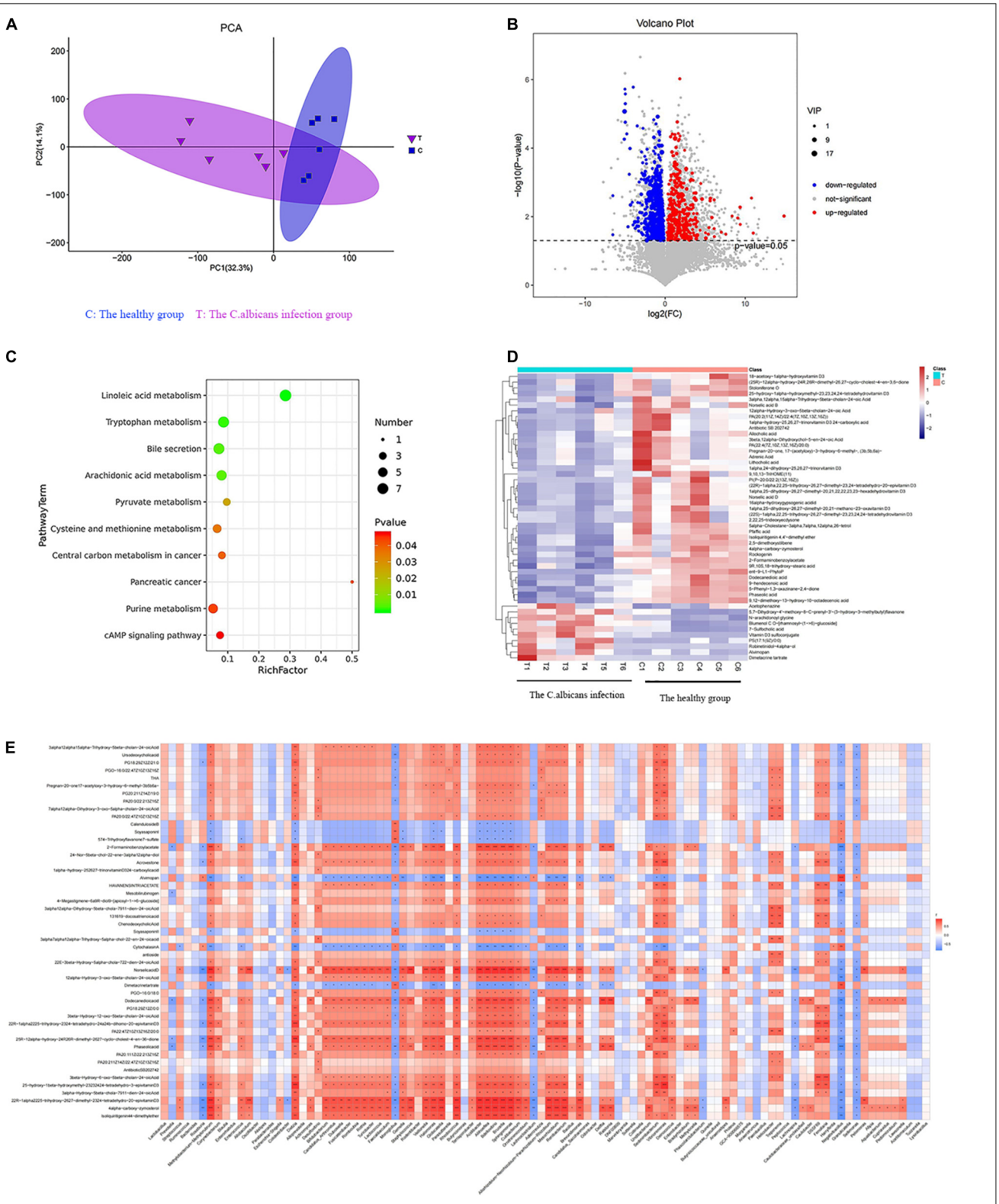

FIGURE 3 | Invasive *C. albicans* infection disrupts fecal metabolites in humans. **(A)** The PCA scatter plots of metabolomic analysis. **(B)** The volcano plot of differentially expressed metabolites. **(C)** The KEGG pathway enrichment analysis. **(D)** Heatmap of the top 50 differentially expressed metabolites. **(E)** Spearman correlation analysis. T, The *Candida albicans* infection group; C, The healthy control group.

TABLE 1 | Tryptophan metabolites from intestinal flora.

Metabolites	VIP	*P*-value	log2(FC)	T1	T2	T3	T4	T5	T6	C1	C2	C3	C4	C5	C6
Quinoline-4,8-diol	4.352005841	0.000456894	−0.98202032	2578.587561	3520.021674	3697.555233	1843.168192	3303.395711	3228.180323	5454.841879	5656.129382	6014.92193	5524.328808	6625.031145	6616.462545
Kynurenic acid	3.310455392	5.6894E-05	−3.598873938	880.2494609	1046.944327	1066.181466	186.0590311	994.0790165	1041.443168	1772.814592	2128.751426	2904.104664	2858.509106	2939.756655	3192.521016
Quinaldic acid	1.860736485	1.26426E-05	−1.318803137	315.9288544	432.2407231	408.3470075	173.5258084	413.5516563	430.9509149	745.9731837	808.7144176	875.3788752	871.9824855	1027.467941	1095.082788

T, Candida albicans infection group; C, Healthy control group (T vs. C).
Three differentially expressed metabolites were screened out: quinoline-4,8-diol, kynurenic acid, and quinaldic acid.

suggesting that KynA can reduce the colonization of *C. albicans* in the intestinal tract (**Figure 4C**). On the fifth day after infection, the liver, kidney, and spleen were collected for analysis to determine the distribution and toxicity of *C. albicans* by fungal culture. The *C. albicans* load in the kidneys, spleen, and liver was significantly lower in the CA+KynA group than in the CA group ($P < 0.05$) (**Figure 4D**). The levels of D-lactic acid, IL-1β, and TNF-α were significantly decreased in the CA+KynA group compared to those of the CA group ($P < 0.05$) (**Figures 4E–G**). Zonula occludens-1 (ZO-1) and occludin are important integral membrane proteins that contribute to the structural integrity of tight junctions during the development of the intestinal mucosal barrier (Li et al., 2015). Compared to the CA group, the expression of ZO-1 and occludin proteins in the intestinal epithelial cells of mice from the CA+KynA group was significantly increased, indicating that KynA protected the intestinal barrier (**Figure 4H**, $P < 0.01$). The Chiu pathologic scores of mucosal injuries were used to assess the extent of the intestinal histological injury. HE results showed an intact colonic mucosa structure in the control group, closely arranged large intestine glands with no signs of ulcers on the epithelial cells, and more goblet cells than in the CA group. In contrast, there were ulcers in the superficial layer of the colonic mucosa in mice from the CA group, and the entire tissue structure of the mucosal layer was destroyed with signs of inflammatory cell infiltration. The impaired structure of the colonic mucosa was improved in the CA+KynA group, no obvious ulcers were observed, and epithelial cells were not significantly damaged, but the number of goblet cells was reduced. Chiu's pathological scoring system revealed that mice from the CA+KynA group had less intestinal mucosal damage than the mice of the CA group (**Figure 4I**).

Kynurenic Acid Activates Aryl Hydrocarbon Receptor Expression in the Intestinal Epithelium

We studied the effect of kynA on the expression levels of AHR in the intestinal epithelium. Western blot analysis showed that protein levels of AHR increased significantly in the intestinal epithelium of mice in the CA+KynA group compared to the mice of the CA group ($P < 0.01$). These results were confirmed by immunohistochemistry analysis (**Figures 5A,B**).

KynA Suppressed the MLCK-pMLC Signaling Pathway by Activating Aryl Hydrocarbon Receptor

The increased expression of myosin light chain kinase (MLCK) is known to activate myosin light chain phosphorylation to induce contraction of the peri-junctional actomyosin ring, reducing intestinal permeability and improving the functions of the epithelial barrier (Xiong et al., 2016). To further investigate the effect of AHR activation on the MLCK-pMLC signaling pathway, we detected MLCK expression and MLC phosphorylation.

In Caco-2 cells, after treatment with KynA alone, the expression of the AHR downstream protein CYP1A1 increased significantly, as did the expression of the tight junction proteins ZO-1 and occludin. However, the expression of MLCK and

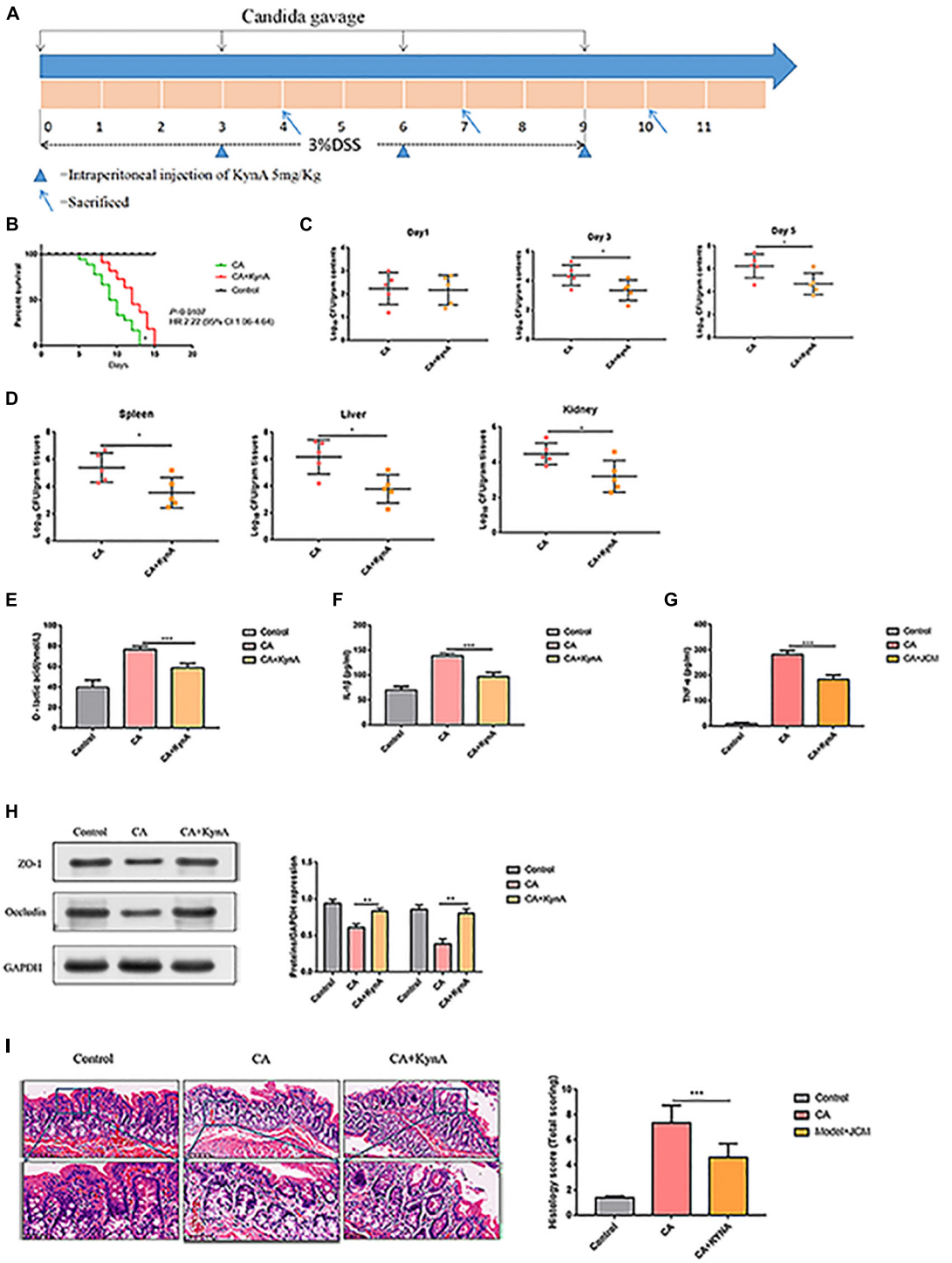

FIGURE 4 | Kynurenic acid alleviates intestinal injury caused by invasive *C. albicans* infection. **(A)** Experimental design including KynA administration and Candida gavage. **(B)** Mice infected with *C. albicans* exhibited higher mortality than mice treated with KynA. **(C)** KynA treatment decreased the colonization of intestinal *C. albicans*. Fungal load in feces collected from untreated and KynA groups at 1, 3, and 5 days after infection. **(D)** Fungal load in kidneys, spleen, and liver samples from euthanized mice collected immediately in the KynA-treated groups and 10 days post-infection in the untreated groups. **(E–G)** The levels of D-lactic acid, IL-1β, and TNF-α were significantly decreased in the CA+KynA group compared to those of the CA group ($P < 0.05$). **(H)** Expression of ZO-1 and occludin in the intestinal epithelial cells of the CA+KynA group was significantly higher than in the CA group. **(I)** Chiu's pathological scoring system revealed that mice from the CA+ KynA group had less intestinal mucosal damage than the mice in the CA group. Statistical significance was evaluated using the Mann–Whitney *U* test. *P*-values < 0.05 (*) or < 0.01 (**) were considered statistically significant. CA, *Candida albicans* infection; KynA, Kynurenic acid.

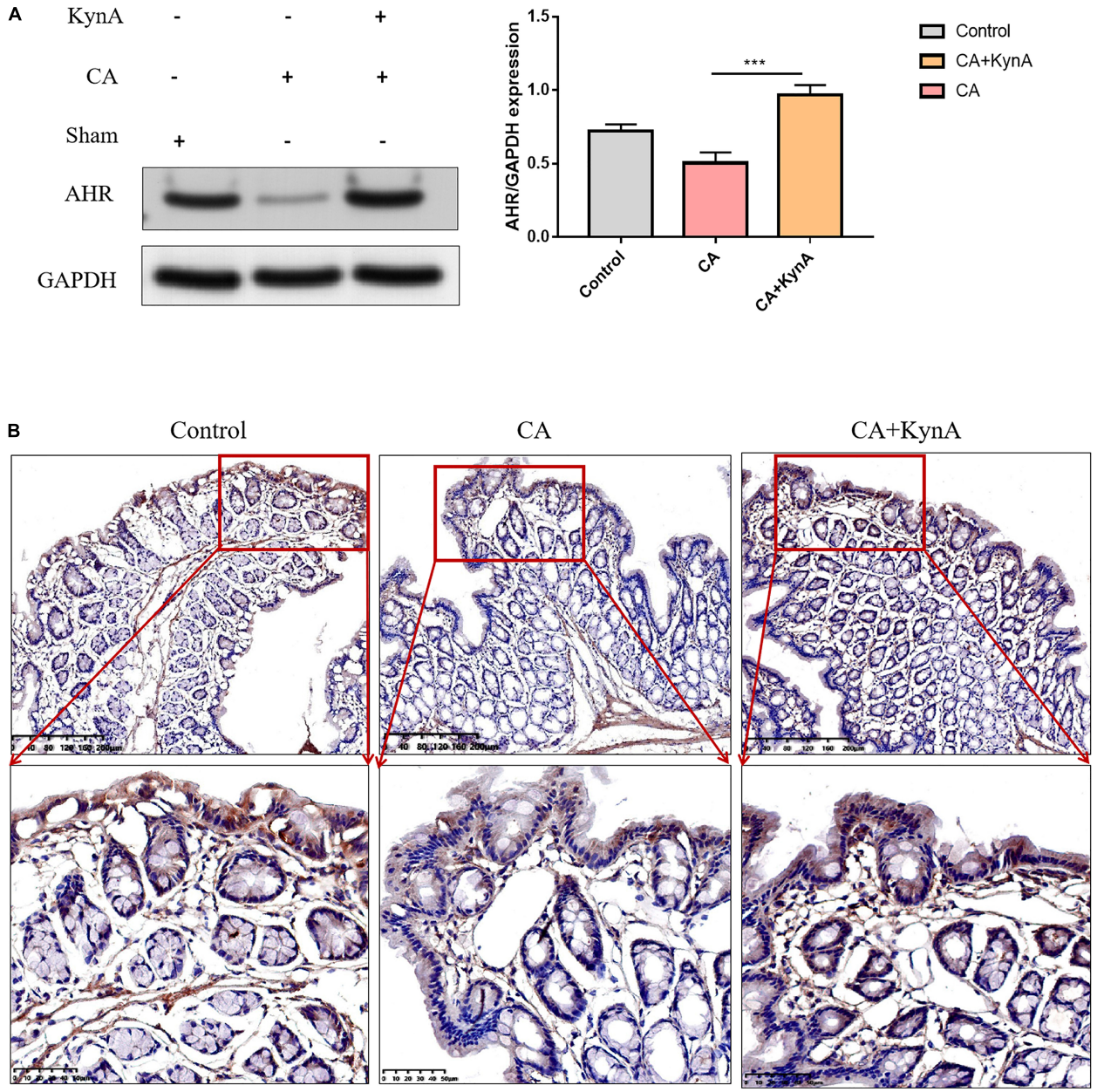

FIGURE 5 | Kynurenic acid activates AHR expression in the intestinal epithelium. **(A,B)** Western blot analysis and immunohistochemistry show higher expression of AHR in the CA+KynA group than in the CA group. Statistical significance was evaluated using the Mann–Whitney *U* test. *P*-values < 0.05 (*) or < 0.01 (**) were considered statistically significant. CA, *Candida albicans* infection; KynA, Kynurenic acid.

pMLC decreased significantly ($P < 0.01$). The expression levels of CYP1A1, ZO-1, and occludin proteins were significantly reduced in the CA-Caco-2 cell model, whereas the levels of MLCK and pMLC were significantly higher ($P < 0.01$). After treatment with KynA and the AHR agonist FICZ, the expression of CYP1A1 in Caco-2 cells increased significantly, as did the expression of the tight junction proteins ZO-1 and Occludin ($P < 0.01$), whereas the expression of MLCK and pMLC decreased significantly ($P < 0.01$). However, after treatment with an AHR inhibitor (CH223191), the expression of CYP1A1, ZO-1, and occludin proteins decreased significantly, whereas the expression of MLCK and pMLC increased ($P < 0.01$). These findings suggest that AHR activation might protect the intestinal epithelial barrier from disruption caused by *C. albicans* infection by suppressing the MLCK-pMLC signaling pathway. Therefore, we suggest that KynA can inhibit the MLCK-PMLC signaling pathway by activating the AHR receptor and promoting the expression of intestinal tight junction proteins,

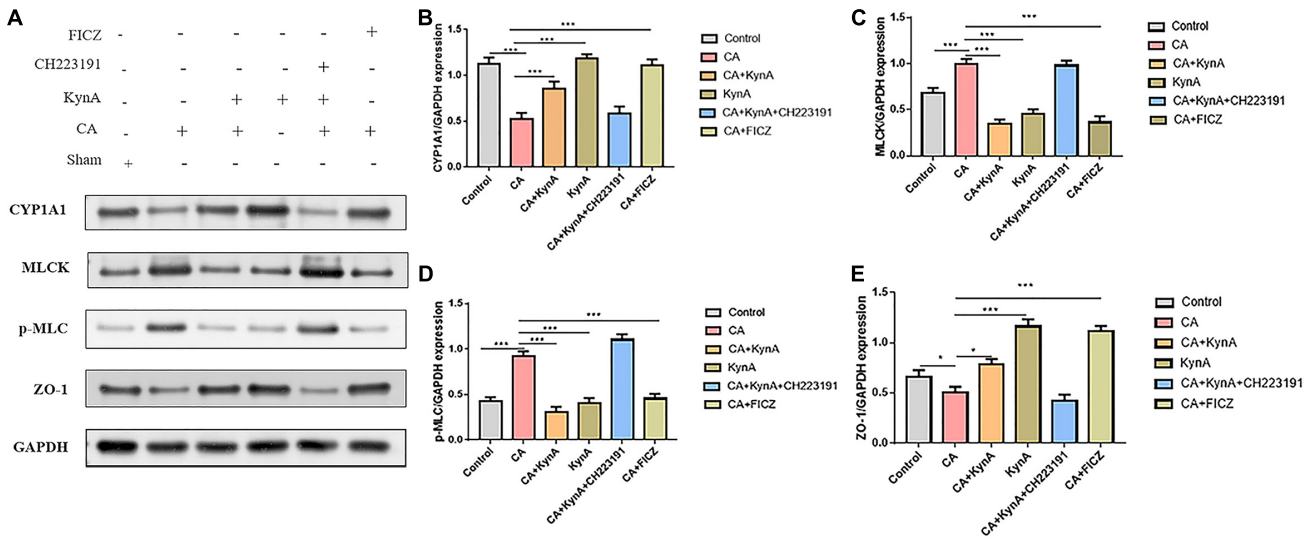

FIGURE 6 | KynA activates the suppression of MLCK-pMLC signaling pathway by AHR. The detection of MLCK expression and MLC phosphorylation was carried out to determine the effect of AHR activation on the MLCK-pMLC signaling pathway. In Caco-2 cells, after KynA treatment, the expression of the AHR downstream protein CYP1A1 increased significantly, as did the expression of the tight junction proteins ZO-1 and occludin. The expression of MLCK and pMLC decreased significantly. In the CA-Caco-2 cell model, expression levels of CYP1A1, ZO-1, and occludin were significantly decreased, but the expression levels of MLCK and pMLC increased. After treatment with KynA and the AHR agonist FICZ, expression of CYP1A1 increased significantly, as did the expression of ZO-1 and occludin, but the expression of MLCK and pMLC decreased. Treatment with an AHR inhibitor (CH223191), led to a decrease in the expression of CYP1A1, ZO-1, and occludin, and to an increase in the expression of MLCK and pMLC. Statistical significance was evaluated using the Mann–Whitney *U* test. *P*-values < 0.05 (*) or < 0.001 (***) were considered statistically significant. CA, Candida albicans infection; KynA, Kynurenic acid; FICZ, 6-Formylindolo[3,2-b]carbazole.

thereby helping to maintain the integrity of the intestinal barrier (**Figure 6**).

KynA Suppressed the MK2-P-MK2 Signaling Pathway by Activating Aryl Hydrocarbon Receptor

The P38/MK2 [mitogen-activated protein kinase (MAPK)-activated protein kinase-2, also known as MAKAP kinase-2] is a member of the mitogen-activated protein kinase (MAPK) family with a role in inflammation (Newton and Holden, 2006). The p38-MAPK/MK2 signaling pathway leads to tristetraprolin (TTP) phosphorylation, resulting in its proteasomal degradation (Huang et al., 2016). Several reports have shown that AHR activation can have an anti-inflammatory effect *in vitro* and *in vivo* during inflammatory processes and immune responses (Brandstatter et al., 2016). However, the effect of AHR activation on MK2 has not been reported (Riemschneider et al., 2021). Therefore, we investigated the regulation of TTP and changes in the expression of MK2 and p-MK2 following AHR activation at the cellular level.

In Caco-2 cells, KynA treatment led to significant increases in the expression levels of CYP1A1 and TTP ($P < 0.05$) but to a significant decrease in MK2 expression ($P < 0.05$). Following infection of Caco-2 cells with *C. albicans*, the expression levels of proteins CYP1A1 and TTP decreased significantly, but the expression levels of p-MK2 increased ($P < 0.01$). FICZ, a KynA and AHR agonist, significantly increased the expression levels of CYP1A1 and TTP in Caco-2 cells but decreased p-MK2 ($P < 0.01$). However, after treatment with the AHR inhibitor CH223191, the expression of CYP1A1, TTP, and p-MK2 was similar to that in the CA group ($P < 0.01$). No significant differences were found in the expression levels of MK2. These findings suggest that AHR regulates TTP expression *via* the MK2/p-MK2 pathway. Our study demonstrates that KynA increased the expression of TTP by activating the AHR receptor, which further suppressed the activation of the MK2/p-MK2 pathway (**Figure 7**).

DISCUSSION

Candida is one of the most common fungi of the GI tract; however, bacterial dysbiosis can cause *Candida* commensalism to become pathogenic, resulting in prolonged infections and *Candidiasis* (Strati et al., 2016). Sepsis can lead to the impairment of the intestinal barrier structure and function due to inflammation, ischemia, and hypoxia (Quan et al., 2020). Invasive *C. albicans* infection can further impair the intestinal barrier and lead to disseminated candidiasis, which disrupts the microflora of the gut (Geng et al., 2020). The extent of inflammation is correlated to the severity of gut microbiota dysbiosis (Lin et al., 2019).

In this study, we examined the alterations in intestinal flora in patients with candidemia compared to the intestinal flora of healthy individuals. At the genus level, the relative abundances of *Lachnoclostridium*, *Bacteroides*, and *Lactococcus* were significantly decreased in patients with candidemia

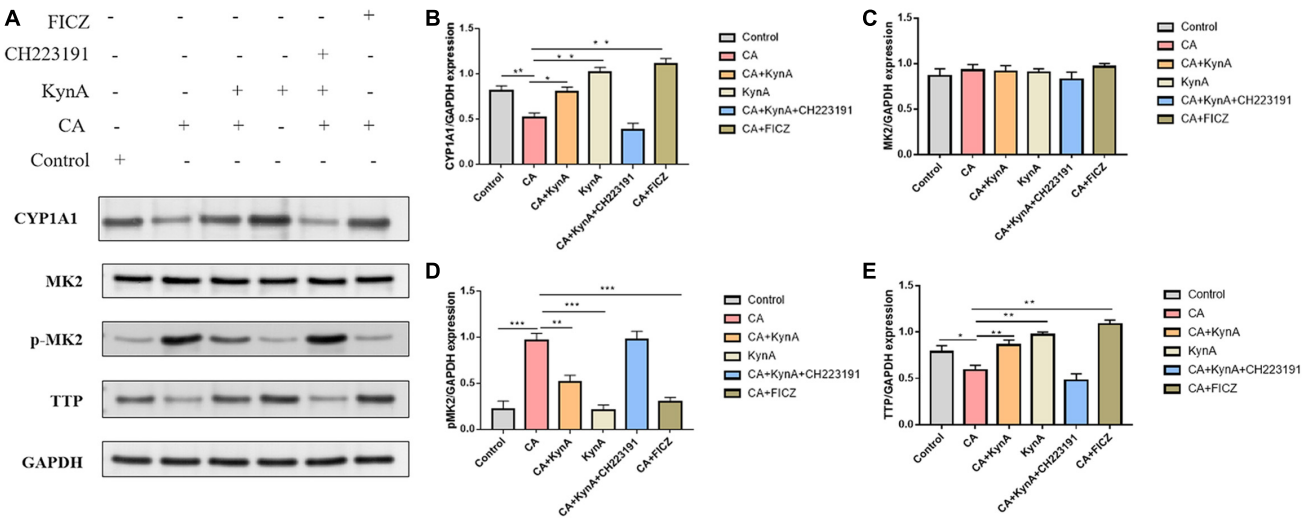

FIGURE 7 | KynA suppressed the MK2/p-MK2 signaling pathway by activating AHR. We investigated the regulation of TTP and expression changes of MK2 and P-MK2 induced by AHR activation at the cellular level. In Caco-2 cells, after treatment with KynA, expression of CYP1A1 increased significantly, as did expression of TTP also ($P < 0.05$), while expression of MK2 decreased significantly ($P < 0.05$). In the CA- Caco-2 cell model, the expression of proteins CYP1A1 and TTP decreased significantly, but the expression of p-MK2 increased ($P < 0.01$). After the treatment of Caco-2 cells with KynA and the AHR agonist FICZ, the expression of CYP1A1 and TTP was significantly increased, but the expression of p-MK2 decreased significantly ($P < 0.01$). Treatment with an AHR inhibitor (CH223191) led to a decrease in the expression of CYP1A1 and TTP, and an increase in the expression of p-MK2 ($P < 0.01$). Statistical significance was evaluated using the Mann–Whitney *U* test. *P*-values < 0.05 (*) or < 0.01 (**) were considered statistically significant. CA, *Candida albicans* infection; KynA, Kynurenic acid; FICZ, 6-Formylindolo[3,2-b]carbazole. *P*-values < 0.001 (***).

compared to healthy individuals. Metabolites involved in tryptophan metabolism, such as quinoline-4,8-diol, kynurenic acid, and quinaldic acid, were also significantly decreased in these patients. We investigated a possible relationship between altered gut microbiota composition and fecal co-metabolites by Spearman correlation analysis, and showed that gut microbiota dysbiosis is closely associated with intestinal metabolites. Metabolites derived from gut microbiota can regulate host immune function and are involved in the metabolic functions of the host. One example of such an organism is *L. reuteri*, which prevents gastrointestinal disturbances, such as diarrhea, by restoring microbial flora and regulating intestinal immune function (Wang et al., 2020). Recent studies in gut microbial metabolomics have demonstrated that an increased abundance of probiotics could increase the concentration of bacterial metabolites, such as propionate and butyrate, thus enhancing the activity of immune cells in the gut (Xu et al., 2020). The production of kynurenic acid is significantly lower in patients with invasive *C. albicans* infection. By using an established mouse model of disseminated candidiasis, we showed that KynA treatment could alleviate the intestinal inflammatory response and decrease the production of serum inflammatory mediators, thus preserving the intestinal barrier function. Therefore, our results suggest a protective role for the intestinal metabolism in intestinal barrier maintenance.

Aryl hydrocarbon receptor is a ligand-dependent transcriptional factor that is widely expressed in barrier tissues consisting of immune cells, epithelial cells, endothelial cells, and stromal cells (Zhou et al., 2019). A number of studies have shown that AHR and AHR agonists maintain gut health and protect against intestinal diseases (Jin et al., 2014). AHR activation in the intestinal tract is dependent on the concentration of tryptophan and its metabolites (Wei et al., 2018). Kynurenine is synthesized from tryptophan (Williams et al., 2014), which has been shown to activate AHR (Moffett et al., 2020). In this study, we found that KynA activated AHR receptors in the intestine both *in vitro* and *in vivo*. Recent research suggested that AHR activation might help preserve the intestinal epithelial barrier function and protect it from disruption caused by TNF-alpha/IFN-gamma, by suppressing the MLCK-pMLC signaling pathway (Yu et al., 2018).

We used Caco-2 cells co-cultured with *C. albicans* to verify the effect of AHR activation on cell damage caused by infection and the role of the MLCK-pMLC signaling pathway. Our findings showed that KynA inhibited the MLCK-pMLC signaling pathway by activating the AHR receptor, promoting the expression of intestinal tight junction proteins, and helping in maintaining the intestinal barrier intact. TTP is a p38-MAPK/MK2 kinase target that changes its RNA affinity when phosphorylated (Perlewitz et al., 2010). In the absence of AHR, disruption of the intestinal barrier was increased in the colitis model, whereas FICZ activated AHR to alleviate DSS-induced colitis *via* the MK2/p-MK2/TTP pathway (Wang Q. et al., 2018). KynA increased TTP expression by activating the AHR receptor, which subsequently suppressed the activation of the MK2/p-MK2 pathway.

In conclusion, this study demonstrated that the intestinal metabolite KynA can protect against intestinal injury induced by C. albicans by activating AHR involved in regulating the

MLCK-pMLC signaling pathway and MK2-p-MK2 signaling pathway, which would offer new potential strategies for the clinical treatment of invasive *C. albicans* infection.

DATA AVAILABILITY STATEMENT

The datasets presented in this study can be found in online repositories. The names of the repository/repositories and accession number(s) can be found below: https://www.ncbi.nlm.nih.gov/, PRJNA835672.

ETHICS STATEMENT

The studies involving human participants were reviewed and approved by the Shanghai Fifth People's Hospital, Shanghai, China. The patients/participants provided their written informed consent to participate in this study. The animal study was reviewed and approved by the East China Normal University's Animal Center.

AUTHOR CONTRIBUTIONS

All authors listed have made a substantial, direct, and intellectual contribution to the work, and approved it for publication.

FUNDING

This research was supported by the scientific research project of the Shanghai Science and Technology Commission "Science and Technology Innovation Action Plan" Natural Science Foundation Project (Grant No. 20ZR1443800).

REFERENCES

Arda-Pirincci, P., and Bolkent, S. (2014). The role of epidermal growth factor in prevention of oxidative injury and apoptosis induced by intestinal ischemia/reperfusion in rats. *Acta Histochem.* 116, 167–175. doi: 10.1016/j.acthis.2013.07.005

Brandstatter, O., Schanz, O., Vorac, J., Konig, J., Mori, T., Maruyama, T., et al. (2016). Balancing intestinal and systemic inflammation through cell type-specific expression of the aryl hydrocarbon receptor repressor. *Sci. Rep.* 6:26091. doi: 10.1038/srep26091

Chen, J., Chen, W., Zhao, N., Wu, M. C., and Schaid, D. J. (2016). Small sample kernel association tests for human genetic and microbiome association studies. *Genet. Epidemiol.* 40, 5–19.

Cheng, X., Wang, X., Wan, Y., Zhou, Q., Zhu, H., and Wang, Y. (2015). Myosin light chain kinase inhibitor ML7 improves vascular endothelial dysfunction via tight junction regulation in a rabbit model of atherosclerosis. *Mol. Med. Rep.* 12, 4109–4116. doi: 10.3892/mmr.2015.3973

Dinan, T. G., and Cryan, J. F. (2017). The microbiome-gut-brain axis in health and disease. *Gastroenterol. Clin. North Am.* 46, 77–89.

Gasaly, N., de Vos, P., and Hermoso, M. A. (2021). Impact of bacterial metabolites on gut barrier function and host immunity: a focus on bacterial metabolism and its relevance for intestinal inflammation. *Front. Immunol.* 12:658354. doi: 10.3389/fimmu.2021.658354

Geng, S. T., Zhang, Z. Y., Wang, Y. X., Lu, D., Yu, J., Zhang, J. B., et al. (2020). Regulation of gut microbiota on immune reconstitution in patients with acquired immunodeficiency syndrome. *Front. Microbiol.* 11:594820. doi: 10.3389/fmicb.2020.594820

Ghiboub, M., Verburgt, C. M., Sovran, B., Benninga, M. A., de Jonge, W. J., and Van Limbergen, J. E. (2020). Nutritional therapy to modulate tryptophan metabolism and Aryl hydrocarbon-receptor signaling activation in human diseases. *Nutrients* 12:2846. doi: 10.3390/nu12092846

He, Y., Xu, R., Wang, W., Zhang, J., and Hu, X. (2020). Probiotics, prebiotics, antibiotic, Chinese herbal medicine, and fecal microbiota transplantation in irritable bowel syndrome: protocol for a systematic review and network meta-analysis. *Medicine (Baltimore)* 99:e21502. doi: 10.1097/MD.0000000000021502

Hirao, L. A., Grishina, I., Bourry, O., Hu, W. K., Somrit, M., Sankaran-Walters, S., et al. (2014). Early mucosal sensing of SIV infection by paneth cells induces IL-1beta production and initiates gut epithelial disruption. *PLoS Pathog* 10:e1004311. doi: 10.1371/journal.ppat.1004311

Hu, W., Huang, L., Zhou, Z., Yin, L., and Tang, J. (2021). Diallyl Disulfide (DADS) ameliorates intestinal candida albicans infection by modulating the gut microbiota and metabolites and providing intestinal protection in mice. *Front. Cell Infect. Microbiol.* 11:743454. doi: 10.3389/fcimb.2021.743454

Huang, L., Yu, Z., Zhang, Z., Ma, W., Song, S., and Huang, G. (2016). Interaction with pyruvate kinase M2 destabilizes tristetraprolin by proteasome degradation and regulates cell proliferation in Breast Cancer. *Sci. Rep.* 6:22449. doi: 10.1038/srep22449

Jenull, S., Mair, T., Tscherner, M., Penninger, P., Zwolanek, F., Silao, F. S., et al. (2021). The histone chaperone HIR maintains chromatin states to control nitrogen assimilation and fungal virulence. *Cell Rep.* 36:109406. doi: 10.1016/j.celrep.2021.109406

Jin, U. H., Lee, S. O., Sridharan, G., Lee, K., Davidson, L. A., Jayaraman, A., et al. (2014). Microbiome-derived tryptophan metabolites and their aryl hydrocarbon receptor-dependent agonist and antagonist activities. *Mol. Pharmacol.* 85, 777–788. doi: 10.1124/mol.113.091165

Kuang, Z., Jin, T., Wu, C., Zong, Y., Yin, P., Dong, W., et al. (2021). Lentinan attenuates damage of the small intestinal mucosa, liver, and lung in mice with gut-origin sepsis. *J. Immunol. Res.* 2021:2052757. doi: 10.1155/2021/2052757

Li, H. Y., Lin, Y. J., Zhang, L., Zhao, J., Xiao, D. Y., and Li, P. W. (2021). Autophagy in intestinal injury caused by severe acute pancreatitis. *Chin. Med. J. (Engl)* 134, 2547–2549.

Li, M., Lu, C., Zhang, L., Zhang, J., Du, Y., Duan, S., et al. (2015). Oral administration of escin inhibits acute inflammation and reduces intestinal mucosal injury in animal models. *Evid. Based Complement Alternat. Med.* 2015:503617. doi: 10.1155/2015/503617

Li, X. J., Wang, M., Xue, Y., Duan, D., Li, C., Ye, J., et al. (2021). Characterization and comparison of the bacterial community between complete intensive and extensive feeding patterns in pigs. *AMB Express* 11:32. doi: 10.1186/s13568-021-01191-y

Lin, Y., Zheng, X., Chen, J., Luo, D., Xie, J., Su, Z., et al. (2019). Protective effect of *Bruguiera gymnorrhiza* (L.) lam. fruit on dextran sulfate sodium-induced ulcerative colitis in mice: role of Keap1/Nrf2 pathway and gut microbiota. *Front. Pharmacol.* 10:1602. doi: 10.3389/fphar.2019.01602

Liu, Z., Li, L., Chen, W., Wang, Q., Xiao, W., Ma, Y., et al. (2018). Aryl hydrocarbon receptor activation maintained the intestinal epithelial barrier function through Notch1 dependent signaling pathway. *Int. J. Mol. Med.* 41, 1560–1572. doi: 10.3892/ijmm.2017.3341

Meng, J., Yu, H., Ma, J., Wang, J., Banerjee, S., Charboneau, R., et al. (2013). Morphine induces bacterial translocation in mice by compromising intestinal barrier function in a TLR-dependent manner. *PLoS One* 8:e54040. doi: 10.1371/journal.pone.0054040

Moffett, J. R., Arun, P., Puthillathu, N., Vengilote, R., Ives, J. A., Badawy, A. A., et al. (2020). Quinolinate as a marker for kynurenine metabolite formation and the unresolved question of NAD(+) synthesis during inflammation and infection. *Front. Immunol.* 11:31. doi: 10.3389/fimmu.2020.00031

Newton, R., and Holden, N. S. (2006). New aspects of p38 mitogen activated protein kinase (MAPK) biology in lung inflammation. *Drug. Discov. Today Dis. Mech.* 3, 53–61. doi: 10.1016/j.ddmec.2006.02.007

Pappas, P. G., Kauffman, C. A., Andes, D., Benjamin, D. K. Jr., Calandra, T. F., et al. (2009). Clinical practice guidelines for the management of candidiasis:

2009 update by the infectious diseases society of America. *Clin. Infect. Dis.* 48, 503–535. doi: 10.1086/596757

Parent, A. S., Naveau, E., Gerard, A., Bourguignon, J. P., and Westbrook, G. L. (2011). Early developmental actions of endocrine disruptors on the hypothalamus, hippocampus, and cerebral cortex. *J. Toxicol. Environ. Health B. Crit. Rev.* 14, 328–345. doi: 10.1080/10937404.2011.578556

Patil, C. S., Liu, M., Zhao, W., Coatney, D. D., Li, F., VanTubergen, E. A., et al. (2008). Targeting mRNA stability arrests inflammatory bone loss. *Mol. Ther.* 16, 1657–1664. doi: 10.1038/mt.2008.163

Perlewitz, A., Nafz, B., Skalweit, A., Fahling, M., Persson, P. B., and Thiele, B. J. (2010). Aldosterone and vasopressin affect {alpha}- and {gamma}-ENaC mRNA translation. *Nucleic Acids Res.* 38, 5746–5760. doi: 10.1093/nar/gkq267

Quan, R., Chen, C., Yan, W., Zhang, Y., Zhao, X., and Fu, Y. (2020). BAFF blockade attenuates inflammatory responses and intestinal barrier dysfunction in a murine endotoxemia model. *Front. Immunol.* 11:570920. doi: 10.3389/fimmu.2020.570920

Riemschneider, S., Hoffmann, M., Slanina, U., Weber, K., Hauschildt, S., and Lehmann, J. (2021). Indol-3-Carbinol and quercetin ameliorate chronic DSS-Induced colitis in C57BL/6 mice by AhR-Mediated anti-inflammatory mechanisms. *Int. J. Environ. Res. Public Health* 18:2262. doi: 10.3390/ijerph18052262

Serlin, Y., Shelef, I., Knyazer, B., and Friedman, A. (2015). Anatomy and physiology of the blood-brain barrier. *Semin. Cell Dev. Biol.* 38, 2–6.

Song, W., Chen, Q., Wang, Y., Han, Y., Zhang, H., and Li, B. (2019). Identification and structure-activity relationship of intestinal epithelial barrier function protective collagen peptides from alaska pollock skin. *Mar. Drugs* 17:450. doi: 10.3390/md17080450

Strati, F., Cavalieri, D., Albanese, D., De Felice, C., Donati, C., Hayek, J., et al. (2016). Altered gut microbiota in Rett syndrome. *Microbiome* 4:41.

Sun, J., Wang, L. C., Fridlender, Z. G., Kapoor, V., Cheng, G., Ching, L. M., et al. (2011). Activation of mitogen-activated protein kinases by 5,6-dimethylxanthenone-4-acetic acid (DMXAA) plays an important role in macrophage stimulation. *Biochem. Pharmacol.* 82, 1175–1185. doi: 10.1016/j.bcp.2011.07.086

Tian, J., Bai, B., Gao, Z., Yang, Y., Wu, H., Wang, X., et al. (2021). Alleviation effects of GQD, a traditional chinese medicine formula, on diabetes rats linked to modulation of the gut microbiome. *Front. Cell Infect. Microbiol.* 11:740236. doi: 10.3389/fcimb.2021.740236

Wang, H., Zhou, C., Huang, J., Kuai, X., and Shao, X. (2020). The potential therapeutic role of *Lactobacillus reuteri* for treatment of inflammatory bowel disease. *Am. J. Transl. Res.* 12, 1569–1583.

Wang, Q., Yang, K., Han, B., Sheng, B., Yin, J., Pu, A., et al. (2018). Aryl hydrocarbon receptor inhibits inflammation in DSSinduced colitis via the MK2/pMK2/TTP pathway. *Int. J. Mol. Med.* 41, 868–876. doi: 10.3892/ijmm.2017.3262

Wang, W., Li, X., Yao, X., Cheng, X., and Zhu, Y. (2018). The characteristics analysis of intestinal microecology on cerebral infarction patients and its correlation with apolipoprotein E. *Medicine (Baltimore)* 97:e12805. doi: 10.1097/MD.0000000000012805

Wei, Y. L., Chen, Y. Q., Gong, H., Li, N., Wu, K. Q., Hu, W., et al. (2018). Fecal microbiota transplantation ameliorates experimentally induced colitis in mice by upregulating AhR. *Front. Microbiol.* 9:1921. doi: 10.3389/fmicb.2018.01921

Williams, C. M., Watanabe, M., Guarracino, M. R., Ferraro, M. B., Edison, A. S., Morgan, T. J., et al. (2014). Cold adaptation shapes the robustness of metabolic networks in *Drosophila melanogaster*. *Evolution* 68, 3505–3523. doi: 10.1111/evo.12541

Xiong, Y., Wang, J., Chu, H., Chen, D., and Guo, H. (2016). Salvianolic acid B restored impaired barrier function via downregulation of MLCK by microRNA-1 in rat colitis model. *Front. Pharmacol.* 7:134. doi: 10.3389/fphar.2016.00134

Xu, X., Lv, J., Guo, F., Li, J., Jia, Y., Jiang, D., et al. (2020). Gut microbiome influences the efficacy of PD-1 antibody immunotherapy on MSS-Type colorectal cancer via metabolic pathway. *Front. Microbiol.* 11:814. doi: 10.3389/fmicb.2020.00814

Yu, M., Wang, Q., Ma, Y., Li, L., Yu, K., Zhang, Z., et al. (2018). Aryl hydrocarbon receptor activation modulates intestinal epithelial barrier function by maintaining tight junction integrity. *Int. J. Biol. Sci.* 14, 69–77.

Zhou, Y. H., Sun, L., Chen, J., Sun, W. W., Ma, L., Han, Y., et al. (2019). Tryptophan metabolism activates Aryl hydrocarbon receptor-mediated pathway to promote HIV-1 infection and reactivation. *mBio* 10:e02591-19. doi: 10.1128/mBio.02591-19

Conflict of Interest: The authors declare that the research was conducted in the absence of any commercial or financial relationships that could be construed as a potential conflict of interest.

Publisher's Note: All claims expressed in this article are solely those of the authors and do not necessarily represent those of their affiliated organizations, or those of the publisher, the editors and the reviewers. Any product that may be evaluated in this article, or claim that may be made by its manufacturer, is not guaranteed or endorsed by the publisher.

frontiers | Frontiers in Microbiology

TYPE Original Research
PUBLISHED 05 August 2022
DOI 10.3389/fmicb.2022.981181

OPEN ACCESS

EDITED BY
Wenjie Fang,
Shanghai Changzheng Hospital,
China

REVIEWED BY
Mohsan Ullah Goraya,
University of Agriculture, Faisalabad,
Pakistan
Sadeeq Ur Rahman,
University College Cork,
Ireland

*CORRESPONDENCE
Yuebin Zeng
zeng_yb@163.com

†These authors share first authorship

SPECIALTY SECTION
This article was submitted to Antimicrobials, Resistance and Chemotherapy, a section of the journal Frontiers in Microbiology

RECEIVED 29 June 2022
ACCEPTED 25 July 2022
PUBLISHED 05 August 2022

CITATION
Bilal H, Hou B, Shafiq M, Chen X, Shahid MA and Zeng Y (2022) Antifungal susceptibility pattern of *Candida* isolated from cutaneous candidiasis patients in eastern Guangdong region: A retrospective study of the past 10 years. *Front. Microbiol.* 13:981181. doi: 10.3389/fmicb.2022.981181

Antifungal susceptibility pattern of *Candida* isolated from cutaneous candidiasis patients in eastern Guangdong region: A retrospective study of the past 10 years

Hazrat Bilal[1†], Bing Hou[2†], Muhammad Shafiq[3], Xinyu Chen[1], Muhammad Akbar Shahid[4] and Yuebin Zeng[1*]

[1]Department of Dermatology, The Second Affiliated Hospital of Shantou University Medical College, Shantou, China, [2]Skin and Venereal Diseases Prevention and Control Hospital of Shantou City, Shantou, Guangdong, China, [3]Department of Cell Biology and Genetics, Shantou University Medical College, Shantou, China, [4]Department of Pathobiology, Faculty of Veterinary Sciences, Bahauddin Zakariya University, Multan, Pakistan

Cutaneous candidiasis is one of the most prevalent mycotic infections caused by *Candida* species. The severity of infection mounts faster when the species shows antifungal resistance. In the current retrospective study, we aimed to analyze the occurrence, causes of cutaneous candidiasis, and antifungal susceptibility pattern of *Candida* isolates from Skin and Venereal Diseases Prevention and Control Hospital of Shantou, located in eastern Guangdong, China. The laboratory data of all patients (n=3,113) suffering from various skin and venereal infections during January 2012 to December 2021 was analyzed through Excel and GraphPad prism. Our analysis indicate that cutaneous candidiasis was 22.29% (n=694), of which 78.53% (n=554) of patients were males and 21.47% (n=149) of patients were females. The median age of patients with cutaneous candidiasis was 38-year [interquartile range (30–48)]. Most cases occurred in the adult age group (19–50 years). Regarding the species type, the *Candida albicans* were prominently detected (n=664, 95.68%), while non-*C. albicans* were found only in 30 (4.32%) patients, which were *C. glabrata* (n=18), *C. krusei* (n=8), *C. tropicalis* (n=3), and *C. parapsilosis* (n=1). The *C. albicans* susceptibility rate for terbinafine, miconazole, voriconazole, itraconazole, fluconazole, ketoconazole, nystatin, 5-flucytosine and amphotericin B were 10.83, 29.32, 59.39, 78.53, 85.28, 87.75, 99.59, 99.41, and 100%, respectively. Finally, all *C. glabrata* isolates were found susceptible to all tested azole drugs with exception to miconazole against which 8.33% of isolates showed resistance. The findings of this study will help healthcare officials to establish better antifungal stewardship in the region.

KEYWORDS

cutaneous candidiasis, antifungal resistance, *C. albicans*, retrospective study, China

Introduction

Cutaneous candidiasis is a superficial infection of skin and mucus membranes caused by yeast from genus *Candida* (Nurdin et al., 2021). *Candida albicans* is the most common specie responsible for candidiasis in humans; however other species like *C. glabrata*, *C. tropicalis*, *C. krusei*, *C. parapsilosis*, and many others are also causing skin infections (Bhattacharya et al., 2020). The *C. albicans* is an opportunistic yeast that mainly causes infections in immunocompromised patients or those with nutritional deficiencies and endocrine disorders. Besides these, local factors like xerostomia, ulcerations, radiation-induced mucositis, trauma-induced skin damage, and skin maceration increase the morbidity rate (Sadeghi et al., 2019). Types of cutaneous candidiasis are candidal vulvovaginitis, candidal balanitis, congenital candidiasis, candidal diaper dermatitis, oral candidiasis, intertrigo, decubital candidiasis, paronychia, perianal dermatitis, and erosio interdigitalis blastomycetica. Pustules, papules, ulcerations, and vesicles are typical signs of cutaneous candidiasis (Edwards, 2015). A study reported that 7% of all inpatients and 1% of all outpatients' visits to dermatological hospitals had cutaneous candidiasis (Taudorf et al., 2019). The mortality rate of cutaneous infections is relatively low; nevertheless, if the infections remain enigmatic or untreated for a long time, they might cause systematic and invasive candidiasis, with an approximately 25–50% mortality rate (Tortorano et al., 2021).

The global therapeutic guidelines for rare yeast infections are available, but cutaneous candidiasis remains unaddressed (Chen et al., 2021). Physicians prescribe various topical and oral antifungal agents combined with antibacterial, anti-inflammatory, and corticosteroid drugs for its treatment. Common topical antifungal drugs for cutaneous candidiasis are clotrimazole, nystatin, and miconazole. The terbinafine, ketoconazole, and fluconazole are also studied as systematic therapeutic agents for cutaneous candidiasis (Taudorf et al., 2019). Due to the lack of national guidelines for treating cutaneous candidiasis, the misuse of available antifungal drugs occurs, which endorses antifungal drug resistance (Markogiannakis et al., 2021). Antimicrobial resistance is a worldwide health concern; prolonged hospital stays, increased patient cost burden, and mortality rates (Ur Rahman et al., 2018).

Locally and country-wise antifungal drug resistance surveillance studies need to be performed to depict the current scenario. These surveillance studies will help physicians and healthcare officials to properly manage and treat infections (Badali and Wiederhold, 2019). Therefore, the purpose of the current study was to retrospectively analyze the prevalence of cutaneous candidiasis reported over the past 10 years in the Skin and Venereal Diseases Prevention and Control Hospital of Shantou in eastern Guangdong, China. Furthermore, the current study sorted out candidiasis in different age groups and gender, data about various *Candida* species, and their antifungal drug susceptibility profiles.

Materials and methods

Study design

The current retrospective study was conducted at Skin and Venereal Diseases Prevention and Control Hospital of Shantou city, Guangdong, China. Data about cutaneous candidiasis were obtained from laboratory records of the hospital for the past 10 years (January 2012 to December 2021).

Study variables

The data of all patients with cutaneous infections were obtained for which direct microscopy, candida growth culture, and antifungal susceptibility tests had performed. The patient's age, gender, date of sample collection, sample type, *Candida* species type, and the antifungal susceptibility profile for each species were obtained from laboratory records and saved in an Excel sheet for further analysis.

Routine laboratory protocols

In routine, every patient with cutaneous fungal infections was first recommended for direct microscopy with potassium hydroxide to visualize fungal pathogens. The positive samples with the *Candida*-like growth were cultured on CHROMagar-*Candida* medium to examine and identify *Candida* following the standard protocol (Saud et al., 2020). Furthermore, the antifungal susceptibility tests for positive *Candida* cultures were performed using CLSI-recommended broth microdilution methods or ATB fungus-2 kit. From 2012 to 2018, antifungal susceptibility tests were performed for fluconazole, miconazole, terbinafine, ketoconazole, itraconazole, and nystatin according to CLSI broth microdilution method (Espinel-Ingroff, 2022). Onward 2019, the tests were performed by ATB fungus-2 kit, and the tested antifungal agents were 5-flucytosine, voriconazole, fluconazole, amphotericin B, and itraconazole. The susceptibility, intermediated, and resistant results were interpreted according to the CLSI M60 or epidemiological cutoff values guidelines (CLSI, 2017; Procop, 2020).

Data analysis

The patients' data were classified into four groups depending on age: infants; less than 1 year of age, pediatrics; aged from 1 to 18 years, adults; aged from 18 to 65 years, and older adults; ages greater than 65. The adult age group was further divided into four groups: group I; 18–30 years of age, group II; 31–40 years of age, group III; 41–50 years of age, group IV; 50–65 years of age. The number and percentage of *Candida* species in each age group, patient gender type, and year of the report were noted. The

antifungal susceptibility patterns for each *Candida* species were amalgamated over the past decade. The percentage of susceptible, intermediate, and resistant *Candida* species against the examined antifungal drugs was determined.

Moreover, the year-wise antifungal susceptibility pattern of *C. albicans* was determined. The trend of year-wise susceptibility patterns of fluconazole and itraconazole were resolved. The data numeration and percentages were calculated by Microsoft Excel 2016, while the statistical analysis and graphs constructions were performed by GraphPad prism v.8.0 software. The total number of *C. albicans* cases occurred each year, and the number of cases in different age groups of patients were compared using student's *t*-tests. Furthermore, gender base significance was calculated by ratio paired *t*-test. Statistical significance was calculated by two-tailed tests, and $p < 0.05$ was considered statistically significant.

Results

Incidence of *Candida* species in past 10 years

In the past 10 years, 3,113 patients with cutaneous mycosis were examined by direct microscopy and fungal routine culture, in which 694 (22.29%) were diagnosed with cutaneous candidiasis. Among the candidiasis patients, 545 (78.53%) were male, and 149 (21.47%) were female. Regarding the *Candida* species type, the *C. albicans* were prominently detected in 664/694 (95.68%) patients, while non-*C. albicans* were found only in 30/694 (4.32%) patients. The high number of *C. albicans* were reported in year 2013 ($n = 121$, 18.22%), followed by 2012 ($n = 111$, 16.71%) and 2018 ($n = 103$, 15.51%). Among the 30 non-*C. albicans* species *C. glabrata* were reported in 18/694 (2.59%) patients, *C. krusei* in 8/694 (1.15%), *C. tropicalis* in 3/694 (0.43%), and *C. parapsilosis* was detected only in one patient ($n = 1/694$, 0.14%). The year-wise incidence of *C. albicans* and non-*C. albicans* species are presented in Figure 1.

Occurrence of *Candida albicans* in different age and gender groups

The median age of patients was 38-year, range (from 8 months to 82 years), interquartile range (30–48 years). Most cases occurred in the adult age group (19–50 years). For *C. albicans* only three (0.45%) cases were reported in infants, and seven (1.05%) were from the pediatric group; three were male, and four were female pediatric patients. From the older adult group, 18 (2.71%) *C. albicans* were isolated, of which 17 were from male patients, and only one was from a female patient. From the adult age group (19–65 years), a total of 636 (95.78%) cases were reported, of which 500/636 (78.61%) were from males, and 136/636 (21.38%) were from female patients. In the current study, we found that the *C. albicans* causing cutaneous candidiasis occurred in a high proportion in males ($n = 522$ out of 664, 78.61%) compared to females ($n = 142$ out of 664, 21.39%; p-value = 0.0001). Among the age groups, the adult age group II for males and adult age group I for females were more vulnerable to *C. albicans*. The year-wise occurrence of *C. albicans* in different age groups and gender and their statistical significance (p-values) are summarized in Table 1.

Occurrence of non-*Candida albicans* in different age and gender groups

The number of non-*C. albicans* ($n = 30$ out of 694, 4.32%) were relatively much smaller than *C. albicans* detected in the present study. Four different types of non-*C. albicans* species were detected, which were *C. glabrata* ($n = 18$ out 30, 60%), *C. krusei* ($n = 8$ out 30, 26.67%), *C. tropicalis* ($n = 3$ out of 30, 10%) and *C. parapsilosis* ($n = 1$ out of 30, 3.33%). The number of non-*C. albicans* isolates from male patients (n = 22 out of 30, 73.33%) were high compared to females (n = 8 out of 30, 26.67%). The number of different non-*C. albicans* species concerning different age and gender groups are presented in Table 2.

Antifungal susceptibility patterns of *Candida albicans*

For *C. albicans* the lowest antifungal susceptibility was reported for terbinafine, with only 10% of the isolates susceptible out of 157 tested strains. Among the azole class, miconazole showed the lowest susceptibility with 29.32% out of 440 tested isolates, while 40.23% of isolates were intermediate and 30.45% resistant. Besides, itraconazole and fluconazole, two of the most extensively used antifungal drugs, have resistance rates of 16.10 and 9.34%, respectively. Among the other tested antifungal drugs, only two isolates in 2012 were intermediate-resistant to nystatin, while only one isolate in 2021 was found resistant to 5-flucytosine, and none of the isolates exhibited resistance to amphotericin B. The antifungal susceptibility profile of all tested antifungal agents against the *C. albicans* is summarized in Table 3.

The terbinafine was tested in 2012 and 2013 and showed the highest resistance, 84.47, and 90.47%, respectively. In 2014, the highest resistance was reported against miconazole, which was 57.14% out of 21 tested isolates. From 2015 to 2018, the resistance rate was comparatively lower except for the miconazole, which was 18.18% in 2015, 9.23% in 2016, 10.52% in 2017, and 12.74% in 2018. Onward 2019, antifungal susceptibility tests were performed by ATB fungus-2 kit, in which the highest resistance was observed for itraconazole, fluconazole, and voriconazole. In 2019 resistance to itraconazole, voriconazole, and fluconazole were 53.16, 53.42, and 36.98%, in 2020 it was 40.81, 38.77, and 32.65%, while in 2021 it was 27.90, 13.95, and 13.95%, respectively.

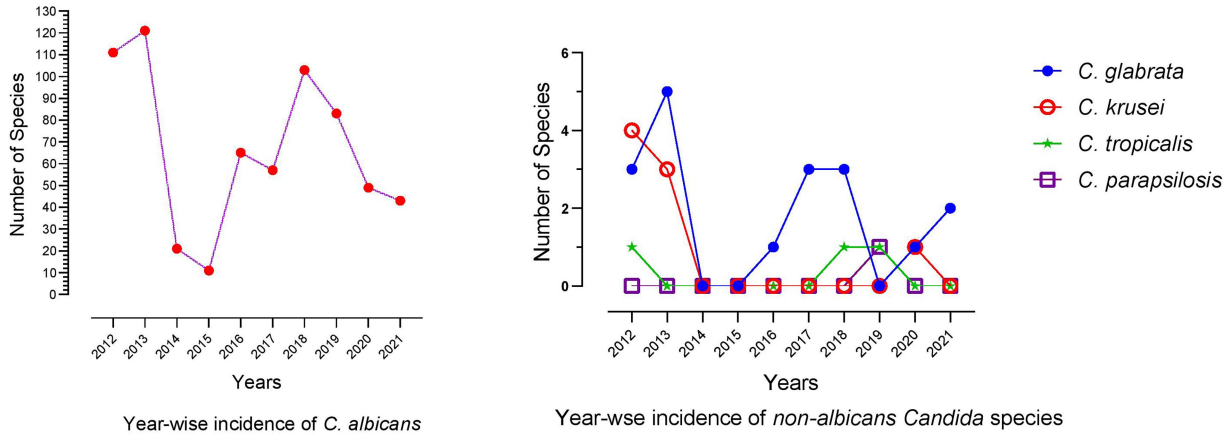

FIGURE 1
Candida species from cutaneous candidiasis reported in the past 10 years (2012–2021).

TABLE 1 Occurrence of *Candida albicans* in different age groups and gender.

Year	Cases	M:F	Age groups							*p*-value[#]
			<1	1–18	19–39	31–40	41–50	51–65	>65	
2012	111	104:07	1	1	39	33	28	8	1	<0.05
2013	121	115:06	0	0	34	41	25	18	3	<0.05
2014	21	17:04	0	0	6	9	4	2	0	0.0645
2015	11	9:02	0	0	0	4	4	3	0	0.0815
2016	65	47:18	0	0	14	24	13	11	3	<0.05
2017	57	46:11	0	0	10	15	18	12	2	<0.05
2018	103	59:44	0	3	27	29	29	15	0	<0.05
2019	83	56:27	1	2	21	22	23	10	4	<0.05
2020	49	37:12	1	0	7	13	17	9	2	<0.05
2021	43	32:11	0	1	9	11	14	5	3	<0.05
SUM	664	261:71	3	7	167	201	175	93	18	<0.05
p-value	<0.05[#]	0.0001*								

M:F = Male ratio female.
*Ratio paired *t*-test.
[#]Student's *t*-test.

Year-wise antifungal susceptibility profiles of *C. albicans* against all tested drugs are presented in Figure 2.

Trend of fluconazole and itraconazole susceptibility in *Candida albicans* over time

From a broader perspective, the last 10 years' fluconazole and itraconazole resistance patterns showed little similarity. However, the combined susceptibility rate of fluconazole was 85.28%, while itraconazole was 78.53%. The lowest resistance rates were noted in 2018 and reached the highest for both drugs in the next 2 years (2019 and 2020). The similarity in pattern between these two drugs indicates that the exact molecular mechanism might be involved in developing resistance against azole drugs. The trend of fluconazole and itraconazole susceptibility patterns over time is shown in Figure 3.

Antifungal susceptibility pattern of non-*Candida albicans* species

The *C. parapsilosis* showed resistance to fluconazole, itraconazole, and voriconazole and was susceptible to amphotericin B and 5-flucytosine. Among the three *C. tropicalis* isolates, resistance to terbinafine and miconazole were observed in only one isolate. For *C. krusei,* 80% of isolates were resistant to

TABLE 2 Occurrence of non-*Candida albicans* species in different age groups and gender.

Species	*C. glabrata*	*C. krusei*	*C. tropicalis*	*C. parapsilosis*	SUM
Total cases	18	8	3	1	30
Male:female	2:1	7:1	2:1	1:0	11:4
Age < 1	0	1	0	0	1
Age 19–30	5	3	0	0	8
Age 31–40	1	2	1	0	4
Age 41–50	6	0	0	1	7
Age 51–65	4	2	2	0	8
Age > 65	2	0	0	0	2

TABLE 3 Antifungal susceptibility profile of *C. albicans* for all tested drugs in the past 10 years.

Antifungal agents	Tested isolates	Susceptible (%)	Intermediate (%)	Resistant (%)
5-Flucytosine	170	99.41	0	0.59
Amphotericin B	172	100	0	0
Fluconazole	632	85.28	5.38	9.34
Itraconazole	652	78.53	5.37	16.10
Ketoconazole	490	87.75	9.80	2.45
Miconazole	440	29.32	40.23	30.45
Nystatin	490	99.59	0.41	0
Terbinafine	157	10.83	3.82	85.35
Voriconazole	165	59.39	1.82	38.79

terbinafine out of five tested strains, while all other isolates were susceptible to amphotericin B and 5-flucytosine. For *C. glabrata,* one isolate detected in 2021 was resistant to 5-flucytosine; however, it was susceptible to amphotericin B and all tested azole drugs. Similarly, another isolate of *C. glabrata* reported in 2013 showed resistance to nystatin, the only nystatin-resistant isolate in the current study. The antifungal susceptibility profile of *C. glabrata* is summarized in Table 4.

Discussion

The prevalence of cutaneous candidiasis varies regarding the geography, demography of patients, type of the fungal pathogen, and many other environmental factors (Kühbacher et al., 2017). In the current study, the prevalence rate of cutaneous candidiasis over the past decade was 22.29% which makes it different from other regions of the world, where it is reported to be 40.5% in Iran, 57% in Serbia, and 82.9% in Brazil (de Albuquerque Maranhão et al., 2019; Otašević et al., 2019; Khodadadi et al., 2021). The difference in the prevalence might be due to different environmental conditions and the social status of the populations (Zareshahrabadi et al., 2021). In the present study, the infection rate was highly reported in the male population (78.53%) compared to females (21.47%). In different countries, gender-based prevalence varies; a previous study from China, Italy, and France reported an equal proportion of males and females infected with cutaneous mycosis (Vena et al., 2012; Cai et al., 2016; Faure-Cognet et al., 2016). Studies from South Korea and Chile reported a high proportion of *Candida*-infected females (Cruz Ch et al., 2011; Yoon et al., 2014). However, a study from Iran showed resemblance to our finding, with high cases of cutaneous candidiasis among males (Zamani et al., 2016). These contradictions depend on differences in occupational activities, personal hygiene, and exposure to contamination of male and female populations (de Albuquerque Maranhão et al., 2019). In our study, cutaneous candidiasis mainly occurred in the adult age group (from 19 to 50 years). Some other studies reported that patients below 20 are more vulnerable to candidiasis; however, the studies from Iran, South Korea, and India agreed with our findings (Nawal et al., 2012; Yoon et al., 2014; Cai et al., 2016; Khodadadi et al., 2021). The main reason for the adult age group's link with cutaneous candidiasis might be that these populations have more involvement in job markets and social activities with a high chance of exposure to *Candida* infections (Khodadadi et al., 2021).

More than 200 *Candida* species have been identified, of which over 15 are known for human pathogenicity, among which the *C. albicans* are highly reported (Palese et al., 2018). Similarly, in our study, 95.68% of cutaneous candidiasis was caused by *C. albicans*. The high infection rate of *C. albicans* is due to its ability to grow in different morphological forms like true hyphae, pseudo-hyphae, and unicellular budding yeast, which enhance its virulence and invading host cell activity (Nam et al., 2022). Moreover, underlying diseases, immunosuppressive states, antibiotic therapy, and skin environment variation are the factors due to which the commensal *C. albicans* switched into a true pathogen (Palese et al., 2018). In the present study, the *C. glabrata* was detected in 18 cases, the highest among non-*C. albicans* species. This differs from the studies reported in Cameroon, Nigeria, and India, where *C. tropicalis* are more prevalent than *C. glabrata* (Verma et al., 2021). However, a similar drift was observed in North America and many European countries (Song et al., 2020). After *C. glabrata*, the *C. krusei* was reported as the second high in number among the non-*C. albicans* species. It is a matter of concern because *C. krusei* is one of the multidrug-resistant species and is intrinsically resistant to fluconazole (Jamiu et al., 2021).

In the current study, the *C. albicans* show high resistance to terbinafine, i.e. 85.35% of 157 tested isolates. Similarly, for *C. glabrata* and *C. krusei*, 80% of the isolates were resistant to terbinafine. This high resistance might be due to the weak inhibitory activity of terbinafine against all *Candida* species except *C. parapsilosis* (Ameen et al., 2014; Noguchi et al., 2019). In the azole class, the high resistance (30.45%) was reported for miconazole, while 40.23% of 440 tested *C. albicans* isolates were intermediated resistant. The high resistance to miconazole is due to its improper usage as a topical therapeutic agent for cutaneous candidiasis (Taudorf et al., 2019).

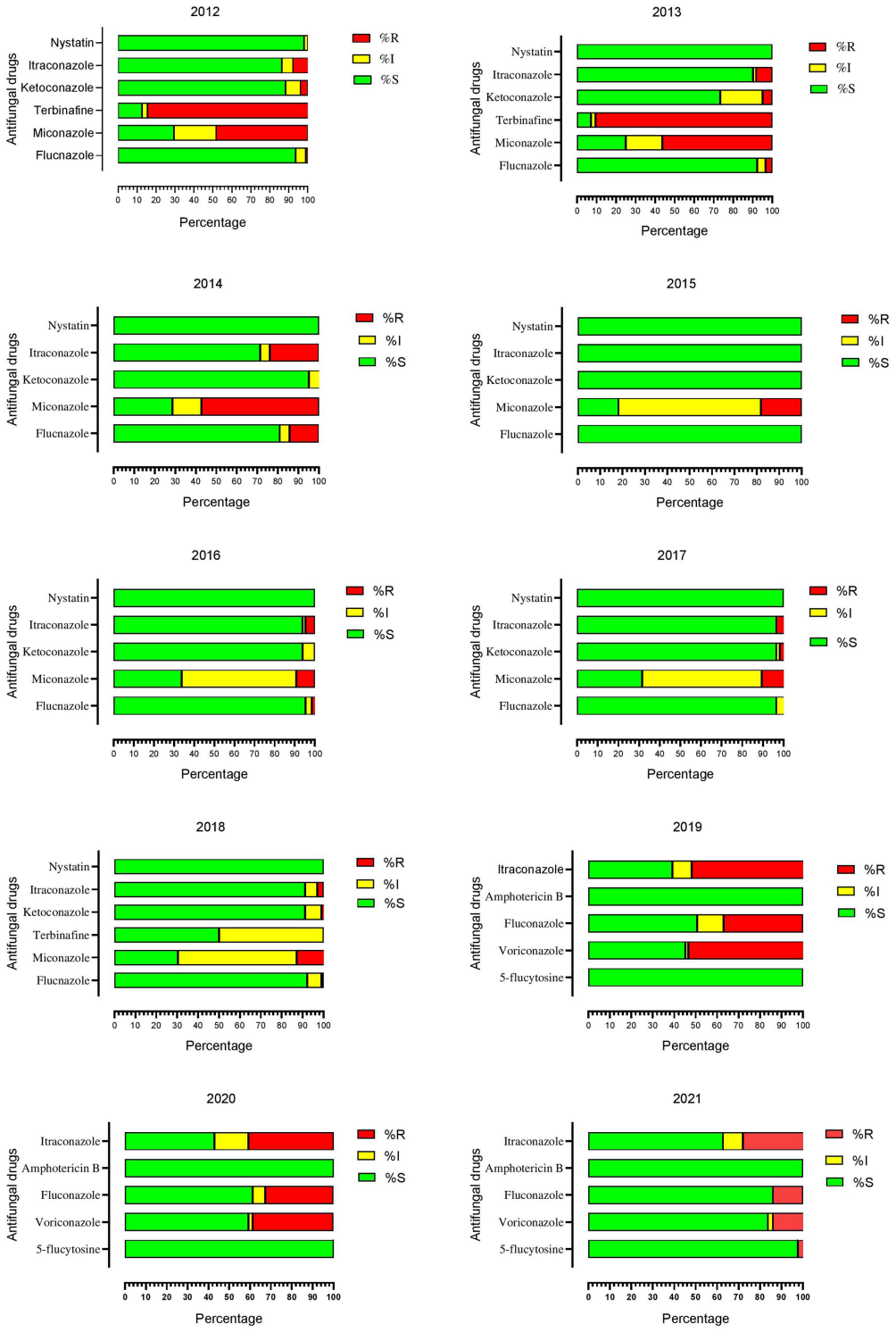

FIGURE 2
Year-wise antifungal susceptibility patterns of *Candida albicans* against all tested drugs.

Similarly, high resistance was reported for voriconazole; 38.79% out of 175 tested isolates. For fluconazole and itraconazole, the resistant rate was 9.34 and 16.10%, while 5.38 and 5.37% of the isolate were intermediate resistant, respectively. In this study, the azoles are comparatively less susceptible than polyenes and flucytosine. The high resistance to azole might be due to its inappropriate usage in agriculture and clinical settings in China (Zhou et al., 2022). Moreover, the

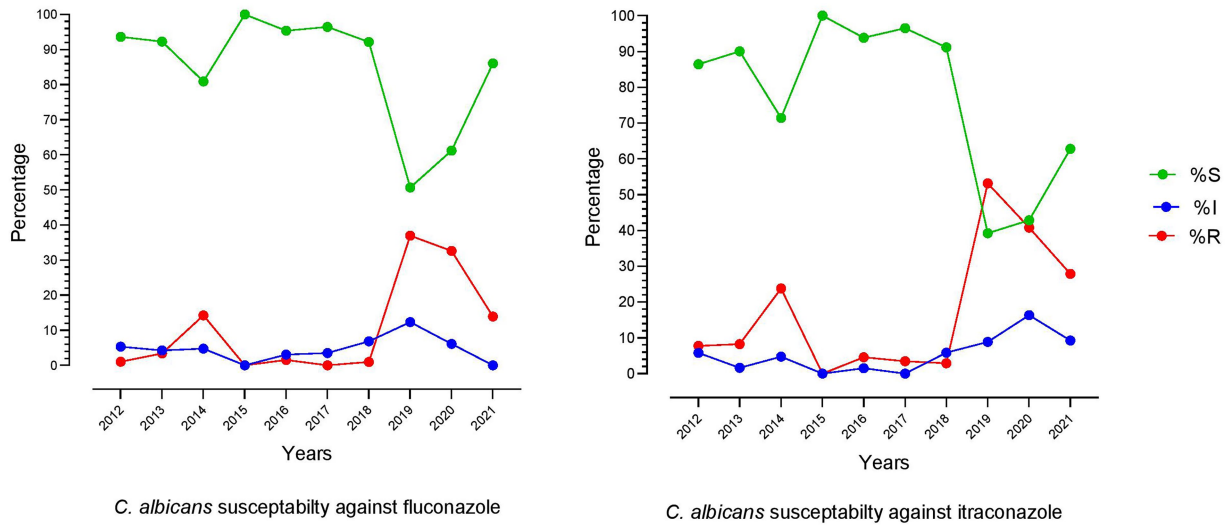

FIGURE 3
Trend of fluconazole and itraconazole susceptibility patterns of *C. albicans* over the last 10 years (2012–2021).

TABLE 4 Antifungal susceptibility profile of *C. glabrata* for all tested drugs in the past 10 years.

Antifungal agents	Tested isolates	Susceptible (%)	Intermediate resistant (%)	Resistant (%)
5-Flucytosine	3	66.67	0	33.33
Amphotericin B	3	100	0	0
Fluconazole	17	88.24	11.76	0
Itraconazole	18	100	0	0
Ketoconazole	12	91.67	8.33	0
Miconazole	12	50	41.67	8.33
Nystatin	15	93.33	0	6.67
Terbinafine	5	20	0	80
Voriconazole	3	100	0	0

fungistatic nature of azole drugs imposes a robust direct selection of antifungal-resistant species (Das et al., 2019). Only one isolate of *C. albicans* and *C. glabrata* show resistance to 5-flucytosine. For nystatin, only one *C. glabrata* isolate was resistant, and two *C. albicans* were intermediate resistant, while none of the isolates was resistant to amphotericin B. According to a report, a single antifungal agent and corticosteroid drugs are good options for curing cutaneous candidiasis (Taudorf et al., 2019). Hence, based on our findings, we suggest nystatin, a topical antifungal agent, and a corticosteroid drug for curing cutaneous candidiasis in our regions.

Moreover, it is suggested that the general population not to take antifungal drugs without a proper diagnosis of mycotic infections and prescriptions from a dermatologist. The laboratory screening of candidiasis needs to be performed molecularly or by MALDI TOF MS to correctly identify *Candida* species (Zhao et al., 2018). Furthermore, national guidelines for treating cutaneous mycotic infections need to be developed for proper medication and to halt the incidence of antifungal-resistant pathogens.

The current study has some limitations; our study was based on a single center in the eastern Guangdong province. Hence our findings might not be generalized to other regions because the prevalence of cutaneous candidiasis varies due to environmental and socio-economic factors (Dhillon and Chopra, 2022). Moreover, our study was based on the available laboratory records; therefore, clinical and detailed demographic features were not analyzed. To provide new insights, from now on, we intend to collect the clinical and patient demographic data for future research work and scientific base treatment of cutaneous candidiasis. On a vaster glimpse, the premise of this study entails significant epidemiological findings that are valuable for scheming approaches to improve the management of cutaneous candidiasis.

Conclusion

In the current study, we summarized the significant updated data about the prevalence of cutaneous candidiasis, species distribution, and antifungal susceptibility patterns of *Candida* species. Over the past decade of surveillance, *C. albicans* was a primary cause of cutaneous candidiasis, and resistances to terbinafine and azole were prominent. The *C. glabrata* were reported in high number among the few non-*C. albicans* isolates. Amphotericin B and 5-flucytosine were more susceptible drugs in the last 3 years. Over the years, nystatin has shown excellent activity against all *Candida* species. National trends of antifungal susceptibility and continuous monitoring are needed. The epidemiological outcomes of the present study will provide baselines for more

in-depth research and help healthcare officials to tackle the challenges of antifungal resistance.

Data availability statement

The raw data supporting the conclusions of this article will be made available by the authors, without undue reservation.

Ethics statement

The studies involving human participants were reviewed and approved by the Ethics Committee of Skin and Venereal Diseases Prevention and Control Hospital of Shantou city, Guangdong, China. The ethics committee waived the requirement of written informed consent for participation.

Author contributions

HB and YZ: study idea and plan. HB and BH: attainment of data. HB, MS, and XC: analysis and interpretation of data. HB, MAS, and YZ: drafting of the manuscript. YZ and MAS: critical revision of the manuscript for important intellectual content. YZ: administrative, technical, material support, and institutional study supervision. All authors contributed to the article and approved the submitted version.

Funding

This study is funded by the Second Affiliated Hospital of Shantou University Medical College to HBil and his mentor YZ.

Conflict of interest

The authors declare that the research was conducted in the absence of any commercial or financial relationships that could be construed as a potential conflict of interest.

Publisher's note

All claims expressed in this article are solely those of the authors and do not necessarily represent those of their affiliated organizations, or those of the publisher, the editors and the reviewers. Any product that may be evaluated in this article, or claim that may be made by its manufacturer, is not guaranteed or endorsed by the publisher.

References

Ameen, M., Lear, J., Madan, V., Mohd Mustapa, M., Richardson, M., Hughes, J., et al. (2014). British association of dermatologists' guidelines for the management of onychomycosis 2014. *Br. J. Dermatol.* 171, 937–958. doi: 10.1111/bjd.13358

Badali, H., and Wiederhold, N. P. (2019). Antifungal resistance testing and implications for management. *Curr. Fungal Inf. Rep.* 13, 274–283. doi: 10.1007/s12281-019-00354-6

Bhattacharya, S., Sae-Tia, S., and Fries, B. C. (2020). Candidiasis and mechanisms of antifungal resistance. *Antibiotics (Basel)* 9:312. doi: 10.3390/antibiotics9060312

Cai, W., Lu, C., Li, X., Zhang, J., Zhan, P., Xi, L., et al. (2016). Epidemiology of superficial fungal infections in Guangdong, southern China: a retrospective study from 2004 to 2014. *Mycopathologia* 181, 387–395. doi: 10.1007/s11046-016-9986-6

Chen, S. C., Perfect, J., Colombo, A. L., Cornely, O. A., Groll, A. H., Seidel, D., et al. (2021). Global guideline for the diagnosis and management of rare yeast infections: an initiative of the ECMM in cooperation with Isham and ASM. *Lancet Infect. Dis.* 21, E375–E386. doi: 10.1016/S1473-3099(21)00203-6

CLSI (2017). *M60. Performance Standards for Antifungal Susceptibility Testing of Yeasts, 1st Edn*. Wayne, PA: Clinical and Laboratory Standards Institute.

Cruz Ch, R., Ponce, E. E., Calderón, R. L., Delgado, V. N., Vieille, O. P., and Piontelli, L. E. (2011). Superficial mycoses in the city of Valparaiso, Chile: period 2007-2009. *Rev. Chil. Infectol.* 28, 404–409. doi: 10.4067/S0716-10182011000600002

Das, K. H., Mangayarkarasi, V., and Sen, M. (2019). Antifungal resistant in non-Albicans Candida species are emerging as a threat to antenatal women with vulvovaginal candidiasis. *Biomed. Pharmacol. J.* 12, 1369–1378. doi: 10.13005/bpj/1765

de Albuquerque Maranhão, F. C., Oliveira-Júnior, J. B., Dos Santos Araújo, M. A., and Silva, D. M. W. (2019). Mycoses in northeastern Brazil: epidemiology and prevalence of fungal species in 8 years of retrospective analysis in Alagoas. *Braz. J. Microbiol.* 50, 969–978. doi: 10.1007/s42770-019-00096-0

Dhillon, A., and Chopra, A. (2022). An observational study of infant dermatoses at a tertiary care health center in Delhi region. *Egypt. J. Dermatol. Venerol.* 42:115. doi: 10.4103/ejdv.ejdv_21_21

Edwards, J. E. (2015). "258- Candida Species," in *Mandell, Douglas, and Bennett's principles and practice of infectious diseases (Eighth Edition)*. eds. J. E. Bennett, R. Dolin and M. J. Blaser (Philadelphia, PA: W.B. Saunders).

Espinel-Ingroff, A. (2022). Commercial methods for antifungal susceptibility testing of yeasts: strengths and limitations as predictors of resistance. *J. Fungi* 8:309. doi: 10.3390/jof8030309

Faure-Cognet, O., Fricker-Hidalgo, H., Pelloux, H., and Leccia, M. T. (2016). Superficial fungal infections in a French teaching hospital in Grenoble area: retrospective study on 5470 samples from 2001 to 2011. *Mycopathologia* 181, 59–66. doi: 10.1007/s11046-015-9953-7

Jamiu, A. T., Albertyn, J., Sebolai, O. M., and Pohl, C. H. (2021). Update on *Candida Krusei*, a potential multidrug-resistant pathogen. *Med. Mycol.* 59, 14–30. doi: 10.1093/mmy/myaa031

Khodadadi, H., Zomorodian, K., Nouraei, H., Zareshahrabadi, Z., Barzegar, S., Zare, M. R., et al. (2021). Prevalence of superficial-cutaneous fungal infections in Shiraz, Iran: a five-year retrospective study (2015-2019). *J. Clin. Lab. Anal.* 35:E23850. doi: 10.1002/jcla.23850

Kühbacher, A., Burger-Kentischer, A., and Rupp, S. (2017). Interaction of Candida species with the skin. *Microorganisms* 5:32. doi: 10.3390/microorganisms5020032

Markogiannakis, A., Korantanis, K., Gamaletsou, M. N., Samarkos, M., Psichogiou, M., Daikos, G., et al. (2021). Impact of a non-compulsory antifungal stewardship program on overuse and misuse of antifungal agents in a tertiary care hospital. *Int. J. Antimicrob. Agents* 57:106255. doi: 10.1016/j.ijantimicag.2020.106255

Nam, M., Kim, S. H., Jeong, J. H., Kim, S., and Kim, J. (2022). Roles of the pro-apoptotic factors Canma111 and Caybh3 in apoptosis and virulence Of *Candida Albicans*. *Sci. Rep.* 12:7574. doi: 10.1038/s41598-022-11682-y

Nawal, P., Patel, S., Patel, M., Soni, S., and Khandelwal, N. (2012). A study of superficial mycoses in tertiary care hospital. *J Age* 6:11. Available at: https://typeset.io/papers/a-study-of-superficial-mycoses-in-tertiary-care-hospital-5eg4oww8k3

Noguchi, H., Matsumoto, T., Kimura, U., Hiruma, M., Kano, R., Yaguchi, T., et al. (2019). Fungal Melanonychia caused by *Candida Parapsilosis* successfully treated with oral Fosravuconazole. *J. Dermatol.* 46, 911–913. doi: 10.1111/1346-8138.15024

Nurdin, R. S. C., Vitayani, S., Amin, S., Kadir, D., Djamaluddin, W., and Adriani, A. (2021). Cutaneous candidiasis caused by Candida Kefyr. *Pan Afr. Med. J.* 38:178. doi: 10.11604/pamj.2021.38.178.28054

Otašević, S., Momčilović, S., Golubović, M., Ignjatović, A., Rančić, N., Đorđević, M., et al. (2019). Species distribution and epidemiological characteristics of superficial fungal infections in southeastern Serbia. *Mycoses* 62, 458–465. doi: 10.1111/myc.12900

Palese, E., Nudo, M., Zino, G., Devirgiliis, V., Carbotti, M., Cinelli, E., et al. (2018). Cutaneous candidiasis caused by *Candida Albicans* in a young non-immunosuppressed patient: an unusual presentation. *Int. J. Immunopathol. Pharmacol.* 32:2058738418781368. doi: 10.1177/2058738418781368

Procop, G. W. (2020). *Epidemiological Cutoff Values for Antifungal Susceptibility Testing*. Wayne, PA: Clinical and Laboratory Standards Institute.

Sadeghi, G., Ebrahimi-Rad, M., Shams-Ghahfarokhi, M., Jahanshiri, Z., Ardakani, E. M., Eslamifar, A., et al. (2019). Cutaneous candidiasis in Tehran-Iran: from epidemiology to multilocus sequence types, virulence factors and antifungal susceptibility of etiologic Candida species. *Iran J. Microbiol.* 11, 267–279. doi: 10.18502/ijm.v11i4.1463

Saud, B., Bajgain, P., Paudel, G., Shrestha, V., Bajracharya, D., Adhikari, S., et al. (2020). Fungal infection among diabetic and nondiabetic individuals in Nepal. *Interdiscip. Perspect. Infect. Dis.* 2020:7949868. doi: 10.1155/2020/7949868

Song, Y., Chen, X., Yan, Y., Wan, Z., Liu, W., and Li, R. (2020). Prevalence and antifungal susceptibility of pathogenic yeasts in China: a 10-year retrospective study in a teaching hospital. *Front. Microbiol.* 11:1401. doi: 10.3389/fmicb.2020.01401

Taudorf, E. H., Jemec, G. B. E., Hay, R. J., and Saunte, D. M. L. (2019). Cutaneous candidiasis-an evidence-based review of topical and systemic treatments to inform clinical practice. *J. Eur. Acad. Dermatol. Venereol.* 33, 1863–1873. doi: 10.1111/jdv.15782

Tortorano, A. M., Prigitano, A., Morroni, G., Brescini, L., and Barchiesi, F. (2021). Candidemia: evolution of drug resistance and novel therapeutic approaches. *Infect. Drug Resist.* 14, 5543–5553. doi: 10.2147/IDR.S274872

Ur Rahman, S., Ali, T., Ali, I., Khan, N. A., Han, B., and Gao, J. (2018). The growing genetic and functional diversity of extended spectrum beta-lactamases. *Biomed. Res. Int.* 2018:9519718. doi: 10.1155/2018/9519718

Vena, G. A., Chieco, P., Posa, F., Garofalo, A., Bosco, A., and Cassano, N. (2012). Epidemiology of dermatophytoses: retrospective analysis from 2005 to 2010 and comparison with previous data From 1975. *New Microbiol.* 35, 207–213. Available at: https://pubmed.ncbi.nlm.nih.gov/22707134/

Verma, R., Pradhan, D., Hasan, Z., Singh, H., Jain, A. K., and Khan, L. A. (2021). A systematic review on distribution and antifungal resistance pattern of Candida species in the Indian population. *Med. Mycol.* 59, 1145–1165. doi: 10.1093/mmy/myab058

Yoon, H. J., Choi, H. Y., Kim, Y. K., Song, Y. J., and Ki, M. (2014). Prevalence of fungal infections using National Health Insurance Data From 2009-2013. *South Korea. Epidemiol. Health* 36:E2014017. doi: 10.4178/epih/e2014017

Zamani, S., Sadeghi, G., Yazdinia, F., Moosa, H., Pazooki, A., Ghafarinia, Z., et al. (2016). Epidemiological trends of dermatophytosis in Tehran, Iran: a five-year retrospective study. *J. Mycol. Med.* 26, 351–358. doi: 10.1016/j.mycmed.2016.06.007

Zareshahrabadi, Z., Totonchi, A., Rezaei-Matehkolaei, A., Ilkit, M., Ghahartars, M., Arastehfar, A., et al. (2021). Molecular identification and antifungal susceptibility among clinical isolates of dermatophytes in shiraz, Iran (2017-2019). *Mycoses* 64, 385–393. doi: 10.1111/myc.13226

Zhao, Y., Tsang, C. C., Xiao, M., Chan, J. F. W., Lau, S. K. P., Kong, F., et al. (2018). Yeast identification by sequencing, biochemical kits, Maldi-Tof Ms and rep-PCR DNA fingerprinting. *Med. Mycol.* 56, 816–827. doi: 10.1093/mmy/myx118

Zhou, D., Wang, R., Li, X., Peng, B., Yang, G., Zhang, K.-Q., et al. (2022). Genetic diversity and azole resistance among natural Aspergillus Fumigatus populations in Yunnan, China. *Microb. Ecol.* 83, 869–885. doi: 10.1007/s00248-021-01804-w

frontiers | Frontiers in Microbiology

TYPE Original Research
PUBLISHED 23 August 2022
DOI 10.3389/fmicb.2022.992275

OPEN ACCESS

EDITED BY
Wenjie Fang,
Shanghai Changzheng Hospital,
China

REVIEWED BY
Pratyusha Vavilala,
University Of Delhi,
India
Hong Zhang,
First Affiliated Hospital of Jinan University,
China

*CORRESPONDENCE
Bing Han
hbshcn@163.com
Lan Yan
ylansmmu@sina.com

†These authors have contributed equally to this work

SPECIALTY SECTION
This article was submitted to Antimicrobials, Resistance and Chemotherapy, a section of the journal Frontiers in Microbiology

RECEIVED 12 July 2022
ACCEPTED 04 August 2022
PUBLISHED 23 August 2022

CITATION
Wang X, Liu P, Jiang Y, Han B and Yan L (2022) The prophylactic effects of monoclonal antibodies targeting the cell wall Pmt4 protein epitopes of *Candida albicans* in a murine model of invasive candidiasis.
Front. Microbiol. 13:992275.
doi: 10.3389/fmicb.2022.992275

The prophylactic effects of monoclonal antibodies targeting the cell wall Pmt4 protein epitopes of *Candida albicans* in a murine model of invasive candidiasis

Xiaojuan Wang[1,2†], Peng Liu[3†], Yuanying Jiang[4], Bing Han[2*] and Lan Yan[1*]

[1]School of Pharmacy, Naval Medical University, Shanghai, China, [2]Department of Pharmacy, Minhang Hospital, Fudan University, Shanghai, China, [3]Department of Gastroenterology, Institute for Regenerative Medicine, Shanghai East Hospital, Tongji University School of Medicine, Shanghai, China, [4]Department of Pharmacology, Shanghai Tenth People's Hospital, Tongji University School of Medicine, Shanghai, China

Candida albicans (*C. albicans*) is the most prevalent opportunistic human pathogen, accounting for approximately half of all clinical cases of candidemia. Resistance to the existing antifungal drugs is a major challenge in clinical therapy, necessitating the development and identification of novel therapeutic agents and potential treatment strategies. Monoclonal antibody-based immunotherapy represents a promising therapeutic strategy against disseminated candidiasis. Protein mannosyltransferase (Pmt4) encodes mannosyltransferases initiating O-mannosylation of secretory proteins and is essential for cell wall composition and virulence of *C. albicans*. Therefore, the Pmt4 protein of *C. albicans* is an attractive target for the discovery of alternative antibody agents against invasive *C. albicans* infections. In the present study, we found that monoclonal antibodies (mAbs) C12 and C346 specifically targeted the recombinant protein mannosyltransferase 4 (rPmt4p) of *C. albicans*. These mAbs were produced and secreted by hybridoma cells isolated from the spleen of mice that were initially immunized with the purified rPmt4p to generate IgG antibodies. The mAbs C12 and C346 exhibited high affinity to *C. albicans* whole cells. Remarkably, these mAbs reduced the fungal burden, alleviated inflammation in the kidneys, and prolonged the survival rate significantly in the murine model of systemic candidiasis. Moreover, they could activate macrophage opsonophagocytic killing and neutrophil killing of *C. albicans* strain *in vitro*. These results suggested that anti-rPmt4p mAbs may provide immunotherapeutic interventions against disseminated candidiasis *via* opsonophagocytosis and opsonic killing activity. Our findings provide evidence for mAbs as a therapeutic option for the treatment of invasive candidiasis.

KEYWORDS

Candida albicans*, monoclonal antibodies, anti-Candida mAbs, invasive candidiasis, *PMT4

Introduction

Invasive fungal infections (IFI) contribute to significant annual morbidity and mortality on a global scale. Approximately 1.7 million annual lethality is attributed to lethal invasive fungal infections, which is comparable to those due to tuberculosis or AIDS, and more than those owing to malaria, breast tumor, or prostate cancer (Brown et al., 2012; Kainz et al., 2020). Strikingly, *Candida* species are the most common causes of severe fungal infections and the fourth leading cause of healthcare-associated infections in the United States (Ostrosky-Zeichner et al., 2010). Among them, *Candida albicans* is the most prevalent opportunistic fungal species, resulting in both superficial mucosal and invasive infections, including those of internal organs and candidemia (Kim and Sudbery, 2011). The annual incidence of invasive *C. albicans* infections has increased notably in immunocompromised patients suffering from malignant tumors, solid organ transplantation, or AIDS (Gow et al., 2011; Bongomin et al., 2017; Pappas et al., 2018). Furthermore, the mortality rate associated with systemic candidiasis is reportedly higher than 30% (Wisplinghoff et al., 2014). At present, the arsenal of antifungal drugs used for systemic candidiasis, including fluconazole, amphotericin B, caspofungin, and 5-flucytosine, is limited. The effective treatment of systemic infections is hindered by the emergence of resistance to currently used antifungal drugs and long-term treatment regimens (Ruggero and Topal, 2014; Lee et al., 2021). Considering the side effects, drug–drug interactions and resistance to the limited number of antifungal drugs, new therapeutic strategies against lethal fungal infections are needed (Arastehfar et al., 2020).

Antibody represents a critical component of the adaptive immune responses and is a key weapon to eradicate microbial infections (Boniche et al., 2020; Ulrich and Ebel, 2020). Targeting specific molecular targets in bacteria and viruses using monoclonal antibodies can overcome the limitations of small-molecule drugs (Zurawski and McLendon, 2020). Nowadays, it has been increasingly appreciated that antibodies are important for the effective elimination of fungal infections. Remarkably, in a pioneering study, robust antibodies responding to specific proteins of *C. albicans* were found to be generated in systemic candidiasis recovered patients, while no, minimal, or waning immune responses were exhibited in those who succumbed to these infections (Matthews et al., 1987). Therefore, passive immunization in severely immunocompromised patients with monoclonal antibodies has the potential to directly combat fungal pathogens and/or activate the residual antifungal immune responses. Unfortunately, although a few mAbs show modest efficacy in the murine model of systemic *C. albicans* infection, no antifungal mAbs are currently available for use in routine clinical practice (Lee et al., 2011; Rudkin et al., 2018; Antoran et al., 2020; Shukla et al., 2021).

The fungal cell wall maintains its shape and plays an important role in hyphal growth, adhesion, and invasion (Chaffin, 2008; Gow et al., 2011; Hiller et al., 2011; Gow and Hube, 2012; Arita et al., 2022). Concurrently, it is crucial for protecting fungi from environmental stress and simultaneously mediating the fungus-host interactions (Mckenzie et al., 2010; Gow and Hube, 2012; Gow et al., 2017). Several studies have revealed that the molecular composition and the expression of the cell wall components change in response to growth pressures, including alterations in the carbon source, iron restriction, hypoxia, and exposure to antifungal agents, indicating that these proteins may either be up- or down-regulated *in vivo* during infections (Ruiz-Herrera et al., 2006). Furthermore, cell wall proteins, as essential components of fungi, represent ideal targets for developing antifungal vaccines and antibodies (Boniche et al., 2020; Ibe and Munro, 2021). Of note, protein mannosyltransferase (Pmt4), encoding mannosyltransferases initiating O-mannosylation of secretory proteins, is one of the five members of the PMT gene family of *C. albicans*, and is critically involved in cell wall composition and virulence of *C. albicans* (Prill et al., 2005; Lengeler et al., 2008). In our previous study, vaccination with the recombinant mannosyltransferase 4 (rPmt4p) exhibited a significant protective effect in mice with invasive *C. albicans* infection. Specifically, the rPmt4p vaccine reduced mortality rate and activated both humoral and cellular immune responses (Wang et al., 2015a).

Herein, we isolated and prepared several hybridomas from the mice vaccinated with different peptides of rPmt4p. These hybridomas produced a panel of monoclonal antibodies (mAbs), displaying a range of specific binding profiles to rPmt4p. After measurements of the specificity and affinity of their binding with *C. albicans* whole cells *via* enzyme-linked immunosorbent assay (ELISA), two specific mAbs targeting rPmt4p, C12 and C346, were selected for further analysis. We focused on the potential prophylactic value of mAbs C12 and C346 in a disseminated candidiasis murine model. The mAbs significantly increased the survival rates in these fungi-infected mice and attenuated kidney damage. Furthermore, mAbs C12 and C346 enhanced the macrophage opsonophagocytic activity and neutrophil killing effects against the *C. albicans* strain *in vitro*. Our findings highlight the prophylactic value of mAbs in the treatment of disseminated candidiasis and provide an effective antibody-based therapeutic option against systemic *C. albicans* infection.

Materials and methods

Animals

Female C57BL/6 and BALB/c mice aged 6–8 weeks and weighing 18–22 g were procured from SLAC Laboratory Animal Co., Ltd. (Shanghai, China). All animals were housed with free access to tap water and rodent chow in a temperature-controlled animal facility with a 12-h light/dark cycle.

Candida albicans strains and culture conditions

C. albicans SC5314 was provided by Dr. William A. Fonzi (Georgetown University, Washington, D.C., United States).

C. albicans SC5314 were thawed from glycerol stocks stored at −80°C, plated onto SDA plates (4% dextrose, 1.8% agar, and 1% peptone), and grown in YPD broth (2% glucose, 2% peptone, and 1% yeast extract) at 30°C. For hyphal growth, exponentially growing *C. albicans* yeast cells were washed in phosphate-buffered saline (PBS) buffer and cultured in Spider or Lee's liquid medium for 3 h at 37°C. RPMI1640 medium was used for biofilm formation assays.

Production of mAbs

The mAbs were prepared by the Abmart Antibody Production Company (Abmart, Shanghai, China). Briefly, based on the amino acid sequence, physicochemical properties, secondary structure, and antigenicity of Pmt4p of *C. albicans*, B cell epitopes were predicted. According to the results, several specific peptides were synthesized and used to subcutaneously immunize BALB/c mice. The antibody titers in sera of the vaccinated mice were determined by indirect enzyme-linked immunosorbent assay (ELISA). Mice with high antibody titers were selected for monoclonal antibody preparation. The spleen was removed and cells were dispersed to obtain a single cell suspension. The immunized mice spleen and myeloma SP2/0 cells were fused to produce hybridoma cell lines. Positive hybridomas capable of secreting mAbs against the corresponding peptides were identified by ELISA and subjected to cloning and subcloning by the limiting dilution method. The positive hybridoma cells were injected intraperitoneally into BALB/c mice to obtain ascites fluid. The mAbs were collected and purified by the protein-G affinity column (Abmart, Shanghai, China).

ELISA

ELISA was performed in 96-well plates to detect antibody titers (Costar, United States). After overnight culture, *C. albicans* cells were washed thrice with PBS and subsequently resuspended in RPMI 1640 medium to a final concentration of 1×10^6 cells/mL. To a 96-well plate, 100 μl of cell suspensions and coating buffer (0.1 M $NaHCO_3$ and 0.1 M Na_2CO_3; pH 9.6) were added. Following overnight incubation at 4°C, the wells were washed five times with PBS containing 0.05% Tween 20 (PBST); blocked with 200 μl of blocking solution (0.1% BSA in PBS), and incubated for 2 h at 37°C. After washing thrice with PBST, 100 μl of purified mAb in blocking buffer was added per well and the plates were incubated at 37°C for 2 h. PBST and IgG were the negative controls. Wells were washed thrice before the addition of horseradish peroxidase (HRP)-conjugated goat anti-mouse IgG (H + L; KPL) at 1:5000 dilution and incubated at 37°C for 1 h. Following a final round of washing, 3,3′,5,5′-tetramethylbenzidine (TMB, Sigma) substrate (100 μl) was added. The plates were incubated at room temperature for 10 min in the dark, followed by the addition of 50 μl of 2 M H_2SO_4 to terminate the reactions. The absorbance of each well was measured at 450 nm on a plate reader (Multiskan MK3, Finland). GraphPad Prism 9 was used to generate concentration-response curves for half-maximal effective concentration (EC_{50}) determination.

Murine model of systemic candidiasis

To assess the antifungal effects of mAbs *in vivo*, survival rate and kidney histopathological assessments were determined in the murine model of disseminated candidiasis. *C. albicans* SC5314 strain was harvested, resuspended in saline, and counted. BALB/c mice were challenged with 1×10^5 *C. albicans* SC5314 through tail vein injection. At 2 h prior to challenge, saline, IgG control, 1, 2, 3, or 4 mg/kg of mAbs were administered to the corresponding mice by intravenous injection. The mice were monitored for 40 days post-inoculation. The kidneys from 6 mice in each group were aseptically harvested, weighed, and homogenized in PBS on day 2 post-infection. The serial dilutions of each group were plated on SDA plates and incubated overnight at 30°C. The colony-forming units (CFU) were counted. The fungal burdens of kidneys were computed as a ratio of CFU/g of the organ. For histopathological assessment, the kidneys were fixed with 10% neutral formalin, dehydrated in graded alcohol solutions, embedded in paraffin, and stained with hematoxylin and eosin (H&E) or periodic acid-Schiff (PAS) solutions.

Determination of macrophage phagocytosis and neutrophil killing

Macrophage phagocytosis and neutrophil killing assays were conducted as reported previously with slight modifications (Zhang et al., 2016; Chen et al., 2020). Briefly, from healthy 6-8-week-old C57BL/6 mice, peritoneal macrophages and neutrophils stimulated by thioglycollate were isolated. Following three washes with PBS, the concentration of overnight cultured *C. albicans* SC5314 was adjusted to 1×10^5 cells/mL. For the macrophage phagocytosis killing assay, *C. albicans* SC5314 was co-cultured with peritoneal macrophages at MOI = 0.4 in the presence of 50, 100, or 150 μg/ml mAbs for 1 h at 37°C, followed by washing thrice in PBS. The mixture was plated on YPD agar for 48 h at 30°C and the surviving *C. albicans* strain was counted.

For the neutrophil killing assay, overnight cultured *C. albicans* SC5314 was incubated with indicated concentrations of mAbs for 1 h at 37°C. After washing with PBS, the concentration of *C. albicans* was adjusted to 1×10^5 cells/mL. Neutrophils were co-cultured with mAb-treated *C. albicans* strain at MOI = 0.05 for 1 h at 4°C before further incubation for another 1 h at 37°C. The mixture was plated on YPD agar at 30°C for 48 h and the surviving

C. albicans strain was counted. The killing rates were finally calculated using the following formula:

$$\left(1-\frac{\text{colonies of } C.albicans \text{ incubated with macrophages or neutrophils}}{\text{colonies of } C.albicans \text{ incubated without macrophages or neutrophils}}\right)\times 100\%$$

Hyphal growth assay

To evaluate the effects of mAbs on hyphal growth, *C. albicans* SC5314 cultured overnight was washed thrice in PBS and resuspended in Spider or Lee's medium at 1×10^6 cells/ml. To each well of a 96-well plate, 100 µl of the suspension was added. A final concentration of 100, 150, or 200 µg/ml of mAbs was added. Saline and IgG were the controls. The samples were incubated at 37°C for 3 h, and hyphal morphologies of the *C. albicans* strain were photographed under the EVOS inverted microscope (AMG, United States).

Biofilm formation assay

The *in vitro* biofilm formation assay was conducted following an established protocol with minor modifications (Pierce et al., 2008). Briefly, *C. albicans* SC5314 strain was grown in YPD overnight at 30°C. After washing thrice with PBS, the strain was diluted in RPMI 1640 medium till optical density (OD) was 0.1. To a 96-well plate, 100 µl of the diluted *C. albicans* strain suspension was added to each well, and allowed to adhere for 90 min at 37°C. Each well was gently washed with PBS to remove non-adherent cells. Fresh RPMI1640 medium (100 µl) with the indicated concentrations of mAbs was added to the corresponding wells and incubated at 37°C for 24 h. IgG and saline were the negative controls. The inhibition of biofilm formation by mAbs was assessed by the previously reported 2,3-bis-(2-methoxy-4-nitro-5-sulfophenyl)-2H-tetrazolium-5-carboxanilide (XTT, Sigma) reduction assay (Ramage et al., 2001).

Statistical analysis

GraphPad Prism 9 software was used to analyze the statistical significance of all data. At least three independent replicates were conducted for all experiments unless otherwise stated and $p<0.05$ was considered statistically significant. Data analysis of mice survival was performed by the log-rank test. For parametric data, the unpaired two-tailed Student's *t*-test was used for between-group comparison and one-way analysis of variance (ANOVA) for multiple-group comparison. For nonparametric data, the nonparametric *t*-test or analysis of variance (ANOVA) was applied.

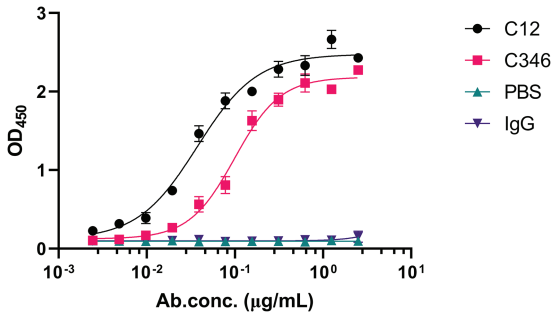

FIGURE 1
ELISA for detecting the binding ability of the purified anti-rPmt4p mAbs to *C. albicans* whole cells. Data are expressed as means ± SEM (n=3).

Results

Anti-rPmt4p mAbs C12 and C346 bind to *Candida albicans* with high specificity and affinity

The hybridomas were preliminarily screened by ELISA to detect their capability of binding to the recombinant *C. albicans* Pmt4p. A total of 22 positive hybridoma cells with an ELISA titer higher than 100 K were obtained. Among them, based on their binding abilities, anti-rPmt4p mAbs C12 and C346, corresponding to the peptide antigens, HVPGSNPKKEKN and LESPLAAHSKPV, respectively, were further selected by ELISA screening against *C. albicans* whole cells. Anti-rPmt4p mAb C12 showed strong binding to *C. albicans* whole cells with EC_{50} value between 30.70 and 45.27 ng/ml (Figure 1). Anti-rPmt4p mAb C346 bound to *C. albicans* whole cells with relatively lower affinity and the EC_{50} value ranged from 87.64 to 113.40 ng/ml. Therefore, mAbs showing specific binding to *C. albicans* cells were generated.

Anti-rPmt4p mAbs C12 and C346 protect mice against disseminated candidiasis

To investigate the protective efficacy of the antibodies *in vivo*, the survival rate of mice pretreated with mAb C12 or mAb C346 in the disseminated candidiasis mice was assessed (Figure 2A). The survival rates (at the end of the monitoring period) in mice administrated mAb C12 at 1, 2, and 3 mg/kg were 70, 50, and 60%, respectively. The lower dose of mAb C12 1 mg/kg significantly increased the 40-day survival rate of mice from 10 to 70% relative to the saline group. Moreover, the protective effects were superior to those in the IgG group with a survival rate of 20% (Figure 2B). The median survival time in the saline and IgG groups was 22 and 22.5 days, respectively. 2 mg/kg of mAb C12 significantly enhanced the median survival time to 33 days. In particular, 1 mg/kg of mAb C12 prevented death in 70% mice ($p<0.05$).

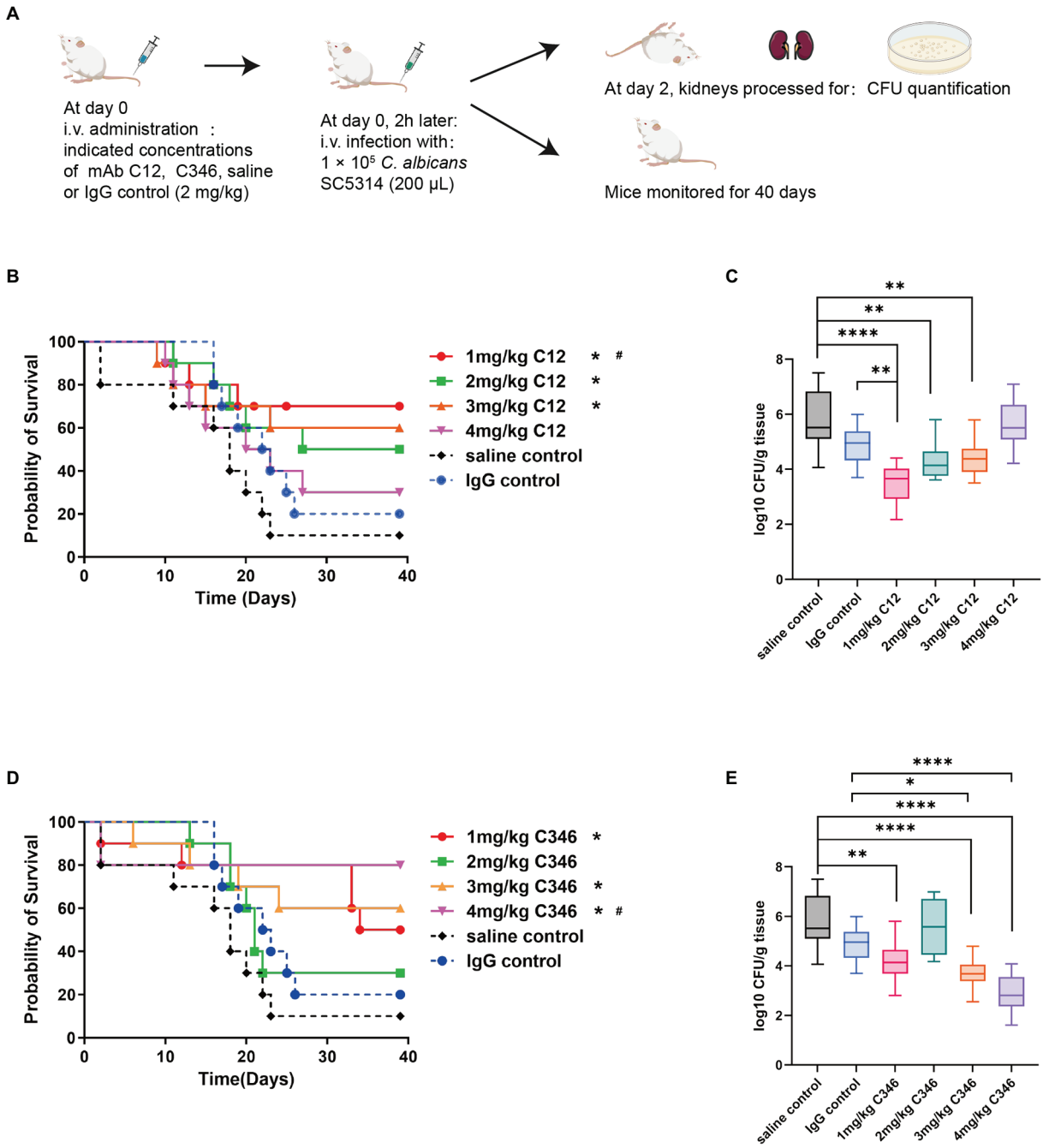

FIGURE 2
The *in vivo* antifungal efficacy of anti-rPmt4p mAbs in the murine model of disseminated candidiasis. **(A)** Schematic process of pre-treatment with mAb C12 or mAb C346 in the murine model of disseminated candidiasis. **(B,C)** Mice were prophylactically administrated 1, 2, 3, 4mg/kg of mAb C12, saline, or 2mg/kg of IgG. Two hours later, mice were challenged with 1×10^5 *C. albicans* SC5314 cells/mouse *via* the lateral tail vein. **(B)** The Kaplan–Meier survival curves of mice monitored for 40days post-inoculation (n=10 per group). **(C)** Quantification of fungal burden in the kidneys from mAb C12 treated mice on day 2 post-infection (n=6 per group). **(D,E)** Mice were prophylactically administrated 1, 2, 3, 4mg/kg of mAb C346, saline, or 2mg/kg of IgG. Two hours later, mice were challenged with 1×10^5 *C. albicans* SC5314 cells/mouse *via* the lateral tail vein. **(D)** The Kaplan–Meier survival curves of mice monitored for 40days post-inoculation (n=10 per group). **(E)** Quantification of fungal burden in the kidneys from mAb C346 treated mice on day 2 post-infection (n=6 per group). *, p<0.05 vs. saline control group; #, p<0.05 vs. IgG control group (**B,D**; Log-rank test). *, p<0.05; **, p<0.01; ****, p<0.0001 (**C,E**; Nonparametric One-way ANOVA).

Nevertheless, the protective effects of mAbs *in vivo* were not induced in a dose-dependent manner. Additionally, disease progression was measured based on the fungal burden in the kidneys. Prophylactic administration of 1, 2, and 3 mg/kg of mAb C12 significantly reduced the fungal burden in the kidneys compared to the saline control, consistent with the

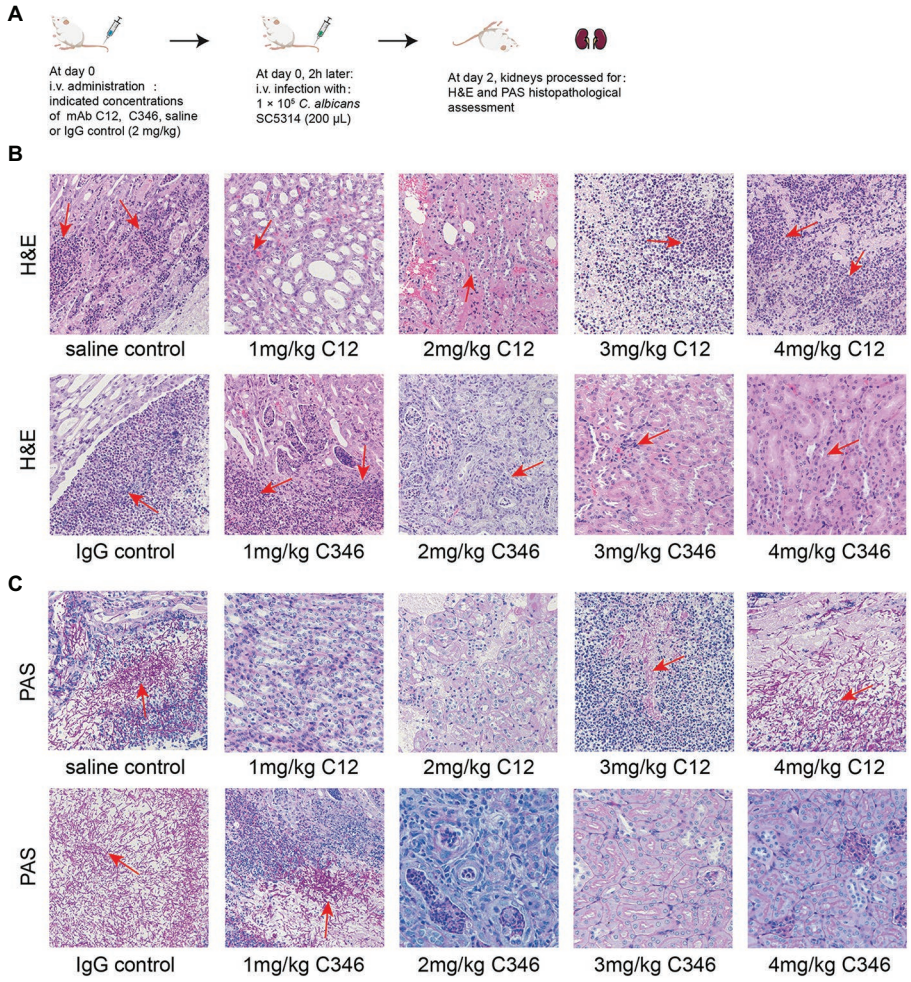

FIGURE 3
The effects of pre-treatment with mAb C12 or mAb C346 on renal histopathological damage in the murine model of disseminated candidiasis. **(A)** Schematic process of pretreatment with mAb C12 or mAb C346 in the murine model of disseminated candidiasis. The kidneys were dissected on day 2 post-infection with *C. albicans* SC5314. **(B,C)** Representative histopathological assessments of the kidneys by H&E staining for inflammatory cell influx and extent of tissue necrosis **(B)** and PAS staining for *C. albicans* strain **(C)**. Arrows indicate inflammatory cell influx and tissue necrosis (H&E staining), and *C. albicans* filaments in the tissues (PAS staining). The representative results of three independent experiments are shown. Magnification 200×.

results of the survival analysis (Figure 2C). Compared with the IgG group, pre-administration of mAb C12 (1 mg/kg) also significantly reduced the fungal burden in kidneys ($p < 0.01$).

Similarly, the mAb C346 exerted protective effects against disseminated candidiasis (Figure 2D). Relative to the saline group, administration of 1, 3, and 4 mg/kg of mAb C346 improved the survival rates of mice from 10 to 50, 60, and 80%, respectively. Furthermore, significant survival extension upon administration of 4 mg/kg mAb C346 relative to IgG was observed ($p < 0.05$). Likewise, mAb C346 administration (3 and 4 mg/kg) reduced the fungal burden in kidneys relative to those in the saline and IgG groups significantly (Figure 2E). These results suggested that the anti-rPmt4p mAbs C12 and C346 provided prophylactic protection in the murine model of the disseminated candidiasis.

mAbs attenuate the damage caused by the *Candida albicans* strain and reduce inflammation in the kidneys

Furthermore, the histopathological status of kidneys challenged by *C. albicans* was assessed by H&E and PAS staining assays. As shown in Figure 3B, H&E staining revealed massive renal medullary necrosis and inflammatory cell infiltration in the saline and IgG groups. PAS staining showed colonization by hyphae and pseudohyphae in the renal medulla and pelvis in both the saline and IgG groups (Figure 3C). In contrast, kidney tissue necrosis and inflammatory responses were remarkably ameliorated and no obvious *C. albicans* colonization or infection lesion was found upon treatment with mAb C12 (1 mg/kg) or mAb C346 (4 mg/kg), consistent with the results of survival and kidney fungal burden analyses.

These results suggested that mAbs C12 and C346 have promising potential antifungal activity *in vivo* as they exerted protective effects against the invasion of *C. albicans* strain in the kidneys and prolonged the survival in the murine model of disseminated candidiasis.

Anti-rPmt4p mAbs C12 and C346 promote macrophage opsonophagocytic and neutrophil killing activity against the *Candida albicans* strain

To determine whether the mAbs contributed to the killing of *C. albicans* by regulating mAb-mediated fungal opsonophagocytosis and opsonic-killing, killing assays were performed using mice macrophages and neutrophils. As shown in Figure 4, mAbs C12 and C346 exhibited opsonophagocytosis and opsonic-killing activity in a dose-dependent manner when co-incubated with macrophages or neutrophils, and challenged by the *C. albicans* strain. Rates of phagocytosis by macrophages and neutrophil killing increased significantly when macrophages or neutrophils were pre-incubated with mAb C12 or C346 at 100 and 150 μg/ml. Taken together, mAb C12 and mAb C346 enhanced the antibody-dependent opsonophagocytosis and opsonic-killing activity of macrophages and neutrophils against the *C. albicans* strain.

Anti-rPmt4p mAbs C12 and C346 do not inhibit hyphal growth or biofilm formation

To investigate whether mAb C12 or C346 could inhibit hyphal growth and biofilm formation, *C. albicans* strain SC5314 was cultured with or without the mAbs in Lee's or Spider medium. As shown in Figure 5, normal hyphae and biofilm formation were observed upon mAb treatment at indicated concentrations in each medium, relative to the control group. Thus, the mAbs did not inhibit hyphal growth or biofilm formation. Therefore, we reasonably speculate that anti-rPmt4p mAbs' antifungal effects may be through antibody-dependent opsonophagocytosis and opsonic-killing rather than direct inhibition of hyphal or biofilm formation.

Discussion

The treatment and management of invasive fungal infections are compromised by long-term treatment regimens and antifungal drug resistance in many fungal genera (Pappas et al., 2018). Vaccines or antibodies alone or in combination with chemotherapy can prevent post-treatment sequelae and reestablish a protective immune response (Biswas, 2021). Several studies have confirmed the immunogenicity and efficacy of vaccines using live attenuated *C. albicans* strains, purified recombinant proteins (Als1p, Sap2p, Hsp90p, Hyr1p, and Als3p), glycoconjugate vaccines (β-Glucan conjugate vaccine, β-mannan, and peptide conjugates,), and cell wall extract (β-mercaptoethanol extract) against candidiasis in animal models (Wang et al., 2015b). Among them, the rAls3p vaccine showed efficacy and safety according to a phase II clinical trial (Edwards et al., 2018). mAbs alone or their combinations are expected to show great protective potential in antifungal therapy, particularly to reduce the high morbidity and mortality in immunocompromised patients (Boniche et al., 2020). Monoclonal antibodies against fungi have been evaluated as an alternative therapeutic option against life-threatening systemic candidiasis. Indeed, several reports have validated the generation of protective antibodies as a critical aspect of recovery from infection (Pelfrene et al., 2019; Boniche et al., 2020; Ulrich and Ebel, 2020). mAbs recognize antigens that are specific to the fungi, such as polysaccharides and proteins in the fungal cell wall (β-glucan, Als3, Sap2, Hsp90, Hry1, Eno1, Utr2, and Pga31 implicated in fungal integrity, assembly, adhesion, virulence, morphogenesis, and pathogenesis) and show protection against fungal infections (De Bernardis et al., 1997; Matthews et al., 2003; Pachl et al., 2006; Rachini et al., 2007; Laforce-Nesbitt et al., 2008; Beucher et al., 2009; Coleman et al., 2009; Torosantucci et al., 2009; Rudkin et al., 2018; Matveev et al., 2019; Chen et al., 2020; Heredia et al., 2020; Leu et al., 2020). For example, antibodies associated with Als3p include mAbs C7, 3D9.3, 2G8, and scFv3 (Laforce-Nesbitt et al., 2008; Beucher et al., 2009; Coleman et al., 2009; Torosantucci et al., 2009). The mAb 2G8 provides marked protection against both systemic and mucosal candidiasis, evidenced in passive vaccination experiments in mice (Torosantucci et al., 2009), while scFv3 can suppress *C. albicans* adhesion to human cells (Laforce-Nesbitt et al., 2008). Thus, antibody neutralizing virulence factors of *C. albicans* are valuable in the treatment of candidiasis, especially in immunocompromised hosts.

Remarkably, cell wall proteins are extremely important for fungi to maintain cell morphology and pathogenicity, and adapt to the external environment. Furthermore, cell wall components can be recognized by the innate immune system, the first line of defense against fungal invasion (Sukhithasri et al., 2013). Thus, vaccines or mAb-based strategies that selectively and effectively inhibit the virulence factors have the clinical development potential. Protein mannosyltransferase 4 represents one of the PMT gene family localized to the *C. albicans* cell wall; it encodes five isoforms of protein mannosyltransferases, which initiates O-mannosylation of secretory proteins, and is essential for the maintenance of hyphal growth, virulence, and cell wall composition (Prill et al., 2005). Previously, we have confirmed that rPmt4p vaccination improves the survival rate in a murine model of disseminated candidiasis and can serve as a vaccine candidate against systemic candidiasis (Wang et al., 2015a). Herein, we prepared anti-rPmt4p mAbs to investigate whether these mAbs protected mice against disseminated candidiasis and examined the potential protective mechanisms.

Anti-rPmt4p mAbs C12 and C346 bound specifically to *C. albicans* whole cells (Figure 1). Additionally, *in vivo* protective

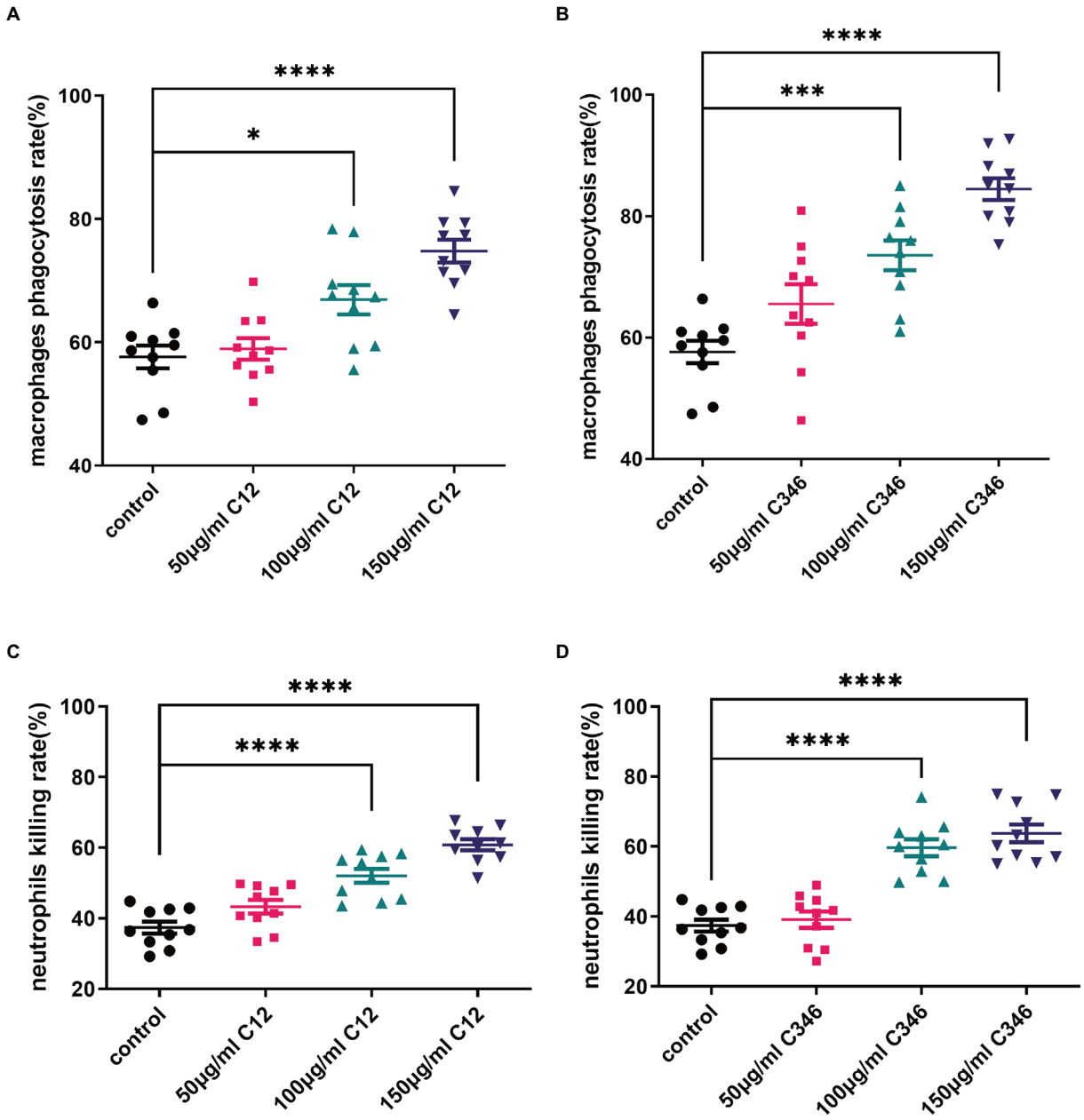

FIGURE 4
The phagocytosis and killing rates of thioglycollate-elicited peritoneal macrophages and neutrophils pretreated with anti-rPmt4p antibodies against *C. albicans* SC5314. *C. albicans* SC5314 was incubated with thioglycollate-elicited peritoneal macrophages (MOI=0.4) in the presence of indicated concentrations of mAb C12 **(A)** and mAb C346 **(B)** for 1h at 37°C, followed by washing thrice in PBS. The suspension was plated on YPD agar at 30°C for 48h; the colonies were counted and the phagocytosis rate was calculated. *C. albicans* SC5314 cells were co-cultured with thioglycollate-elicited peritoneal neutrophils (MOI=0.05) with the indicated concentrations of mAb C12 **(C)** and mAb C346 **(D)** at 37°C for 1h. The suspension was then plated on YPD agar for 48h. *C. albicans* colonies were counted and the killing rates were calculated. Data in **(A–D)** are representative of three independent experiments. *, $p<0.05$; ***, $p<0.001$; ****, $p<0.0001$, one-way ANOVA.

efficacy of these mAbs against systemic candidiasis was convincingly demonstrated in the murine model of disseminated candidiasis (Figure 2). However, this beneficial effect did not show a clear dose-dependence. mAb C12, in particular, when administered at a single dose of 1 mg/kg followed by the *C. albicans* attack, conferred improved survival rates to 70% compared to the saline (10%) and IgG (20%) controls (Figure 2B). The benefits of these antibodies were also reflected by significant reductions in the fungal burden in the kidneys of mice administered 1 mg/kg, 2 mg/kg, or 3 mg/kg mAb C12 (Figure 2C). In contrast, 4 mg/kg of mAb C346 was administered as a prophylactic before the *C. albicans* challenge and showed the most significant survival benefit and reduction in fungal burden (Figures 2D,E). Simultaneously, H&E and PAS staining assays in kidneys showed

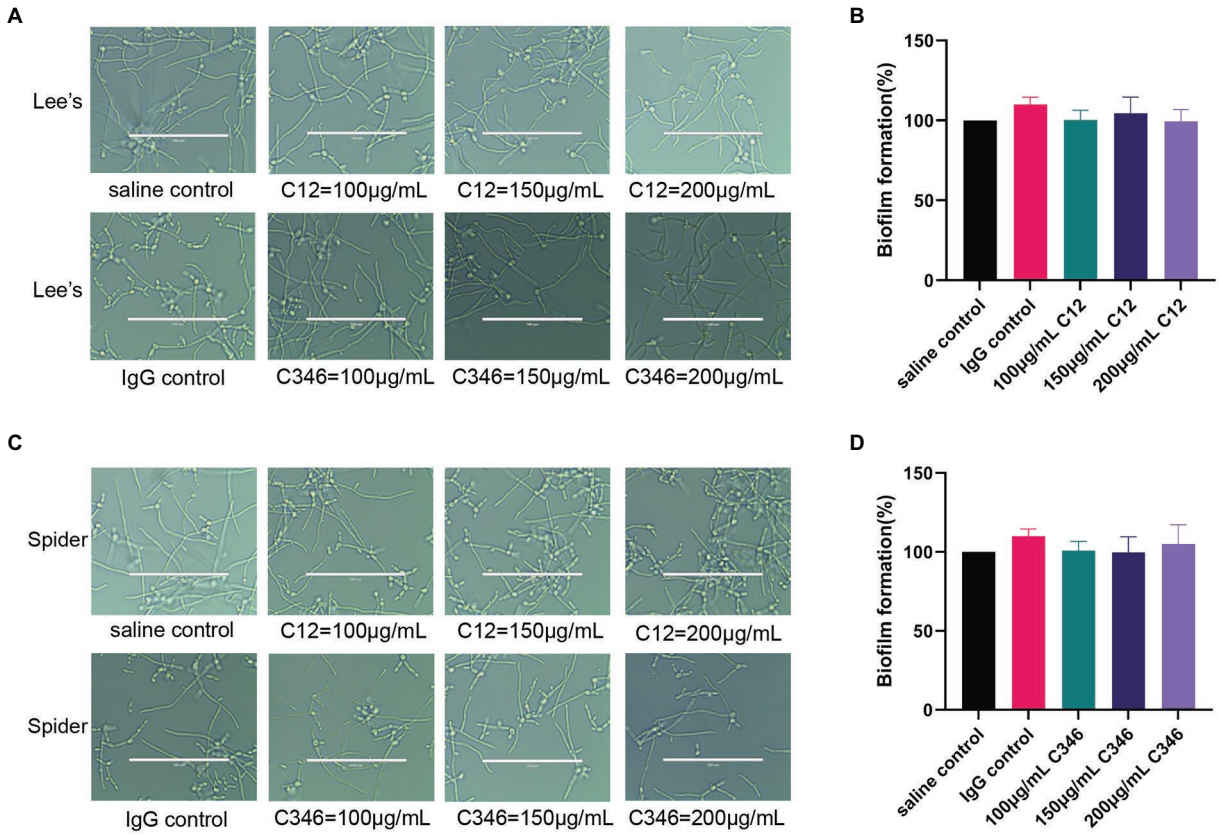

FIGURE 5
No obvious inhibitory effects of anti-rPmt4p mAbs C12 and C346 on hyphal growth or biofilm formation. Exponentially growing *C. albicans* SC5314 cells were transferred to Lee's liquid medium **(A)** or Spider medium **(C)**, followed by co-incubation with different concentrations of mAbs. The cellular morphologies were photographed after incubation at 37°C for 3h. Scale bar=100μm for **(A,C)**. Exponentially growing *C. albicans* SC5314 cells were transferred to RPMI1640 liquid medium in a 96-well plate for 90min, followed by addition and incubation for 24h with mAbs, C12 **(B)** or C346 **(D)**. Biofilm formation was evaluated by the XTT reduction assay. The results are presented as the percentage compared to the biofilm formed in the saline control group. Data in **(A,C)** are representative of three independent experiments. Data in **(B,D)** are expressed as means ± SD (*n*=3).

that renal injury and inflammation in the antibody-pretreated group reduced significantly relative to the saline and IgG groups (Figure 3). These results revealed that mAb C12 and mAb C346 exerted protective effects against the murine model of disseminated candidiasis at appropriate dosing and increased the clearance of *C. albicans*, thereby reducing kidney damage.

Antibodies combat pathogens mostly by direct neutralization or subsequently elicit innate immune cells opsonophagocytosis and cytotoxic responses through antibodies' Fc domains (Lu et al., 2018). Macrophages and neutrophils are the most important effector cells of the innate immune system against *C. albicans* (Kumar and Sharma, 2010; Wang, 2015; Pappas et al., 2018). The innate immune defense system is activated after invasion by *C. albicans*. The binding between the antibody and *C. albicans* strain induces innate host immune cell-mediated phagocytosis and killing (Chen et al., 2020). Previously published studies have focused on *in vivo* efficacy, whereby mAbs were either pre-incubated with *C. albicans* or administered as a prophylactic before the challenge, resulting in survival benefits and reduction in the fungal burden in various organs (Rudkin et al., 2018; Matveev et al., 2019). Therefore, mAbs are already available in the systemic circulation and can bind to the *C. albicans* strain, thus facilitating opsonophagocytosis and clearance with increased protection. The rPmt4p-specific antibodies attenuated the kidney fungal burden in the mice received prophylactic treatment, thus indicating that mAbs can bind to *C. albicans in vivo*, probably by inhibition of cell replication and/or by enhancement of macrophage recruitment and neutrophil-mediated phagocytosis and clearance. Our results depicted that mAb C12 and C346 significantly promoted the clearance of *C. albicans* cells by opsonizing macrophage phagocytic killing and neutrophil killing activity (Figure 4).

Many therapeutic mAbs exert their protective effects through direct inhibition of hyphal growth and biofilm formation (Carrano et al., 2019; Leu et al., 2020; Palliyil et al., 2022). We investigated the inhibitory effects of anti-rPmt4p antibodies on the yeast-to-hypha morphological transition and the formation of biofilm in *C. albicans*. Unexpectedly, both mAb C12 and mAb C346 did not show inhibition of hyphal growth or biofilm formation at different

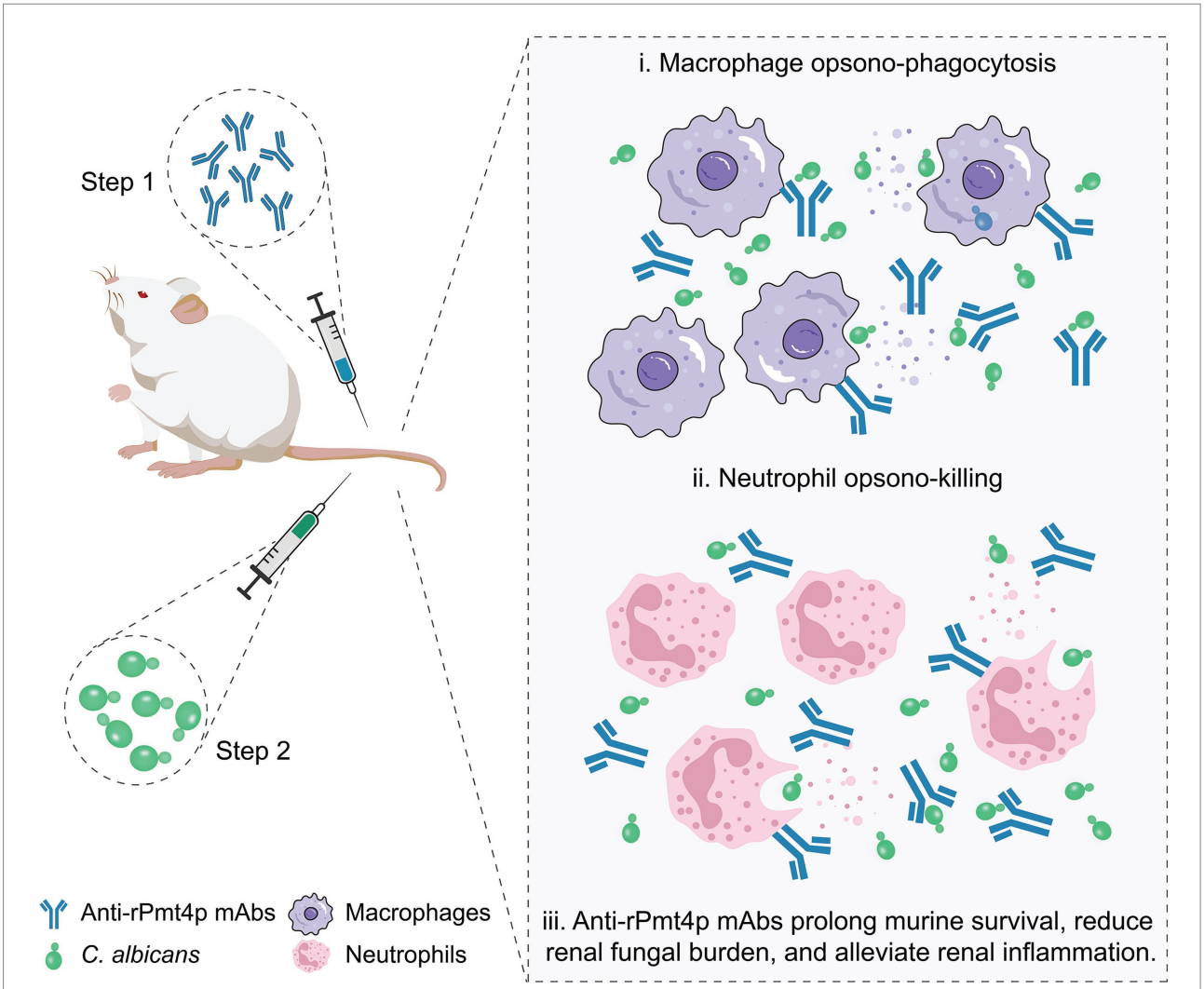

FIGURE 6
A schematic illustration of anti-rPmt4p mAbs eliciting beneficial effects in the murine model of disseminated candidiasis. The mAbs exert protective effects *via* a mechanism that involves mAb-induced macrophage opsonophagocytic (i) and neutrophil killing activities (ii). Prophylactic mAb administration prolongs the survival time, reduces the fungal burden, and alleviates renal inflammation in mice with disseminated candidiasis (iii).

concentrations (Figure 5). As biofilm is developed by the hyphae, these results are consistent and reasonable. Taken together, mAb C12 and mAb C346 may exert protection by enhancing host opsonophagocytic activity instead of inhibiting hyphal growth or biofilm formation.

The present study has some limitations. First, the absence of binding to a *PMT4* knockout strain in *C. albicans* would further enhance the specificity of mAbs C12 and C346. The binding affinities of anti-rPmt4p mAbs were only assessed in *C. albicans* strain. Further investigation of the binding profiles to other pathogenic fungi is needed to be validated. Second, invasive fungal infections can also be caused by fluconazole-resistant *C. albicans*, *C. glabrata*, or *C. parapsilosis*. The protective effects of anti-rPmt4p mAbs on these systemic fungal infections need further evaluation. Third, a single dosage of anti-rPmt4p mAbs was evaluated herein. The effects of repeated treatment with anti-rPmt4p mAbs or their combination with currently used antifungal agents remain unknown. Therefore, the prophylactic and therapeutic efficacies of anti-rPmt4p mAbs in animal models and the potential clinical use of such antibodies in the future warrant further investigation.

In conclusion, two anti-rPmt4p mAbs were designed, produced, and shown to have prominent binding affinities to *C. albicans* whole cell. A murine model of systemic candidiasis was utilized to assess the prophylactic efficacy of the anti-rPmt4p mAbs *in vivo*. We confirmed that the mAbs exerted their protective effects through the recruitment of macrophages and neutrophils *via* antibody-mediated opsonophagocytosis and clearance (Figure 6). Thus, these findings provide new insights into anti-*C. albicans* immunotherapy and the possibility of developing potential novel antifungal therapeutic mAbs targeting the cell wall proteins.

Data availability statement

The original contributions presented in the study are included in the article/Supplementary material, further inquiries can be directed to the corresponding authors.

Ethics statement

The animal study was reviewed, approved, and conducted following the Animal Care Ethics guidelines with protocols approved by the Animal Care and Use Committees of Naval Medical University and Fudan University (2021JSMinhang Hospital-036).

Author contributions

XW, PL, YJ, BH, and LY conceptualized the study design. XW and PL assessed the prophylactic value of mAbs in the murine model of disseminated candidiasis, wrote the first version of the manuscript, and conducted hyphal growth and biofilm formation analyses. XW analyzed IgG antibody's affinity to *Candida albicans* and performed opsonophagocytosis and opsonic-killing experiments. YJ, BH, and LY supervised the study. LY revised the manuscript. All authors contributed to the article and approved the submitted version.

Funding

This research was supported by grants from the National Natural Science Foundation of China (Nos.: 82173867, 82103095, and 82104242), the Shanghai Science and Technology Innovation Action Plan, the International Science and Technology Cooperation Project (21430713000), Shanghai Pujiang Program (21PJD0081), the Project of Shanghai Minhang District Health and Family Planning Commission (2021MW18), and Minhang District Healthcare System Program for Outstanding Young Medical Technical and Pharmacology Scholars (mwyjyx01).

Acknowledgments

All authors are grateful to William A. Fonzi (Department of Microbiology and Immunology, Georgetown University, Washington, DC, United States) for providing *C. albicans* strains.

Conflict of interest

The authors declare that the research was conducted in the absence of any commercial or financial relationships that could be construed as a potential conflict of interest.

Publisher's note

All claims expressed in this article are solely those of the authors and do not necessarily represent those of their affiliated organizations, or those of the publisher, the editors and the reviewers. Any product that may be evaluated in this article, or claim that may be made by its manufacturer, is not guaranteed or endorsed by the publisher.

References

Antoran, A., Aparicio-Fernandez, L., Pellon, A., Buldain, I., Martin-Souto, L., Rementeria, A., et al. (2020). The monoclonal antibody Ca37, developed against *Candida albicans* alcohol dehydrogenase, inhibits the yeast in vitro and in vivo. *Sci. Rep.* 10:9206. doi: 10.1038/s41598-020-65859-4

Arastehfar, A., Gabaldón, T., Garcia-Rubio, R., Jenks, J. D., Hoenigl, M., Salzer, H. J. F., et al. (2020). Drug-resistant fungi: An emerging challenge threatening our limited antifungal armamentarium. *Antibiotics (Basel)* 9:877. doi: 10.3390/antibiotics9120877

Arita, G. S., Faria, D. R., Capoci, I. R. G., Kioshima, E. S., Bonfim-Mendonça, P. S., and Svidzinski, T. I. E. (2022). Cell wall associated proteins involved in filamentation with impact on the virulence of *Candida albicans*. *Microbiol. Res.* 258:126996. doi: 10.1016/j.micres.2022.126996

Beucher, B., Marot-Leblond, A., Billaud-Nail, S., Oh, S. H., Hoyer, L. L., and Robert, R. (2009). Recognition of *Candida albicans* Als3 by the germ tube-specific monoclonal antibody 3D9.3. *FEMS Immunol. Med. Microbiol.* 55, 314–323. doi: 10.1111/j.1574-695X.2008.00502.x

Biswas, P. S. (2021). Vaccine-induced immunological memory in invasive fungal infections - A dream so close yet so far. *Front. Immunol.* 12:671068. doi: 10.3389/fimmu.2021.671068

Bongomin, F., Gago, S., Oladele, R. O., and Denning, D. W. (2017). Global and multi-National Prevalence of fungal diseases-estimate precision. *J Fungi (Basel)* 3:57. doi: 10.3390/jof3040057

Boniche, C., Rossi, S. A., Kischkel, B., Barbalho, F. V., Moura, Á. N. D., Nosanchuk, J. D., et al. (2020). Immunotherapy against systemic fungal infections based on monoclonal antibodies. *J Fungi (Basel)* 6:31. doi: 10.3390/jof6010031

Brown, G. D., Denning, D. W., Gow, N. A., Levitz, S. M., Netea, M. G., and White, T. C. (2012). Hidden killers: human fungal infections. *Sci. Transl. Med.* 4:165rv13. doi: 10.1126/scitranslmed.3004404

Carrano, G., Paulone, S., Lainz, L., Sevilla, M. J., Blasi, E., and Moragues, M. D. (2019). Anti-Candidaalbicans germ tube antibodies reduce in vitro growth and biofilm formation of *C. albicans*. *Rev. Iberoam. Micol.* 36, 9–16. doi: 10.1016/j.riam.2018.07.005

Chaffin, W. L. (2008). Candida albicans cell wall proteins. *Microbiol. Mol. Biol. Rev.* 72, 495–544. doi: 10.1128/mmbr.00032-07

Chen, S. M., Zou, Z., Guo, S. Y., Hou, W. T., Qiu, X. R., Zhang, Y., et al. (2020). Preventing *Candida albicans* from subverting host plasminogen for invasive infection treatment. *Emerg Microbes Infect* 9, 2417–2432. doi: 10.1080/22221751.2020.1840927

Coleman, D. A., Oh, S. H., Zhao, X., Zhao, H., Hutchins, J. T., Vernachio, J. H., et al. (2009). Monoclonal antibodies specific for Candida albicans Als3 that immunolabel fungal cells in vitro and in vivo and block adhesion to host surfaces. *J. Microbiol. Methods* 78, 71–78. doi: 10.1016/j.mimet.2009.05.002

De Bernardis, F., Boccanera, M., Adriani, D., Spreghini, E., Santoni, G., and Cassone, A. (1997). Protective role of antimannan and anti-aspartyl proteinase antibodies in an experimental model of *Candida albicans* vaginitis in rats. *Infect. Immun.* 65, 3399–3405. doi: 10.1128/iai.65.8.3399-3405.1997

Edwards, J. E. Jr., Schwartz, M. M., Schmidt, C. S., Sobel, J. D., Nyirjesy, P., Schodel, F., et al. (2018). A fungal immunotherapeutic vaccine (NDV-3A) for treatment of recurrent Vulvovaginal candidiasis-A phase 2 randomized, double-blind, placebo-controlled trial. *Clin. Infect. Dis.* 66, 1928–1936. doi: 10.1093/cid/ciy185

Gow, N. A., and Hube, B. (2012). Importance of the *Candida albicans* cell wall during commensalism and infection. *Curr. Opin. Microbiol.* 15, 406–412. doi: 10.1016/j.mib.2012.04.005

Gow, N. A. R., Latge, J. P., and Munro, C. A. (2017). The fungal Cell Wall: structure, biosynthesis, and function. *Microbiol. Spectr.* 5, 1–25. doi: 10.1128/microbiolspec.FUNK-0035-2016

Gow, N. A., Van De Veerdonk, F. L., Brown, A. J., and Netea, M. G. (2011). *Candida albicans* morphogenesis and host defence: discriminating invasion from colonization. *Nat. Rev. Microbiol.* 10, 112–122. doi: 10.1038/nrmicro2711

Heredia, M. Y., Ikeh, M. A. C., Gunasekaran, D., Conrad, K. A., Filimonava, S., Marotta, D. H., et al. (2020). An expanded cell wall damage signaling network is comprised of the transcription factors Rlm1 and Sko1 in *Candida albicans*. *PLoS Genet.* 16:e1008908. doi: 10.1371/journal.pgen.1008908

Hiller, E., Zavrel, M., Hauser, N., Sohn, K., Burger-Kentischer, A., Lemuth, K., et al. (2011). Adaptation, adhesion and invasion during interaction of *Candida albicans* with the host--focus on the function of cell wall proteins. *Int. J. Med. Microbiol.* 301, 384–389. doi: 10.1016/j.ijmm.2011.04.004

Ibe, C., and Munro, C. A. (2021). Fungal cell wall: An underexploited target for antifungal therapies. *PLoS Pathog.* 17:e1009470. doi: 10.1371/journal.ppat.1009470

Kainz, K., Bauer, M. A., Madeo, F., and Carmona-Gutierrez, D. (2020). Fungal infections in humans: the silent crisis. *Microb Cell* 7, 143–145. doi: 10.15698/mic2020.06.718

Kim, J., and Sudbery, P. (2011). *Candida albicans*, a major human fungal pathogen. *J. Microbiol.* 49, 171–177. doi: 10.1007/s12275-011-1064-7

Kumar, V., and Sharma, A. (2010). Neutrophils: Cinderella of innate immune system. *Int. Immunopharmacol.* 10, 1325–1334. doi: 10.1016/j.intimp.2010.08.012

Laforce-Nesbitt, S. S., Sullivan, M. A., Hoyer, L. L., and Bliss, J. M. (2008). Inhibition of *Candida albicans* adhesion by recombinant human antibody single-chain variable fragment specific for Als3p. *FEMS Immunol. Med. Microbiol.* 54, 195–202. doi: 10.1111/j.1574-695X.2008.00465.x

Lee, J. H., Jang, E. C., and Han, Y. (2011). Combination immunotherapy of MAb B6.1 with fluconazole augments therapeutic effect to disseminated candidiasis. *Arch. Pharm. Res.* 34, 399–405. doi: 10.1007/s12272-011-0307-9

Lee, Y., Puumala, E., Robbins, N., and Cowen, L. E. (2021). Antifungal drug resistance: molecular mechanisms in *Candida albicans* and Beyond. *Chem. Rev.* 121, 3390–3411. doi: 10.1021/acs.chemrev.0c00199

Lengeler, K. B., Tielker, D., and Ernst, J. F. (2008). Protein-O-mannosyltransferases in virulence and development. *Cell. Mol. Life Sci.* 65, 528–544. doi: 10.1007/s00018-007-7409-z

Leu, S. J., Lee, Y. C., Lee, C. H., Liao, P. Y., Chiang, C. W., Yang, C. M., et al. (2020). Generation and characterization of single chain variable fragment against alpha-Enolase of *Candida albicans*. *Int. J. Mol. Sci.* 21:2903. doi: 10.3390/ijms21082903

Lu, L. L., Suscovich, T. J., Fortune, S. M., and Alter, G. (2018). Beyond binding: antibody effector functions in infectious diseases. *Nat. Rev. Immunol.* 18, 46–61. doi: 10.1038/nri.2017.106

Matthews, R. C., Burnie, J. P., and Tabaqchali, S. (1987). Isolation of immunodominant antigens from sera of patients with systemic candidiasis and characterization of serological response to *Candida albicans*. *J. Clin. Microbiol.* 25, 230–237. doi: 10.1128/jcm.25.2.230-237.1987

Matthews, R. C., Rigg, G., Hodgetts, S., Carter, T., Chapman, C., Gregory, C., et al. (2003). Preclinical assessment of the efficacy of mycograb, a human recombinant antibody against fungal HSP90. *Antimicrob. Agents Chemother.* 47, 2208–2216. doi: 10.1128/aac.47.7.2208-2216.2003

Matveev, A. L., Krylov, V. B., Khlusevich, Y. A., Baykov, I. K., Yashunsky, D. V., Emelyanova, L. A., et al. (2019). Novel mouse monoclonal antibodies specifically recognizing β-(1→3)-D-glucan antigen. *PLoS One* 14:e0215535. doi: 10.1371/journal.pone.0215535

Mckenzie, C. G., Koser, U., Lewis, L. E., Bain, J. M., Mora-Montes, H. M., Barker, R. N., et al. (2010). Contribution of *Candida albicans* cell wall components to recognition by and escape from murine macrophages. *Infect. Immun.* 78, 1650–1658. doi: 10.1128/iai.00001-10

Ostrosky-Zeichner, L., Casadevall, A., Galgiani, J. N., Odds, F. C., and Rex, J. H. (2010). An insight into the antifungal pipeline: selected new molecules and beyond. *Nat. Rev. Drug Discov.* 9, 719–727. doi: 10.1038/nrd3074

Pachl, J., Svoboda, P., Jacobs, F., Vandewoude, K., Van Der Hoven, B., Spronk, P., et al. (2006). A randomized, blinded, multicenter trial of lipid-associated amphotericin B alone versus in combination with an antibody-based inhibitor of heat shock protein 90 in patients with invasive candidiasis. *Clin. Infect. Dis.* 42, 1404–1413. doi: 10.1086/503428

Palliyil, S., Mawer, M., Alawfi, S. A., Fogg, L., Tan, T. H., De Cesare, G. B., et al. (2022). Monoclonal antibodies targeting surface-exposed epitopes of *Candida albicans* Cell Wall proteins confer In vivo protection in an infection model. *Antimicrob. Agents Chemother.* 66:e0195721. doi: 10.1128/aac.01957-21

Pappas, P. G., Lionakis, M. S., Arendrup, M. C., Ostrosky-Zeichner, L., and Kullberg, B. J. (2018). Invasive candidiasis. *Nat rev dis primers.* 4:18026. doi: 10.1038/nrdp.2018.26

Pelfrene, E., Mura, M., Cavaleiro Sanches, A., and Cavaleri, M. (2019). Monoclonal antibodies as anti-infective products: a promising future? *Clin. Microbiol. Infect.* 25, 60–64. doi: 10.1016/j.cmi.2018.04.024

Pierce, C. G., Uppuluri, P., Tristan, A. R., Wormley, F. L. Jr., Mowat, E., Ramage, G., et al. (2008). A simple and reproducible 96-well plate-based method for the formation of fungal biofilms and its application to antifungal susceptibility testing. *Nat. Protoc.* 3, 1494–1500. doi: 10.1038/nport.2008.141

Prill, S. K., Klinkert, B., Timpel, C., Gale, C. A., Schröppel, K., and Ernst, J. F. (2005). PMT family of Candida albicans: five protein mannosyltransferase isoforms affect growth, morphogenesis and antifungal resistance. *Mol. Microbiol.* 55, 546–560. doi: 10.1111/j.1365-2958.2004.04401.x

Rachini, A., Pietrella, D., Lupo, P., Torosantucci, A., Chiani, P., Bromuro, C., et al. (2007). An anti-beta-glucan monoclonal antibody inhibits growth and capsule formation of Cryptococcus neoformans in vitro and exerts therapeutic, anticryptococcal activity in vivo. *Infect. Immun.* 75, 5085–5094. doi: 10.1128/iai.00278-07

Ramage, G., Vande Walle, K., Wickes, B. L., and López-Ribot, J. L. (2001). Standardized method for in vitro antifungal susceptibility testing of *Candida albicans* biofilms. *Antimicrob. Agents Chemother.* 45, 2475–2479. doi: 10.1128/aac.45.9.2475-2479.2001

Rudkin, F. M., Raziunaite, I., Workman, H., Essono, S., Belmonte, R., Maccallum, D. M., et al. (2018). Single human B cell-derived monoclonal anti-Candida antibodies enhance phagocytosis and protect against disseminated candidiasis. *Nat. Commun.* 9:5288. doi: 10.1038/s41467-018-07738-1

Ruggero, M. A., and Topal, J. E. (2014). Development of echinocandin-resistant *Candida albicans* candidemia following brief prophylactic exposure to micafungin therapy. *Transpl. Infect. Dis.* 16, 469–472. doi: 10.1111/tid.12230

Ruiz-Herrera, J., Elorza, M. V., Valentín, E., and Sentandreu, R. (2006). Molecular organization of the cell wall of *Candida albicans* and its relation to pathogenicity. *FEMS Yeast Res.* 6, 14–29. doi: 10.1111/j.1567-1364.2005.00017.x

Shukla, M., Chandley, P., and Rohatgi, S. (2021). The role of B-cells and antibodies against Candida vaccine antigens in invasive candidiasis. *Vaccines (Basel)* 9:1159. doi: 10.3390/vaccines9101159

Sukhithasri, V., Nisha, N., Biswas, L., Anil Kumar, V., and Biswas, R. (2013). Innate immune recognition of microbial cell wall components and microbial strategies to evade such recognitions. *Microbiol. Res.* 168, 396–406. doi: 10.1016/j.micres.2013.02.005

Torosantucci, A., Chiani, P., Bromuro, C., De Bernardis, F., Palma, A. S., Liu, Y., et al. (2009). Protection by anti-beta-glucan antibodies is associated with restricted beta-1, 3 glucan binding specificity and inhibition of fungal growth and adherence. *PLoS One* 4:e5392. doi: 10.1371/journal.pone.0005392

Ulrich, S., and Ebel, F. (2020). Monoclonal antibodies as tools to combat fungal infections. *J Fungi (Basel)* 6:22. doi: 10.3390/jof6010022

Wang, Y. (2015). Looking into *Candida albicans* infection, host response, and antifungal strategies. *Virulence* 6, 307–308. doi: 10.1080/21505594.2014.1000752

Wang, X. J., Sui, X., Yan, L., Wang, Y., Cao, Y. B., and Jiang, Y. Y. (2015b). Vaccines in the treatment of invasive candidiasis. *Virulence* 6, 1–7. doi: 10.4161/21505594.2014.983015

Wang, L., Yan, L., Li, X. X., Xu, G. T., An, M. M., and Jiang, Y. Y. (2015a). Vaccination with recombinant non-transmembrane domain of protein Mannosyltransferase 4 improves survival during murine disseminated candidiasis. *Biol. Pharm. Bull.* 38, 1779–1787. doi: 10.1248/bpb.b15-00475

Wisplinghoff, H., Ebbers, J., Geurtz, L., Stefanik, D., Major, Y., Edmond, M. B., et al. (2014). Nosocomial bloodstream infections due to *Candida spp.* in the USA: species distribution, clinical features and antifungal susceptibilities. *Int. J. Antimicrob. Agents* 43, 78–81. doi: 10.1016/j.ijantimicag.2013.09.005

Zhang, S. Q., Zou, Z., Shen, H., Shen, S. S., Miao, Q., Huang, X., et al. (2016). Mnn 10 maintains pathogenicity in *Candida albicans* by extending α-1, 6-mannose backbone to evade host Dectin-1 mediated antifungal immunity. *PLoS Pathog.* 12:e1005617. doi: 10.1371/journal.ppat.1005617

Zurawski, D. V., and Mclendon, M. K. (2020). Monoclonal antibodies as an antibacterial approach Against bacterial pathogens. *Antibiotics (Basel)* 9:155. doi: 10.3390/antibiotics9040155

frontiers | Frontiers in Microbiology

TYPE Original Research
PUBLISHED 20 September 2022
DOI 10.3389/fmicb.2022.992582

OPEN ACCESS

EDITED BY
Weihua Pan,
Shanghai Changzheng Hospital,
China

REVIEWED BY
Mahdi Abastabar,
Mazandaran University of Medical Sciences,
Iran
Shahram Mahmoudi,
Iran University of Medical Sciences, Iran

*CORRESPONDENCE
Kang Liao
liaokang1971@163.com
Yaqin Peng
pyqdream@163.com

†These authors have contributed equally to this work and share first authorship

SPECIALTY SECTION
This article was submitted to Antimicrobials, Resistance and Chemotherapy,
a section of the journal
Frontiers in Microbiology

RECEIVED 12 July 2022
ACCEPTED 22 August 2022
PUBLISHED 20 September 2022

CITATION
Guo P, Chen J, Tan Y, Xia L, Zhang W, Li X, Jiang Y, Li R, Chen C, Liao K and Peng Y (2022) Comparison of molecular and MALDI-TOF MS identification and antifungal susceptibility of clinical *Fusarium* isolates in Southern China.
Front. Microbiol. 13:992582.
doi: 10.3389/fmicb.2022.992582

Comparison of molecular and MALDI-TOF MS identification and antifungal susceptibility of clinical *Fusarium* isolates in Southern China

Penghao Guo[1†], Jianlong Chen[1†], Yiwei Tan[2], Li Xia[3], Weizheng Zhang[4], Xiaojie Li[5], Yujie Jiang[6], Ruiying Li[7], Chunmei Chen[8], Kang Liao[1*] and Yaqin Peng[1*]

[1]Department of Clinical Laboratory, The First Affiliated Hospital, Sun Yat-sen University, Guangzhou, China, [2]Department of Clinical Laboratory, Zhongshan Ophthalmic Center, Sun Yat-Sen University, Guangzhou, China, [3]Department of Clinical Laboratory, Jieyang People's Hospital, Jieyang, China, [4]Department of Clinical Laboratory, Guangzhou No.11 People's Hospital, Guangzhou, China, [5]Department of Clinical Laboratory, The Third Affiliated Hospital, Sun Yat-Sen University, Guangzhou, China, [6]Department of Clinical Laboratory, Central Hospital of Guangdong Nongken, Zhanjiang, China, [7]Department of Clinical Laboratory, The First Affiliated Hospital, Guangdong Pharmaceutical University, Guangzhou, China, [8]Department of Clinical Laboratory, The Seventh Affiliated Hospital, Sun Yat-Sen University, Shenzhen, China

Background: *Fusarium* species are opportunistic causative agents of superficial and disseminated human infections. Fast and accurate identification and targeted antifungal therapy give help to improve the patients' prognosis.

Objectives: This study aimed to evaluate the effectiveness of matrix-assisted laser desorption ionisation time of flight mass spectrometry (MALDI-TOF MS) for *Fusarium* identification, and investigate the epidemiology and antifungal susceptibility profiles of clinical *Fusarium* isolates in Southern China.

Methods: There were 95 clinical *Fusarium* isolates identified by DNA sequencing of translation elongation factor 1-alpha (TEF1α) and MALDI-TOF MS, respectively. Antifungal susceptibility testing of isolates was performed by broth microdilution according to the CLSI approved standard M38-A3 document.

Results: Seven species complexes (SC) with 17 *Fusarium* species were identified. The most prevalent SC was the *F. solani* SC (70.5%, 67/95), followed by the *F. fujikuroi* SC (16.8%, 16/95). *F. keratoplasticum* within the *F. solani* SC was the most prevalent species (32.6%, 31/95). There were 91.6% (87/95) of isolates identified by MALDI-TOF MS at the SC level. In most of species, amphotericin B and voriconazole showed lower MICs compared to itraconazole and terbinafine. The *F. solani* SC showed higher MICs to these antifungal agents compared to the other SCs. There were 10.5% (10/95) of strains with high MICs for amphotericin B (≥8μg/ml), terbinafine (≥32μg/ml) and itraconazole (≥32μg/ml) simultaneously, mostly focusing on *F. keratoplasticum* (9/10).

Conclusion: MALDI-TOF MS exhibited good performance on the identification of *Fusarium* strains at the SC level. The *F. solani* SC was the most prevalent

clinical SC in Southern China. The MICs varied significantly among different species or SCs to different antifungal agents.

KEYWORDS

Fusarium, humans, sequence analysis, mass spectrometry, microbial sensitivity tests

Introduction

The genus *Fusarium* is an important phytopathogen; only a few species can cause a broad spectrum of human infections (Al-Hatmi et al., 2016b; Van Diepeningen and de Hoog, 2016). Almost 70 *Fusarium* species have been reported as opportunistic human pathogens, with the increasing rates of infection over the past years (Tortorano et al., 2014; Triest et al., 2015). The clinical manifestations of *Fusarium* disease are diverse, depending largely on the immune status of the host and the portal of entry (Tortorano et al., 2014). In immunocompetent patients, *Fusarium* species mainly lead to superficial infections such as keratitis and onychomycosis, while the invasive or disseminated infections tend to affect critically ill and immunosuppressed patients with a high mortality rate (Zhao et al., 2021).

The clinically relevant *Fusarium* species are mainly grouped into six species complexes (SC), including the *F. solani* SC (FSSC), *F. oxysporum* SC (FOSC), *F. fujikuroi* SC (FFSC), *F. dimerum* SC (FDSC), *F. incarnatum-equiseti* SC (FIESC), and *F. chlamydosporum* SC (FCSC; Triest et al., 2015). It has been found that antifungal susceptibility may vary among different species within a single species complex (O'Donnell et al., 2008; Al-Hatmi et al., 2015b; Song et al., 2021), which indicates it is necessary to identify the aetiological agent up to the species level for clinical treatment. In the clinical laboratory, these closely related species are often morphologically indistinguishable. Molecular analysis can provide the gold standard for species identification, while it has the disadvantages of being time-consuming and costly. A rapid, simple, cost-effective, and reproducible tool has received increasingly interest for mold identification, i.e., matrix-assisted laser desorption ionisation time of flight mass spectrometry (MALDI-TOF MS; Triest et al., 2015; Al-Hatmi et al., 2015a; Normand et al., 2021). This approach has been found to enhance the correct identification rate of non-*Aspergillus* filamentous fungi with a 31%–61% increase (Ranque et al., 2014). However, more data are needed for the verification and standardization of *Fusarium* identification due to the potential impacts of different instrument platforms and reference spectrum databases on its performance.

In clinic, amphotericin B and azole drugs, e.g., voriconazole and itraconazole, are commonly used for *Fusarium* infection (Nucci and Anaissie, 2007; Tortorano et al., 2014; Oliveira et al., 2020). Amphotericin B or voriconazole is used for the disseminated infections as first-line drugs (Al-Hatmi et al., 2018). *Fusarium* keratitis is mainly treated with voriconazole and natamycin, and the treatment of onychomycosis should include terbinafine, voriconazole and sometimes itraconazole (Al-Hatmi et al., 2018). However, it has been reported that clinical *Fusaria* have relatively decreased susceptibility to these commonly used antifungal drugs (Taj-Aldeen et al., 2016; Rosa et al., 2019). Different patterns of *in vitro* susceptibility have been found in different *Fusarium* species (Song et al., 2021). Remarkably, since neither clinical breakpoints nor epidemiological cutoff values have been established for *Fusarium* according to Clinical and Laboratory Standards Institute (CLSI) M59-3ed (CLSI, 2020) and EUCAST database,[1] information on the correlation between minimum inhibitory concentration (MIC) and drug efficacy is not clear. Given that a limited number of studies on *in vitro* susceptibility are available, more data are necessary for the epidemiology and therapy purpose.

Studies on clinical *fusaria* are limited in Asia, especially in Southern China. In this study, we aim to investigate the prevalence characteristics and antifungal susceptibility profiles of clinical *Fusarium* strains collected from eight hospitals in Southern China. And the effectiveness of *Fusarium* identification by MALDI-TOF MS was also investigated.

Materials and methods

Fusarium strains

Ninety-five clinical *Fusarium* strains were collected from eight hospitals in Southern China between January 2018 and December 2020. These isolates were recovered from corneal scrapings (47.4%, 45/95) and skin secretions (40.0%, 38/95), followed by pus (4.2%, 4/95), blood (4.2%, 4/95), sputum (3.2%, 3/95) and urine (1.0%, 1/95). Duplicated isolates were excluded if they were obtained from the same patient. Given samples were totally collected during routine patient care in this retrospective investigation, the need for informed consent was waived by the institutional review board of the First Affiliated Hospital of Sun Yat-sen University.

The *Fusarium* strains were cultured for 5 days on potato dextrose agar medium at 28°C. All cultures were handled within a class II biological safety cabinet.

1 https://www.eucast.org/

DNA sequencing

A single colony was picked up in a 1.5-ml Eppendorf (EP) tube containing 1.0 ml PBS, with the turbidity adjusted to 1.0 McFarland. DNA extraction was performed using the Yeast Genomic DNA Rapid Extraction Kit (Sangon Biotech, Shanghai, China) according to the manufacturer's instructions.

The sequence of the translation elongation factor 1-alpha gene (TEF1α) was amplified using the primers EF1 (5′-ATGGGTAAGGARGACAAGAC-3′) and EF2 (5′-GGARGTACCAGTSATCATGTT-3′) as previously described with some modifications (O'Donnell et al., 2008). The PCR amplification was conducted in a 50-μL reaction mixture containing 10 μl 10 × PCR buffer, 5 μl templates, 1 μl forward primer, 1 μl reverse primer, 0.5 μl Taq enzyme, 8 μl dNTP mixture, and 24.5 μl double-distilled water. The PCR amplification condition is as follows: 1 cycle of 95°C 10 min; 40 cycles of 95°C 30 s, 56°C 30 s, 72°C 30 s; 1 cycle of 72°C 10 min. The PCR products were subjected to Sanger sequencing (Sangon Biotech, China). The sequences were identified by BLAST analysis in GenBank[2] (Da et al., 2021).

The MALDI-TOF MS analysis

The colonies were picked by sterile swabs in a 1.5-mL EP tube containing 0.9 ml 75% ethanol and 20–30 glass beads, mixed for 2 min. Then the suspension was removed to a new tube for centrifugation at 13,000 rpm for 2 min. The supernatant was removed, and 40 μl freshly prepared 70% formic acid was added to the tube and mixed for 1 min. Then, 40 μl acetonitrile was added to the tube and mixed for 1 min. The tube was centrifuged at 13,000 rpm for 2 min. One μl of supernatant was added on the spot of the target plate, and 1 μl CHCA matrix was added after the 1-μl supernatant dried. After the matrix dried, the target plate was taken to the mass spectrometer's ionization chamber. The mass spectra of the strains were acquired using a VITEK MS Plus (bioMérieux, France) in IVD mode and analyzed by the IVD knowledge base V3.2 for *Fusarium* identification.

The dendrogram showing taxonomic relationships was carried out using VITEK MS RUO/SARAMIS (bioMérieux, France) according to the manufacturer's instructions. Firstly, spectra were manually imported to the SARAMIS™ RUO database version 4.17 using the button "import spectra to spectra database." Then the dendrogram was generated according to the whole spectra. Consensus spectra were analyzed with a single link agglomerative clustering algorithm, applying the relative taxonomy analysis tool of SARAMIS premium software to show the resulting dendrogram with differences and similarities in relative terms (percent matching masses).

For instrument calibration, the *Escherichia coli* strain (ATCC 8739) was applied. And the *Candida glabrata* strain (ATCC MYA-2950) was used as quality control.

In vitro antifungal susceptibility testing

Four commonly antifungal agents (Shanghai Aladdin Bio-Chem Technology Co., Ltd., China), i.e., amphotericin B, voriconazole, itraconazole and terbinafine were included and dissolved in dimethyl sulfoxide to 3.2 mg/ml as stock solutions. The work concentrations of these agents ranged from 0.06 to 32 μg/ml. The broth microdilution was performed according to CLSI M38-A3 method (CLSI, 2017). The colonies were picked up and transferred into a 1.5-ml EP tube containing 1.0 ml PBS, with turbidity adjusted to 0.5 McFarland. The suspensions were then diluted in RPMI 1640 to the desired concentration of 0.4×10^4–5×10^4 CFU/ml by counting on a hemocytometer, 100 μl of which were added in the microdilution plates for 48-h incubation at 35°C. The MICs were defined as the lowest concentration with complete growth inhibition compared to the drug-free growth. MIC_{50} and MIC_{90} values were defined as the lowest concentrations that inhibited the growth of 50% or 90% of the strains. WHONET software version 5.6 was used for determining MIC_{50}, MIC_{90}, geometric mean (GM) and MIC range.

The strains of *Candida parapsilosis* (ATCC 22019) and *Candida krusei* (ATCC 6258) were used as quality controls.

Sequence accession numbers

All sequences identified in this study were deposited in GenBank (ON959267–ON959361).

Results

Identification

The 95 isolates were identified by DNA sequencing of TEF1α as members of 7 species complexes (SC) with 17 *Fusarium* species (Table 1): FSSC (70.5%, 67/95), FFSC (16.8%, 16/95), FOSC (7.4%, 7/95), FDSC (2.1%, 2/95), one isolate of FIESC, FCSC and *F. nisikadoi* SC (FNSC), respectively. The FSSC was the most prevalent SC, including *F. keratoplasticum* (32.6%, 31/95), *F. falciforme* (20.0%, 19/95), *F. solani sensu stricto* (6.3%, 6/95), *F. ambrosium* (5.3%, 5/95), *F. petroliphilum* (4.2%, 4/95) and *F. lichenicola* (2.1%, 2/95). The FFSC included *F. proliferatum* (7.4%, 7/95), *F. sacchari* (3.2%, 3/95), *F. concentricum* (3.2%, 3/95), *F. verticillioides* (2.1%, 2/95) and *F. napiforme* (1.1%, 1/95). The FOSC included *F. oxysporum* (6.3%, 6/95) and one isolate of *F. acutatum*.

For the 45 isolates obtained from cornea scrapings, the detection rates of FSSC, FFSC and FOSC were 73.3% (33/45),

2 http://www.ncbi.nlm.nih.gov/genbank/

TABLE 1 Comparison of identification results of 95 clinical *Fusarium* strains using DNA sequencing of TEF1α and MALDI-ToF MS methods.

DNA sequencing (No.)	MALDI-TOF MS, No.					
	SC level			Species level		
	Correct	Unidentified	Misidentified	Correct	Unidentified	Misidentified
***F. solani* SC (67)**						
F. keratoplasticum (31)	31	0	0	0	31	0
F. falciforme (19)	19	0	0	0	19	0
F. solani sensu stricto (6)	6	0	0	0	6	0
F. ambrosium (5)	5	0	0	0	5	0
F. petroliphilum (4)	4	0	0	0	4	0
F. lichenicola (2)	2	0	0	0	2	0
***F. fujikuroi* SC (16)**						
F. proliferatum (7)	7	0	0	7	0	0
F. sacchari (3)	2	1	0	0	1	2
F. concentricum (3)	1	2	0	0	2	1
F. verticillioides (2)	2	0	0	2	0	0
F. napiforme (1)	0	1	0	0	1	0
***F. oxysporum* SC (7)**						
F. oxysporum (6)	6	0	0	0	6	0
F. acutatum (1)	0	1	0	0	1	0
***F. dimerum* SC (2)**						
F. dimerum (2)	2	0	0	2	0	0
***F. chlamydosporum* SC (1)**						
F. chlamydosporum (1)	0	1	0	0	1	0
***F. incarnatum-equiseti* SC (1)**						
F. incarnatum (1)	0	1	0	0	1	0
***F. nisikadoi* SC (1)**						
F. commune (1)	0	1	0	0	1	0
All isolates	87	8	0	11	81	3

TEF1α, translation elongation factor 1-alpha; MALDI-ToF MS, matrix-assisted laser desorption ionisation time of flight mass spectrometry; SC, species complex.

20.0% (9/45) and 4.4% (2/45), respectively. Both *F. keratoplasticum* (28.9%, 13/45) and *F. falciforme* (28.9%, 13/45) within FSSC were the most common species from cornea scrapings (Figure 1). And 63.2% (24/38) of isolates originating from skin secretions belonged to FSSC, followed by FFSC (13.2%, 5/38) and FOSC (13.2%, 5/38). The most prevalent species from skin secretions was *F. keratoplasticum* (34.2%, 13/38; Figure 1).

MALDI-TOF MS

Comparison of data with DNA sequencing and MALDI-TOF MS is listed in Table 1. The results showed that 91.6% (87/95) of isolates were identified at the SC level by MALDI-TOF MS. For FSSC ($n=67$) and FDSC ($n=2$), all the isolates were correctly recognized. Most of isolates were also identified by MALDI-TOF MS for FFSC (75.0%, 12/16) and FOSC (85.7%, 6/7). However, MALDI-TOF MS correctly identified 11.6% (11/95) of the isolates down to the species level, including all isolates of *F. proliferatum* ($n=7$), *F. verticillioides* ($n=2$) and *F. dimerum* ($n=2$). One isolate of *F. concentricum* and two isolates of *F. sacchari* were misidentified as *F. proliferatum* but were correct at the SC level. Further, we analyzed the MALDI-TOF MS profiles of *Fusarium* species corresponding to the morphological characteristics of cultures. Although it was hard to differentiate them by morphology, the discrepancies of MS profile characteristics were observed significantly among these species (Figure 2).

In the MALDI-TOF dendrogram, almost all of members were found to cluster together in the FSSC except *F. lichenicola* (Figure 3). However, members of FFSC and FOSC were randomly interspersed with those of other species complexes. The strains of the *F. keratoplasticum* within FSSC were found to cluster together in the dendrogram. Differences between *F. proliferatum* and other strains were also unambiguous.

Antifungal susceptibility

The MICs varied among different species complexes to these antifungal agents (Table 2). Compared to itraconazole and terbinafine, voriconazole and amphotericin B showed lower MICs to most of species. *Fusarium* isolates showed variable MICs to

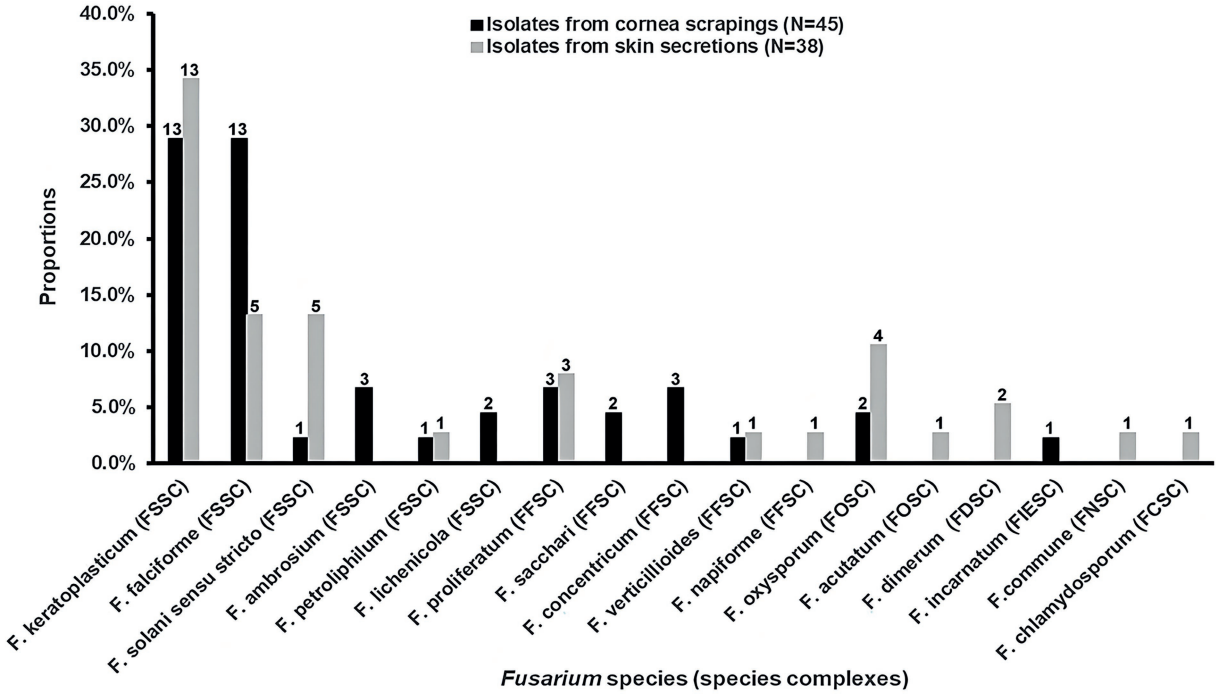

FIGURE 1
The distributions and proportions of *Fusarium* strains among isolates from cornea scrapings and skin secretions, respectively. FSSC, *F. solani* species complex (SC); FFSC, *F. fujikuroi* SC; FOSC, *F. oxysporum* SC; FDSC, *F. dimerum* SC; FIESC, *F. incarnatum-equiseti* SC; FNSC, *F. nisikadoi* SC; FCSC, *F. chlamydosporum* SC.

voriconazole ranging between 0.5 and 16 μg/ml. Amphotericin B had good activity against most of species, with 1–16 μg/ml in FSSC, 1–4 μg/ml in FFSC and 1–2 μg/ml in FOSC, respectively. Interestingly, 10.5% (10/95) of strains for amphotericin B had high MICs (≥8 μg/ml), totally belonging to the FSSC. For itraconazole, 93.7% (89/95) of strains showed high MICs (≥32 μg/ml). There were 76.8% (73/95) of strains with high MICs (≥8 μg/ml) for terbinafine. And terbinafine showed low MICs in FFSC (GM = 2.3 μg/ml) and FCSC (1 μg/ml). Compared to the other species complexes, FSSC presented relatively higher MICs to these antifungal agents.

We further analyzed antifungal activities of species within FSSC (Table 3). The MICs of *Fusarium* isolates to voriconazole ranged from 1 to 16 μg/ml. All strains within FSSC showed high MICs (≥32 μg/ml) for itraconazole. For terbinafine, there were 65.3% (62/95) of strains with highest MICs (≥32 μg/ml). Among the 10 strains with high MICs (≥8 μg/ml) for amphotericin B, nine strains belonged to *F. keratoplasticum* and only one were in *F. falciforme*. Remarkably, high MICs (≥ 32 μg/ml) both for terbinafine and itraconazole were observed among these 10 strains.

Discussion

Along with the rising numbers of severely immunocompromised patients in recent decades, invasive or disseminated *Fusarium* infections with high mortality have been found to increase remarkably (Muhammed et al., 2013; Al-Hatmi et al., 2016a). Considering the relatively low susceptibility of *Fusarium* species to most of commonly used antifungal drugs, the prevalence and resistance profile of clinical *Fusarium* species can contribute to enhance the management of the infection (O'Donnell et al., 2008; Guarro, 2013). As a major challenge, it is lack of an accurate, quick and easy to operate approach for the identification of clinical *Fusarium* strains so far. In most of clinical laboratories, *Fusarium* identification mainly depends on different morphological characteristics of size and shape of macro- and microconidia and presence or absence of chlamydospores as well as colony appearance (Najafzadeh et al., 2020; Da et al., 2021). However, a series of factors can affect the morphological characteristics of cultures such as the temperature, the culture medium and maybe the thickness of the medium (Da et al., 2021). *Fusarium* at the SC level are usually hard to be distinguished by this conventional and time-consuming approach if not for experienced experts.

We observed that MALDI-TOF MS had excellent performance of *Fusarium* identification at the SC level with the correct rate up to 91.6% (87/95), taking DNA sequencing of TEF1α as the gold standard (Herkert et al., 2019; Oliveira et al., 2020; Da et al., 2021). Similar results were achieved by Paziani et al. (94.4%) and Song et al. (95.2%; Paziani et al., 2019; Song et al., 2021). To a large extent, it attributed to a success ratio of 100% correct identifications for the most prevalent SC (FSSC; Table 1). High

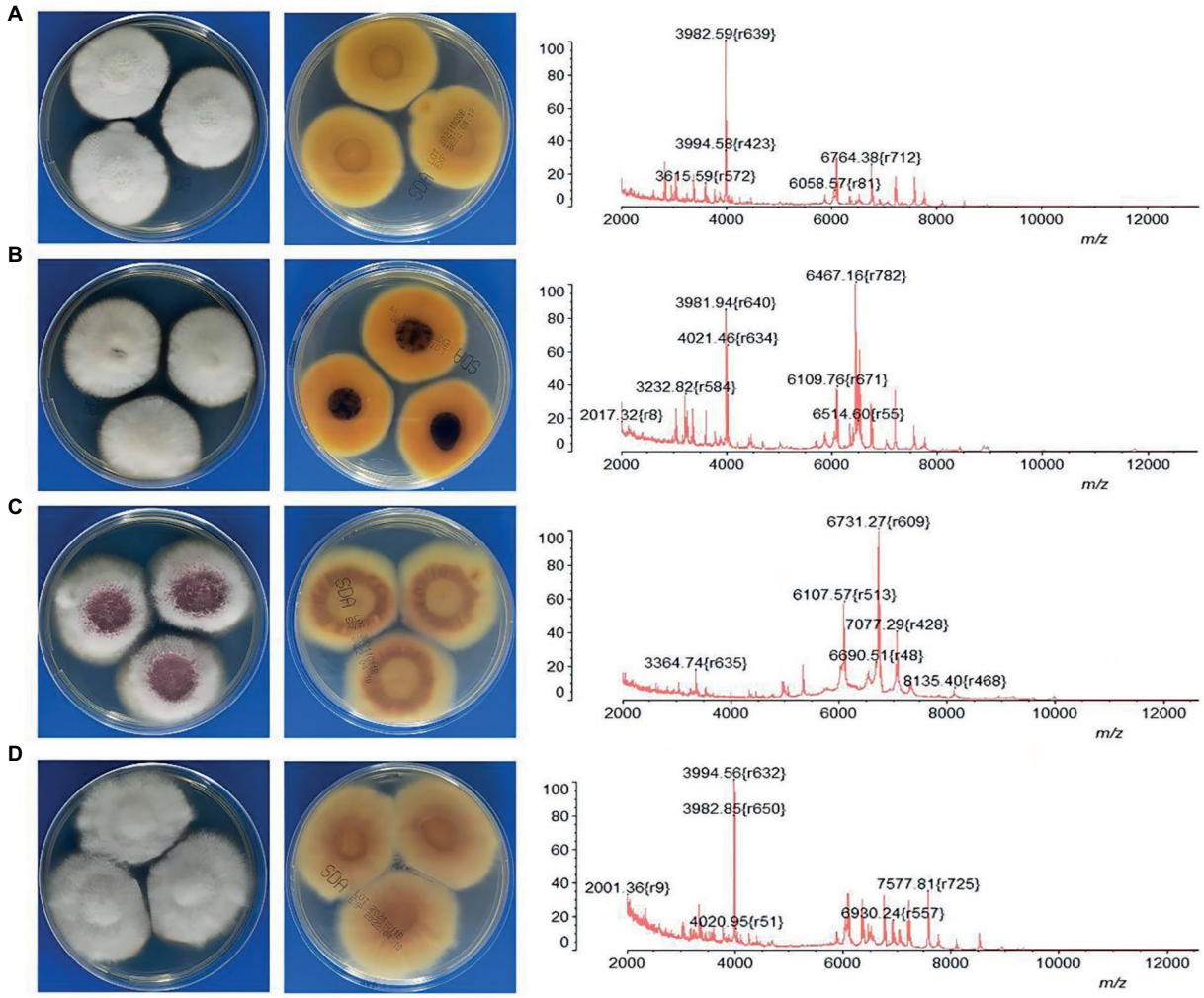

FIGURE 2
The characteristics of MALDI-TOF MS profiles corresponding to the morphologies of four common *Fusarium* species. **(A)** *F. keratoplasticum*; **(B)** *F. falciforme*; **(C)** *F. proliferatum*; **(D)** *F. oxysporum*.

correct rates were also observed for FDSC (100%, 2/2) and FOSC (85.7%, 6/7). For FFSC ($n = 16$), there were four strains unable to be identified by MALDI-TOF MS which were *F. sacchari* ($n = 1$), *F. concentricum* ($n = 2$) and *F. napiforme* ($n = 1$), respectively. Some studies showed good performance of *Fusarium* identification by MALDI-TOF MS down to the species level (Triest et al., 2015; Song et al., 2021). Regrettably, only 11.6% (11/95) of isolates could be correctly identified to the species level in this study. It might be limited by small species and strain representations in commercial libraries (Sleiman et al., 2016). Triest's study presented a correct rate of the identifications (91.0%) to the species level by constructing an in-house reference spectrum database combined with a standardized MALDI-TOF MS assay (Triest et al., 2015). Song et al. found MALDI-TOF MS recognized 89.04% of *Fusarium* species though a combination of the Bruker library and an expanded version in the BMU database (Song et al., 2021). Further studies will be needed to improve species identification in our laboratory. In the dendrogram, we found all strains except one clustered together in the FSSC, which was similar as Triest's finding (Triest et al., 2015). However, most of members of the other species complexes were randomly distributed. Normand et al. also demonstrated about 30% of the strains clustered correctly in the dendrograms (Herkert et al., 2019). Given the identification probably depends on recognition of a limited number of conserved proteins regardless of intraspecific variability, phylogenetic interpretation of MALDI-TOF data is not recommended.

The discrepancy of *Fusarium* distribution has been thought to be associated with several factors such as geographical regions, clinical patient populations and infection sites. When being judged from numerous literature data, members of *fusaria* encountered in human infections are mostly found in three species complexes: FSSC, FFSC, and FOSC. FSSC is considered as the most frequently detected SC worldwide, mainly causing superficial infections such as keratitis and onychomycosis under tropical and subtropical climatic conditions, especially in Asia and

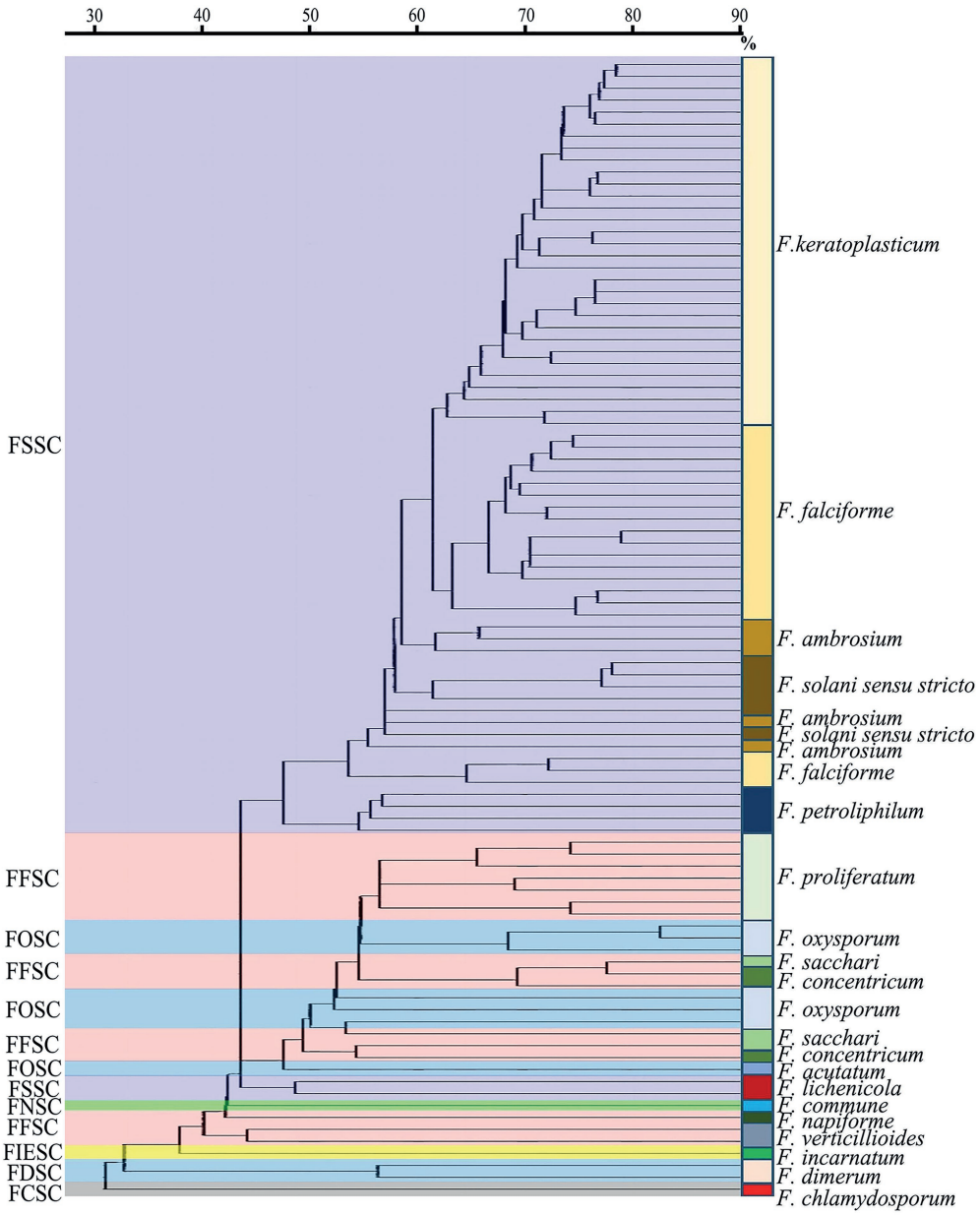

FIGURE 3
The MALDI-ToF dendrogram of 95 clinical *Fusarium* strains. FSSC, *F. solani* species complex (SC); FFSC, *F. fujikuroi* SC; FOSC, *F. oxysporum* SC; FNSC, *F. nisikadoi* SC; FIESC, *F. incarnatum-equiseti* SC; FDSC, *F. dimerum* SC; FCSC, *F. chlamydosporum* SC.

Latin America (Castro López et al., 2009; Salah et al., 2015; Sun et al., 2015; Guevara-Suarez et al., 2016; Muraosa et al., 2017; Rosa et al., 2017; Tupaki-Sreepurna et al., 2017; Dallé da Rosa et al., 2018; Najafzadeh et al., 2020). Several studies showed FFSC to be the prevalent SC in some areas such as Iran and Turkey, whereas FOSC was more common in Europe (Dalyan Cilo et al., 2015; Abastabar et al., 2018; Oliveira et al., 2019; Najafzadeh et al., 2020; Walther et al., 2021). Our results demonstrated FSSC (70.5%, 67/95) was the most prevalent group mainly originating from corneal scrapings (33/45), followed by FFSC (16.8%, 16/95) and FOSC (7.4%, 7/95). The prevalence of *Fusarium* SC here showed similar as Song's finding in Northern China and Sun's finding in central China (Sun et al., 2015; Song et al., 2021).

There were 40.0% (38/95) of isolates in this study that were obtained from skin secretions, a proportion of which were collected from inpatients with burns or diabetes mellitus (data not shown). Severe burns and poorly controlled diabetes are thought to be high risk factors for invasive mold infections (Nucci and Anaissie, 2007; Enoch et al., 2017). However, little is known about the epidemiology of *Fusarium* strains causing locally invasive skin infection in patients with burns or diabetes mellitus, limited by sporadic case reports (Nucci and Anaissie, 2002; Taj-Aldeen et al.,

10.3389/fmicb.2022.992582

TABLE 2 Activities of antifungal agents against seven *Fusarium* species complexes (SC).

SC (No.)	Antifungal agents MIC (μg/ml)			
	Voriconazole	Itraconazole	Amphotericin B	Terbinafine
***F. solani* SC (67)**				
MIC_{50}	2	≥32	2	≥32
MIC_{90}	8	≥32	8	≥32
MIC range	1–16	≥32	1–16	4–≥32
GM MIC	2.8	32.0	2.9	28.3
***F. fujikuroi* SC (16)**				
MIC_{50}	2	≥32	1	2
MIC_{90}	4	≥32	2	4
MIC range	1–8	2–≥32	1–4	1–4
GM MIC	2.4	19.0	1.5	2.3
***F. oxysporum* SC (7)**				
MIC_{50}	4	≥32	2	≥32
MIC_{90}	8	≥32	2	≥32
MIC range	1–8	4–≥32	1–2	1–≥32
GM MIC	3.0	23.8	1.5	11.9
***F. dimerum* SC (2)**				
MIC range	2	≥32	1–2	4–8
***F. chlamydosporum* SC (1)**				
MIC	0.5	1	0.5	1
***F. nisikadoi* SC (1)**				
MIC	8	≥32	0.25	≥32
***F. incarnatum-equiseti* SC (1)**				
MIC	4	≥32	2	≥32

MIC, minimal inhibitory concentration; MIC_{50}, the lowest concentration that inhibited the growth of half of the strains; MIC_{90}, the lowest concentration that inhibited the growth of 90% of the strains; GM MIC, the geometric mean of MICs.

2006; Pai et al., 2010; Atty et al., 2014; Rosanova et al., 2016; Karadag et al., 2020; Tram et al., 2020; Liza et al., 2021). We observed 63.2% (24/38) of isolates from skin secretions belonged to FSSC. Limited by incomplete clinical data here, further studies will be needed to investigate the association of *Fusarium* strains and locally invasive skin infection among these patients. Remarkably, we found one isolate of *F. commune* obtained from skin secretion. *F. commune* within FNSC has been reported as a plant pathogen (Mezzalama et al., 2021; Wang et al., 2022). To the best of our knowledge, this is the first to report this species in clinical specimens.

In Nucci's review, *F. solani sensu stricto* was regarded as the most common species, followed by *F. oxysporum* and *F. verticillioides* (Nucci and Anaissie, 2007). However, the three most common species were *F. falciforme* and *F. keratoplasticum*, followed by *F. oxysporum* in Al-Hatmi's review (Al-Hatmi et al., 2016a). Song et al. demonstrated the most prevalent species was *F. solani sensu stricto* (93.8%, 135/144) within the FSSC, and *F. verticillioides* (60.6%, 40/66) within the FFSC (Song et al., 2021). Walther et al. presented *F. petroliphilum* within the FSSC was the most prevalent species (Walther et al., 2021). We here found that 46.3% (31/67) of isolates belonged to *F. keratoplasticum* within the FSSC, followed by *F. falciforme* (28.4%, 19/67) and *F. solani sensu stricto* (9.0%, 6/67). For FFSC, *F. proliferatum* (43.8%, 7/16) was the most common species. Given species-specific differences in antifungal susceptibility, the discrepancy of species distribution should be considered on the treatment options.

Currently, most of *Fusarium* infection still based on empirical antifungal therapy. A limited number of studies on *in vitro* susceptibility were available, showing variable results. In this study, antifungal susceptibility profiles of 95 strains were analyzed for four commonly used agents, i.e., amphotericin B, voriconazole, itraconazole and terbinafine. Our results showed high MICs for itraconazole (93.7%, MIC ≥ 32 μg/ml) and terbinafine (76.8%, MIC ≥ 8 μg/ml) in most of species. Rosa et al. presented higher MICs (≥64 μg/ml) for itraconazole and terbinafine in general (Rosa et al., 2017), while more than 50% of *Fusarium* strains were sensitive to these agents in Sun's study (Sun et al., 2015). Here, terbinafine showed low MICs in FFSC (GM = 2.3 μg/ml), showing similar results as Song's study (Song et al., 2021). However, Song et al. presented good activities for terbinafine against FSSC (GM = 2.4 μg/ml) and FOSC (GM = 2.5 μg/ml), which were significantly different from our results (Table 3). For voriconazole, it is thought to be clinically effective against *Fusarium* spp., despite variable *in vitro* activity (Walther et al., 2021). Similarly, the MICs for voriconazole here

TABLE 3 Activities of antifungal agents against different species in *F. solani* species complex.

Species (No.)	Antifungal agents MIC(μg/ml)			
	Voriconazole	Itraconazole	Amphotericin B	Terbinafine
***F. keratoplasticum* (31)**				
MIC_{50}	2	≥32	4	≥32
MIC_{90}	4	≥32	8	≥32
MIC range	1–8	≥32	2–16	≥32
GM MIC	2.6	32.0	4.4	32.0
***F. falciforme* (19)**				
MIC_{50}	2	≥32	2	≥32
MIC_{90}	8	≥32	4	≥32
MIC range	1–8	≥32	1–8	8–≥32
GM MIC	2.4	32.0	2.4	29.7
***F. solani sensu stricto* (6)**				
MIC_{50}	4	≥32	2	≥32
MIC_{90}	4	≥32	2	≥32
MIC range	4	≥32	1–2	8–≥32
GM MIC	4.0	32.0	1.8	25.4
***F. ambrosium* (5)**				
MIC_{50}	8	≥32	1	8
MIC_{90}	16	≥32	1	≥32
MIC range	2–16	≥32	1–2	4–≥32
GM MIC	7.0	32.0	1.3	10.6
***F. petroliphilum* (4)**				
MIC_{50}	4	≥32	2	≥32
MIC_{90}	4	≥32	2	≥32
MIC range	2–4	≥32	1–2	≥32
GM MIC	3.4	32.0	1.7	32.0
***F. lichenicola* (2)**				
MIC range	1–2	≥32	2	≥32

MIC, minimal inhibitory concentration; MIC_{50}, the lowest concentration that inhibited the growth of half of the strains; MIC_{90}, the lowest concentration that inhibited the growth of 90% of the strains; GM MIC, the geometric mean of MICs.

ranged from 0.5 to 16 μg/ml. Castro López et al. showed *F. solani sensu stricto* had the highest MIC for voriconazole (Castro López et al., 2009). Interestingly, here the MIC of all the *F. solani sensu stricto* strains was 4 μg/ml for voriconazole. In line with our results, several studies showed low MICs for amphotericin B to the majority of isolates (Al-Hatmi et al., 2015b; Rosa et al., 2017; Oliveira et al., 2019, 2020). Remarkably, we observed 10.5% (10/95) of strains with high MICs for amphotericin B (≥8 μg/ml), terbinafine (≥32 μg/ml) and itraconazole (≥32 μg/ml) simultaneously, which were totally belonged to the FSSC. More attentions should be paid on these multi-resistance strains within the FSSC. It is worth noting that information on the relationships between low MIC and clinical response to therapy is still unavailable due to lack of species-specific clinical breakpoints.

Our study has some limitations. Clinical data was not fully collected, preventing us to decipher whether these clinical isolates were related to proven fusariosis or could be associated with contamination of organs. In summary, our results demonstrated that MALDI-TOF MS exhibited good performance on the identification of *Fusarium* strains at the SC level. In most of species, amphotericin B and voriconazole showed lower MICs compared to itraconazole and terbinafine. *F. keratoplasticum* within the FSSC was the most prevalent species in southern China, showing relatively high MICs for these antifungal agents. Further studies will be needed for investigating the correlations of low and high MICs with the prognosis of patients as well as the resistance mechanisms of *Fusarium* strains.

Data availability statement

The data presented in the study are deposited in the GenBank repository, accession number ON959267–ON959361.

Author contributions

KL and YP participated in research design and data analysis. PG participated in the writing of the manuscript and data analysis. JC performed the experiments. YT, LX, WZ, XL, YJ, RL, and CC

participated in the collection of *Fusarium* strains. All authors contributed to the article and approved the submitted version.

Conflict of interest

The authors declare that the research was conducted in the absence of any commercial or financial relationships that could be construed as a potential conflict of interest.

Publisher's note

References

Abastabar, M., Al-Hatmi, A., Vafaei, M. M., de Hoog, G. S., Haghani, I., Aghili, S. R., et al. (2018). Potent activities of luliconazole, lanoconazole, and eight comparators against molecularly characterized *Fusarium* species. *Antimicrob. Agents Chemother.* 62. doi: 10.1128/AAC.00009-18

Al-Hatmi, A., Bonifaz, A., Ranque, S., Sybren, D. H. G., Verweij, P. E., and Meis, J. F. (2018). Current antifungal treatment of fusariosis. *Int. J. Antimicrob. Agents* 51, 326–332. doi: 10.1016/j.ijantimicag.2017.06.017

Al-Hatmi, A. M., Hagen, F., Menken, S. B., Meis, J. F., and de Hoog, G. S. (2016a). Global molecular epidemiology and genetic diversity of *Fusarium*, a significant emerging group of human opportunists from 1958 to 2015. *Emerg. Microbes Infect.* 5:e124. doi: 10.1038/emi.2016.126

Al-Hatmi, A. M., Meis, J. F., and de Hoog, G. S. (2016b). *Fusarium*: molecular diversity and intrinsic drug resistance. *PLoS Pathog.* 12:e1005464. doi: 10.1371/journal.ppat.1005464

Al-Hatmi, A. M., Normand, A. C., van Diepeningen, A. D., Hendrickx, M., de Hoog, G. S., and Piarroux, R. (2015a). Rapid identification of clinical members of *Fusarium fujikuroi* complex using MALDI-TOF MS. *Future Microbiol.* 10, 1939–1952. doi: 10.2217/fmb.15.108

Al-Hatmi, A. M., van Diepeningen, A. D., Curfs-Breuker, I., de Hoog, G. S., and Meis, J. F. (2015b). Specific antifungal susceptibility profiles of opportunists in the *Fusarium fujikuroi* complex. *J. Antimicrob. Chemother.* 70, 1068–1071. doi: 10.1093/jac/dku505

Atty, C., Alagiozian-Angelova, V. M., and Kowal-Vern, A. (2014). Black plaques and white nodules in a burn patient. *Fusarium* and Mucormycosis. *JAMA Dermatol* 150, 1355–1356. doi: 10.1001/jamadermatol.2014.2463

Castro López, N., Casas, C., Sopo, L., Rojas, A., del Portillo, P., Cepero de García, M. C., et al. (2009). *Fusarium* species detected in onychomycosis in Colombia. *Mycoses* 52, 350–356. doi: 10.1111/j.1439-0507.2008.01619.x

CLSI (2017). *Reference Method for Broth Dilution Antifungal Susceptibility Testing of Filamentous Fungi. CLSI Standard M38, 3rd Edn*. Wayne, PA: Clinical and Laboratory Standards Institute.

CLSI (Ed.) (2020). "Epidemiological cutoff values for antifungal susceptibility testing," in *CLSI supplement M59. 3rd Edn*. (Wayne, PA: Clinical and Laboratory Standards Institute)

Da, R. P., Aquino, V., Fuentefria, A. M., and Goldani, L. Z. (2021). Diversity of *Fusarium* species causing invasive and disseminated infections. *J. Mycol. Med.* 31:101137. doi: 10.1016/j.mycmed.2021.101137

Dallé da Rosa, P., Nunes, A., Borges, R., Batista, B., Meneghello Fuentefria, A., and Goldani, L. Z. (2018). In vitro susceptibility and multilocus sequence typing of *Fusarium* isolates causing keratitis. *J. Mycol. Med.* 28, 482–485. doi: 10.1016/j.mycmed.2018.05.001

Dalyan Cilo, B., al-Hatmi, A. M. S., Seyedmousavi, S., Rijs, A. J., Verweij, P. E., Ener, B., et al. (2015). Emergence of fusarioses in a university hospital in Turkey during a 20-year period. *Eur. J. Clin. Microbiol. Infect. Dis.* 34, 1683–1691. doi: 10.1007/s10096-015-2405-y

Enoch, D. A., Yang, H., Aliyu, S. H., and Micallef, C. (2017). The changing epidemiology of invasive fungal infections. *Methods Mol. Biol.* 1508, 17–65. doi: 10.1007/978-1-4939-6515-1_2

Guarro, J. (2013). Fusariosis, a complex infection caused by a high diversity of fungal species refractory to treatment. *Eur. J. Clin. Microbiol. Infect. Dis.* 32, 1491–1500. doi: 10.1007/s10096-013-1924-7

Guevara-Suarez, M., Cano-Lira, J. F., Cepero de García, M. C., Sopo, L., de Bedout, C., Cano, L. E., et al. (2016). Genotyping of *Fusarium* isolates from onychomycoses in Colombia: detection of two new species within the *Fusarium solani* species complex and in vitro antifungal susceptibility testing. *Mycopathologia* 181, 165–174. doi: 10.1007/s11046-016-9983-9

Herkert, P. F., al-Hatmi, A. M. S., de Oliveira Salvador, G. L., Muro, M. D., Pinheiro, R. L., Nucci, M., et al. (2019). Molecular characterization and antifungal susceptibility of clinical *Fusarium* species from Brazil. *Front. Microbiol.* 10:737. doi: 10.3389/fmicb.2019.00737

Karadag, A. S., Cebeci, F., Aslan Kayıran, M., Özakkaş, F., Çobanoğlu, B., Kuru, B. C., et al. (2020). *Fusarium solani* infection in a diabetic patient treated with itraconazole and debridement. *Dermatol. Ther.* 33:e14203. doi: 10.1111/dth.14203

Liza, D., Divya, D., Kirti, G., Mahesh, P., Bhanu, M., et al. (2021). Eumycetoma of the foot due to *Fusarium solani* in a person with diabetes mellitus: report of a case and review of literature. *Mycopathologia* 186, 277–288. doi: 10.1007/s11046-020-00524-y

Mezzalama, M., Guarnaccia, V., Martino, I., Tabome, G., and Gullino, M. L. (2021). First report of *Fusarium* commune causing root and crown rot on maize in Italy. *Plant Dis.* 105:4156. doi: 10.1094/PDIS-01-21-0075-PDN

Muhammed, M., Anagnostou, T., Desalermos, A., Kourkoumpetis, T. K., Carneiro, H. A., Glavis-Bloom, J., et al. (2013). *Fusarium* infection: report of 26 cases and review of 97 cases from the literature. *Medicine (Baltimore)* 92, 305–316. doi: 10.1097/MD.0000000000000008

Muraosa, Y., Oguchi, M., Yahiro, M., Watanabe, A., Yaguchi, T., and Kamei, K. (2017). Epidemiological study of *Fusarium* species causing invasive and superficial fusariosis in Japan. *Med. Mycol. J.* 58, E5–E13. doi: 10.3314/mmj.16-00024

Najafzadeh, M. J., Dolatabadi, S., de Hoog, S., Esfahani, M. K., Haghani, I., Aghili, S. R., et al. (2020). Phylogenetic analysis of clinically relevant *Fusarium* species in Iran. *Mycopathologia* 185, 515–525. doi: 10.1007/s11046-020-00460-x

Normand, A. C., Imbert, S., Brun, S., al-Hatmi, A. M. S., Chryssanthou, E., Cassaing, S., et al. (2021). Clinical origin and species distribution of *Fusarium* spp. isolates identified by molecular sequencing and mass spectrometry: a European multicenter hospital prospective study. *J. Fungi.* 7:246. doi: 10.3390/jof7040246

Nucci, M., and Anaissie, E. (2002). Cutaneous infection by *Fusarium* species in healthy and immunocompromised hosts: implications for diagnosis and management. *Clin. Infect. Dis.* 35, 909–920. doi: 10.1086/342328

Nucci, M., and Anaissie, E. (2007). *Fusarium* infections in immunocompromised patients. *Clin. Microbiol. Rev.* 20, 695–704. doi: 10.1128/CMR.00014-07

O'Donnell, K., Sutton, D. A., Fothergill, A., McCarthy, D., Rinaldi, M. G., Brandt, M. E., et al. (2008). Molecular phylogenetic diversity, multilocus haplotype nomenclature, and in vitro antifungal resistance within the *Fusarium solani* species complex. *J. Clin. Microbiol.* 46, 2477–2490. doi: 10.1128/JCM.02371-07

Oliveira, D. S. C., Kolwijck, E., van der Lee, H. A., Tehupeiory-Kooreman, M. C., al-Hatmi, A. M. S., Matayan, E., et al. (2019). In vitro activity of Chlorhexidine compared with seven antifungal agents against 98 *Fusarium* isolates recovered from fungal keratitis patients. *Antimicrob. Agents Chemother.* 63:e02669-18. doi: 10.1128/AAC.02669-18

Oliveira, D. S. C., Kolwijck, E., van Rooij, J., Stoutenbeek, R., Visser, N., Cheng, Y. Y., et al. (2020). Epidemiology and clinical management of *Fusarium* keratitis in the Netherlands, 2005-2016. *Front. Cell. Infect. Microbiol.* 10:133. doi: 10.3389/fcimb.2020.00133

Pai, R., Boloor, R., Shreevidya, K., and Shenoy, D. (2010). *Fusarium solani*: an emerging fungus in chronic diabetic ulcer. *J. Lab. Physicians* 2, 037–039. doi: 10.4103/0974-2727.66710

Paziani, M. H., Tonani Carvalho, L., Melhem, M. S. C., Almeida, M. T. G., Nadaletto Bonifácio da Silva, M. E., Martinez, R., et al. (2019). First comprehensive report of clinical *Fusarium* strains isolated in the state of Sao Paulo (Brazil) and identified by MALDI-TOF MS and molecular biology. *Microorganisms* 8:66. doi: 10.3390/microorganisms8010066

Ranque, S., Normand, A. C., Cassagne, C., Murat, J. B., Bourgeois, N., Dalle, F., et al. (2014). MALDI-TOF mass spectrometry identification of filamentous fungi in the clinical laboratory. *Mycoses* 57, 135–140. doi: 10.1111/myc.12115

Rosa, P. D., Heidrich, D., Correa, C., Scroferneker, M. L., Vettorato, G., Fuentefria, A. M., et al. (2017). Genetic diversity and antifungal susceptibility of *Fusarium* isolates in onychomycosis. *Mycoses* 60, 616–622. doi: 10.1111/myc.12638

Rosa, P., Ramirez-Castrillon, M., Borges, R., Aquino, V., Meneghello, F. A., Zubaran, G. L., et al. (2019). Epidemiological aspects and characterization of the resistance profile of *Fusarium* spp. In patients with invasive fusariosis. *J. Med. Microbiol.* 68, 1489–1496. doi: 10.1099/jmm.0.001059

Rosanova, M. T., Brizuela, M., Villasboas, M., Guarracino, F., Alvarez, V., Santos, P., et al. (2016). *Fusarium* spp. infections in a pediatric burn unit: nine years of experience. *Braz. J. Infect. Dis.* 20, 389–392. doi: 10.1016/j.bjid.2016.04.004

Salah, H., Al-Hatmi, A. M., Theelen, B., Abukamar, M., Hashim, S., van Diepeningen, A. D., et al. (2015). Phylogenetic diversity of human pathogenic *Fusarium* and emergence of uncommon virulent species. *J. Infect.* 71, 658–666. doi: 10.1016/j.jinf.2015.08.011

Sleiman, S., Halliday, C. L., Chapman, B., Brown, M., Nitschke, J., Lau, A. F., et al. (2016). Performance of matrix-assisted laser desorption ionization-time of flight mass spectrometry for identification of *Aspergillus*, *Scedosporium*, and *Fusarium* spp. in the Australian clinical setting. *J. Clin. Microbiol.* 54, 2182–2186. doi: 10.1128/JCM.00906-16

Song, Y., Liu, X., Yang, Z., Meng, X., Xue, R., Yu, J., et al. (2021). Molecular and MALDI-TOF MS differentiation and antifungal susceptibility of prevalent clinical *Fusarium* species in China. *Mycoses* 64, 1261–1271. doi: 10.1111/myc.13345

Sun, S., Lyu, Q., Han, L., Ma, Q., Hu, H., He, S., et al. (2015). Molecular identification and in vitro susceptibility of *Fusarium* from fungal keratitis in Central China. *Zhonghua Yan Ke Za Zhi* 51, 660–667. doi: 10.3760/cma.j.issn.0412-4081.2015.09.005

Taj-Aldeen, S. J., Gene, J., Al, B. I., Buzina, W., Cano, J. F., and Guarro, J. (2006). Gangrenous necrosis of the diabetic foot caused by *Fusarium acutatum*. *Med. Mycol.* 44, 547–552. doi: 10.1080/13693780500543246

Taj-Aldeen, S. J., Salah, H., Al-Hatmi, A. M., Hamed, M., Theelen, B., van Diepeningen, A. D., et al. (2016). In vitro resistance of clinical *Fusarium* species to amphotericin B and voriconazole using the EUCAST antifungal susceptibility method. *Diagn. Microbiol. Infect. Dis.* 85, 438–443. doi: 10.1016/j.diagmicrobio.2016.05.006

Tortorano, A. M., Richardson, M., Roilides, E., van Diepeningen, A., Caira, M., Munoz, P., et al. (2014). ESCMID and ECMM joint guidelines on diagnosis and management of hyalohyphomycosis: *Fusarium* spp., *Scedosporium* spp. and others. *Clin. Microbiol. Infect.* 20, 27–46. doi: 10.1111/1469-0691.12465

Tram, Q. A., Minh, N. T. N., Anh, D. N., Lam, N. N., Dung, T. N., Thi Minh Chau, N., et al. (2020). A rare case of fungal burn wound infection caused by *Fusarium solani* in Vietnam. *J. Investig. Med. High Impact Case Rep.* 8:232470962091212. doi: 10.1177/2324709620912122

Triest, D., Stubbe, D., De Cremer, K., Pierard, D., Normand, A. C., Piarroux, R., et al. (2015). Use of matrix-assisted laser desorption ionization-time of flight mass spectrometry for identification of molds of the *Fusarium* genus. *J. Clin. Microbiol.* 53, 465–476. doi: 10.1128/JCM.02213-14

Tupaki-Sreepurna, A., Al-Hatmi, A. M., Kindo, A. J., Sundaram, M., and de Hoog, G. S. (2017). Multidrug-resistant *Fusarium* in keratitis: a clinico-mycological study of keratitis infections in Chennai, India. *Mycoses* 60, 230–233. doi: 10.1111/myc.12578

Van Diepeningen, A. D., and de Hoog, G. S. (2016). Challenges in *Fusarium*, a trans-kingdom pathogen. *Mycopathologia* 181, 161–163. doi: 10.1007/s11046-016-9993-7

Walther, G., Zimmermann, A., Theuersbacher, J., Kaerger, K., von Lilienfeld-Toal, M., Roth, M., et al. (2021). Eye infections caused by filamentous fungi: spectrum and antifungal susceptibility of the prevailing agents in Germany. *J. Fungi* 7:511. doi: 10.3390/jof7070511

Wang, H., Hou, X., Huang, X., Gao, M., Chen, T., Gao, Q., et al. (2022). First report of *Fusarium* commune causing leaf spot disease on *Bletilla striata* in China. *Plant Dis.* 106:1070. doi: 10.1094/PDIS-07-21-1486-PDN

Zhao, B., He, D., and Wang, L. (2021). Advances in *Fusarium* drug resistance research. *J. Glob. Antimicrob. Resist.* 24, 215–219. doi: 10.1016/j.jgar.2020.12.016

frontiers | Frontiers in Microbiology

TYPE Original Research
PUBLISHED 05 October 2022
DOI 10.3389/fmicb.2022.1007576

OPEN ACCESS

EDITED BY
Weihua Pan,
Shanghai Changzheng Hospital, China

REVIEWED BY
Wenqiang Chang,
Shandong University, China
Wenjuan Wu,
Tongji University School of Medicine, China

*CORRESPONDENCE
Yuanying Jiang
jiangyy@smmu.edu.cn
Bing Han
hbshcn@163.com
Yongbing Cao
ybcao@vip.sina.com

†These authors have contributed equally to this work

SPECIALTY SECTION
This article was submitted to Antimicrobials, Resistance, and Chemotherapy, a section of the journal Frontiers in Microbiology

RECEIVED 30 July 2022
ACCEPTED 16 September 2022
PUBLISHED 05 October 2022

CITATION
Wang X, Wang X, Cai T, Qin Y, Li L, Jiang Y, Han B and Cao Y (2022) Development and validation of a sensitive LC-MS/MS method for determination of intracellular concentration of fluconazole in *Candida albicans*. *Front. Microbiol.* 13:1007576. doi: 10.3389/fmicb.2022.1007576

Development and validation of a sensitive LC-MS/MS method for determination of intracellular concentration of fluconazole in *Candida albicans*

Xiaofei Wang[1,2,3†], Xiaojuan Wang[2,4†], Tongkai Cai[1,2], Yulin Qin[2,4], Ling Li[1], Yuanying Jiang[2*], Bing Han[4*] and Yongbing Cao[1*]

[1]Institute of Vascular Disease, Shanghai TCM-Integrated Hospital, Shanghai University of Traditional Chinese Medicine, Shanghai, China, [2]School of Pharmacy, Naval Medical University, Shanghai, China, [3]Department of Pharmacy, Mudanjiang First People's Hospital, Mudanjiang, China, [4]Department of Pharmacy, Minhang Hospital, Fudan University, Shanghai, China

Systemic candidiasis is the fourth leading cause of healthcare-associated infections worldwide. The combination therapy based on existing antifungal agents is well-established to overcome drug resistance and restore antifungal efficacy against drug-resistant strains. In this study, a simple and sensitive liquid chromatography with tandem mass spectrometry (LC-MS/MS) method was developed to quantify the intracellular fluconazole (FLC) content in the opportunistic human fungal pathogen *Candida albicans*. The cell lysates were prepared by lysing *C. albicans* cells with Precellys homogenizers and FLC was extracted with methylene chloride. The entire extraction approach was simple, precise and reliable. The extracts were separated on a Zorbax SB-C18 column using a mobile phase of acetonitrile (solvent A) and deionized water plus 0.1% formic acid. FLC and ketoconazole (KCZ, internal standard) were monitored in positive mode using electrospray ionization source. The multiple reaction monitoring transitions (precursor to product) were monitored for FLC m/z 307.1 → 238.2 and for the internal standard KCZ m/z 531.2 → 489.1. The linear for this method were in the range from 5.0 to 1000.0 ng/mL. The precision and accuracy of the samples were relative standard deviations (RSD) < 1.0% for intra-day and RSD < 0.51% for inter-day. The overall recovery of FLC from samples was higher than 77.61%. Furthermore, this method was successfully applied and validated in 36 clinical isolated strains. Taken together, we established a highly accurate, efficient, and reproducible method for quantifying the intracellular content of FLC in *C. albicans*.

KEYWORDS

fluconazole, *Candida albicans*, liquid-liquid extraction, LC-MS/MS, intracellular concentration

Introduction

Candida albicans (*C. albicans*) is one of the most common commensal fungal species located in the gastrointestinal and reproductive tracts of healthy individuals, causing both mucosal and systemic infections in immunocompromised individuals (Brown et al., 2012; de Oliveira Santos et al., 2018; Quindós et al., 2018). Systemic candidiasis is a serious healthcare-associated infection in Europe and US, and associated with high mortality rates (40%) among hospitalized patients, particularly in individuals with hematological malignancies, undergoing major surgery, cytotoxic chemotherapy, and organ transplantation (Magill et al., 2014; Bongomin et al., 2017; Pappas et al., 2018; Hou et al., 2022). Currently, fluconazole (FLC), a highly selective inhibitor of fungal cytochrome P-450 sterol C-14 alpha-demethylation, is the most widely administered antifungal for treating invasive, life-threatening fungal infections (Robbins et al., 2017; Revie et al., 2018). However, high administration frequency and long duration treatment of FLC contribute to the rising number of drug resistant *C. albicans* worldwide (Berkow and Lockhart, 2017; Campitelli et al., 2017; Pristov and Ghannoum, 2019). The primary mechanism of drug resistance is the reduction of intracellular accumulation of azole in *C. albicans*, due to reduced drug uptake or increased drug efflux (Arendrup and Patterson, 2017; Wiederhold, 2017). Therefore, the development of new therapeutic agents to restore *C. albicans* susceptibility to FLC is an effective strategy for the treatment of fungal infections.

The use of drug combination therapy has been successfully implemented for difficult-to-treat infections, such as malaria, tuberculosis, and AIDS (Robbins et al., 2017). Indeed, combination therapy represents an effective method to overcome the emergence of drug-resistant fungi and decrease toxicity (Zacchino et al., 2017; Ribeiro de Carvalho et al., 2018). However, many studies have shown results that range from antagonism to synergy effects due to the different concentrations of each drug combination (Johnson et al., 2004; Campitelli et al., 2017; Tome et al., 2018). The discrepancy may be caused by different measurements of intracellular drug content. In order to accurately detect the intracellular concentration, high performance liquid chromatography with tandem mass spectrometry (HPLC–MS/MS) was used to measure the intracellular FLC levels in *C. albicans*. At present, several fast HPLC–MS/MS methods have been validated and reported for monitoring the antifungal drug concentration in plasma or other body liquid, including FLC, itraconazole, and other antifungal agents (Van De Steene and Lambert, 2008; Tang et al., 2010; Zhang et al., 2011; Alebic-Kolbah and Modesitt, 2012; Beste et al., 2012; Zgoła-Grześkowiak and Grześkowiak, 2013; de Moraes et al., 2014; Wadsworth et al., 2017; Różalska et al., 2018; Xiang et al., 2018). Actually, quantitative analysis of FLC in *C. albicans via* HPLC-MS/MS has not been reported. In this study, we developed a specific, reliable and sensitive liquid chromatography with tandem mass spectrometry (LC-MS/MS) method for determining the intracellular levels of FLC in *C. albicans*.

Materials and methods

Strains and growth conditions

The FLC-resistant *C. albicans* strains NOs. 100 and 103 were obtained from Changhai hospital (MIC_{80} > 1,024 μg/mL). In addition, 36 clinical isolated strains of FLC-resistant or FLC-sensitive *C. albicans* were obtained from Tianjin University. All strains were stored with 15% glycerol at −80°C and subcultured on sabouraud dextrose agar (SDA) plates (4% dextrose, 1.8% agar, and 1% peptone) at 30°C. Exponentially growing *C. albicans* cells were routinely grown in yeast-peptone-dextrose (YPD) liquid medium (2% peptone, 2% dextrose, and 1% yeast extract) at 30°C in a shaking incubator overnight for the following experiments.

Chemicals and reagents

FLC and ketoconazole (KCZ) (> 99.0%) were purchased from Sigma-Aldrich (St Louis, MO, USA). Acetonitrile was liquid chromatography (LC) grade and purchased from Merck (Darmstadt, Germany). HPLC-grade formic acid was purchased from Tedia Company (Fairfield, OH, USA). Dichloromethane, sodium hydroxide and dimethyl sulfoxide were purchased from Shanghai Chemical Reagent Company (Shanghai, China). Deionized water was prepared from Milli-Q water purifying system (Millipore Corporation, Bedford, MA, USA). Methanol was purchased from Merck (Darmstadt, Germany).

Internal standards and calibration standards

FLC and KCZ were weighed and solved in methanol at a concentration of 1.00 mg/mL, respectively. Working solution of FLC (100, 10, and 1.0 μg/mL) was prepared by the dilution of the stock solution. The stock solution of KCZ and H_2O were mixed to obtain working solution at a concentration of 100 μg/mL. Stock solutions were stored at −70°C and the standard solutions were prepared immediately before use.

Liquid chromatography with tandem mass spectrometry conditions

The LC-MS/MS analysis was performed using the triple quadrupole mass spectrometer (Aglient 6410A, Santa Clara,

USA) in the selected reaction monitoring (SRM) mode. The columns were chromatographic column Zorbax SB-C18 column (3.5 μm, 100 mm × 2.1 mm i.d., Agilent, Palo Alto, CA). The mobile phase was composed of acetonitrile (solvent A) and 0.1% formic acid in distilled deionized water (solvent B), a 40:60 (v/v) mixture of solvent A and B. Flow rate was 0.3 mL/min; run time was 2.3 min. The column temperature was maintained at 35°C and the injection volume was 10 μ L.

The LC-MS/MS conditions were as follows: electrospray ionization (ESI) in positive mode; capillary voltage, 4,000 V; vaporizer temperature, 40°C; atomization gas (nitrogen) pressure, 0.276 MPa; desolution gas (nitrogen) temperature, 350°C, flow rate, 10.0 L/min. The collision gas (high purity nitrogen) pressure was 0.1 MPa. Half width of the mass spectrum was 0.7 amu. The mass spectrometer was operated under multiple reaction monitoring (MRM) modes with collision energy of 18 eV for FLC and 40 eV for KCZ. The following MRM transitions (precursor to product) were monitored for FLC m/z 307.1 → 238.2 and for the internal standard (IS) KCZ m/z 531.2 → 489.1 (**Table 1**).

Sample preparation

Candida albicans lysates preparation

The logarithmic growth *C. albicans* was harvested and re-suspended to 5 × 10^9 CFU/mL with YPD liquid medium. FLC stock solution (1 mg/mL) were added to the suspension. The final concentration of *C. albicans* was adjusted to 5 × 10^7 CFU/mL and FLC concentration was diluted to 16 μg/mL. The mixture was incubated at 30°C with agitation at 200 rpm for 16 h. Subsequently, *C. albicans* cells were collected by centrifuging the suspension for 30 s at 5,000 × *g*. Samples were washed for four times with equivalent volume of the original culture medium and centrifuged to remove residual medium and FLC. After that, the precipitation was resuspended and centrifuged four times at 16,200 × *g* to remove the liquid. 500.0 mg of fungal cells were added to the Eppendorf tube together with a volume of 1.5 mL deionized water and 180.0 μL 0.5 mm glass beads, 180.0 μL 0.1 mm glass beads, 180.0 μL 1 mm ceramic bead and two 3 mm ceramic beads. All samples were crushed in a Precellys 24 biological sample homogenizer (Bertin Technologies, Montignyle-Bretonneux, France) with the following protocol: 6,500 rpm/min, 30 s, 3 times, interval of 30 s; 3 cycles, interval of 5 min. All samples were kept on ice during the circulation interval. *C. albicans* lysates solution was harvested after centrifugation.

TABLE 1 Optimized MRM (multiple reaction monitoring) parameters for FLC and KCZ.

	Precursor ion (m/z)	Fragmentor energy (V)	Collision energy (eV)	Product ion (m/z)
FLC	307.1	80.0	18.0	238.2
KCZ (IS)	531.2	100.0	40.0	489.1

Candida albicans lysates extraction

The *C. albicans* lysates solution (100 μL) was added into a centrifuge tube containing internal standard solution, 20.0 μL KCZ (1.0 μg/mL) and 10.0 μL NaOH (20.0 μg/mL). After vortexing for 30 s, 3.0 mL of dichloromethane (CH_2Cl_2) was finally added and mixed thoroughly. The liquid system was divided into two layers after 10 min centrifugation at 9,982 × *g*. Next, 2.4 mL of liquid was removed from the lower layer and the CH_2Cl_2 phase was transferred into a clean centrifuge tube and evaporated to dryness in the centrifugal thickener (35°C heat, heat time: 50 min, run time: 200 min). After that, 80 μL of mobile phase [acetonitrile: 0.1% formic acid = 40:60 (v/v)] was added to the evaporated sample tubes and vortex-mixed for 1 min. The liquid was transferred to a new 1.5 mL centrifuge tube and centrifuged at 21,000 × *g* for 10 min. Following, the supernatant was then transferred to the vial (containing the inner tube) for LC-MS/MS analysis.

Validation of the liquid chromatography with tandem mass spectrometry method

The validation including selectivity, matrix effect, linearity, precision, and accuracy, the limits of detection (LOD) and quantification (LOQ), extraction recovery and stability were conducted in accordance with the regulatory guidelines on bioanalytical method validation.

Selectivity

The product ions of m/z 307.1→238.2 (FLC) and m/z 531.2→489.1 (KCZ) were analyzed by full scanning, and the fragment ions were used as product ions monitored during the quantitative analysis.

Linearity

The linearity was investigated by analyzing a seven-point (5.0, 10.0, 50.0, 100.0, 200.0, 500.0, and 1,000.0 ng/mL) calibration curve of FLC in *C. albicans* lysate in triplicate. Calibration curve were constructed by plotting the peak area ratios of FLC/internal standard vs. the concentrations of FLC in *C. albicans* lysate, using weighted ($1/c^2$) least squares linear regression. Slope, intercept, and correlation coefficient were calculated as regression parameters by using a 1/x weighed linear regression.

Precision and accuracy

Precision and accuracy were assessed in within-run (repeatability and accuracy in 1 day) and between-run

conditions (intermediate precision and intermediate accuracy). Precision was calculated as relative standard deviations (RSD) in percentage, whereas accuracy was calculated as relative error (RE) in percentage, between a nominal concentration value in the calibration sample and a concentration obtained from the calibration curve. Low, medium and high concentrations of FLC (10.0, 100.0, and 500.0 ng/mL, respectively) were used to analyze intra-day precision and accuracy. Moreover, five replicates of each sample at low, medium and high concentration levels were analyzed on the same day. The assay was performed in three consecutive days to evaluate inter-day precision and accuracy.

Limit of detection and limit of quantification

LOD and LOQ were determined by spiking a decreasing concentration of the mixed stock solution into blank *C. albicans* lysate. The LOD was defined as the lowest concentration point at which the instrument exhibits a signal-to-noise (S/N) ratio equal to 3. The LOQ was defined as the lowest concentration reliably quantified and fulfilled the criteria of not exceeding ± 20% mean relative error (MRE) and < 20% RSD.

Extraction recovery and matrix effect

The samples were spiked with blank *C. albicans* lysate and prepared with FLC final concentrations of 10.0, 100.0, and 500.0 ng/mL. The extractions of the samples containing different concentrations of FLC were prepared as described in section "*Candida albicans* lysates extraction." Then, the samples extractions and different concentrations of FLC standard solution were detected by LC-MS/MS. The extraction recovery rates of samples containing different concentrations of FLC were obtained by comparing the chromatographic peak areas of the same concentration of extraction sample and the FLC standard solution.

In order to develop a reliable and reproducible method, the matrix effect was also investigated. The matrix effect was evaluated by the following experiment. Triplicates of QC samples at three levels of FLC and IS were added into 100 μL *C. albicans* lysates and water separately, and then the spiked samples were pretreated with exactly the same procedure as described in *Candida albicans* lysates preparation section. Then, the samples extractions were detected by LC-MS/MS. Comparison of the chromatograms of the blank and the spiked *C. albicans* lysates was used to assay the selectivity of the method. The matrix effect was determined by observing the signal of the chromatogram.

Stability

Stability of FLC in extracted samples was evaluated at three concentrations (high, medium, low) in triplicate under different conditions, including three freeze (−80°C)/thaw (25°C) cycles, 1-month storage in −20°C or 6 h storage at room temperature. The post-preparative stability was also evaluated by keeping samples in mobile phase at room temperature for 24 h.

Statistical analysis

GraphPad Prism 9 was applied to analyze the statistical significance of data. At least three independent replicates were conducted for all experiments unless otherwise stated and $P < 0.05$ was considered statistically significant. For multiple comparisons, *P*-values were calculated by using one-way analysis of variance (ANOVA). For single comparison, *P*-values were calculated by using two-tailed Student's *t*-test.

Results

Liquid chromatography with tandem mass spectrometry optimization

The suitable internal standard was selected to correct the errors that might occur in each process of sample pretreatment, and it is especially important to correct errors caused by instrument instability when mass spectrometry was used as a detector. Internal standards are usually required to have same or similar structural and physical and chemical properties as the analyte. Therefore, KCZ was chosen as the internal standard of this experiment. The structure of KCZ has a certain similarity compared with FLC. In the positive ESI mode, the analyte and IS formed predominately protonated molecular ions $[M + H]^+$ in full scan mass spectra. **Figure 1** displayed product ion spectra of $[M + H]^+$ ions from two compounds. Two fragment ions were observed in the product ion spectra. The major fragment ions at m/z 307.1→238.2 and m/z 531.2→489.1 were chosen in the MRM acquisition for FLC and IS, respectively. Moreover, KCZ was not detected in *C. albicans* lysate. Hence, KCZ met the conditions as an internal standard.

Sample preparation

In order to make the intracellular FLC fully release from *C. albicans*, efficient and flexible Precellys 24 biological sample homogenizer offered by Bertin technologies was used for grinding samples prior to analysis. The method could make the cell wall broken completely and conducive to the extraction and separation of FLC from the *C. albicans* cells. Moreover, the method was simple and efficient. At the beginning of the study, liquid-liquid extraction solvents such as methyl tertiary butyl ether, ethyl acetate or dichloromethane were investigated to process biological samples. After dissolved with the mobile phase [A phase is acetonitrile, B phase is water (containing 0.1% formic acid), A:B = 40:60 (v/v)], the liquid samples were detected by LC-MS/MS. Our results showed that the extraction recovery rate significantly increased to about 81%, and more importantly, samples obtained were clean with less impurities when dichloromethane was used

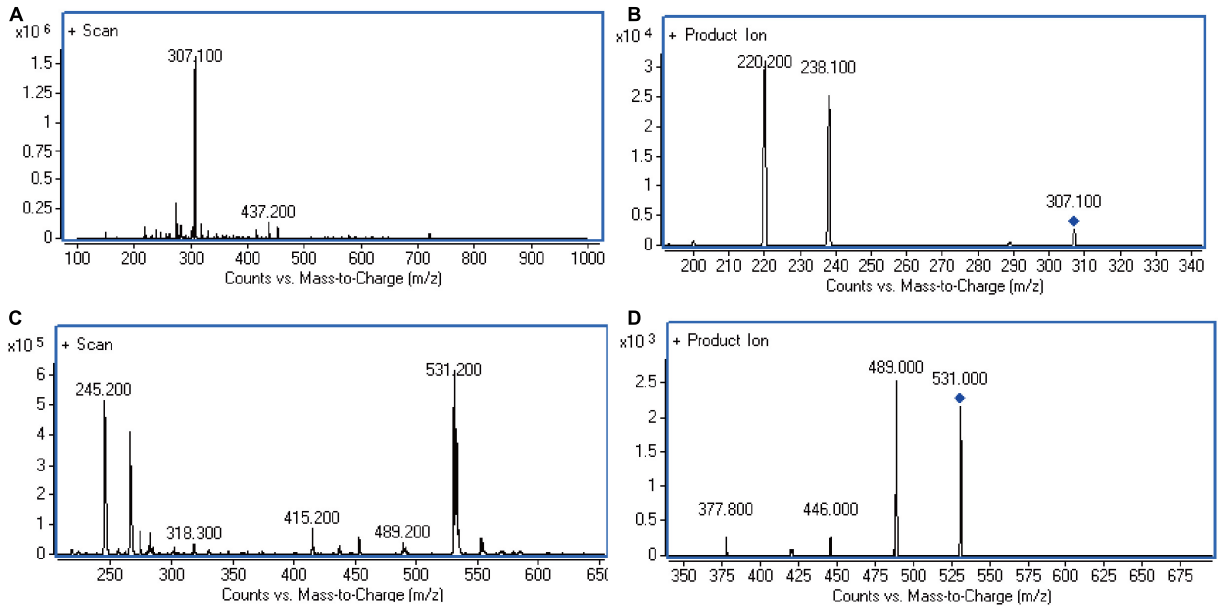

FIGURE 1
LC-MS/MS chromatograms. **(A)** Full-scan of FLC in standard solution. **(B)** Product ion of FLC in standard solution. **(C)** Full-scan of KCZ in internal standard solution. **(D)** Product ion of KCZ in internal standard solution. The representative results of three independent experiments are shown.

with a small amount of sodium hydroxide (Table 2). Indeed, when samples were re-dissolved and liquid samples were injected after the mobile phase, ideal peak shapes with highest extraction recovery rate (∼ 81%) were observed. Therefore, liquid-liquid extraction to treat *C. albicans* lysate samples was used with dichloromethane and a small amount of sodium hydroxide.

Validation

Selectivity

The LC–MS/MS detection has high selectivity that only ions generated from the selected precursor ions can be monitored. Comparison the chromatograms of the blank and the spiked *C. albicans* lysate, the retention times of the analytes and the IS has no significant interference (Figure 2). The retention time of FLC and KCZ were 1.06 and 1.49 min, respectively. The endogenous impurities in *C. albicans* lysates did not interfere with determination of FLC and KCZ, indicating that the method was specific for FLC analysis in *C. albicans*.

TABLE 2 Extract recovery of FLC (n = 3).

Theoretical concentration (%)	**100.00**
Methyl tert-butyl-ether (%)	30.51 ± 4.45
Ethyl acetate (4 μL of 5 mol sodium hydroxide, %)	67.28 ± 7.76
Ethyl acetate (40 μL of 2 mol ammonia water, %)	44.19 ± 6.51
Dichloromethane (40 μL of 2 mol ammonia water, %)	65.28 ± 4.13
Dichloromethane (4 μL of 5 mol sodium hydroxide, %)	81.30 ± 8.96

Linearity

The calibration curves were linear ranging from 5.0 to 1000.0 ng/mL with the correlation coefficient was 0.9963. The results showed that the standard curve equation of FLC in *C. albicans* lysates solution was Y = 0.1742C–2.8763 (n = 5). Moreover, the LOQ was 5.0 ng/mL. The standard curve of FLC in *C. albicans* lysate is shown in Figure 3.

Precision and accuracy

Precision and accuracy were determined by replicating the analyses of three known concentrations over the calibration curve on 3 different days. The intra-day accuracy ranged from −12.9 to 10.8%, and the precision ranged from 1.00 to 1.54% (Table 3). The inter-day accuracy and precision were −12.6 ∼11.6% and 0.51 ∼ 0.85%, respectively. The deviation of the measured concentrations from the true value was reached ± 15% of nominal (theoretical) concentrations. These results demonstrated that the method was reproducible and accurate.

Extraction recovery and matrix effect

We evaluated the extraction recoveries of FLC at three different concentrations (10.0, 100.0, and 500.0 ng/mL). As shown in Table 4, the extraction relative recoveries of low, medium, and high concentrations were 87.10 ± 0.09%, 110.82 ± 1.62%, and 88.87 ± 13.64%, respectively. High

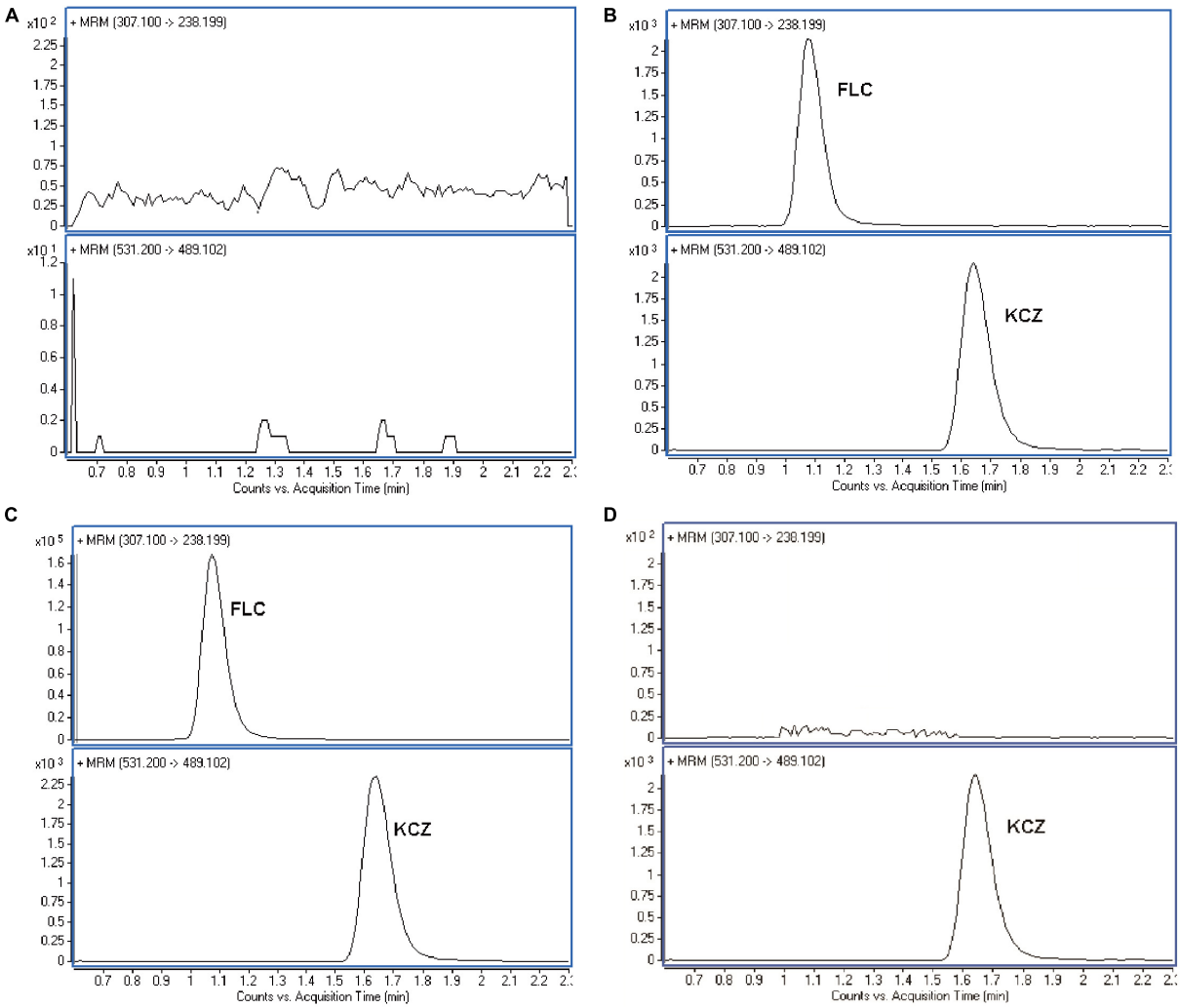

FIGURE 2
Representative MRM chromatograms of FLC in *C. albicans* lysate. **(A)** Blank sample. **(B)** Blank sample with FLC and KCZ (internal standard). **(C)** The testing *C. albicans* lysate. **(D)** Blank sample with KCZ (internal standard). The representative results of three independent experiments are shown.

extraction recoveries were observed in *C. albicans* lysate samples, suggesting that extraction efficiency ensured FLC stability. The results of matrix effect experiments showed that there was no significant difference between the peak areas of samples prepared from *C. albicans* lysate and water, indicating that no co-eluting unknown compounds had apparent effect on the ionization of analytes and IS (Figure 2).

Limit of detection and limit of quantification

The LOD of FLC was 0.5 ng/mL with an RSD of 2.38%. The present LC–MS/MS method offered an LOQ 5.0 ng/mL with an accuracy of −7.6% in terms of RE and a precision of 5.42% in terms of RSD (n = 5). This indicated a highly sensitive method was established.

Stability

FLC remained stable during sample preparation and storage. The stability of FLC was evaluated under various conditions and summarized in Table 5. The relative deviation of samples undergoing the three freeze (−80°C)-thawed (25°C) cycle was RSD < 2.5%, RSD < 2.1%, and RSD < 3.4% for samples in low, medium and high-quality control samples, respectively. In addition, RSD < 3.8%, RSD < 9.5%, and RSD < 6.1% was observed for samples treated in the mobile phase at room temperature for 24 h in low, medium, and high quality control samples. Moreover, the content of FLC was no significant decreased while *C. albicans* lysate samples has been stored at −20°C for 30 days. Relative recovery was more than 94.69% in all the quality control samples, indicating that FLC was stable in *C. albicans* lysate during the whole analytical process.

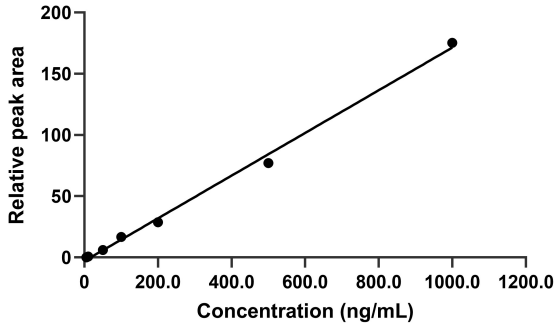

FIGURE 3
Plot of back-calculated concentrations of calibration standards of FLC. The standard curve equation was Y = 0.1742C−2.8763 (n = 5). The limits of detection for this method were in the range from 5.0 to 1000.0 ng/mL. The representative results of three independent experiments are shown.

TABLE 3 Intra-day and inter-day assay precision and accuracy of FLC in *C. albicans* lysate samples (n = 5).

Conditions	Concentration (ng/mL)	Accuracy (%)	Precision (%)
Intra-day	10.0	−12.9	1.00
	100.0	10.8	1.46
	500.0	−11.1	1.54
Inter−day	10.0	−12.6	0.51
	100.0	11.6	0.68
	500.0	−10.9	0.85

TABLE 4 Recovery of FLC in *C. albicans* lysate samples (n = 5).

Drug	Nominal concentration (ng/mL)	Measured concentration (ng/mL)	Relative recovery (%)	RSD (%)
FLC	10.0	8.71 ± 0.09	87.10 ± 0.09	1.00
	100.0	110.82 ± 1.62	110.82 ± 1.62	1.46
	500.0	444.36 ± 6.84	88.87 ± 13.64	1.54

Application to clinical *Candida albicans* strains

The method validated in this study was applied to clinical isolated *C. albicans* strains, including FLC-sensitive and FLC-resistant strains. **Figures 4A,B** showed the concentrations changes in FLC-resistant strains NO. 100 and NO. 103 treated with 4 and 64 μg/mL FLC, respectively. The concentration of intracellular FLC in *C. albicans* were gradually increased and then decreased during the 48 h detect time, with a maximum level at 24∼36 h. Furthermore, the concentration of FLC was also measured in 36 clinical isolated *C. albicans* that was incubation with FLC at a concentration of 1.0 μg/mL. As shown in **Figure 4C**, the mean intracellular concentration of fluconazole in FLC-sensitive *C. albicans* strains (green columns) was significantly higher than FLC-resistant *C. albicans* (red columns). However, no major differences in the intracellular FLC concentration were observed between several sensitive strains (strain13, 14, and 19) and the majority of FLC-resistant strains. Although the reason for this discrepancy is unclear, it might result from the different expression of drug efflux genes in *C. albicans* cell wall, including *CDR1*, *CDR2,* and *MDR1* (Kofla et al., 2011; Rocha et al., 2017; Dhasarathan et al., 2021; Xu et al., 2021).

Discussion

The effective combination-based therapy is a feasible regimen for the majority of refractory infections disease. FLC represents one of the most commonly available antifungal drugs in clinical practice (Lu et al., 2021). Our previous research has shown that the combination of FLC and berberine (BBR) has a significant synergistic against FLC-resistant *C. albicans*, but the synergistic effect was not observed in FLC-sensitive *C. albicans* (Quan et al., 2006). To elucidate whether FLC exerts discrepant effects against *C. albicans* due to intracellular FLC, we performed LC-MS/MS approach to quantify the concentration of FLC in *C. albicans* strains. LC-MS/MS is frequently used as a detector to monitor selected ions and specific fragment ions generated by the ions. Currently, available assays for detecting intracellular FLC include bioassays, gas chromatography assays, and high-performance liquid chromatographic methods. In this study, a sensitive and convenient LC-MS/MS method for the determination of intracellular levels of FLC in *C. albicans* was developed and validated.

Indeed, it is well known that sample extraction plays a particular role in LC analysis, especially for small volume samples requiring purification. The conventional sample preparation approaches of *C. albicans* lysates for LC analysis include protein precipitation, liquid-liquid extraction or solid phase extraction (Diez et al., 2005; Beste et al., 2012). Although drug extraction rate prepared by solid phase extraction is higher and the sample is clean and automated solid phase extraction instrument can achieve rapid pretreatment of large samples, this method is rarely used because of the expensive columns. Compared to protein precipitation and solid phase extraction, liquid-liquid extraction is one of the most commonly used methods for sample pretreatment (Kim et al., 2018). Relatively pure samples can be obtained by using liquid-liquid extraction with low cost, but this method is not suitable to the low extraction rate or instability drugs.

In the present study, a simple sample preparation and extraction protocol including the use of Precellys homogenizers and methylene chloride for FLC extraction were optimized to provide adequate sensitivity, appropriate samples cleanliness,

TABLE 5 Freeze thawing of FLC in *C. albicans* lysate samples (n = 3).

Storage conditions (n = 3)	Nominal concentration FLC (ng/mL)	Calculation concentration FLC (ng/mL)		
		Mean	Relative recovery (%)	RSD (%)
Pre-preparative stability (25°C, 6 h)	10.00	9.84	98.40	3.88
	100.00	103.47	103.47	6.05
	500.00	512.44	102.49	9.59
Pre-preparative stability (25°C, 24 h)	10.00	9.88	98.87	3.77
	100.00	94.69	94.69	9.42
	500.00	531.06	106.21	6.05
Long-term storage stability (−20°C, 30 days)	10.00	9.97	99.73	3.21
	100.00	101.26	101.26	7.59
	500.00	505.99	101.20	6.96
Three freeze (−80°C) and thaw (25°C) cycles	10.00	9.60	96.01	2.45
	100.00	110.99	110.99	2.00
	500.00	552.88	110.58	3.36

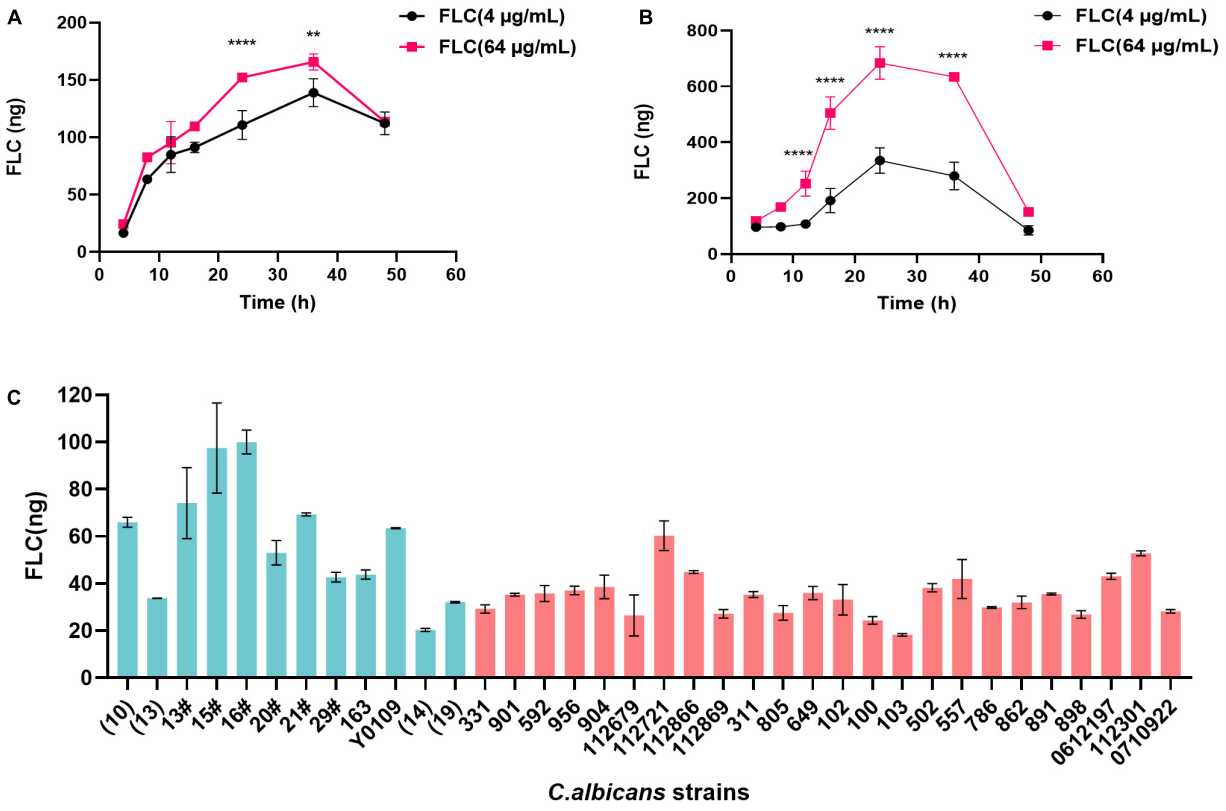

FIGURE 4
Intracellular levels of FLC in 500.0 mg wet *C. albicans* samples. **(A)** Levels of FLC in samples derived from NO. 103 FLC-resistant *C. albicans* strain at different time points. **(B)** Levels of FLC in samples derived from NO. 100 FLC-resistant *C. albicans* strain at different time points. **(C)** Levels of FLC in *C. albicans* samples after 1-h incubation with 1 μg/mL FLC. The green columns represent FLC-sensitive *C. albicans* strains, and the red columns represent FLC-resistant *C. albicans* strains. Data are mean ± SD from triplicates of one representative experiment of three. $^{**}P < 0.01$, $^{****}P < 0.0001$ [**(A,B)**, one-way analysis of variance (ANOVA)].

excellent recovery rate. The method was fully validated based on international guidelines and all evaluated parameters met the pre-established criteria (Zimmer, 2014). Moreover, the suitability of the method was applied to 36 clinical isolated *C. albicans* strains.

In order to release the intracellular FLC of *C. albicans*, efficient and flexible Precellys 24 biological sample homogenizer offered by Bertin technologies was applied for grinding samples prior to analysis. Moreover, the sample preparation method was further optimized by using glass beads to homogenize *Candida* cells. The glass beads allowed the cell wall broken completely, facilitating the extraction and isolation of FLC from *C. Candida* cells. The integrity of the *C. albicans* cell was observed under the microscope and the protein content was determined after extraction. Importantly, this extraction method based on the release of FLC from cell breakage was simple and not laborious. It can be used in routine microbiology laboratories to quantify FLC in fungi and improve experimental operation to increase the reproducibility and accuracy.

Internal standard with similar structural and physicochemical properties provides multiple advantages in HPLC-MS/MS bioanalytical process, including reduction of analysis run time, improvement of the intra-injection reproducibility, reduction of matrix and ionization effects (Bergeron et al., 2009). KCZ and FLC have the similar structural and physicochemical properties and belong to the same antifungal drug class. Our results demonstrated that using KCZ as the internal standard was feasible (**Table 1**). Subsequently, the characteristics of LC-MS/MS approach, including selectivity, linearity, LOD, LOQ, precision, accuracy, extraction recovery, matrix effect, and stability were validated (**Tables 2–5** and **Figures 1–3**).

Furthermore, the established LC-MS/MS method was validated in 36 clinical isolated *C. albicans* strains. According to **Figures 4A,B**, the concentration of FLC *C. albicans* cells was low at the early stage therapeutic exposures. Specifically, intracellular drug concentrations were gradually increased, reaching the maximum concentration between 24 and 36 h, and then gradually decreased over time. We speculate that the changes of FLC concentration may be due to the logarithmic reproduction of *C. albicans* after 24 h culture, as the most active division and reproduction of *C. albicans*. During this stage, a large number of substances need to be absorbed from the culture medium for reproduction, and thus FLC was more efficiently untaken by *C. albicans*. With the rapid increase in the number of *C. albicans* and the continuous consumption of culture media, *C. albicans* become tolerant to drugs, and the efflux of intracellular drugs continues to increase, resulting in decreased content of intracellular drug after 36 h.

The intracellular content of FLC is not the same among different *C. albicans* strains in the same co-culture time (**Figure 4C**). The intracellular FLC content of a majority of sensitive *C. albicans* is significantly higher than that of drug-resistant *C. albicans*, which may be due to membrane permeability or the high expression of *CDR1*, *CDR2,* and *MDR1* in FLC-resistant *C. albicans* strains, and the reduction of intracellular azole drug content caused by drug efflux (Kofla et al., 2011; Rocha et al., 2017; Dhasarathan et al., 2021; Xu et al., 2021). However, the results also showed that intracellular FLC content of FLC-sensitive *C. albicans* strains (strain 13, 14, and 19) is lower than most of FLC-resistant *C. albicans* strains. Mechanisms of FLC-resistance amongst *C. albicans* isolates are highly variable and often clade specific, the nuances of which are still being elucidated (Perea et al., 2001; Flowers et al., 2015).

To investigate whether the intracellular FLC content can be affected in the presence of other drugs which exhibits synergistic effects with FLC against FLC-resistant *C. albicans* 103 strain, we applied the established approach to detect the intracellular FLC content in the combination of Flos Rosae Chinensis (FRC), BBR, or other herbal extracts derived from the traditional Chinese medicine and FLC. The results showed that the effects of different drugs on intracellular concentration of FLC were diverse. Among these drugs exhibiting synergistic anti-FLC-resistant *C. albicans* activity with FLC, some drugs did increase the intracellular concentration of FLC at the different time points analyzed, some drugs did not affect the intracellular FLC concentration, but some drugs even decreased the intracellular concentration of FLC (data not shown). These data indicated that the mechanisms of these synergistic effects were different from each other. Given the complex and heterogeneity of resistance mechanisms, further investigations are required to explore the exact molecular mechanisms underlying these phenomena. In addition, detection of intracellular FLC content when applying our approach to a combination therapy regimen may be affected by other compounds, such as phosphorus-containing compounds can adsorb onto active sites in the sample flow path, particularly at trace levels, compromising the accuracy of the chromatography. Furthermore, some compounds are more difficult to elute from the column, such as BBR, requiring additional elution time to resolve this. However, combination drugs that affect the stability of FLC have not been encountered.

Taken together, we developed a LC-MS/MS approach, providing a highly accurate, efficient, and reproducible method for quantifying the intracellular concentration of FLC in *C. albicans*. However, the present study has several limitations. First, this LC-MS/MS method was applied to 36 clinical isolated *C. albicans* strains, more clinical isolated *C. albicans* strains would be needed to further investigate this relationship between intracellular drug concentration of FLC-sensitive and FLC-resistant *C. albicans*. Second, the combination therapy regimens can be easily implemented to treat fungal infections (Iyer et al., 2020). Our current easy-to-use detection method may further obtain data on the intracellular drug concentration to explore the underlying mechanism of synergistic antifungal therapy by increasing the intracellular drug content. Third,

whether the differences of drug concentration between FLC-sensitive and FLC-resistant *C. albicans* is related to membrane permeability or drug efflux genes needs to be further investigated.

Data availability statement

The original contributions presented in the study are included in the article/supplementary material, further inquiries can be directed to the corresponding author/s.

Author contributions

XFW, XJW, YJ, BH, and YC conceptualized the study design. XFW, XJW, TC, and LL conducted experiments. XJW, YQ, and LL wrote the manuscript. YJ, BH, and YC supervised the study and revised the manuscript. All authors contributed to the article and approved the submitted version.

Funding

This research was supported by the National Natural Science Foundation of China (grant nos. 81872910, 81673478, 82103095, and 82104242), the Shanghai Key Basic Research Project (grant no. 19JC1414900), the Shanghai Traditional Chinese Medicine New Interdisciplinary Program and the Natural Science Foundation of Shanghai (grant no. 19ZR1451800), the Project of Shanghai Minhang District Health and Family Planning Commission (grant no. 2021MW18), and the Minhang District Healthcare System Program for Outstanding Young Medical Technical and Pharmacology Scholars (grant no. mwyjyx01).

Acknowledgments

We are grateful to Changhai Hospital (Shanghai, China) and Tianjin University (Tianjin, China) for providing *C. albicans* strains.

Conflict of interest

The authors declare that the research was conducted in the absence of any commercial or financial relationships that could be construed as a potential conflict of interest.

Publisher's note

References

Alebic-Kolbah, T., and Modesitt, M. S. (2012). Anidulafungin–challenges in development and validation of an LC-MS/MS bioanalytical method validated for regulated clinical studies. *Anal. Bioanal. Chem.* 404, 2043–2055. doi: 10.1007/s00216-012-6272-4

Arendrup, M. C., and Patterson, T. F. (2017). Multidrug-resistant *Candida*: Epidemiology, molecular mechanisms, and treatment. *J. Infect. Dis.* 216:S445–S451. doi: 10.1093/infdis/jix131

Bergeron, A., Furtado, M., and Garofolo, F. (2009). Importance of using highly pure internal standards for successful liquid chromatography/tandem mass spectrometric bioanalytical assays. *Rapid Commun. Mass Spectrom.* 23, 1287–1297. doi: 10.1002/rcm.4001

Berkow, E. L., and Lockhart, S. R. (2017). Fluconazole resistance in *Candida species*: A current perspective. *Infect. Drug Resist.* 10, 237–245. doi: 10.2147/idr.S118892

Beste, K. Y., Burkhardt, O., and Kaever, V. (2012). Rapid HPLC-MS/MS method for simultaneous quantitation of four routinely administered triazole antifungals in human plasma. *Clin. Chim. Acta* 413, 240–245. doi: 10.1016/j.cca.2011.09.042

Bongomin, F., Gago, S., Oladele, R. O., and Denning, D. W. (2017). Global and multi-national prevalence of fungal diseases-estimate precision. *J. Fungi* 3:57. doi: 10.3390/jof3040057

Brown, G. D., Denning, D. W., and Levitz, S. M. (2012). Tackling human fungal infections. *Science* 336:647. doi: 10.1126/science.1222236

Campitelli, M., Zeineddine, N., Samaha, G., and Maslak, S. (2017). Combination antifungal therapy: A review of current data. *J. Clin. Med. Res.* 9, 451–456. doi: 10.14740/jocmr2992w

de Moraes, F. C., Bittencourt, S. F., Perissutti, E., Frencentese, F., Arruda, A. M., Chen, L. S., et al. (2014). Quantification of dapaconazole in human plasma using high-performance liquid chromatography coupled to tandem mass spectrometry: Application to a phase I study. *J. Chromatogr. B* 958, 102–107. doi: 10.1016/j.jchromb.2014.01.053

de Oliveira Santos, G. C., Vasconcelos, C. C., Lopes, A. J. O., De Sousa Cartágenes, M. D. S., Filho, A., Do Nascimento, F. R. F., et al. (2018). *Candida* infections and therapeutic strategies: Mechanisms of action for traditional and alternative agents. *Front. Microbiol.* 9:1351. doi: 10.3389/fmicb.2018.01351

Dhasarathan, P., Alsalhi, M. S., Devanesan, S., Subbiah, J., Ranjitsingh, A. J. A., Binsalah, M., et al. (2021). Drug resistance in *Candida albicans* isolates and related changes in the structural domain of Mdr1 protein. *J. Infect. Public Health* 14, 1848–1853. doi: 10.1016/j.jiph.2021.11.002

Diez, L., Martenka, E., Dabrowska, A., Coulon, J., and Leroy, P. (2005). Assessment of in situ cellular glutathione labeling with naphthalene-2,3-dicarboxaldehyde using high-performance liquid chromatography. *J. Chromatogr. B Anal. Technol. Biomed. Life Sci.* 827, 44–50. doi: 10.1016/j.jchromb.2005.02.007

Flowers, S. A., Colón, B., Whaley, S. G., Schuler, M. A., and Rogers, P. D. (2015). Contribution of clinically derived mutations in ERG11 to azole resistance in *Candida albicans*. *Antimicrob. Agents Chemother.* 59, 450–460. doi: 10.1128/aac.03470-14

Hou, J., Deng, J., Liu, Y., Zhang, W., Wu, S., Liao, Q., et al. (2022). Epidemiology, clinical characteristics, risk factors, and outcomes of candidemia in a large tertiary teaching hospital in Western China: A retrospective 5-year study from 2016 to 2020. *Antibiotics* 11:788. doi: 10.3390/antibiotics11060788

Iyer, K. R., Camara, K., Daniel-Ivad, M., Trilles, R., Pimentel-Elardo, S. M., Fossen, J. L., et al. (2020). An oxindole efflux inhibitor potentiates azoles and impairs virulence in the fungal pathogen *Candida auris*. *Nat. Commun.* 11:6429. doi: 10.1038/s41467-020-20183-3

Johnson, M. D., Macdougall, C., Ostrosky-Zeichner, L., Perfect, J. R., and Rex, J. H. (2004). Combination antifungal therapy. *Antimicrob. Agents Chemother.* 48, 693–715. doi: 10.1128/aac.48.3.693-715.2004

Kim, C., Ryu, H. D., Chung, E. G., Kim, Y., and Lee, J. K. (2018). A review of analytical procedures for the simultaneous determination of medically important veterinary antibiotics in environmental water: Sample preparation, liquid chromatography, and mass spectrometry. *J. Environ. Manag.* 217, 629–645. doi: 10.1016/j.jenvman.2018.04.006

Kofla, G., Turner, V., Schulz, B., Storch, U., Froelich, D., Rognon, B., et al. (2011). Doxorubicin induces drug efflux pumps in *Candida albicans*. *Med. Mycol.* 49, 132–142. doi: 10.3109/13693786.2010.512022

Lu, H., Shrivastava, M., Whiteway, M., and Jiang, Y. (2021). *Candida albicans* targets that potentially synergize with fluconazole. *Crit. Rev. Microbiol.* 47, 323–337. doi: 10.1080/1040841x.2021.1884641

Magill, S. S., Edwards, J. R., Bamberg, W., Beldavs, Z. G., Dumyati, G., Kainer, M. A., et al. (2014). Multistate point-prevalence survey of health care-associated infections. *N. Engl. J. Med.* 370, 1198–1208. doi: 10.1056/NEJMoa1306801

Pappas, P. G., Lionakis, M. S., Arendrup, M. C., Ostrosky-Zeichner, L., and Kullberg, B. J. (2018). Invasive candidiasis. *Nat. Rev. Dis. Primers* 4:18026. doi: 10.1038/nrdp.2018.26

Perea, S., López-Ribot, J. L., Kirkpatrick, W. R., Mcatee, R. K., Santillán, R. A., Martínez, M., et al. (2001). Prevalence of molecular mechanisms of resistance to azole antifungal agents in *Candida albicans* strains displaying high-level fluconazole resistance isolated from human immunodeficiency virus-infected patients. *Antimicrob. Agents Chemother.* 45, 2676–2684. doi: 10.1128/aac.45.10.2676-2684.2001

Pristov, K. E., and Ghannoum, M. A. (2019). Resistance of *Candida* to azoles and echinocandins worldwide. *Clin. Microbiol. Infect.* 25, 792–798. doi: 10.1016/j.cmi.2019.03.028

Quan, H., Cao, Y. Y., Xu, Z., Zhao, J. X., Gao, P. H., Qin, X. F., et al. (2006). Potent *in vitro* synergism of fluconazole and berberine chloride against clinical isolates of *Candida albicans* resistant to fluconazole. *Antimicrob. Agents Chemother.* 50, 1096–1099. doi: 10.1128/aac.50.3.1096-1099.2006

Quindós, G., Marcos-Arias, C., San-Millán, R., Mateo, E., and Eraso, E. (2018). The continuous changes in the aetiology and epidemiology of invasive candidiasis: From familiar *Candida albicans* to multiresistant *Candida auris*. *Int. Microbiol.* 21, 107–119. doi: 10.1007/s10123-018-0014-1

Revie, N. M., Iyer, K. R., Robbins, N., and Cowen, L. E. (2018). Antifungal drug resistance: Evolution, mechanisms and impact. *Curr. Opin. Microbiol.* 45, 70–76. doi: 10.1016/j.mib.2018.02.005

Ribeiro de Carvalho, R., Chaves Silva, N., Cusinato, M., Tranches Dias, K. S., Dos Santos, M. H., Viegas Junior, C., et al. (2018). Promising synergistic activity of fluconazole with bioactive guttiferone-a and derivatives against non-albicans *Candida species*. *J. Mycol. Med.* 28, 645–650. doi: 10.1016/j.mycmed.2018.07.006

Robbins, N., Caplan, T., and Cowen, L. E. (2017). Molecular evolution of antifungal drug resistance. *Annu. Rev. Microbiol.* 71, 753–775. doi: 10.1146/annurev-micro-030117-020345

Rocha, M. F. G., Bandeira, S. P., De Alencar, L. P., Melo, L. M., Sales, J. A., Paiva, M. A. N., et al. (2017). Azole resistance in *Candida albicans* from animals: Highlights on efflux pump activity and gene overexpression. *Mycoses* 60, 462–468. doi: 10.1111/myc.12611

Różalska, B., Sadowska, B., Budzyńska, A., Bernat, P., and Różalska, S. (2018). Biogenic nanosilver synthesized in metarhizium robertsii waste mycelium extract - as a modulator of *Candida albicans* morphogenesis, membrane lipidome and biofilm. *PLoS One* 13:e0194254. doi: 10.1371/journal.pone.0194254

Tang, J., Wei, H., Liu, H., Ji, H., Dong, D., Zhu, D., et al. (2010). Pharmacokinetics and biodistribution of itraconazole in rats and mice following intravenous administration in a novel liposome formulation. *Drug Deliv.* 17, 223–230. doi: 10.3109/10717541003667822

Tome, M., Zupan, J., Tomičić, Z., Matos, T., and Raspor, P. (2018). Synergistic and antagonistic effects of immunomodulatory drugs on the action of antifungals against *Candida glabrata* and Saccharomyces cerevisiae. *PeerJ* 6:e4999. doi: 10.7717/peerj.4999

Van De Steene, J. C., and Lambert, W. E. (2008). Comparison of matrix effects in HPLC-MS/MS and UPLC-MS/MS analysis of nine basic pharmaceuticals in surface waters. *J. Am. Soc. Mass Spectrom.* 19, 713–718. doi: 10.1016/j.jasms.2008.01.013

Wadsworth, J. M., Milan, A. M., Anson, J., and Davison, A. S. (2017). Development of a liquid chromatography tandem mass spectrometry method for the simultaneous measurement of voriconazole, posaconazole and itraconazole. *Ann. Clin. Biochem.* 54, 686–695. doi: 10.1177/0004563216686378

Wiederhold, N. P. (2017). Antifungal resistance: Current trends and future strategies to combat. *Infect. Drug Resist.* 10, 249–259. doi: 10.2147/idr.S124918

Xiang, J., Yu, Q., Liang, M. Z., Qin, Y. P., and Nan, F. (2018). [Determination of voriconazole in human plasma and its bioequivalence by HPLC-MS/MS]. *Sichuan Da Xue Xue Bao Yi Xue Ban* 49, 102–106.

Xu, Y., Lu, H., Zhu, S., Li, W. Q., Jiang, Y. Y., Berman, J., et al. (2021). Multifactorial mechanisms of tolerance to ketoconazole in *Candida albicans*. *Microbiol. Spectr.* 9:e0032121. doi: 10.1128/Spectrum.00321-21

Zacchino, S. A., Butassi, E., Cordisco, E., and Svetaz, L. A. (2017). Hybrid combinations containing natural products and antimicrobial drugs that interfere with bacterial and fungal biofilms. *Phytomedicine* 37, 14–26. doi: 10.1016/j.phymed.2017.10.021

Zgoła-Grześkowiak, A., and Grześkowiak, T. (2013). Application of dispersive liquid-liquid microextraction followed by HPLC-MS/MS for the trace determination of clotrimazole in environmental water samples. *J. Sep. Sci.* 36, 2514–2521. doi: 10.1002/jssc.201300271

Zhang, H., Wang, X., Qian, M., Wang, X., Xu, H., Xu, M., et al. (2011). Residue analysis and degradation studies of fenbuconazole and myclobutanil in strawberry by chiral high-performance liquid chromatography-tandem mass spectrometry. *J. Agric. Food Chem.* 59, 12012–12017. doi: 10.1021/jf202975x

Zimmer, D. (2014). New US FDA draft guidance on bioanalytical method validation versus current FDA and EMA guidelines: Chromatographic methods and ISR. *Bioanalysis* 6, 13–19. doi: 10.4155/bio.13.298

frontiers | Frontiers in Microbiology

TYPE Original Research
PUBLISHED 06 October 2022
DOI 10.3389/fmicb.2022.1006375

OPEN ACCESS

EDITED BY
Weihua Pan,
Shanghai Changzheng Hospital,
China

REVIEWED BY
Nan Hong,
Jinling Hospital,
China
Lianjuan Yang,
Shanghai Dermatology Hospital,
China

*CORRESPONDENCE
Wei Liu
liuwei@bjmu.edu.cn

†These authors have contributed equally to this work and share first authorship

SPECIALTY SECTION
This article was submitted to Antimicrobials, Resistance and Chemotherapy, a section of the journal Frontiers in Microbiology

RECEIVED 29 July 2022
ACCEPTED 20 September 2022
PUBLISHED 06 October 2022

CITATION
Wang Q, Cai X, Li Y, Zhao J, Liu Z, Jiang Y, Meng L, Li Y, Pan S, Ai X, Zhang F, Li R, Zheng B, Wan Z and Liu W (2022) Molecular identification, antifungal susceptibility, and resistance mechanisms of pathogenic yeasts from the China antifungal resistance surveillance trial (CARST-fungi) study.
Front. Microbiol. 13:1006375.
doi: 10.3389/fmicb.2022.1006375

Molecular identification, antifungal susceptibility, and resistance mechanisms of pathogenic yeasts from the China antifungal resistance surveillance trial (CARST-fungi) study

Qiqi Wang[1†], Xuan Cai[2†], Yun Li[3], Jianhong Zhao[4], Zhiyong Liu[5], Yan Jiang[6], Ling Meng[7], Yanming Li[8], Shiyang Pan[9], Xiaoman Ai[10], Fang Zhang[11], Ruoyu Li[1], Bo Zheng[3], Zhe Wan[1] and Wei Liu[1*] on behalf of the China Antifungal Resistance Surveillance Trial (CARST-fungi) Study Group

[1]Department of Dermatology and Venereology, Peking University First Hospital, National Clinical Research Center for Skin and Immune Diseases, Research Center for Medical Mycology, Beijing Key Laboratory of Molecular Diagnosis on Dermatoses, Peking University, Beijing, China, [2]Department of Clinical Laboratory, Renmin Hospital of Wuhan University, Wuhan, China, [3]Institute of Clinical Pharmacology, Peking University First Hospital, Beijing, China, [4]Department of Clinical Laboratory Medicine, Second Hospital of Hebei Medical University, Shijiazhuang, China, [5]Department of Laboratory Medicine, Southwest Hospital, Army Medical University, Chongqing, China, [6]Center for Clinical Laboratories, Affiliated Hospital of Guizhou Medical University, Guiyang, China, [7]Lanzhou University Second Hospital, Lanzhou, China, [8]Department of Clinical Laboratory, Xiangya Hospital, Central South University, Changsha, China, [9]First Affiliated Hospital of Nanjing Medical University, Nanjing, China, [10]Department of Medical Laboratory, Beijing Hospital, National Center of Gerontology, Institute of Geriatric Medicine, Chinese Academy of Medical Sciences, Beijing, China, [11]Medical Research and Laboratory Diagnostic Center, Central Hospital Affiliated to Shandong First Medical University, Jinan, China

To have a comprehensive understanding of epidemiology and antifungal susceptibilities in pathogenic yeasts, the China Antifungal Resistance Surveillance Trial (CARST-fungi) study was conducted. All yeast isolates were identified by ribosomal DNA sequencing. Antifungal susceptibilities were performed using CLSI M27-A4 broth microdilution method. Sequence and expression level of resistant-related genes in resistant/non-wide-type (NWT) *Candida* isolates were analyzed. Totally 269 nonduplicate yeast isolates from 261 patients were collected. About half of the yeast isolates (127, 47.2%) were recovered from blood, followed by ascetic fluid (46, 17.1%). *C. albicans* remained the most prevalent (120, 44.6%), followed by *C. parapsilosis* complex (50, 18.6%), *C. tropicalis* (40, 14.9%), and *C. glabrata* (36, 13.4%). Fourteen (11.7%) *C. albicans* isolates and 1 (2.0%) *C. parapsilosis* isolate were resistant/NWT to triazoles. Only 42.5% (17/40) *C. tropicalis* were susceptible/WT to all the triazoles, with 19 (47.5%) isolates NWT to posaconazole and 8 (20%) cross-resistant to triazoles. Among *C. glabrata*, 20 (55.6%) and 8 (22.2%) isolates were resistant/NWT to voriconazole and posaconazole, respectively,

and 4 (10.3%) isolates were cross-resistant to triazoles. Isavuconazole was the most active triazole against common *Candida* isolates. Except for 2 isolates of *C. glabrata* cross-resistant to echinocandins which were also NWT to POS and defined as multidrug-resistant, echinocandins exhibit good activity against common *Candida* species. All isolates were WT to AMB. For less common species, *Rhodotorula mucilaginosa* exhibited high MICs to echinocandins and FLC, and 1 isolate of *Trichosporon asahii* showed high MICs to all the antifungals except AMB. Among triazole-resistant *Candida* isolates, *ERG11* mutations were detected in 10/14 *C. albicans* and 6/23 *C. tropicalis*, while 21/23 *C. tropicalis* showed *MDR1* overexpression. Overexpression of *CDR1*, *CDR2*, and *SNQ2* exhibited in 14, 13, and 8 of 25 triazole-resistant *C. glabrata* isolates, with 5 isolates harboring *PDR1* mutations and 2 echinocandins-resistant isolates harboring S663P mutation in *FKS2*. Overall, the CARST-fungi study demonstrated that although *C. albicans* remain the most predominant species, non-*C. albicans* species accounted for a high proportion. Triazole-resistance is notable among *C. tropicalis* and *C. glabrata*. Multidrug-resistant isolates of *C. glabrata* and less common yeast have been emerging.

KEYWORDS

pathogenic yeasts, invasive fungal diseases, *Candida* spp., antifungal susceptibility, triazoles, echinocandins, multidrug resistance

Introduction

Invasive fungal diseases (IFDs) are life-threatening diseases with considerable morbidity and mortality, primarily occurring in immunocompromised and critically ill hosts (Bassetti et al., 2017). About 80% of IFDs were caused by *Candida* species, the third most frequently isolated microorganism of all infections in a worldwide ICU prevalence study (Kett et al., 2011). Although *C. albicans* continues to be the most prevalent *Candida* spp. causing IFDs, the past decades have witnessed changing epidemiology of IFDs shift to non-*albicans* spp., which may be more resistant to antifungal therapy (Bassetti et al., 2017). Other uncommon yeasts, such as *Cryptococcus* spp., *Saccharomyces* spp., *Trichosporon* spp., and *Rhodotorula* spp., although remained relatively rare in IFDs, were emerging as opportunistic pathogens and made diagnosis challenging and treatment suboptimal (Miceli et al., 2011). The management of IFDs was hindered owing to the paucity of rapid diagnostic assays (such as molecular identification methods). However, numerous clinicians still rely on traditional culture-based methods which are not rapid and sensitive. Therefore, empirical antifungal therapy often needs to be initiated and may contribute to increasing and inappropriate use of antifungals, which will not only alter *Candida* spp. distribution but also decrease antifungal susceptibility, making antifungal resistance an emerging problem worldwide (Lamoth et al., 2018).

There are 4 major classes of antifungals available to treat IFDs, including (1) polyenes, such as amphotericin B (AMB), destabilize membrane by binding to ergosterol; (2) triazoles, including fluconazole (FLC) itraconazole (ITC), voriconazole (VRC), posaconazole (POS), isavuconazole (ISA), target the enzyme 14-α-demethylase (Erg11p), a key step in the biosynthesis of ergosterol; (3) echinocandins, including caspofungin (CAS), anidulafungin (ANF), micafungin (MCF), block the catalytic subunit of the β-1,3 glucan synthase and thus inhibit cell wall biosynthesis; (4) pyrimidine analogs, such as 5-fluorocytosine (5-FC), are metabolized by fungal cells into fluorinated pyrimidines, which destabilize nucleic acids and result in growth arrest. Among these antifungals, triazoles represent the most widely prescribed antifungal class for IFDs. However, triazole-resistance has become a growing problem worldwide. The major mechanisms of triazole-resistance in *Candida* spp. include alteration in the *ERG11* gene encoding Erg11p, upregulation of the *ERG11* gene due to mutations in transcriptional factors such as *UPC2*, and overexpression of drug efflux pumps such as Mdr1p and Cdr1p/Cdr2p occurring mainly as a result of gain-of-function (GOF) mutations in transcription factors genes such as *MRR1*, *TAC1* and *PDR1* in *C. glabrata*. Echinocandins have now been recommended as first-line drugs for candidiasis (Pappas et al., 2016). Although the resistance rate remains generally low, echinocandin-resistance is rising as usage broadens among *Candida* spp., most notably *C. glabrata*, which was reported as high as >13% in some centers (Alexander et al., 2013). The mechanism of echinocandin resistance involves mutations in *FKS* genes encoding subunits of glucan synthase (Arastehfar et al., 2020). Different resistance mechanisms vary by species and geographic distribution, and the underlying mechanisms in some species have not been well defined. A better understanding of antifungal resistance mechanisms will provide insights to reclaim those antifungal classes as an option for empiric treatment of IFDs.

Under these circumstances, surveillance of IFDs plays a significant role in understanding epidemiology and antifungal susceptibility data to guide empirical therapy and aid antifungal

stewardship efforts (Pfaller et al., 2019). The China Antifungal Resistance Surveillance Trial (CARST-fungi) study was a prospective national surveillance program for IFDs in mainland China. The study described the epidemiology and antifungal susceptibilities of clinical yeast isolates, including *Candida* spp., *Cryptococcus neoformans*, *Trichosporon asahii*, and other less common yeast species recovered from patients across major cities in China during 2019 and 2020. Additionally, to preliminarily elucidate the mechanisms underlying the resistant phenotypes, sequences of resistance-related genes *ERG11*, *PDR1*, *FKS*, and expression profiles of *ERG11* and efflux pump genes including *CDR1*, *CDR2*, *MDR1*, and *SNQ2*, were analyzed.

Materials and methods

Study design

The CARST-fungi study was a multi-center, prospective, observational, and laboratory-based study of IFDs with its inception in July 2019 and finished in June 2020. Nine "rank-A tertiary" hospitals distributed throughout 9 major cities in China took part in the study. All *Candida*, *Cryptococcus*, and other yeast isolates recovered from sterile sites including blood, other sterile body fluids (ascitic fluid, pleural fluid, cerebrospinal fluid [CSF]), pus, tissue from patients with invasive yeast diseases, bronchoalveolar lavage fluid (BALF), central venous catheter (CVC) tips, biliary tract fluid were collected. Additionally, yeast strains from considered colonizers such as urine, feces, sputum, and the genital tract were also included. For each episode of yeast isolation, the information including the patient's age, gender, the ward location (e.g., emergency department, surgical, medical, and ICU), the time of sample collection, the specimen type, and the initial species identification made by the referring laboratory were collected. All isolates were sent to the Research Center for Medical Mycology at Peking University First Hospital, Beijing, China, for further study.

Species identification

To ensure the accuracy of identification, all clinical yeast isolates were identified to the species level in the central laboratory. Six colonies from primary culture plates were subcultured and identified using sequence-based methods for the internal transcribed spacer (ITS) region, 28S ribosomal subunit (D1/D2), and the intergenic spacer (IGS, for *Trichosporon* spp. and *Cryptococcus* spp.), primers used for identification were listed in Supplementary Table S1. Those sequences were aligned using CBS database[1] (Pfaller et al., 2012).

Antifungal susceptibility testing

Antifungal susceptibility testing was performed according to the Clinical and Laboratory Standards Institute (CLSI) M27-A4 microbroth dilution method (CLSI, 2017), and the tested drugs including AMB (from North China Pharmaceutical Co. Ltd., Shijiazhuang, China), FLC, ITC, VRC, POS, ISA, CAS, ANF, MCF and 5-FC, (all from Harveybio Gene Technology Co. Ltd., Beijing, China) were prepared according to CLSI methods.

Minimum inhibitory concentrations (MICs) were determined after 24 h incubation at 35°C for *Candida* spp. and *Trichosporon* spp. and after 72 h incubation for *Cryptococcus* spp. MICs were read as the lowest drug concentration producing a prominent decrease in turbidity translating to 50% (triazoles, echinocandins, and 5-FC) or 100% (AMB) growth reduction compared with the drug-free control. Quality control was performed with each test run using *C. parapsilosis* ATCC22019 and *C. krusei* ATCC6258.

The interpretation of susceptibility was performed by applying the updated species-specific clinical breakpoints (CBPs) according to CLSI M60 document (CLSI, 2020a). In the absence of CBPs, isolates were defined as having a wild-type (WT) or a non-WT (NWT) drug susceptibility phenotype according to the epidemiological cutoff values (ECVs) as determined by the CLSI M59 document (CLSI, 2020b). Cross-resistance was defined as resistance to at least two antifungals of the same drug class. Multidrug-resistance was defined as resistance to at least two classes of antifungal drugs (Orasch et al., 2014).

Resistance-related genes amplification and sequencing

Genomic DNA of resistant or non-WT yeast strains was extracted using the QIAamp DNA Mini Kit (Qiagen, Hilden, Germany). Primers to amplify the full open reading frame of *ERG11*, *PDR1* (for *C. glabrata*), and *FKS1*, *FKS2* for (*C. glabrata*) were designed (Supplementary Table S1) according to the genome of *C. albicans* SC5314, *C. glabrata* CBS138, *C. tropicalis* MYA-3404, and *C. parapsilosis* CDC317 from the Candida Genome Database[2] as reference. The amplified products were sent to the BGI Company (Beijing, China) for sequencing and the sequences were aligned with the reference strain using the Clustal Omega.[3]

RNA extraction and quantitative real-time reverse-transcription (RT)-PCR

Suspensions of *Candida* isolates cells (OD_{600}, 0.1) freshly prepared in YPD medium were grown at 35°C to reach the mid-exponential phase (OD_{600}, 0.6–0.8). The cells were washed

1 http://www.cbs.knaw.nl/

2 http://www.candidagenome.org/

3 https://www.ebi.ac.uk/Tools/msa/clustalo/

twice with sterile water. Total RNA was extracted using the RNeasy Mini kit (QIAGEN Science, Maryland, USA) following the manufacturer's instructions. The RNA was then treated with RNase-free DNase (Thermo Fisher Scientific, USA) according to the manufacturer's recommendations. cDNA was synthesized using an Advantage RT-for-PCR kit (Clontech) according to the manufacturer's instructions. RT-qPCR was performed on an Applied Biosystems ViiA7 Real-Time PCR system using SYBR green reagent (Applied Biosystems). Optimal thermal cycling conditions consisted of a 10-min initial denaturation at 95°C, followed by 40 cycles of denaturation at 95°C for 15 s, and annealing/extension at 60°C for 10 s. The experiments were carried out in triplicate for each data point. The cycle threshold (CT) value of the gene was normalized to that of internal control *ACT1* gene for *C. albicans*, *C. tropicalis*, *C. tropicalis*, and *RND5.8* gene for *C. glabrata* as ΔCT value. Relative gene expression ($2^{\Delta\Delta Ct}$) was calculated as the fold change in expression of the isolates compared to the mean expression values in drug-susceptible control strains including *C. albicans* SC5314, *C. glabrata* CBS138, *C. tropicalis* ATCC01463, and *C. parapsilosis* ATCC22019. The primers used were listed in Supplementary Table S1.

Statistical analysis

Comparisons were performed using SPSS software version 22 (SPSS, Chicago, IL, USA). Continuous variables were compared using the Mann–Whitney test, and categorical variables were analyzed using the χ^2 test or Fisher's exact test. A value of $p < 0.05$ was considered statistically significant.

Results

Patient demographics

A total of 269 nonduplicate yeast isolates from 261 patients were collected, among which more than 1 isolate was recovered from 8 patients. Of the yeast isolates investigated, 161 (59.9%) were cultured from male patients, and 108 (40.1%) were from female patients. The patients' ages ranged from 0 to 98 years (median, 57 years; interquartile range, 36 to 72 years). Most isolates (252/269, 93.7%) were from hospital inpatients (including those in ICUs [23.4%], medical wards [28.3%], surgical wards [33.8%], obstetrics and gynecology departments [5.2%], paediatrics departments [3.0%]), and remaining 6.3% were from patients in emergency settings.

Distribution of species by specimen type

Of the various specimen types, about half of the yeast isolates (127, 47.2%) were recovered from blood, followed by ascitic fluid (46, 17.1%), pus (17, 6.3%), CVC (13, 4.8%), CSF (11, 4.1%), bile (9, 3.3%), tissue (7, 2.6%), and other sterile sites (3, 1.1%, including bone marrow, BALF; Figure 1). Thirty-six yeast isolates (13.4%)

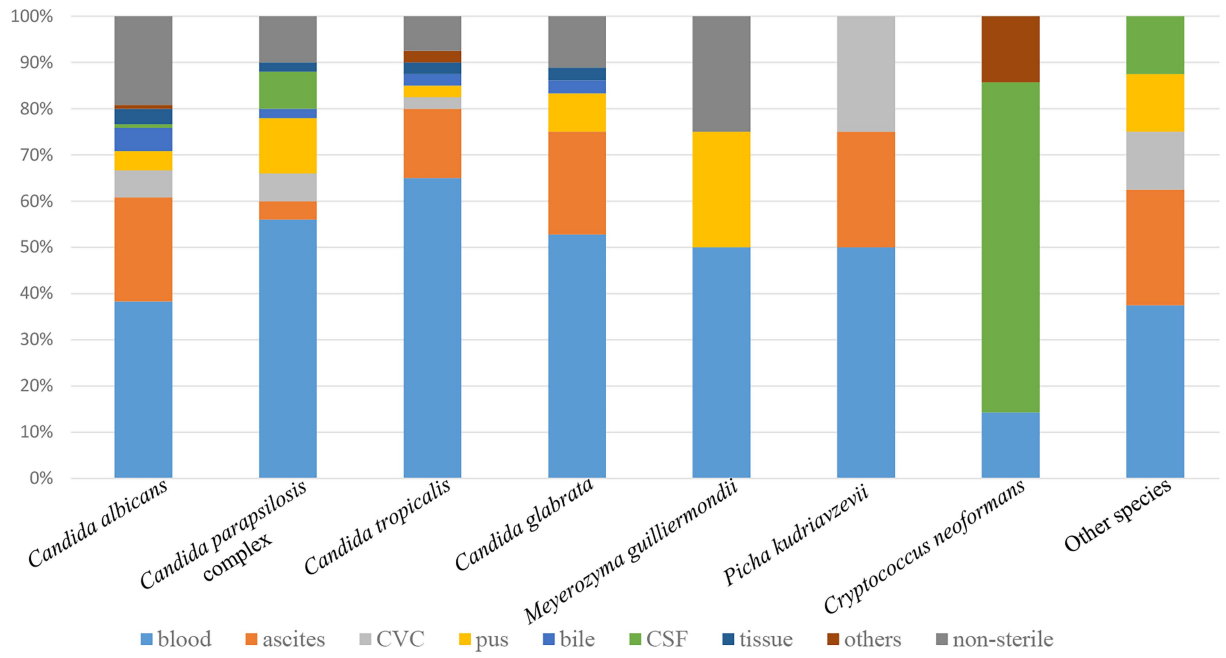

FIGURE 1
Distribution of yeast species by specimen type. Other species include 2 each of *Clavispora lusitaniae*, *Trichosporon asahii*, and *Wickerhamomyces anomalus*, 1 each of *Cyberlindnera fabianii* and *Rhodotorula mucilaginosa*. Other sterile sites include bone marrow and bronchoalveolar lavage fluid (BALF). Non-sterile samples include urine, feces, sputum, and genital tract secretion. CVC, central venous catheter; CSF, cerebrospinal fluid.

were from non-sterile samples and considered colonizers (such as urine, feces, sputum, and genital tract secretion). The proportion of non-*albicans Candida* isolates recovered from blood (78/127, 61.4%) was significantly higher than that recovered from other specimen types (58/142, 40.8%) ($p < 0.01$).

Yeast species distribution

Thirteen species were identified among the 269 yeast isolates (Figure 2). *C. albicans* remained the most prevalent (120, 44.6%), followed by *C. parapsilosis* complex (including *C. parapsilosis sensu stricto* [41, 15.2%] and *C. metapsilosis* [9, 3.3%]), *C. tropicalis* (40, 14.9%), and *C. glabrata* (36, 13.4%). Other yeast species including 7 isolates of *Cryptococcus neoformans*, 4 each of *Picha kudriavzevii* (*Candida krusei*) and *Meyerozyma guilliermondii* (*Candida guilliermondii*), 2 each of *Clavispora lusitaniae* (*Candida lusitaniae*), *Trichosporon asahii*, and *Wickerhamomyces anomalus* (*Candida pelliculosa*), 1 each of *Cyberlindnera fabianii* (*Candida fabianii*) and *Rhodotorula mucilaginosa*, accounted for tiny proportion.

Mixed species detection in the same specimen

Eight out of 261 samples (3.1%) in our study were co-isolated more than 1 yeast species (Table 1). Of the 8 specimens, 5 were from blood, 1 each from ascites, paracentesis fluid, and urine, among which 4 cases were *C. albicans*/*C. glabrata* mixed, 1 each *C. albicans*/*C. tropicalis mixed and C. parapsilosis sensu stricto*/*C. metapsilosis* mixed. Interestingly, 2 isolates of *T. asahii* in blood specimens were both co-isolated with *C. albicans*. Of note, most specimens contained yeast isolates that were resistant/NWT to at least one antifungal (Table 1).

In vitro susceptibility to triazoles

In vitro susceptibility of antifungal drugs against yeast species is shown in Table 2. Among the common *Candida* species, 5 (4.2%), 6 (5.0%), and 10 (8.4%) isolates of *C. albicans* were resistant/NWT to FLC, VRC, and POS, respectively. As for the *C. parapsilosis* complex, only 1 (2.4%) isolate of

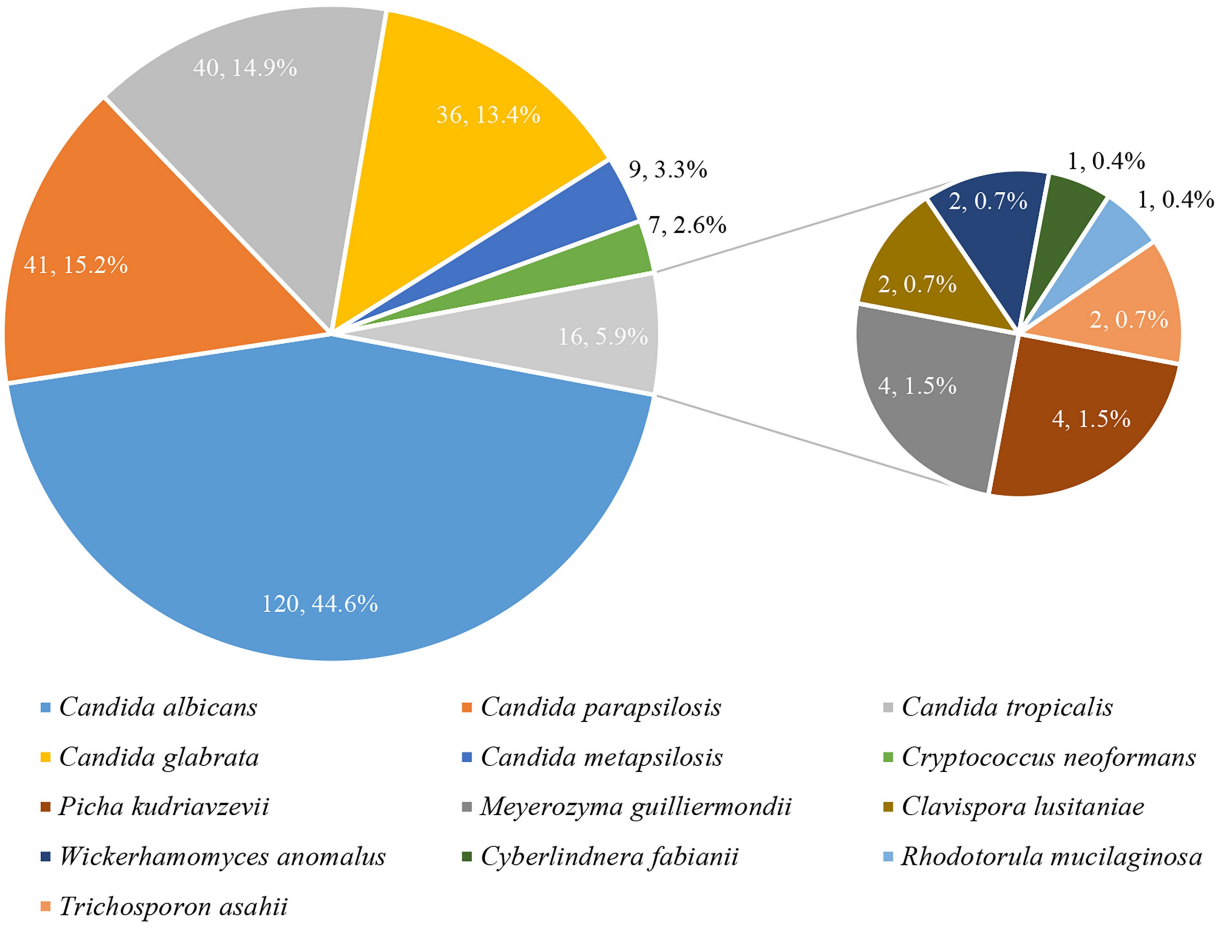

FIGURE 2
Species distribution of common and less common yeast isolates.

TABLE 1 Distribution of co-isolated yeast species in specimens and their antifungal susceptibility profiles.

Specimen	Initial identification	Pathogens detected	Antifungal susceptibility MICs (μg/ml)									
			FLC	ITC	VRC	POS	ISA	AMB	ANF	MCF	CAS	5-FC
Blood	*C. parapsilosis*	*C. tropicalis*	4	0.25	0.5	0.5	0.25	1	0.12	0.06	0.06	>64
		C. albicans	0.5	0.06	0.008	0.03	0.008	1	0.06	0.008	0.06	<0.06
Blood	*C. glabrata*	*C. glabrata*	32	1	0.5	1	0.12	1	0.03	<0.008	0.03	<0.06
		C. albicans	0.12	0.06	0.008	0.015	0.015	0.5	0.12	0.008	0.12	0.06
Blood	*C. parapsilosis*	*C. parapsilosis*	0.25	0.12	0.008	0.06	0.008	0.5	1	1	0.5	0.06
		C. metapsilosis	2	0.25	0.03	0.12	0.008	0.5	0.5	0.5	0.25	0.06
Blood	*T. asahii*	*C. albicans*	4	0.25	0.5	0.06	4	0.5	0.015	0.015	0.015	0.5
		T. asahii	4	0.25	0.06	0.25	0.12	0.5	>8	>8	>8	4
Blood	*T. asahii*	*C. albicans*	4	0.25	1	0.12	0.008	1	0.06	0.008	0.03	64
		T. asahii	>256	>16	>8	>8	16	0.5	>8	>8	>8	>64
Paracentesis fluid	*C. albicans*	*C. albicans*	0.5	0.12	0.015	0.03	0.015	0.5	0.12	0.015	0.06	1
		C. glabrata	32	1	1	1	0.5	1	0.03	0.015	0.03	0.06
Urine	*C. glabrata*	*C. glabrata*	8	0.5	0.06	0.5	0.12	1	0.03	0.008	0.06	0.06
		C. albicans	4	0.06	0.06	1	0.015	1	0.06	0.008	0.06	0.06
Ascites	*C. glabrata*	*C. glabrata*	32	1	1	1	0.015	0.5	0.03	0.015	0.06	0.06
		C. albicans	0.5	0.12	0.015	0.03	0.008	0.5	0.12	0.008	0.06	0.06

FLC, fluconazole; ITC, itraconazole; VRC, voriconazole, POS, posaconazole; ISA, isavuconzaole; AMB, amphotericin B; ANF, anidulafungin; MCF, micafungin; CAS, caspofungin; 5-FC, 5-fluorocytosine; MICs, minimum inhibitory concentrations. MICs highlighted in red represent the isolate non-susceptible to the antifungal agent.

C. parapsilosis sensu stricto was cross-resistant to FLC and POS, while all the 9 *C. metapsilosis* isolates were WT to triazoles. However, only 42.5% (17/40) of *C. tropicalis* were susceptible/WT to all the triazoles, and 12 (30.0%), 3 (7.5%), 8 (20.0%), 19 (47.5%) isolates were resistant/NWT to FLC, ITC, VRC, and POS, respectively. Among *C. glabrata*, 2 (5.6%) isolates were resistant to FLC while the remaining 34 were susceptible-dose dependent (SDD), 20 (55.6%) and 8 (22.2%) isolates were resistant/NWT to VRC and POS, respectively, and all isolates were WT to ITC.

For less common yeast species, all 4 isolates of *P. kudriavzevii* were susceptible/WT to other triazoles which were assumed to be intrinsically resistant to FLC; *M. guilliermondii* and *C. lusitaniae* were WT to triazoles except 1 isolate of *M. guilliermondii* was NWT to POS. Based on MIC_{90} since neither CBPs nor ECV values have been established for ISA and *Candida* spp., ISA was the most active triazole against *C. albicans* (MIC_{90}, 0.015 μg/ml), *C. parapsilosis* (MIC_{90}, 0.015 μg/ml), *C. tropicalis* (MIC_{90}, 0.25 μg/ml), and *C. glabrata* (MIC_{90}, 0.5 μg/ml), while comparable to other triazoles against *P. kudriavzevii*, *M. guilliermondii*, and other non-*Candida* spp. Two isolates of *W. anomalus* exhibited relatively less susceptible to FLC (MICs 2–8 μg/ml) and POS (MICs 0.5–1 μg/ml) than ITC, VRC, and ISA (MICs 0.12–0.25 μg/ml).

In vitro susceptibility to echinocandins, AMB, and 5-FC

All isolates of *C. albicans* and *C. parapsilosis* were susceptible to echinocandins. Among *C. glabrata*, 2 isolates were cross-resistant to CAS, MCF, ANF (MICs 32 μg/ml, 8 μg/ml, 4 μg/ml, respectively) and 2 isolates were intermediate to CAS (MICs 0.25 μg/ml). There were 1 and 2 isolates of *C. tropicalis* exhibiting intermediate to CAS and ANF, respectively. Among the non-*Candida* yeasts, MICs of the echinocandins were consistently high for all isolates of *C. neoformans*, *R. mucilaginosa*, and *T. asahii* (all MICs >16 μg/ml) (Table 2).

All yeast isolates tested in this study were WT to AMB (MICs ≤2 μg/ml). No ECVs were defined for 5-FC against *Candida* spp., the MICs of 5-FC against 7 isolates of *C. albicans* and 2 isolates of *C. tropicalis* were > 64 μg/ml, while the MICs against the remaining *Candida* isolates were all ≤1 μg/ml. All isolates of *C. neoformans* were WT to 5-FC (ECV 8 μg/ml).

Cross-resistance and multidrug-resistance

For yeast species with established CBPs or ECVs, 18 isolates were cross-resistant to at least 2 triazoles, including 5 (4.2%) isolates of *C. albicans*, 8 (20.0%) isolates of *C. tropicalis*, 4 (10.3%) isolates of *C. glabrata*, and 1 (2.4%) isolate of *C. parapsilosis sensu stricto*. Among triazole-resistant *Candida* isolates, 2 isolates of *C. albicans* and 1 isolate of *C. tropicalis* were also non-susceptible to 5-FC (MICs >64 μg/ml), and 2 isolates of *C. glabrata* were resistant to 3 echinocandins, which were defined as multidrug-resistance.

For less common species or those without CBPs or ECVs, 1 isolate of *R. mucilaginosa* exhibited high MICs to echinocandins and triazoles, and 1 isolate of *T. asahii* showed high MICs to all the antifungals tested except AMB (Table 2).

10.3389/fmicb.2022.1006375

TABLE 2 Activities of 9 antifungal drugs against yeast species according to CLSI clinical breakpoints or ECVs.

Organism/Antifungal agents		FLC	ITC	VRC	POS	ISA	AMB	ANF	MCF	CAS	5-FC
C. albicans, $n = 120$	Breakpoints (*S*, *I*, *R*) (μg/ml)	$S \leq 2$, SDD 4, $R \geq 8$	/	$S \leq 0.1$, $I = 0.25$–0.5, $R \geq 1$	/	/	/	$S \leq 0.25$, $I = 0.5$, $R \geq 1$	$S \leq 0.25$, $I = 0.5$, $R \geq 1$	$S \leq 0.25$, $I = 0.5$, $R \geq 1$	/
	ECV (μg/ml)	/	/	/	0.06	/	2	/	/	/	/
	Range (μg/ml)	0.12–256	0.015–16	0.008–8	0.008–8	0.008–16	0.12–2	0.015–0.25	0.008–0.06	0.015–0.25	0.06–64
	MIC_{50} (μg/ml)	0.5	0.12	0.015	0.03	0.008	0.5	0.12	0.015	0.06	0.06
	MIC_{90} (μg/ml)	1	0.12	0.03	0.06	0.015	1	0.12	0.015	0.12	0.12
	CLSI S	111	/	109	/	/	/	120	120	120	/
	CLSI R	5	/	6	/	/	/	0	0	0	/
	WT	/	/	/	110	/	120	/	/	/	/
	non-WT	/	/	/	10	/	0	/	/	/	/
C. parapsilosis complex, $n = 50$											
C. parapsilosis sensu stricto, $n = 41$	Breakpoints (*S*, *I*, *R*) (μg/ml)	$S \leq 2$, SDD 4, $R \geq 8$	/	$S \leq 0.12$, $I = 0.25$–0.5, $R \geq 1$	/	/	/	$S \leq 2$, $I = 4$, $R \geq 8$	$S \leq 2$, $I = 4$, $R \geq 8$	$S \leq 2$, $I = 4$, $R \geq 8$	/
	ECV (μg/ml)	/	0.5	/	0.25	/	1	/	/	/	/
	Range (μg/ml)	0.25–8	0.03–0.5	0.008–0.03	0.03–0.5	0.008–0.25	0.25–1	0.06–2	0.015–2	0.12–1	0.06–0.25
	MIC_{50} (μg/ml)	0.5	0.12	0.015	0.03	0.008	0.5	2	1	0.5	0.06
	MIC_{90} (μg/ml)	1	0.12	0.03	0.06	0.015	1	2	2	1	0.12
	CLSI S	40	/	40	/	/	/	41	41	41	/
	CLSI R	1	/	0	/	/	/	0	0	0	/
	WT	/	41	/	40	/	41	/	/	/	/
	non-WT	/	0	/	1	/	0	/	/	/	/
C. metapsilosis, $n = 9$	Breakpoints (*S*, *I*, *R*) (μg/ml)	/	/	/	/	/	/	/	/	/	/
	ECV (μg/ml)	4	1	0.06	0.25	/	1	0.5	1	0.25	/
	Range (μg/ml)	0.25–2	0.03–0.25	0.008–0.06	0.03–0.25	0.008–0.06	0.5–1	0.12–0.5	0.015–0.5	0.06–0.25	0.06
	MIC_{50} (μg/ml)	1	0.12	0.03	0.06	0.008	0.5	0.25	0.5	0.12	0.06
	MIC_{90} (μg/ml)	2	0.25	0.06	0.25	0.015	1	0.5	0.5	0.25	0.06
	CLSI S	/	/	/	/	/	/	/	/	/	/
	CLSI R	/	/	/	/	/	/	/	/	/	/
	WT	9	9	9	9	/	9	9	9	9	/
	non-WT	0	0	0	0	/	0	0	0	0	/
C. tropicalis, $n = 40$	Breakpoints (*S*, *I*, *R*) (μg/ml)	$S \leq 2$, SDD 4, $R \geq 8$	/	$S \leq 0.12$, $I = 0.25$–0.5, $R \geq 1$	/	/	/	$S \leq 0.25$, $I = 0.5$, $R \geq 1$	$S \leq 0.25$, $I = 0.5$, $R \geq 1$	$S \leq 0.25$, $I = 0.5$, $R \geq 1$	/
	ECV (μg/ml)	/	0.5	/	0.12	/	2	/	/	/	/
	Range (μg/ml)	0.5–128	0.03–16	0.12–8	0.06–8	0.008–16	0.5–2	0.015–0.25	0.015–0.06	0.015–0.5	0.06–64
	MIC_{50} (μg/ml)	2	0.25	0.12	0.25	0.008	1	0.12	0.03	0.03	0.06
	MIC_{90} (μg/ml)	64	0.5	2	1	0.25	2	0.25	0.06	0.12	0.12

(Continued)

TABLE 2 (Continued)

Organism/Antifungal agents		FLC	ITC	VRC	POS	ISA	AMB	ANF	MCF	CAS	5-FC
	CLSI S	18	/	27	/	/	/	38	40	39	/
	CLSI R	12	/	8	/	/	/	0	0	0	/
	WT	/	37	/	21	/	40	/	/	/	/
	non-WT	/	3	/	19	/	0	/	/	/	/
C. glabrata, $n = 36$	Breakpoints (S, I, R) (μg/ml)	SDD ≤ 32, $R \geq 64$	/	/	/	/	/	$S \leq 0.12$, $I = 0.25$, $R \geq 0.5$	$S \leq 0.06$, $I = 0.12$, $R \geq 0.25$	$S \leq 0.12$, $I = 0.25$, $R \geq 0.5$	/
	ECV (μg/ml)	/	4	0.25	1	/	2	/	/	/	/
	Range (μg/ml)	4–128	0.5–2	0.06–4	0.25–4	0.008–2	0.25–1	0.015–4	0.008–8	0.03–16	0.06–0.25
	MIC_{50} (μg/ml)	32	0.5	0.5	1	0.12	1	0.03	0.015	0.06	0.06
	MIC_{90} (μg/ml)	32	1	1	2	0.5	1	0.12	0.015	0.12	0.06
	CLSI S	0	/	/	/	/	/	34	34	32	/
	CLSI R	2	/	/	/	/	/	2	2	2	/
	WT	/	36	16	28	/	36	/	/	/	/
	non-WT	/	0	20	8	/	0	/	/	/	/
C. krusei, $n = 4$	Breakpoints (S, I, R) (μg/ml)	/	/	$S \leq 0.5$, $I = 1$, $R \geq 2$	/	/	/	$S \leq 0.25$, $I = 0.5$, $R \geq 1$	$S \leq 0.25$, $I = 0.5$, $R \geq 1$	$S \leq 0.25$, $I = 0.5$, $R \geq 1$	/
	ECV (μg/ml)	/	1	/	0.5	/	2	/	/	/	/
	Range (μg/ml)	64	0.25–0.5	0.5	0.25–0.5	0.25–0.5	1–2	0.06–0.12	0.015–0.12	0.5	8–64
	MIC_{50} (μg/ml)	64	0.5	0.5	0.5	0.5	1	0.12	0.12	0.5	16
	MIC_{90} (μg/ml)	/	0.5	0.5	0.5	0.5	2	0.12	0.12	0.5	64
	CLSI S	/	/	4	/	/	/	4	4	0	/
	CLSI R	/	/	0	/	/	/	0	0	0	/
	WT	/	4	/	4	/	4	/	/	/	/
	non-WT	/	0	/	0	/	0	/	/	/	/
Meyerozyma guilliermondii, $n = 4$	Breakpoints (S, I, R) (μg/ml)	/	/	/	/	/	/	$S \leq 2$, $I = 4$, $R \geq 8$	$S \leq 2$, $I = 4$, $R \geq 8$	$S \leq 2$, $I = 4$, $R \geq 8$	/
	ECV (μg/ml)	8	2	/	0.5	/	2	/	/	/	/
	Range (μg/ml)	0.5–8	0.06–0.5	0.03–0.12	0.25–1	0.06–0.5	0.25–0.5	1–2	0.25–0.5	0.25–1	0.06
	MIC_{50} (μg/ml)	1	0.25	0.06	0.25	0.12	0.5	1	0.5	0.5	0.06
	MIC_{90} (μg/ml)	8	0.5	0.12	1	0.5	0.5	2	0.5	1	0.06
	CLSI S	/	/	/	/	/	/	4	4	0	/
	CLSI R	/	/	/	/	/	/	0	0	0	/
	WT	4	4	/	3	/	4	/	/	/	/
	non-WT	0	0	/	1	/	0	/	/	/	/

(Continued)

10.3389/fmicb.2022.1006375

TABLE 2 (Continued)

Organism/Antifungal agents		FLC	ITC	VRC	POS	ISA	AMB	ANF	MCF	CAS	5-FC
Cryptococcus neoformans, *n* = 7	Breakpoints (*S*, *I*, R) (μg/ml)	/	/	/	/	/	/	/	/	/	/
	ECV (μg/ml)	8	0.25	0.25	0.25	/	0.5	/	/	/	8
	Range (μg/ml)	1–8	0.03–0.25	0.015–0.12	0.015–0.25	0.008–0.12	0.25–0.5	>8	>8	>8	1–8
	MIC_{50} (μg/ml)	4	0.12	0.06	0.12	0.03	0.5	>8	>8	>8	4
	MIC_{90} (μg/ml)	8	0.25	0.12	0.25	0.12	0.5	>8	>8	>8	8
	CLSI S	/	/	/	/	/	/	/	/	/	/
	CLSI R	/	/	/	/	/	/	/	/	/	/
	WT	7	7	7	7	/	7	/	/	/	7
	non-WT	0	0	0	0	/	0	/	/	/	0
Uncommon yeast species with <3 isolates											
Clavispora lusitaniae, *n* = 2	MICs	1	0.25	0.015	0.06	0.015	0.5	1	0.12	0.5	0.06
		0.5	0.12	<0.008	0.06	0.008	0.5	0.25	0.12	0.25	<0.06
Trichosporon asahii, *n* = 2		>256	>16	>8	>8	16	0.5	>8	>8	>8	>64
		4	0.25	0.06	0.25	0.12	0.5	>8	>8	>8	4
Wickerhamomyces anomalus, *n* = 2		2	0.12	0.12	0.5	0.25	0.5	0.015	0.03	0.06	0.06
		8	0.25	0.25	0.5	0.25	0.5	0.015	0.015	0.06	0.06
Cyberlindnera fabianii, *n* = 1		1	0.25	0.03	0.5	0.03	0.25	0.03	0.03	0.03	0.06
Rhodotorula mucilaginosa, *n* = 1		>256	1	2	2	0.5	0.5	>8	>8	>8	0.06

FLC, fluconazole; ITC, itraconazole; VRC, voriconazole, POS, posaconazole; ISA, isavuconzaole; AMB, amphotericin B; ANF, anidulafungin; MCF, micafungin; CAS, caspofungin; 5-FC, 5-fluorocytosine; MICs, minimum inhibitory concentrations; ECVs, epidemiological cutoff values; WT, wide-type; non-WT, non-wild-type. *S*, susceptible; *R*, resistant; *I*, intermediate. $MIC_{50/90}$ represent the MIC inhibiting the growth of 50 and 90% of the isolates, respectively.

10.3389/fmicb.2022.1006375

Mutation and expression level of resistance-related genes in resistant/NWT isolates

From the sequencing results of *ERG11* in the 14 triazole-resistant/NWT *C. albicans* isolates, missense mutations were detected in 10 isolates, among which the most common substitution is Y132H exhibiting in 6 isolates. Four isolates without *ERG11* mutations exhibited overexpression of *ERG11*, *CDR1*, *CDR2*, or *MDR1* (Table 3). One isolate of *C. parapsilosis sensu stricto* cross-resistant to FLC and POS harbored R398I substitution in Erg11p as well as *CDR1* overexpression. Among the 23 triazole-resistant/NWT *C. tropicalis* isolates, only 6 isolates exhibited amino acid substitutions in Erg11p, among which S154F was detected in 1 isolate, Y132F with S154F was present in 5 isolates. Overexpression of *MDR1* was most frequent in triazole-resistant isolates (21/23), followed by *ERG11*, *CDR1*, and *CDR2*. In 25 triazole-resistant/NWT *C. glabrata* isolates, no mutations in *ERG11* despite of 5 isolates showed *ERG11* overexpression. Five isolates had *PDR1* modifications, among which P76S, P143T, D243N were detected in 3 isolates, 1 each harboring R250K and Y682C, respectively. Overall, there were 14, 13, and 8 isolates showed overexpression of *CDR1*, *CDR2*, and *SNQ2*, respectively. The entire sequences of *FKS1* and *FKS2* were determined in 2 echinocandin-resistant *C. glabrata* isolates, and S663P substitutions in *FKS2* were detected in both isolates (Table 3).

Discussion

To our knowledge, there are several excellent surveillance studies of IFDs worldwide, such as the SENTRY Antimicrobial Surveillance Program (Pfaller et al., 2019), the ARTEMIS DISK study (Pfaller et al., 2010), the SCOPE Program (Wisplinghoff et al., 2014), and so on. In China, the national-wide surveillance studies include the China Hospital Invasive Fungal Surveillance Net (CHIF-NET) study, which has provided useful data on the epidemiology of IFDs in mainland China (Xiao et al., 2018b), and China-SCAN study determining species distribution and antifungal susceptibility of invasive *Candida* infection (ICI) in ICU across China (Liu et al., 2014). The CARST-fungi study is another multi-center surveillance study of IFDs in mainland China with its inception in July 2019. Totally 9 hospitals participated during the first year with the collection of 269 yeast isolates. As expected, the four major *Candia* species, *C. albicans*, *C. parapsilosis* complex, *C. tropicalis*, and *C. glabrata*, accounted for predominate proportion. Although *C. albicans* remained the most prevalent (120, 44.6%), the proportion of non-*albicans Candida* species was over 50%, especially have been the primary causative pathogen of candidemia, in accordance with previous studies from China (Xiao et al., 2018a; Song et al., 2020), Asia-Pacific regions, and European countries (Pappas et al., 2018).

Mixed species detection in the same specimen was another significant result of our study. Totally, 8 out of 261 samples (3.1%) in our study were co-isolated with more than 1 yeast species, among which 4 cases were *C. albicans*/*C. glabrata* mixed, 1 each *C. albicans*/*C. tropicalis mixed and C. parapsilosis sensu stricto*/*C. metapsilosis* mixed, and 2 cases of *C. albicans* /*T. asahii* co-isolated. Indeed, mixed yeast infections have been detected in 8.78% of the culture-positive samples in an extensive study of 6,192 clinical yeast isolates (Cassagne et al., 2016). Similarly, an 18-year report from a tertiary-care university hospital revealed the incidence of mixed fungaemia was 3.7% (33/883) (Gulmez et al., 2020). Most mixed species in our study were *C. albicans*/*C. glabrata*, in accordance with the above-mentioned studies. Several studies revealed that *C. albicans* and *C. glabrata* are frequently co-isolated and co-adhesion *in vitro* (Tati et al., 2016), demonstrating enhanced invasion and increased tissue damage (Silva et al., 2011; Alves et al., 2014), which probably can be explained for the high proportion of the co-culture of these two species. Of note, most specimens contained yeast isolates that were non-susceptible to one or more antifungals. Mixed infections may further bring additional issues for treatment, especially infected by more than one fungal species with different drug susceptibilities, which highlights that mycological analysis of clinical samples should also reliably detect mixed fungal species, especially those involving yeasts species with a particular antifungal resistance profile. A previous study suggested that detection of mixed infection increased significantly after subculture from yeast-positive blood-culture bottles and routine use of chromogenic agar (Gulmez et al., 2020).

First-line drugs treating IFDs, including echinocandins and triazoles, are relatively effective, but the emergence of antifungal resistance is a matter of concern and poses a global threat (Pappas et al., 2018). In our study, most *C. albicans* and *C. parapsilosis* complex are susceptible to all the antifungals tested. Only 1 isolate (2.0%) of *C. parapsilosis sensu stricto* exhibited triazole-resistance, similar to the global (Pfaller et al., 2019) and domestic data (Wang et al., 2016; Xiao et al., 2018a; Song et al., 2020). The overall triazole-resistant rate of *C. albicans* was 11.6% (14/120), higher than the global data (<1%) (Pfaller et al., 2019). However, triazole susceptibility of *C. tropicalis* and *C. glabrata* was low, with only 42.5% (17/40) *C. tropicalis* and 30.5% (11/36) *C. glabrata* susceptible/WT to all tested triazoles. Of particular note, the POS-resistant rate of *C. tropicalis* isolates was 47.5% and the VRC-resistant rate of *C. glabrata* isolates was 55.6%, consistent with previous reports (Xiao et al., 2018a; Song et al., 2020) and much higher than that of past decade (Liu et al., 2014).

Another noteworthy finding of our study was the emergence of echinocandin resistance, although exhibiting excellent activity to most common *Candida* isolates. Two isolates of *C. glabrata* were cross-resistant to all the echinocandins tested, which also NWT to POS and defined as multidrug-resistant. Echinocandin-resistance among *C. glabrata* isolates ranges from 3–5% in population-based studies, and some centers even report as high as 10–15% (Farmakiotis et al., 2014), but it is less than 1% in China (Hou et al., 2017). Alarmingly, *C. glabrata* often presents as multidrug-resistance, with nearly one-third of echinocandin-resistant isolates also being

TABLE 3 Mutations and expression level of resistance-related genes in resistant/NWT *Candida* isolates.

Species/ Isolates	Antifungal susceptibility/MICs[a] (μg/ml)										Amino acid substitutions[b]			Gene expression[c]				
	FLC	ITC	VRC	POS	ISA	AMB	ANF	MCF	CAS	5-FC	*ERG11*	*PDR1*	*FKS2*	*ERG11*	*CDR1*	*CDR2*	*MDR1*	*SNQ2*
Candida albicans																		
10080	4	0.25	1	0.12	0.008	1	0.06	0.008	0.03	>64	WT	/	/	0.92	0.48	3.26*	0.77	/
10081	8	0.25	0.5	0.06	1	0.5	0.12	0.008	0.03	>64	T123I, Y132H	/	/	0.41	0.71	1.16	0.98	/
10108	>256	>8	>16	>8	>16	1	0.12	0.015	0.12	0.06	S263L, E266D	/	/	1.10	0.45	0.42	1.05	/
10568	1	0.25	0.03	0.12	0.008	1	0.12	0.008	0.06	0.06	S263L, E266D	/	/	2.03	2.03	1.50	2.04*	/
10570	>256	>8	>16	>8	>16	0.5	0.06	0.008	0.03	0.06	D116E, S263L, E266D	/	/	1.07	0.34	0.17	1.12	/
10573	1	0.12	0.03	0.12	0.03	1	0.12	0.015	0.12	0.25	D116E, K128T	/	/	0.42	2.19*	3.17	0.32	/
10574	2	0.25	0.5	0.12	0.5	0.5	0.12	0.015	0.06	0.25	D116E, K128T, Y132H, G465S	/	/	3.07*	0.25	0.25	0.82	/
10576	2	0.25	0.25	0.12	0.25	0.12	0.12	0.015	0.06	0.15	D116E, K128T, Y132H, G465S	/	/	0.25	0.46	0.30	3.03	/
10580	4	0.06	0.06	1	0.015	1	0.06	0.008	0.06	0.06	WT	/	/	0.65	0.57	7.07***	1.02	/
10648	256	>8	>16	>8	>16	0.5	0.06	0.015	0.06	<0.06	WT	/	/	7.54**	7.19**	0.98	1.93	/
10749	8	0.25	2	0.03	0.06	1	0.015	0.015	0.015	0.5	WT	/	/	2.19*	0.22	0.17	3.01**	/
10751	4	0.25	0.5	0.12	4	0.5	0.015	0.015	0.015	0.5	T123I, Y132H	/	/	1.02	2.13	0.78	2.31	/
10813	2	0.12	0.25	0.12	0.25	0.5	0.12	0.015	0.03	0.5	D116E, K128T, Y132H, G665S	/	/	1.14	0.26	0.25	2.02	/
10837	4	0.25	1	0.12	4	1	0.03	0.015	0.015	0.5	T123I, Y132H	/	/	0.82	0.41	2.81	0.59	/
Candida parapsilosis																		
10717	8	0.5	0.25	0.5	0.5	0.5	2	2	0.5	0.06	R398I	/	/	0.46	5.56**	/	0.64	/
Candida tropicalis																		
09956	>256	1	>16	2	0.5	2	0.12	0.03	0.06	0.06	Y132F, S154F	/	/	2.23	1.29	0.91	14.79**	/
10116	>256	1	>16	2	0.25	2	0.06	0.03	0.03	0.06	Y132F, S154F	/	/	6.62*	2.51	3.74	13.57**	/
10582	32	0.25	2	2	0.25	1	0.12	0.03	0.06	0.06	Y132F, S154F	/	/	1.83	0.92	0.97	4.76**	/
10641	64	0.25	2	1	0.25	1	0.12	0.06	0.03	<0.06	Y132F, S154F	/	/	10.28**	0.77	0.82	14.01***	/
09969	32	0.25	1	1	0.5	1	0.12	0.06	0.06	0.06	Y132F, S154F	/	/	1.70	2.45	9.07**	1.65	/
09973	128	0.25	4	1	0.12	1	0.12	0.03	0.03	0.06	WT	/	/	2.51	1.88	1.15	7.33**	/
10687	8	0.25	0.25	0.12	0.06	1	0.12	0.03	0.03	<0.06	WT	/	/	2.33	0.47	1.76	3.83**	/
10756	64	16	2	8	0.008	0.5	0.03	0.03	0.015	<0.06	WT	/	/	2.96	1.37	0.78	4.69***	/
10832	64	0.5	4	1	0.015	1	0.12	0.03	0.03	<0.06	S154F	/	/	4.37***	3.78*	6.74	13.26**	/
10041	4	0.5	0.25	0.5	0.06	1	0.5	0.12	0.06	0.06	WT	/	/	0.21	1.62	0.69	3.21**	/
10052	1	0.25	0.25	0.25	0.008	1	0.03	0.12	0.06	0.12	WT	/	/	1.52	1.34	2.35*	3.81***	/
10075	4	0.5	0.12	0.5	0.03	1	0.06	0.03	0.03	0.06	WT	/	/	4.55*	8.10	2.17	21.11**	/

(Continued)

10.3389/fmicb.2022.1006375

TABLE 3 (Continued)

Species/ Isolates	Antifungal susceptibility/MICs[a] (μg/ml)										Amino acid substitutions[b]			Gene expression[c]				
	FLC	ITC	VRC	POS	ISA	AMB	ANF	MCF	CAS	5-FC	*ERG11*	*PDR1*	*FKS2*	*ERG11*	*CDR1*	*CDR2*	*MDR1*	*SNQ2*
10083	4	0.5	0.12	0.5	0.015	1	0.12	0.015	0.25	0.06	WT	/	/	2.03	1.34	1.16	6.42***	/
10117	4	0.5	0.12	0.25	0.03	1	0.12	0.03	0.25	0.06	WT	/	/	2.21	1.51	0.86	5.34**	/
10113	4	0.5	0.12	0.25	4	1	0.12	0.03	0.12	0.06	WT	/	/	1.90	3.01*	3.20*	7.37***	/
10120	256	0.03	0.06	0.12	0.5	1	0.06	0.03	0.03	0.06	WT	/	/	7.50**	5.90***	3.55**	28.11**	/
10629	4	0.5	0.12	0.25	0.03	0.5	0.06	0.03	0.03	0.06	WT	/	/	1.37	1.02	1.05	9.77**	/
10737	8	0.03	0.12	0.12	0.008	1	0.25	0.06	0.03	0.06	WT	/	/	4.85**	4.77**	2.36	15.49**	/
10752	8	0.5	0.06	0.06	0.008	1	0.03	0.03	0.015	0.06	WT	/	/	1.87	0.83	2.48	5.06***	/
10831	4	0.5	0.25	0.25	8	2	0.25	0.06	0.03	0.06	WT	/	/	2.74	0.76	0.66	7.77***	/
10739	4	0.5	0.5	0.25	0.015	2	0.12	0.03	0.03	0.06	WT	/	/	4.37**	3.78*	6.74**	13.26***	/
10639	4	0.25	0.25	0.25	0.25	1	0.12	0.06	0.06	>64	WT	/	/	3.77**	0.75	2.72	1.80	/
10642	4	0.5	0.12	0.25	0.008	1	0.03	0.03	0.03	0.06	WT	/	/	3.74*	11.59***	2.35	20.68***	/
Candida glabrata																		
10090	32	0.5	1	1	0.12	1	0.06	0.015	0.12	0.25	WT	WT	/	1.85	13.64**	19.97**	/	3.97
10123	128	>8	4	>8	2	1	0.12	0.015	0.12	0.06	WT	Y682C	/	0.54	2.64*	3.68***	/	1.33*
10124	32	1	1	1	0.12	1	0.06	0.008	0.12	0.06	WT	WT	/	5.33	10.27*	2.20	/	2.81
10578	16	1	2	2	0.015	1	0.03	0.008	0.06	0.06	WT	P76S, P143T, D243N	/	0.56	0.68	1.54	/	0.50
10045	16	>8	>16	>8	0.06	1	0.03	0.015	0.06	0.06	WT	WT	/	0.50	1.75	0.14	/	0.50
10055	32	1	1	2	0.12	0.5	0.03	0.008	0.03	0.06	WT	R250K	/	1.42*	7.22***	7.59***	/	2.92
10652	32	1	1	1	0.25	1	0.03	<0.008	0.03	<0.06	WT	WT	/	1.04	3.20*	1.10	/	0.14
09979	16	1	1	2	0.03	0.25	0.03	0.015	0.12	0.06	WT	WT	/	14.66**	6.56***	2.69	/	1.93
10742	64	1	2	2	0.015	0.5	0.06	0.015	0.12	<0.06	WT	WT	/	5.25***	1.45	3.11	/	1.98*
10720	4	2	0.12	4	0.25	1	4	8	>16	0.06	WT	P76S, P143T, D243N	S663P	4.35***	0.97	1.44	/	1.42
10722	4	2	0.12	4	0.25	1	4	8	>16	0.06	WT	P76S, P143T, D243N	S663P	1.12	3.01**	1.04	/	1.37
10082	32	1	1	1	0.5	0.5	0.03	0.015	0.06	0.06	WT	WT	/	1.84	0.59	4.51	/	1.64
10088	32	0.5	0.5	2	0.25	1	0.06	0.015	0.12	0.06	WT	WT	/	0.71	9.76	9.47	/	8.81**
10630	32	1	1	1	0.5	1	0.015	0.015	0.03	<0.06	WT	WT	/	2.27	4.15	13.36***	/	11.34**
10638	32	1	1	1	0.25	1	0.03	0.015	0.06	<0.06	WT	WT	/	4.96**	6.73*	0.74	/	1.40
10644	16	0.5	0.5	1	0.25	1	0.03	0.015	0.06	<0.06	WT	WT	/	0.33	6.72**	15.56***	/	4.24
10645	16	0.5	0.5	1	0.06	0.5	0.015	0.015	0.03	<0.06	WT	WT	/	0.67	10.62***	6.66**	/	2.89
10655	32	0.5	1	1	0.06	1	0.03	0.015	0.03	<0.06	WT	WT	/	2.61	0.36	1.15	/	0.99

(Continued)

10.3389/fmicb.2022.1006375

TABLE 3 (Continued)

Species/ Isolates	Antifungal susceptibility/MICs[a] (μg/ml)									Amino acid substitutions[b]		Gene expression[c]			
	FLC	ITC	VRC	POS	ISA	AMB	ANF	MCF	CAS	5-FC	*ERG11*	*PDR1*	*FKS2*	*ERG11*	*CDR1*	*CDR2*	*MDR1*	*SNQ2*
10827	16	0.5	0.5	1	0.25	1	0.015	0.015	0.03	<0.06	WT	WT	/	0.13	21.96**	31.80**	/	2.74
10828	32	1	1	1	0.25	1	0.03	0.015	0.06	<0.06	WT	WT	/	0.16	2.47	14.10***	/	4.65
10829	32	1	1	1	0.06	1	0.03	0.015	0.06	<0.06	WT	WT	/	0.23	3.34	18.61***	/	3.98*
10830	32	1	1	1	0.015	1	0.03	0.015	0.03	0.06	WT	WT	/	7.50*	11.46***	3.74**	/	1.42
10838	16	0.5	0.5	1	0.25	1	0.03	0.015	0.06	<0.06	WT	WT	/	1.21	1.26	13.26***	/	7.38**
10718	32	0.5	1	1	0.015	1	0.06	0.015	0.06	0.06	WT	WT	/	3.44	3.50*	20.36***	/	4.68*
10728	32	0.5	0.25	2	0.25	1	0.12	0.015	0.12	0.06	WT	WT	/	0.65	4.54**	5.99**	/	7.85*

[a]Antifungal susceptibility MICs were determined by the CLSI M27-A4 broth microdilution method. FLC, fluconazole; ITC, itraconazole; VRC, voriconazole, POS, posaconazole; ISA, isavuconzaole; AMB, amphotericin B; ANF, anidulafungin; MCF, micafungin; CAS, caspofungin; 5-FC, 5-fluorocytosine. MICs highlighted in red represent the isolate non-susceptible to the antifungal agent.

[b]Sequences were align against that of *C. albicans* SC5314, *C. glabrata* CBS138, *C. tropicalis* MYA-3404, and *C. parapsilosis* CDC317 from the Candida Genome Database (http://www.candidagenome.org/) as reference.

[c]Quantification was performed using real-time PCR. Values are averages from three independent experiments and relative gene expression ($2^{\Delta\Delta Ct}$) was calculated as the fold change in expression of the isolates compared to the mean expression values in drug-susceptible control strains including *C. albicans* SC5314, *C. glabrata* CBS138, *C. tropicalis* ATCC01463, and *C. parapsilosis* ATCC22019. Statistical significant overexpression genes relative to that of control strains were indicated as *$p < 0.05$; **$p < 0.01$; ***$p < 0.0001$.

non-susceptible to triazoles, leaving extremely few options to treat patients infected with multidrug-resistant isolates (Healey and Perlin, 2018). Emerging of multidrug-resistance is a significant threat to the treatment of IFD and urges our research group to explore the resistance mechanism of the *C. glabrata* isolates, demonstrating mutations in *FKS2* explaining echinocandin-resistance and overexpression of *CDR1* and *ERG11* contributing to triazole-resistance (Wang et al., 2021).

Except for the above-mentioned common *Candida* species, less common and cryptic yeast species were also identified in this study, among which *C. metapsilosis* accounted for a high proportion of *C. parapsilosis* complex (9/50), indicating the proportion was underestimated. Interestingly, *C. metapsilosis* and *C. parapsilosis* were co-cultured, highlight the significance of subculture and accurate identification. One isolate of *C. fabianii* was identified in our study. *C. fabianii* infections have rarely been reported (Park et al., 2019) and only one case has been reported in China which causes blood infection in a premature infant (Wu et al., 2013). Additionally, *W. anomalus* (previously named *C. pelliculosa*) accounted for a low rate (<1%) and was similar to previous national surveillance in China (Liu et al., 2014), and to our knowledge, one of which in our study is the first isolate of *W. anomalus* reported to be cultured from CSF in China. *W. anomalus* isolates in our study were less susceptible to FLC (MICs 2–8 μg/ml) and POS (MIC, 0.5 μg/ml), while AMB, echinocandins, and 5-FC showed good *in vitro* activity, but recent research revealed that *W. anomalus* isolates showed high MICs against all triazoles tested and 5-FC (Zhang et al., 2021). As for other yeast genera, *C. neoformans*, *R. mucilaginosa*, and *T. asahii* were included in our study. As expected, most *C. neoformans* isolates were isolated from CSF, which is believed to be the prevalent pathogen of fungal meningitis. *R. mucilaginosa* is a multidrug-resistant pathogen with the ability to cause nosocomial infection (Huang et al., 2022), which exhibited high MICs to all the triazoles and echinocandins. Recently, *Trichosporon* spp. which is usually associated with superficial mycosis has recently been recognized as an emergent fungal pathogen capable of causing invasive infections (Padovan et al., 2019). Besides intrinsic echinocandins-resistance, one isolate of *T. asahii* in our study showed high MICs to all triazoles and 5-FC. Several studies have estimated antifungal profiles of rare yeast species (Stavrou et al., 2020), demonstrated that high MICs against azole drugs and echinocandins were common and resistance rates in yeast species are dynamic and variable between medical institutions and countries (Desnos-Ollivier et al., 2021), highlighting the need for an accurate species identification of yeast isolates, which is essential for proper management of patients and prevention of emergence of drug resistance.

Finally, sequence of *ERG11* genes (and *PDR1* in *C. glabrata*) and expression level of *ERG11* and efflux pump genes in triazole-resistant *Candida* isolates and sequence of *FKS* genes in echinocandin-resistant isolates were determined. *ERG11* mutations were found in 10 of 14 triazole-resistant *C. albicans* isolates and 6 of 23 *C. tropicalis* isolates, the most common substitution is Y132H in *C. albicans,* and Y132F with S154F in *C. tropicalis*, similar to Y132F and S154F were the most common substitutions in Erg11p of *C. tropicalis* and proven to mediate triazole resistance (Jiang et al., 2012; Castanheira et al., 2020).

Except for mutations of drug target, overexpression of *MDR1* seems as the predominant mechanism of *C. tropicalis* triazole-resistance in our study. Despite of no *ERG11* mutation was detected in triazole-resistant *C. glabrata* isolates, 5 isolates exhibited *ERG11* overexpression, which was considered to be less common in *C. glabrata*. *PDR1* modifications were detected in 5 isolates, with 3 isolates harboring P76S, P143T, D243N and 1 each harboring R250K and Y682C, respectively. The latter two isolates showed high expression level of ABC transporter genes including *CDR1*, *CDR2*, and *SNQ2*, indicating those *PDR1* modifications maybe GOF mutations resulting in up-regulation of downstream ABC transporter genes, which need further verification. The entire sequences of *FKS1* and *FKS2* were determined in 2 echinocandin-resistant *C. glabrata* isolates and S663P substitutions in *FKS2* were detected in both isolates. Notably, there are numerous isolates without modifications in well-known drug targets or up-regulation of transporter genes, the resistant mechanisms remain to be elucidated.

There are some limitations in our study. First, this paper concluded the first-year data of the CARST-fungi study, which encompass only nine hospitals cannot reveal the dynamic change year by year. The study will continue and more centers will join in to enhance the comprehension of epidemiology and antifungal susceptibilities in pathogenic yeasts across China. Second, the information of the patients is incomplete including mycoses, antibiotics used, basal conditions and other more detailed clinical characteristics. These data need to be included in future study. Nevertheless, this study provides important epidemiological findings of species distribution, antifungal susceptibility profile, and preliminary resistant mechanism exploration, which are instrumental in designing strategies for better management of yeast infections in China.

In conclusion, the CARST-fungi study demonstrated that although *C. albicans* remain the most predominant species, non-*C. albicans* species accounted for a high proportion, especially as the causative pathogen of fungemia. Triazole-resistance is notable among *C. tropicalis* and *C. glabrata* and multidrug-resistant isolates of *C. glabrata* and less common yeast have been emerging.

Data availability statement

The original contributions presented in the study are included in the article/Supplementary material, further inquiries can be directed to the corresponding author.

Author contributions

WL designed the experiments, supervised the data analysis, and contributed to funding acquisition. WL, YL, BZ, and RL administered the project. XC, JZ, ZL, YJ, LM, YML, SP, XA, and FZ collected all the isolates and provided clinical information. QW contributed to the species identification, antifungal susceptibility testing, molecular biology experiments, and original draft preparation. YL and ZW supervised the transformation, collection, and storage of the isolates. QW, XC, and WL contributed to writing and reviewing the manuscript. All authors contributed to the article and approved the submitted version.

Funding

This study was supported by the National Key Research and Development Program of China (2021YFC2302005) and National Natural Science Foundation of China (81971912).

Conflict of interest

The authors declare that the research was conducted in the absence of any commercial or financial relationships that could be construed as a potential conflict of interest.

Publisher's note

Supplementary material

The Supplementary material for this article can be found online at: https://www.frontiersin.org/articles/10.3389/fmicb.2022.1006375/full#supplementary-material

References

Alexander, B. D., Johnson, M. D., Pfeiffer, C. D., Jiménez-Ortigosa, C., Catania, J., Booker, R., et al. (2013). Increasing echinocandin resistance in *Candida glabrata*: clinical failure correlates with presence of *FKS* mutations and elevated minimum inhibitory concentrations. *Clin. Infect. Dis.* 56, 1724–1732.doi: 10.1093/cid/cit136

Alves, C. T., Wei, X. Q., Silva, S., Azeredo, J., Henriques, M., and Williams, D. W. (2014). *Candida albicans* promotes invasion and colonisation of *Candida glabrata* in a reconstituted human vaginal epithelium. *J. Infect.* 69, 396–407. doi: 10.1016/j.jinf.2014.06.002

Arastehfar, A., Lass-Flörl, C., Garcia-Rubio, R., Daneshnia, F., Ilkit, M., Boekhout, T., et al. (2020). The quiet and underappreciated rise of drug-resistant invasive fungal pathogens. *J. Fungi (Basel)* 6:138. doi: 10.3390/jof6030138

Bassetti, M., Garnacho-Montero, J., Calandra, T., Kullberg, B., Dimopoulos, G., Azoulay, E., et al. (2017). Intensive care medicine research agenda on invasive fungal infection in critically ill patients. *Intensiv. Care Med.* 43, 1225–1238. doi: 10.1007/s00134-017-4731-2

Cassagne, C., Normand, A.-C., Bonzon, L., L'Ollivier, C., Gautier, M., Jeddi, F., et al. (2016). Routine identification and mixed species detection in 6, 192 clinical yeast isolates. *Med. Mycol.* 54, 256–265. doi: 10.1093/mmy/myv095

Castanheira, M., Deshpande, L. M., Messer, S. A., Rhomberg, P. R., and Pfaller, M. A. (2020). Analysis of global antifungal surveillance results reveals

predominance of erg 11 Y132F alteration among azole-resistant *Candida parapsilosis* and *Candida tropicalis* and country-specific isolate dissemination. *Int. J. Antimicrob. Agents* 55:105799. doi: 10.1016/j.ijantimicag.2019.09.003

CLSI (2017). *Clinical and Laboratory Standards Institute. Reference Method for Broth Dilution Antifungal Susceptibility Testing of Yeasts. Approved Standard-Fourth Edition*. Wayne, PA: Clinical and Laboratory Standards Institute.

CLSI (2020a). *Clinical and Laboratory Standards Institute. Performance Standards for Antifungal Susceptibility Testing of Yeasts, CLSI Supplement M60. 2nd edn*. Wayne, PA: Clinical and Laboratory Standards Institute.

CLSI (2020b). *Epidemiological Cutoff Values for Antifungal Susceptibility Testing. CLSI Supplement M59. 3rd edn*. Wayne, PA: Clinical and Laboratory Standards Institute.

Desnos-Ollivier, M., Lortholary, O., Bretagne, S., and Dromer, F. (2021). Azole susceptibility profiles of more than 9,000 clinical yeast isolates belonging to 40 common and rare species. *Antimicrob. Agents Chemother.* 65, e02615–e02620. doi: 10.1128/aac.02615-20

Farmakiotis, D., Tarrand, J. J., and Kontoyiannis, D. P. (2014). Drug-resistant *Candida glabrata* infection in cancer patients. *Emerg. Infect. Dis.* 20, 1833–1840. doi: 10.3201/eid2011.140685

Gulmez, D., Alp, S., Gursoy, G., Ayaz, C. M., Dogan, O., Arikan-Akdagli, S., et al. (2020). Mixed fungaemia: an 18-year report from a tertiary-care university hospital and a systematic review. *Clin. Microbiol. Infect.* 26, 833–841. doi: 10.1016/j.cmi.2020.03.030

Healey, K. R., and Perlin, D. S. (2018). Fungal resistance to echinocandins and the MDR phenomenon in *Candida glabrata*. *J. Fungi (Basel)* 4:105. doi: 10.3390/jof4030105

Hou, X., Xiao, M., Chen, S. C., Kong, F., Wang, H., Chu, Y. Z., et al. (2017). Molecular epidemiology and antifungal susceptibility of *Candida glabrata* in China (August 2009 to July 2014): a multi-center study. *Front. Microbiol.* 8:880. doi: 10.3389/fmicb.2017.00880

Huang, J. J., Chen, X. F., Tsui, C. K. M., Pang, C. J., Hu, Z. D., Shi, Y., et al. (2022). Persistence of an epidemic cluster of *Rhodotorula mucilaginosa* in multiple geographic regions in China and the emergence of a 5-flucytosine resistant clone. *Emerg. Microbes. Infect.* 11, 1079–1089. doi: 10.1080/22221751.2022.2059402

Jiang, C., Dong, D., Yu, B., Cai, G., Wang, X., Ji, Y., et al. (2012). Mechanisms of azole resistance in 52 clinical isolates of *Candida tropicalis* in China. *J. Antimicrob. Chemother.* 68, 778–785. doi: 10.1093/jac/dks481

Kett, D. H., Azoulay, E., Echeverria, P. M., and Vincent, J.-L. (2011). *Candida* bloodstream infections in intensive care units: analysis of the extended prevalence of infection in intensive care unit study. *Crit. Care Med.* 39, 665–670. doi: 10.1097/CCM.0b013e318206c1ca

Lamoth, F., Lockhart, S. R., Berkow, E. L., and Calandra, T. (2018). Changes in the epidemiological landscape of invasive candidiasis. *J. Antimicrob. Chemother.* 73, i4–i13. doi: 10.1093/jac/dkx444

Liu, W., Tan, J., Sun, J., Xu, Z., Li, M., Yang, Q., et al. (2014). Invasive candidiasis in intensive care units in China: in vitro antifungal susceptibility in the China-SCAN study. *J. Antimicrob. Chemother.* 69, 162–167. doi: 10.1093/jac/dkt330

Miceli, M. H., Díaz, J. A., and Lee, S. A. (2011). Emerging opportunistic yeast infections. *Lancet Infect. Dis.* 11, 142–151. doi: 10.1016/S1473-3099(10)70218-8

Orasch, C., Marchetti, O., Garbino, J., Schrenzel, J., Zimmerli, S., Muhlethaler, K., et al. (2014). *Candida* species distribution and antifungal susceptibility testing according to European committee on antimicrobial susceptibility testing and new vs. old clinical and laboratory standards institute clinical breakpoints: a 6-year prospective candidaemia survey from the fungal infection network of Switzerland. *Clin. Microbiol. Infect.* 20, 698–705. doi: 10.1111/1469-0691.12440

Padovan, A. C. B., Rocha, W., Toti, A. C. M., Freitas de Jesus, D. F., Chaves, G. M., and Colombo, A. L. (2019). Exploring the resistance mechanisms in *Trichosporon asahii*: triazoles as the last defense for invasive trichosporonosis. *Fungal Genet. Biol.* 133:103267. doi: 10.1016/j.fgb.2019.103267

Pappas, P. G., Kauffman, C. A., Andes, D. R., Clancy, C. J., Marr, K. A., Ostrosky-Zeichner, L., et al. (2016). Clinical practice guideline for the management of candidiasis: 2016 update by the infectious diseases society of America. *Clin. Infect. Dis.* 62, e1–e50. doi: 10.1093/cid/civ933

Pappas, P. G., Lionakis, M. S., Arendrup, M. C., Ostrosky-Zeichner, L., and Kullberg, B. J. (2018). Invasive candidiasis. *Nat. Rev. Dis. Primers.* 4:18026. doi: 10.1038/nrdp.2018.26

Park, J.-H., Oh, J., Sang, H., Shrestha, B., Lee, H., Koo, J., et al. (2019). Identification and antifungal susceptibility profiles of *Cyberlindnera fabianii* in Korea. *Mycobiology* 47, 449–456. doi: 10.1080/12298093.2019.1651592

Pfaller, M. A., Diekema, D. J., Gibbs, D. L., Newell, V. A., Ellis, D., Tullio, V., et al. (2010). Results from the ARTEMIS DISK global antifungal surveillance study, 1997 to 2007: a 10.5-year analysis of susceptibilities of *Candida* species to fluconazole and voriconazole as determined by CLSI standardized disk diffusion. *J. Clin. Microbiol.* 48, 1366–1377. doi: 10.1128/jcm.02117-09

Pfaller, M. A., Diekema, D. J., Turnidge, J. D., Castanheira, M., and Jones, R. N. (2019). Twenty years of the SENTRY antifungal surveillance program: results for *Candida* species from 1997–2016. *Open Forum Infect. Dis.* 6, S79–S94. doi: 10.1093/ofid/ofy358

Pfaller, M. A., Woosley, L. N., Messer, S. A., Jones, R. N., and Castanheira, M. (2012). Significance of molecular identification and antifungal susceptibility of clinically significant yeasts and moulds in a global antifungal surveillance programme. *Mycopathologia* 174, 259–271. doi: 10.1007/s11046-012-9551-x

Silva, S., Henriques, M., Hayes, A., Oliveira, R., Azeredo, J., and Williams, D. W. (2011). Candida glabrata and Candida albicans co-infection of an in vitro oral epithelium. *J. Oral Pathol. Med.* 40, 421–427. doi: 10.1111/j.1600-0714.2010.00981.x

Song, Y., Chen, X., Yan, Y., Wan, Z., Liu, W., and Li, R. (2020). Prevalence and antifungal susceptibility of pathogenic yeasts in China: a 10-year retrospective study in a teaching hospital. *Front. Microbiol.* 11:1401. doi: 10.3389/fmicb.2020.01401

Stavrou, A. A., Perez-Hansen, A., Lackner, M., Lass-Florl, C., and Boekhout, T. (2020). Elevated minimum inhibitory concentrations to antifungal drugs prevail in 14 rare species of candidemia-causing *Saccharomycotina* yeasts. *Med. Mycol.* 58, 987–995. doi: 10.1093/mmy/myaa005

Tati, S., Davidow, P., McCall, A., Hwang-Wong, E., Rojas, I. G., Cormack, B., et al. (2016). *Candida glabrata* binding to *Candida albicans* hyphae enables its development in oropharyngeal candidiasis. *PLoS Pathog.* 12:e1005522. doi: 10.1371/journal.ppat.1005522

Wang, H., Zhang, L., Kudinha, T., Kong, F., Ma, X. J., Chu, Y. Z., et al. (2016). Investigation of an unrecognized large-scale outbreak of *Candida parapsilosis sensu stricto* fungaemia in a tertiary-care hospital in China. *Sci. Rep.* 6:27099. doi: 10.1038/srep27099

Wang, Q., Li, Y., Cai, X., Li, R., Zheng, B., Yang, E., et al. (2021). Two sequential clinical isolates of *Candida glabrata* with multidrug-resistance to posaconazole and echinocandins. *Antibiotics (Basel)* 10:1217. doi: 10.3390/antibiotics10101217

Wisplinghoff, H., Ebbers, J., Geurtz, L., Stefanik, D., Major, Y., Edmond, M. B., et al. (2014). Nosocomial bloodstream infections due to *Candida* spp. in the USA: species distribution, clinical features and antifungal susceptibilities. *Int. J. Antimicrob. Agents* 43, 78–81. doi: 10.1016/j.ijantimicag.2013.09.005

Wu, Y., Wang, J., Li, W., Jia, H., Che, J., Lu, J., et al. (2013). *Pichia fabianii* blood infection in a premature infant in China: case report. *BMC. Res. Notes* 6:77. doi: 10.1186/1756-0500-6-77

Xiao, M., Chen, S. C. A., Kong, F., Fan, X., Cheng, J.-W., Hou, X., et al. (2018a). Five-year China Hospital invasive fungal surveillance net (CHIF-NET) study of invasive fungal infections caused by noncandidal yeasts: species distribution and azole susceptibility. *Infect. Drug Resist.* 11, 1659–1667. doi: 10.2147/IDR.S173805

Xiao, M., Sun, Z. Y., Kang, M., Guo, D. W., Liao, K., Chen, S. C., et al. (2018b). Five-year national surveillance of invasive candidiasis: species distribution and azole susceptibility from the China Hospital invasive fungal surveillance net (CHIF-NET) study. *J. Clin. Microbiol.* 56, e00577–e00518. doi: 10.1128/jcm.00577-18

Zhang, L., Xiao, M., Arastehfar, A., Ilkit, M., Zou, J., Deng, Y., et al. (2021). Investigation of the emerging nosocomial *Wickerhamomyces anomalus* infections at a Chinese tertiary teaching hospital and a systemic review: clinical manifestations, risk factors, treatment, outcomes, and anti-fungal susceptibility. *Front. Microbiol.* 12:744502. doi: 10.3389/fmicb.2021.744502

frontiers | Frontiers in Microbiology

TYPE Original Research
PUBLISHED 13 October 2022
DOI 10.3389/fmicb.2022.1031388

OPEN ACCESS

EDITED BY
Wenjie Fang,
Shanghai Changzheng Hospital, China

REVIEWED BY
Xin Huang,
Tongji University, China
Depin Zhao,
Tongji University, China

*CORRESPONDENCE
Zhao Han
547588989@qq.com
Xin Ye
yexin0223@xjtu.edu.cn
Xiaojing Li
zlmdsh@126.com

†These authors have contributed equally to this work

SPECIALTY SECTION
This article was submitted to Antimicrobials, Resistance and Chemotherapy, a section of the journal Frontiers in Microbiology

RECEIVED 29 August 2022
ACCEPTED 26 September 2022
PUBLISHED 13 October 2022

CITATION
Jiang W, Hu D, Xu Y, Chen Y, Zhu X, Han Z, Ye X and Li X (2022) Loop-mediated isothermal amplification-microfluidic chip for the detection of *Trichophyton* infection.
Front. Microbiol. 13:1031388.
doi: 10.3389/fmicb.2022.1031388

Loop-mediated isothermal amplification-microfluidic chip for the detection of *Trichophyton* infection

Weiwei Jiang[1†], Dongying Hu[1†], Yanyan Xu[2†], Yang Chen[1], Xiaoyang Zhu[1], Zhao Han[2*], Xin Ye[3*] and Xiaojing Li[2*]

[1]Department of Dermatology, 72nd Group Army Hospital of PLA, Huzhou, Zhejiang, China, [2]Affiliated Hospital of Hebei University of Engineering, Handan, Hebei, China, [3]Department of Laboratory Medicine, The First Affiliated Hospital of Xi'an Jiaotong University, Xi'an, Shaanxi, China

Trichophyton is the most pathogenic type of fungal skin infection. It often invades and grows in a keratin-rich matrix, and lesions include human skin, hair, and fingernails (toenails). We designed LAMP primers for *Trichophyton* and developed a LAMP-Microfluidic chip detection system for *Trichophyton*. This system detects six common species of *Trichophyton* in the genus *Trichophyton*, including *Trichophyton rubrum*, *Trichophyton mentagrophyte*, *Trichophyton violaceum*, *Trichophyton tonsurans*, *Trichophyton verrucosum*, and *Trichophyton schoenleinii*. The specificity reached 100%, and the sensitivity could reach about 1×10^2 copies/μl. The entire detection process can be completed within 60 min and does not cross-react with other dermatophytes. The established LAMP-Microfluidic chip detection system has the advantages of simple operation, high specificity, and high sensitivity, and has the potential for clinical application.

KEYWORDS

***Trichophyton*, LAMP, microfluidics, early diagnosis, chip**

Introduction

Trichophyton is the most common group of fungi responsible for superficial fungal infections, which affect 20–25 percent of the world's population (Havlickova et al., 2008; Maraki and Mavromanolaki, 2016; Zhan and Liu, 2017). *Trichophyton* infects a large number of people and can cause tinea capitis, onychomycosis, tinea manuum, tinea pedis, tinea corporis, etc. It spreads easily, causing self-infection and infecting others. Coupled with irregular treatment and other reasons, it is easy to have a repeat infection. The lack of a long-term cure seriously affects the patient's quality of life. In addition, tinea pedis and onychomycosis may be risk factors for developing acute leg cellulitis or erysipelas, especially in patients with diabetes

(Bristow and Spruce, 2009). According to an epidemiological survey of large-scale superficial mycosis in China, the most common pathogenic species of *Trichophyton* are *Trichophyton rubrum*, *Trichophyton mentagrophyte*, *Trichophyton violaceum*, *Trichophyton tonsurans*, *Trichophyton verrucosum*, and *Trichophyton schoenleinii* (Shao-xi et al., 2011). It is recommended to carry out drug treatment from the level of *Trichophyton* (Fuller et al., 2001, 2014; Devliotou-Panagiotidou and Koussidou-Eremondi, 2004; Kakourou et al., 2010). Irregular antifungal treatment increases the difficulty of treating skin diseases, leads to recurrent attacks, prolongs the course of the treatment, and increases the economic burden on the patients. However, due to the lack of timely and accurate diagnostic measures, the current clinical treatment of dermatophytosis is generally only empirical treatment, such as tinea capitis or onychomycosis, which usually requires several months of antifungal treatment. Therefore, an accurate diagnosis is essential before initiating treatment (Feuilhade de Chauvin, 2005).

Traditionally, fungal microscopy and culture methods are used to detect *Trichophyton* infection, and direct microscopy results are highly subjective, with false-negative cases accounting for 15–30% of routine tests (Summerbell et al., 2005; Panasiti et al., 2006). When conidia or hyphae of strict saprophytic fungi are too shallow or too far from the onychomycosis sampling, they can be seen upon direct inspection of the sample, resulting in false-positive results (Gianni et al., 1997). Most *Trichophytons* species are cultured for a longer time (2 weeks). Some supplementary tests, such as urease, nutrients, and other biochemical tests, or *in vitro* hair perforation tests, are also carried out when identifying some *Trichophyton* species (Shadomy and Philpot, 1980). Therefore, it is particularly necessary to develop a rapid diagnostic method for *Trichophyton* with a high detection rate, high accuracy, low reagent cost, low instrument cost, simple operation, certain high throughput, and direct clinical significance.

Loop-mediated isothermal amplification (LAMP) technology is an isothermal nucleic acid amplification technology (Notomi et al., 2000). It has the advantages of high sensitivity, short reaction time, and simple operation. It has been widely used to detect various pathogens (Kasahara et al., 2014; Liu et al., 2016; Tang et al., 2016; Li et al., 2017). Centrifugal microfluidics labs (lab-on-a-chip) can concentrate various unit technologies on a chip, and finally realize the miniaturization and automation of the entire detection integration; due to the integrated function of the microfluidic chip, the pollution of the sample to the environment during manual operation is minimized; the microfluidic chip can design the number of sample tanks and reaction chambers according to needs, which greatly shortens the detection time and improves the detection efficiency compared with the traditional project-by-project detection; in addition, the system needs less detection reagents and test sample size (Madou et al., 2006; Gorkin et al., 2010).

In this study, the real-time LAMP technology was combined with the microfluidic laboratory-on-a-chip technology to achieve a high-throughput and rapid diagnosis of *Trichophyton*. The formulation of the correct clinical drug regimen is of great significance.

Experimental

Experimental strains and nucleic acid extraction

There were 111 strains in total, including 20 strains of *Trichophyton rubrum*, 20 strains of *Trichophyton mentagrophytes*, 11 strains of *Trichophyton violaceum*, 4 strains of *Trichophyton tonsurans*, 3 strains of *Trichophyton verrucosum*, 8 strains of *Trichophyton schoenleinii*, 16 strains of *Microsporum canis*, 3 strains of *Microsporum ferrugineum*, 6 strains of *Epidermophyton floccosum*, 5 strains of common *Candida*, 5 strains of *Malassezia*, 4 strains of *Aspergillus*, 2 strains of *Penicillium*, 2 strains of *Rhodotorula*, and 2 strains of bacteria (**Table 1**). The strain nucleic acid extraction method was a rapid nucleic acid extraction method. The one-step nucleic acid extraction technology was independently developed by the Shanghai igenetec diagnostics Co. Ltd. There was no need to open the lid during extraction, avoiding aerosol contamination. The nucleic acid extraction kit had a high nucleic acid extraction efficiency and fully met the requirements for DNA sequencing, the PCR reaction, and the isothermal amplification experiments. The entire extraction process could be completed within 15 min.

Primer design and screening

First, the genome sequences of common species of *Trichophyton* were retrieved from Genbank, and the target genes were found to be highly similar to those of the species by Geneious software for analysis and comparison. The selected target gene fragments were significantly different from the sequences of other genera or adjacent species on the phylogenetic tree. Then, using the LAMP primer design software primer ExplorerV4, the *Trichophyton* primers were designed (outer primers F3 and B3; inner primers FIP and BIP, and loop primers LB and LF can be added to further shorten the reaction time). A total of three sets of primers were designed, and their sequences are shown in **Table 2**.

The components were thoroughly mixed according to the LAMP reaction system in **Table 3** and amplified using a 9600Plus fluorescence PCR instrument. In the primer screening stage, the reaction temperature was set to 63°C for 60 s, 60 s

TABLE 1 List of strains used in the test.

Genus	Strain	Strain number
Trichophyton	*T. rubrum*	SCZ60001; SCZ60002; SCZ60006; SCZ60009; SCZ60093; SCZ60096; SCZ60097; SCZ60098; SCZ60099; SCZ600100; SCZ94501; SCZ94502 SCZ94503; SCZ94504; SCZ94505; SCZ94506; SCZ94507; SCZ94508; SCZ94509 ATCC-MYA-4438
	T. mentagrophyte	SCZ30008; SCZ30023; SCZ60092; SCZ60245; SCZ60339; SCZ94510; SCZ94511; SCZ94512; SCZ94513 SCZ94514; SCZ94515; SCZ94516; SCZ94517; SCZ94518; SCZ94519; SCZ94520; SCZ94521; SCZ94522; SCZ94523; SCZ94524
	T. tonsurans	SCZ30024; SCZ30025; SCZ60342; SCZ60344
	T. violaceum	SCZ30005; SCZ30039; SCZ30041; SCZ30046; SCZ30050; SCZ30052 SCZ30057; SCZ30061; SCZ30066; SCZ30068; SCZ60352
	T. verrucosum	SCZ30016; SCZ30019; SCZ30020
	T. schoenleinii	SCZ30007; SCZ60033; SCZ60035; SCZ60340; SCZ60349; SCZ60350; SCZ60351; SCZ60353
Microsporum	*M. canis*	SCZ60167; SCZ60168; SCZ60169; SCZ60170; SCZ60171; SCZ60172; SCZ60173; SCZ60174; SCZ60175; SCZ60179; SCZ94525; SCZ94526; SCZ94527; SCZ94528; SCZ94529; SCZ94530
	M. ferrugineum	SCZ30012; SCZ30014; SCZ30015
Epidermophyton	*E. floccosum*	SCZ30031; SCZ30032; SCZ60140; SCZ94531; SCZ94532; SCZ94533
Candida	*C. albicans*	ATCC MYA-2876
	C. parapsilosis	ATCC 22019
	C. tropicalis	ATCC 66029
	C. glabrata	ATCC 28226
	C. krusei	ATCC 2159
Malassezia	*Malassezia*	SCZ94534; SCZ94535; SCZ94536; SCZ94537; SCZ94538
Aspergillus	*A. fumigatus*	ATCC-MYA-3627
	A. niger	SCZ 10135
	A. flavus	SCZ 10138
	A. terrestris	SCZ60285
Penicillium	*Penicillium*	SCZ60287; SCZ60288
Rhodotorula	*Rhodotorula*	SCZ20005; SCZ20007
bacteria	*Staphylococcus epidermidis*	BP-1; BP-2

T, *Trichophyton*; *M*, *Microsporum*; *E*, *Epidermophyton*; *C*, *Candida*; *A*, *Aspergillus*.

TABLE 2 *Trichophyton* primer sequence list.

Primer number	Primer name	Primer sequence
1	F3	CCGTCGCTACTACCGATTG
	B3	TCTGCTCACCCTGATGGA
	FIP	CAACTTTCCGGCCCTGGGC-GTGAGGCC TTCGGACTGG
	BIP	TCCGTAGGTGAACCTGCGGA-ACG TCGGTCCCTATCGTG
2	F3	ACCGATTGAATGGCTCAGTG
	B3	TCTGCTCACCCTGATGGA
	FIP	TGACCAACTTTCCGGC CCTGAGGCCTTCGGACTGGC
	BIP	TCCGTAGGTGAACCTGC GGAACGTCG GTCCCTATCGTG
3	F3	ACCGATTGAATGGCTCAGTG
	B3	ACGTCTGCTCACCCTGATG
	FIP	TGACCAACTTTCCGGCC CTGAGGCCTTCGGACTGGC
	BIP	AGGTTTCCGTAGGTGAACCT GCGAACGTCGGTCCCTATCGTG

TABLE 3 Loop-mediated isothermal amplification (LAMP) reaction system.

Reactive components	Volume (μ l)
LAMP reaction buffer	17.7
FIP	0.40
BIP	0.40
F3	0.05
B3	0.05
LB (H_2O)	0.20
LF (H_2O)	0.20
Bst polymerase	1.0
DNA template	5
Total	25

is a cycle, and the number of cycles was 90. The amplification curve of the reaction was observed in real-time, and the selected primer and the corresponding cut-off value were comprehensively judged in combination with the CT value.

Loop-mediated isothermal amplification system evaluation and verification

Specific experimental testing and validation of the system

Using the 9600Plus fluorescence PCR instrument, according to the reaction system in Table 3, the experimental strain DNA

was prepared according to the primer system after screening to prepare a reaction solution. The amplification test was carried out under the conditions of 63°C for 60 s, and the number of cycles was 60. The DNA concentration was adjusted to 2.5–5 ng/μl. The amplification curve, CT value, etc., were used to determine whether the reaction was amplified, the typical amplification curve of the system reaction is s-type, and the reaction time is determined by combining the CT value at this time. And then, the number of strains was expanded for the experiment and verification.

Sensitivity test and verification of the system

The *Trichophyton* strain DNA was diluted according to the concentration gradient of 10^5 copies/μl, 10^4 copies/μl, 10^3 copies/μl, 10^2 copies/μl, 10^1 copies/μl, and negative control (H_2O). The reaction conditions were the same as the specificity experiment, and the amplification curve and CT value were observed to determine whether the amplification reaction occurred, the typical amplification curve of the system reaction is s-type, and the reaction time is determined by combining the CT value at this time. The experiment was repeated to further verify the sensitivity of the system and obtain the lowest positive concentration before the cut-off value for *Trichophyton*.

Evaluation and verification of the microfluidic chip system

Fabrication of the microfluidic chip system

In this experiment, a microfluidic chip was used, and the microfluidic chip was bought from Shanghai igenetec diagnostics Co. Ltd. (product number: CP01620NK). The microfluidic chip had 8 sample feeding slots, each of which corresponded to 4 reaction wells, for a total of 32 reaction wells (Figure 1). First, the microfluidic chip reaction plate was made. Then, the reaction solution for the microfluidic reaction well was prepared (Table 4 for the specific system). The sample volume of each reaction well was 1.5 μl, and each microfluidic chip had 32 sample wells. A total of 1.5 μl/well of the reaction solution was added to the reaction chamber, and the membrane was sealed for later use.

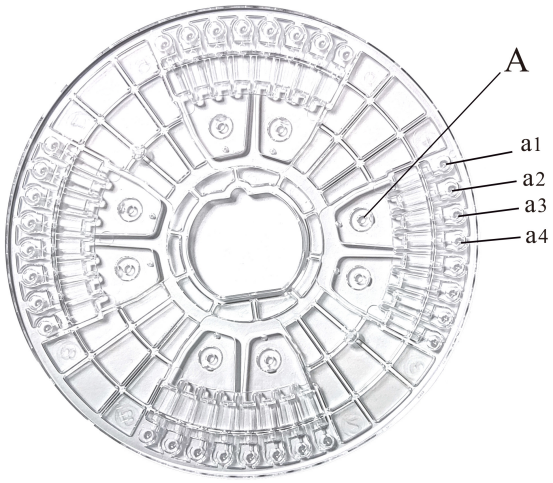

FIGURE 1
Microfluidic chip: (A) Sample tank; (a1–a4) reaction chamber.

TABLE 4 Microfluidic reactor mix.

Reactive components	Volume (μ l)
FIP	0.08
BIP	0.08
F3	0.01
B3	0.01
H_2O	1.06
0.1% trehalose	0.26
Total	1.50

TABLE 5 Sample tank reaction system mix.

Reactive components	Volume (μ l)
Buffer	35.4
Bst polymerase	2
H_2O	2.6
DNA template	10
total	50

The reaction system and reaction conditions of the sample addition tank are shown in Table 5. The sample volume of each sample addition tank was 50 μl. The amplification experiments were carried out using a microfluidic chip isothermal amplification nucleic acid analyzer. The reaction conditions were as follows: the temperature of the reaction hole was 63.0°C; the number of detection cycles was 60 (each cycle was 60 s); the low-speed centrifugal speed was 1,600 rpm; the low-speed centrifugal time was 10 s; the high-speed centrifugal speed was 4,600 rpm; and the high-speed centrifugal time was 30 s.

Specific experiments for the microfluidic chip system

According to the reaction system in Table 5, the strain DNA was used to prepare the reaction solution. The sample DNA and negative control nucleic acid were added to the eight sample addition tanks of the microfluidic control according to the experimental plan, and the DNA concentration was adjusted to 2.5–5 ng/μl. After adding the sample, the sample was sealed with a sealing film and added to the microfluidic amplifier. The experiments were conducted according to the above reaction conditions. The amplification curve and CT value were observed

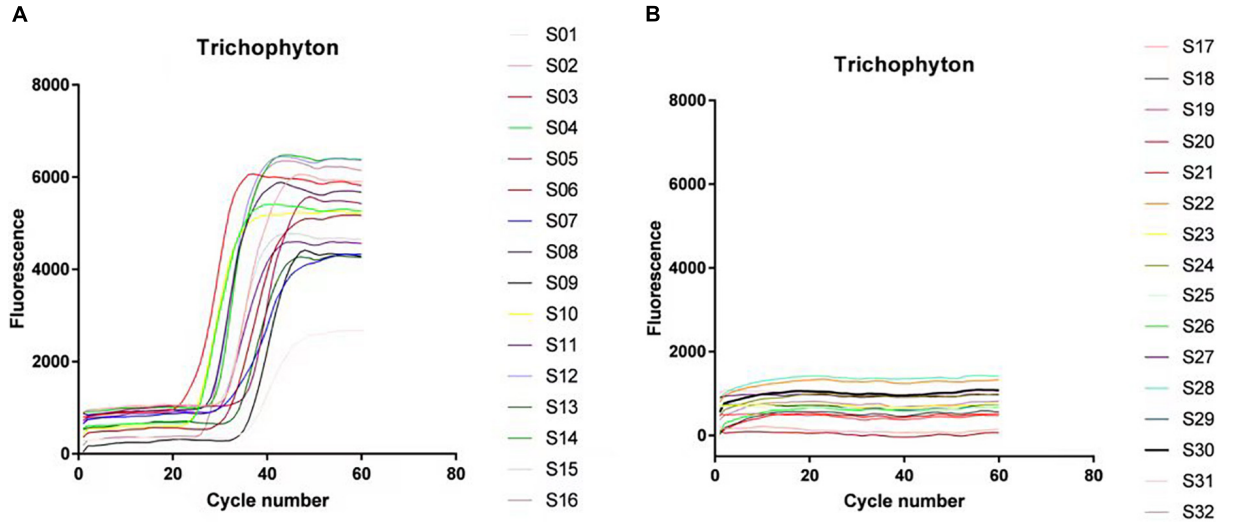

FIGURE 2
Loop-mediated isothermal amplification (LAMP) system specificity experimental results. **(A)** *Trichophyton* test results. **(B)** Experimental results of control strains.

to determine whether an amplification reaction occurred, the typical amplification curve of the system reaction is s-type.

Sensitivity experiment for the microfluidic chip system

The dermatophyte strain DNA was added into the reaction tank according to the diluted concentration gradient, and the gradient was 10^5 copies/μl, 10^4 copies/μl, 10^3 copies/μl, 10^2 copies/μl, 10^1 copies/μl, and negative control (H_2O). The reaction conditions were the same as the specificity experiment, and the amplification curve and CT value were observed to determine whether the amplification reaction occurred, the typical amplification curve of the system reaction is s-type. The experiment was repeated to further verify the sensitivity of the system and obtain the minimum amplification concentration before the cut-off value of *Trichophyton*.

Results and discussion

Loop-mediated isothermal amplification system specificity experimental results

The three groups of *Trichophyton* primers were screened for specificity. The amplification curves of the positive sample of primer No. 3 and the control sample were well distinguished, and the peak time of the control sample was the latest. Therefore, primer No. 3 was selected as the primer for *Trichophyton*. After the preliminary screening of several specific experiments, the positive samples were well amplified before 40 cycles, the negative samples in the optimized system were amplified after 60 cycles, and the positive amplification CT value was set to 40.0.

Loop-mediated isothermal amplification system specificity experimental results

There were 66 strains of *Trichophyton* in total, including 20 strains of *Trichophyton rubrum*, 20 strains of *Trichophyton mentagrophytes*, 11 strains of *Trichophyton violaceum*, 4 strains of *Trichophyton tonsurans*, 3 strains of *Trichophyton verrucosum*, and 8 strains of *Trichophyton schoenleinii*. These strains were all positively amplified before 40 cycles, and the negative strains, including dermatophytes of other genera and other common clinical fungi, bacteria, etc., did not amplify. The LAMP technology of this primer system had a diagnostic specificity of 100% for *Trichophyton*. Figure 2 is the amplification curve diagram. The positive samples S1–16 were: SCZ 60001; SCZ 60006; SCZ 60009; ATCC-MYA-4438; SCZ30008; SCZ30023; SCZ60092; SCZ30024; SCZ30005; SCZ30039; SCZ30016; SCZ30019; SCZ30007; SCZ60033; SCZ60035; SCZ60340. The negative samples S17∼32 were: SCZ60167; SCZ60168; SCZ60169; SCZ60170; SCZ60171; SCZ60172; SCZ30012; SCZ30014; SCZ30031; SCZ30032; ATCC MYA-2876; SCZ94534; ATCC-MYA-3627; SCZ60287; SCZ20005; BP-1.

Loop-mediated isothermal amplification system sensitivity test results

The *Trichophyton* DNA was sequentially diluted according to the concentration gradient and then added to the above LAMP reaction system. Figure 3 shows the isothermal amplification results of the ATCC-MYA-4438 strain

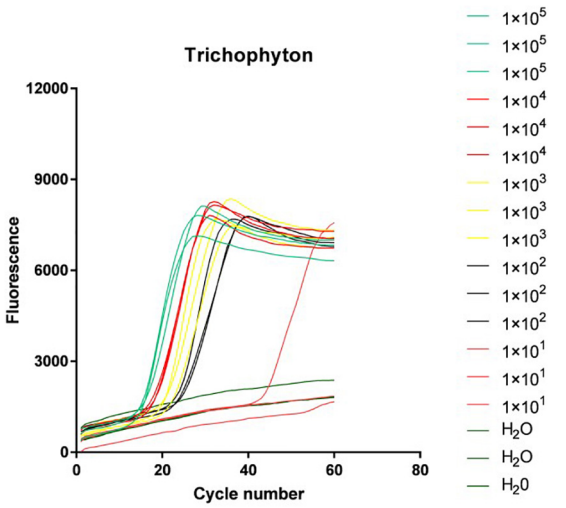

FIGURE 3
Loop-mediated isothermal amplification (LAMP) system sensitivity test results.

samples, which were 1×10^5 copies/μl 1×10^4 copies/μl, 1×10^3 copies/μl, 1×10^2 copies/μl, 1×10^1 copies/μl, and negative control (H_2O). The samples were expanded, and the results were repeated for verification. The sensitivity of LAMP for verifying *Trichophyton* was 1×10^2 copies/μl.

Microfluidic chip system experimental results

The above-verified LAMP system was combined with a microfluidic chip to further verify the specificity and sensitivity of the system on the microfluidic chip platform.

Microfluidic chip system specificity experimental results

In this study, an 8-channel microfluidic chip was used as the reaction carrier, and each channel corresponds to four reaction wells (as shown in Figure 1). It was verified that the DNA of 66 *Trichophyton* strains showed positive amplification before 40 cycles, and the negative strains, including dermatophytes of other genera and other common clinical fungi, bacteria, etc., were not amplified. The amplification specificity of the *Trichophyton* primer system on the microfluidic chip was 100%. Figure 4 shows the amplification curve. The positive samples S1∼4 were: ATCC-MYA-4438; SCZ30023; SCZ30024; SCZ60340; The negative samples S5–8 were: SCZ60167; SCZ30014; SCZ30032; ATCC-MYA-3627.

Microfluidic chip system sensitivity experimental results

The *Trichophyton* DNA was sequentially diluted according to the concentration gradient and added to the reaction wells of the microfluidic chip. Figure 5 shows the isothermal amplification results of the strain ATCC-MYA-4438 samples,

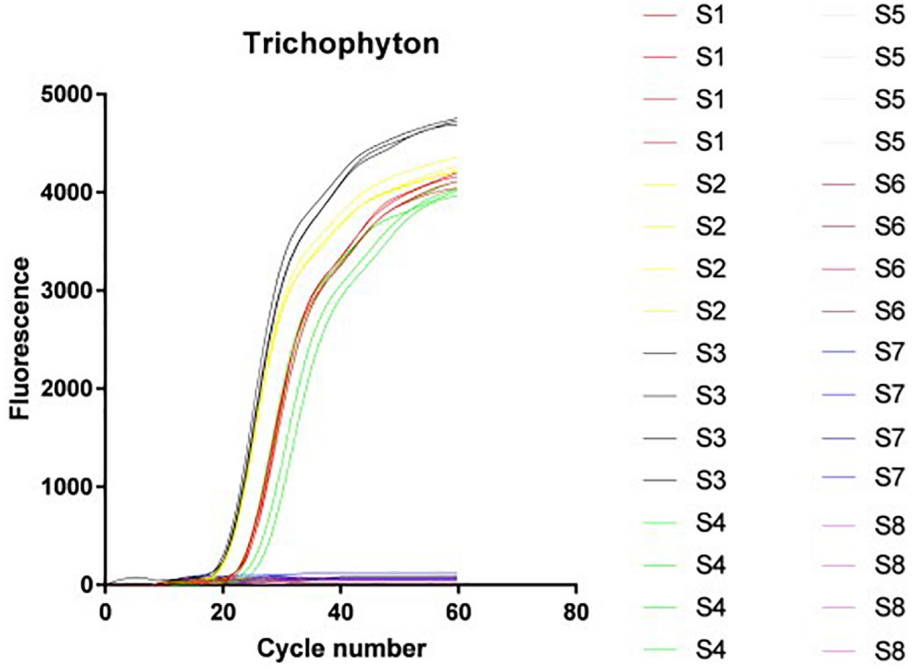

FIGURE 4
Microfluidic chip system specificity experimental results.

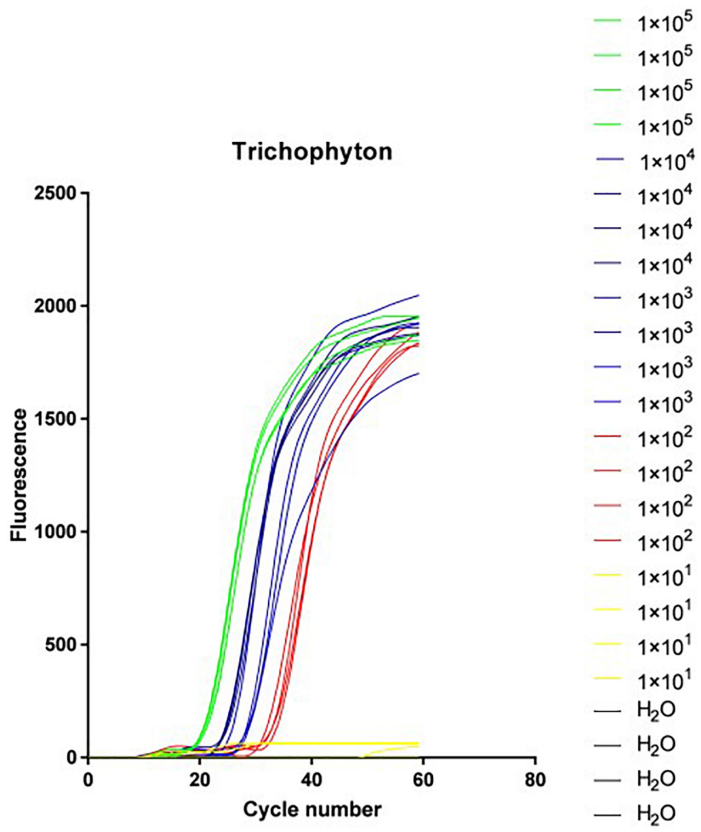

FIGURE 5
Microfluidic system sensitivity experimental results.

from left to right as follows: 1×10^5 copies/μl, 1×10^4 copies/μl, 1×10^3 copies/μl, 1×10^2 copies/μl, 1×10^1 copies/μl, and the negative control (H_2O). The amplified samples were the same as the repeated verification results. The sensitivity of LAMP for *Trichophyton* in the verification was 1×10^2 copies/μl.

Discussion

Trichophyton infection can affect the whole body, the skin, hair, finger (toe) nails, etc. Because of the difficulty in distinguishing *Trichophyton* infection from non-fungal dermatitis, especially dystrophic nails, in most cases, the laboratory helps confirm the diagnosis and initiate the appropriate treatment (Hainer, 2003). Recently, a series of molecular diagnostic methods for fungal infections, such as *Trichophyton*, have been gradually developed and applied in clinical practice. These mainly include two categories: one is based on skin plant protein diagnostic techniques, including Surface-enhanced Raman Spectroscopy (SERS), MALDI - TOF, etc.; the other is diagnostic technologies based on skin plant nucleic acids, including PCR product electrophoresis, multiplex PCR, PCR-TRFLP technology, PCR-ELISA detection method, real-time fluorescent quantitative PCR and isothermal amplification technology, etc. These early diagnostic methods allow for the identification of pathogenic microorganisms within hours with a high degree of specificity compared to traditional diagnostic methods, and the increasing use of MALDI-TOF mass spectrometry in the laboratory should facilitate the identification of microorganisms from cultured strains. The identification of dermatophytes, especially in the case of atypical isolates (L'Ollivier et al., 2013), by recent PCR-based studies has reported positive rates ranging from 74 to 100% (Verrier et al., 2013).

In a study including 60 patients, Rothmund et al. (2013) compared the efficacy of different methods for the diagnosis of onychomycosis. PCR had the highest sensitivity (90%). However, these techniques also have certain limitations. For example, a mass spectrometer (MALDI-TOF), which has been used clinically, is expensive with a high cost of maintenance, making it difficult to popularize. In addition, the current reference library of *Trichophyton* is insufficient, and changes in protein expression related to culture conditions may alter the MALDI-TOF MS results (L'Ollivier and Ranque, 2017). Multiplex PCR, because the same system contains multiple sets of primers, has a high possibility of primer-dimerization, leading

to false positive results. Real-time fluorescent quantitative PCR has higher requirements for the experimental conditions and the operators. Therefore, despite the good sensitivity and specificity of many studies and faster PCR reactions, the routine diagnosis of these superficial fungal diseases currently relies on traditional methods (Petinataud et al., 2016). Therefore, there is an urgent need for an early diagnosis method that is both rapid and cost-effective.

This study combined the LAMP and microfluidic chip technologies, in which LAMP is a novel nucleic acid amplification method that can directly amplify specific DNA under isothermal conditions (Notomi et al., 2000; Nagamine et al., 2001). This technique eliminates the temperature cycling required for polymerase chain reaction (PCR), and most importantly, the method does not require denatured DNA templates (Nagamine et al., 2001) and can amplify 10^9 copies of target DNA within 1 h (Notomi et al., 2000; Nagamine et al., 2001). The microfluidic chip technology was used to establish the above nucleic acid constant temperature amplification system on a miniaturized chip, design corresponding multi-channel reaction wells on the chip according to the experimental purpose and requirements, and pre-establish the reaction requirements on the channel. According to the recommendations of the latest edition of the "International Diagnosis and Treatment Guidelines," using LAMP primer design software to design the corresponding genus primers from the level of *Trichophyton* species, requiring that the primers of the genus must be able to accurately identify common *Trichophyton* species, and can't amplify dermatophytes of other genera and experiment-negative strains while meeting the characteristics of high amplification efficiency, good stability, and no cross-reaction. A total of 111 strains were included in this study, of which 66 were *Trichophyton* and 45 were control strains. After a comprehensive screening and alignment, a set of primers for the genus *Trichophyton* was selected. According to the results of multiple specificity experiments, the cut-off value of the system was determined to be 40 cycles, that is 40 min (one cycle in this study was 60 s). Then, the specificity and sensitivity of the system were tested. The results showed that the specificity of the LAMP technology for the identification of common dermatophytes of the genus *Trichophyton* reached 100%, and the sensitivity reached 1×10^2 copies/μl. After verification, the reaction system was also well-verified on the microfluidic chip, with the same specificity and sensitivity as the LAMP technology. This diagnostic system greatly reduces the cost and time of testing a single patient, while increasing the number of patients tested per unit of time.

Conclusion

In summary, this study successfully established a high-throughput, highly efficient, and low-cost detection platform for six species of *Trichophyton*, including *Trichophyton rubrum*, *Trichophyton mentagrophyte*, *Trichophyton violaceum*, *Trichophyton tonsurans*, *Trichophyton verrucosum*, and *Trichophyton schoenleinii*. The study revealed that the LAMP technology identified the common dermatophytes in *Trichophyton* with a specificity of 100% and a sensitivity of 1×10^2 copies/μl. After verification, the reaction system was also well-verified on the microfluidic chip. The specificity and sensitivity were the same as the LAMP technology, and the whole process could be completed in 60 min. The LAMP-microfluidic chip is simple to operate, easy to popularize, and has a good application prospect for the detection and diagnosis of clinical *Trichophyton* infection.

Data availability statement

The original contributions presented in this study are included in the article/supplementary material, further inquiries can be directed to the corresponding authors.

Author contributions

WJ, DH, and YX conducted the experimental section, in which WJ also wrote the manuscript. YC and XZ were involved in strain identification and primer design. ZH and XY were responsible for experimental guidance and data analysis. XL was responsible for article design, experimental protocol adjustment, and manuscript review. All authors contributed to the article and approved the submitted version.

Funding

This work was supported by the Hebei Provincial Department of Education (B20221018) and the Science and Technology Bureau of Huzhou, Zhejiang Province (2021GYB01).

Conflict of interest

The authors declare that the research was conducted in the absence of any commercial or financial relationships that could be construed as a potential conflict of interest.

Publisher's note

References

Bristow, I. R., and Spruce, M. C. (2009). Fungal foot infection, cellulitis and diabetes: A review. *Diabet. Med.* 26, 548–551. doi: 10.1111/j.1464-5491.2009.02722.x

Devliotou-Panagiotidou, D., and Koussidou-Eremondi, T. H. (2004). Efficacy and tolerability of 8 weeks' treatment with terbinafine in children with tinea capitis caused by *Microsporum canis*: A comparison of three doses. *J. Eur. Acad. Dermatol. Venereol.* 18, 155–159. doi: 10.1111/j.1468-3083.2004.00854.x

Feuilhade de Chauvin, M. (2005). New diagnostic techniques. *J. Eur. Acad. Dermatol. Venereol.* 19, 20–24. doi: 10.1111/j.1468-3083.2005.01287.x

Fuller, L. C., Barton, R. C., Mohd Mustapa, M. F., Proudfoot, L. E., Punjabi, S. P., and Higgins, E. M. (2014). British Association of Dermatologists' guidelines for the management of tinea capitis 2014. *Br. J. Dermatol.* 171, 454–463. doi: 10.1111/bjd.13196

Fuller, L. C., Smith, C. H., Cerio, R., Marsden, R. A., Midgley, G., Beard, A. L., et al. (2001). A randomized comparison of 4 weeks of terbinafine vs. 8 weeks of griseofulvin for the treatment of tinea capitis. *Br. J. Dermatol.* 144, 321–327. doi: 10.1046/j.1365-2133.2001.04022.x

Gianni, C., Cerri, A., and Crosti, C. (1997). Unusual clinical features of fingernail infection by *Fusarium oxysporum*. *Mycoses* 40, 455–459. doi: 10.1111/j.1439-0507.1997.tb00184.x

Gorkin, R., Park, J., Siegrist, J., Amasia, M., Lee, B. S., Park, J. M., et al. (2010). Centrifugal microfluidics for biomedical applications. *Lab. Chip* 10, 1758–1773. doi: 10.1039/b924109d

Hainer, B. L. (2003). Dermatophyte infections. *Am. Fam. Phys.* 67, 101–108.

Havlickova, B., Czaika, V. A., and Friedrich, M. (2008). Epidemiological trends in skin mycoses worldwide. *Mycoses* 51, 2–15. doi: 10.1111/j.1439-0507.2008.01606.x

Kakourou, T., Uksal, U., and European Society for Pediatric (2010). Guidelines for the management of tinea capitis in children. *Pediatr. Dermatol.* 27, 226–228. doi: 10.1111/j.1525-1470.2010.01137.x

Kasahara, K., Ishikawa, H., Sato, S., Shimakawa, Y., and Watanabe, K. (2014). Development of multiplex loop-mediated isothermal amplification assays to detect medically important yeasts in dairy products. *FEMS Microbiol. Lett.* 357, 208–216. doi: 10.1111/1574-6968.12512

Li, Y., Fan, P., Zhou, S., and Zhang, L. (2017). Loop-mediated isothermal amplification (LAMP): A novel rapid detection platform for pathogens. *Microb. Pathog.* 107, 54–61. doi: 10.1016/j.micpath.2017.03.016

Liu, X., Wang, H., Lin, B., Tao, Y., Zhuo, K., and Liao, J. (2016). Loop-mediated isothermal amplification based on the mitochondrial COI region to detect *Pratylenchus zeae*. *Eur. J. Plant Pathol.* 148, 435–446. doi: 10.1007/s10658-016-1102-8

L'Ollivier, C., Cassagne, C., Normand, A. C., Bouchara, J. P., Contet-Audonneau, N., Hendrickx, M., et al. (2013). A MALDI-TOF MS procedure for clinical dermatophyte species identification in the routine laboratory. *Med. Mycol.* 51, 713–720. doi: 10.3109/13693786.2013.781691

L'Ollivier, C., and Ranque, S. (2017). MALDI-TOF-Based Dermatophyte Identification. *Mycopathologia* 182, 183–192. doi: 10.1007/s11046-016-0080-x

Madou, M., Zoval, J., Jia, G., Kido, H., Kim, J., and Kim, N. (2006). Lab on a CD. *Annu. Rev. Biomed. Eng.* 8, 601–628. doi: 10.1146/annurev.bioeng.8.061505.095758

Maraki, S., and Mavromanolaki, V. E. (2016). Epidemiology of Dermatophytoses in Crete. Greece. *Med. Mycol. J.* 57, E69–E75. doi: 10.3314/mmj.16-00008

Nagamine, K., Watanabe, K., Ohtsuka, K., Hase, T., and Notomi, T. (2001). Loop-mediated isothermal amplification reaction using a nondenatured template. *Clin. Chem.* 47, 1742–1743.

Notomi, T., Okayama, H., Masubuchi, H., Yonekawa, T., Watanabe, K., Amino, N., et al. (2000). Loop-mediated isothermal amplification of DNA. *Nucleic Acids Res.* 28:E63. doi: 10.1093/nar/28.12.e63

Panasiti, V., Borroni, R. G., Devirgiliis, V., Rossi, M., Fabbrizio, L., Masciangelo, R., et al. (2006). Comparison of diagnostic methods in the diagnosis of dermatomycoses and onychomycoses. *Mycoses* 49, 26–29. doi: 10.1111/j.1439-0507.2005.01185.x

Petinataud, D., Berger, S., Ferdynus, C., Debourgogne, A., Contet-Audonneau, N., and Machouart, M. (2016). Optimising the diagnostic strategy for onychomycosis from sample collection to fungal identification evaluation of a diagnostic kit for real-time PCR. *Mycoses* 59, 304–311. doi: 10.1111/myc.12471

Rothmund, G., Sattler, E. C., Kaestle, R., Fischer, C., Haas, C. J., Starz, H., et al. (2013). Confocal laser scanning microscopy as a new valuable tool in the diagnosis of onychomycosis - comparison of six diagnostic methods. *Mycoses* 56, 47–55. doi: 10.1111/j.1439-0507.2012.02198.x

Shadomy, H. J., and Philpot, C. M. (1980). Utilization of standard laboratory methods in the laboratory diagnosis of problem dermatophytes. *Am. J. Clin. Pathol.* 74, 197–201. doi: 10.1093/ajcp/74.2.197

Shao-Xi, W., Ning-Ru, G., and Wei-Da, L. (2011). Dynamic epidemiologic survey of pathogenic dermatophytes of China at 1986, 1996 and 2006. *J. Diagnos. Ther. Dermato Venereol.* 18, 144–147+152.

Summerbell, R. C., Cooper, E., Bunn, U., Jamieson, F., and Gupta, A. K. (2005). Onychomycosis: A critical study of techniques and criteria for confirming the etiologic significance of nondermatophytes. *Med. Mycol.* 43, 39–59. doi: 10.1080/13693780410001712043

Tang, Y., Yu, X., Chen, H., and Diao, Y. (2016). An immunoassay-based reverse-transcription loop-mediated isothermal amplification assay for the rapid detection of avian influenza H5N1 virus viremia. *Biosens. Bioelectron.* 86, 255–261. doi: 10.1016/j.bios.2016.06.063

Verrier, J., Krahenbuhl, L., Bontems, O., Fratti, M., Salamin, K., and Monod, M. (2013). Dermatophyte identification in skin and hair samples using a simple and reliable nested polymerase chain reaction assay. *Br. J. Dermatol.* 168, 295–301. doi: 10.1111/bjd.12015

Zhan, P., and Liu, W. (2017). The Changing Face of Dermatophytic Infections Worldwide. *Mycopathologia* 182, 77–86. doi: 10.1007/s11046-016-0082-8

frontiers | Frontiers in Microbiology

TYPE Original Research
PUBLISHED 10 November 2022
DOI 10.3389/fmicb.2022.1036351

OPEN ACCESS

EDITED BY
Wenjie Fang,
Shanghai Changzheng Hospital, China

REVIEWED BY
Macit Ilkit,
Çukurova University, Turkey
László Majoros,
University of Debrecen, Hungary

*CORRESPONDENCE
Meng Xiao
cjtcxiaomeng@aliyun.com
Ying-Chun Xu
xycpumch@139.com

†These authors have contributed equally to this work and share first authorship

SPECIALTY SECTION
This article was submitted to Antimicrobials, Resistance and Chemotherapy, a section of the journal Frontiers in Microbiology

RECEIVED 04 September 2022
ACCEPTED 17 October 2022
PUBLISHED 10 November 2022

CITATION
Chen X-F, Hou X, Zhang H, Jia X-M, Ning L-P, Cao W, Fan X, Huang J-J, Yang W-H, Zhang G, Zhang J-J, Kang W, Xiao M and Xu Y-C (2022) First two fungemia cases caused by *Candida haemulonii var. vulnera* in China with emerged antifungal resistance.
Front. Microbiol. 13:1036351.
doi: 10.3389/fmicb.2022.1036351

First two fungemia cases caused by *Candida haemulonii var. vulnera* in China with emerged antifungal resistance

Xin-Fei Chen[1,2,3†], Xin Hou[4†], Han Zhang[1,3], Xin-Miao Jia[3,5], Li-Ping Ning[6], Wei Cao[7], Xin Fan[8], Jing-Jing Huang[1,2,3], Wen-Hang Yang[1,3], Ge Zhang[1,3], Jing-Jia Zhang[1,3], Wei Kang[1,3], Meng Xiao[1,3]* and Ying-Chun Xu[1,3]*

[1]Department of Laboratory Medicine, State Key Laboratory of Complex Severe and Rare Diseases, Peking Union Medical College Hospital, Chinese Academy of Medical Sciences and Peking Union Medical College, Beijing, China, [2]Graduate School, Chinese Academy of Medical Sciences and Peking Union Medical College, Beijing, China, [3]Beijing Key Laboratory for Mechanisms Research and Precision Diagnosis of Invasive Fungal Diseases (BZ0447), Beijing, China, [4]Department of Laboratory Medicine, Peking University Third Hospital, Beijing, China, [5]Medical Research Center, Peking Union Medical College Hospital, Chinese Academy of Medical Sciences and Peking Union Medical College, Beijing, China, [6]Department of Laboratory Medicine, No.908 Hospital of Joint Logistics Support Force, Nanchang, Jiangxi, China, [7]Department of Laboratory Medicine, The Second Xiangya Hospital, Central South University, Changsha, Hubei, China, [8]Department of Infectious Diseases and Clinical Microbiology, Beijing Institute of Respiratory Medicine, Beijing Chao-Yang Hospital, Capital Medical University, Beijing, China

Candida haemulonii var. vulnera is a rare variant of *C. haemulonii*, which has been previously reported to cause human infections. Owing to the close kinship between *C. haemulonii* sensu stricto and *C. haemulonii var. vulnera*, accurate identification of *C. haemulonii var. vulnera* relied on DNA sequencing assay targeting, for example, rDNA internal transcribed spacer (ITS) region. In this work, two strains of *C. haemulonii var. vulnera* were collected from the China Hospital Invasive Fungal Surveillance Net (CHIF-NET). The identification capacity of three matrix-assisted laser desorption/ionization time-of-flight mass spectrometry (MALDI-TOF MS) and VITEK 2 YST ID biochemical methods were evaluated against ITS sequencing. In addition, antifungal susceptibility testing was performed using Sensititre YeastOne. Moreover, we comprehensively screened drug-resistant related genes by whole-genome sequencing. The two strains were not correctly identified to species variant level using MALDI-TOF MS and YST ID cards. Both strains were resistant to amphotericin B (minimum inhibitory concentration [MIC] > 2 μg/ml). Moreover, strain F4564 and F4584 exhibited high MIC to fluconazole (>256 μg/ml) and 5-flucytosine (>64 μg/ml), respectively, which were supposed to result from key amino acid substitutions Y132F and G307A

in Erg11p and V58fs and G60K substitutions in Fur1p. The rare species *C. haemulonii var. vulnera* has emerged in China, and such drug-resistant fungal species that can cause invasive diseases require further close attention.

KEYWORDS

***Candida haemulonii var. vulnera*, antifungal susceptibility, *ERG11*, *FUR1*, whole-genome sequence, drug resistant mechanisms**

Introduction

Candida haemulonii var. vulnera belongs to the *C. haemulonii* species complex, along with *C. haemulonii* sensu stricto and *C. duobushaemulonii* (Gade et al., 2020; Rodrigues et al., 2021; Ramos et al., 2022). Generally, *C. haemulonii* species complex isolates display high multidrug-resistant rates and transmission properties, which have attracted increased attention (Gade et al., 2020).

In 2012, *C. haemulonii var. vulnera* was reported for the first time by Cendejas-Bueno et al. They found four strains with low rDNA internal transcribed spacer (ITS) sequence identity to *C. haemulonii* sensu stricto type strain (∼96%) (Cendejas-Bueno et al., 2012). Infections caused by *C. haemulonii var. vulnera* were later reported in Brazil, India, Argentina, and Peru (de Almeida et al., 2016; Kumar et al., 2016; Isla et al., 2017; Pérez-Lazo et al., 2021; Ramos et al., 2022). In addition, by retesting a set of previously collected strains, Rodrigues et al. found a *C. haemulonii var. vulnera* strain isolated in 2009, which became the earliest strain of the species variant discovered till now and its genome sequence was elucidated (Rodrigues et al., 2020). Moreover, antifungal resistance to azoles, echinocandins, and amphotericin B has been reported in *C. haemulonii var. vulnera* isolates (Cendejas-Bueno et al., 2012; Isla et al., 2017; Ramos et al., 2022).

In this study, we reported two fungemia cases caused by *Candida haemulonii var. vulnera* found from China Hospital Invasive Fungal Surveillance Net (CHIF-NET) study. Clinical characters, identification capacity of Vitek YST card and three matrix-assisted laser desorption/ionization time-of-flight mass spectrometry (MALDI-TOF MS) systems, isolates' antifungal susceptibility phenotypes, and potential resistant mechanisms were illustrated. To our best knowledge, these were the first *Candida haemulonii var. vulnera* infection cases reported in China, including the first 5-flucytocine resistant strain discovered globally.

Materials and methods

Ethics statement

This study was approved by the Human Research Ethics Committee of the Peking Union Medical College Hospital (No. S-263). Written informed consent was obtained from all patients who participated in this study, which aimed to culture and study the isolates obtained from the patients.

Microorganisms and identification

From 2010 to 2017 (**Table 1**), two *C. haemulonii var. vulnera* isolates were collected from different hospitals in two provinces from the CHIF-NET study. The colony

TABLE 1 Information for two *Candida haemulonii var. vulnera* isolates identified in this study.

Strain	F4564	F4584
General information		
Age/Gender	88/Female	12/Male
Year of isolation	2015	2016
Source of isolate	Blood	Blood
Clinical diagnosis	Pulmonary infection	Abdominal infection
Ward	ICU	General surgery
Location	Nanchang, China	Changsha, China
Identification (identity/score/confidence value)		
ITS sequencing	*C. haemulonii var. vulnera* (100%)	*C. haemulonii var. vulnera* (100%)
Vitek 2 Compact	Low discrimination	*C. haemulonii* (94%)
Vitek MS	*C. haemulonii* (99.9)	*C. haemulonii* (99.9)
Autof-MS 1000	*C. haemulonii* (9.505)	*C. haemulonii* (9.516)
Smart MS	No identification	No identification
Antifungal susceptibility (μg/ml)		
Fluconazole	>256	16
Voriconazole	2	0.12
Itraconazole	0.25	0.25
Posaconazole	0.25	0.12
5-Flucytosine	<0.06	>64
Anidulafungin	0.12	0.12
Micafungin	0.12	0.12
Caspofungin	0.12	0.12
Amphotericin B	4	4
Potential resistance mechanisms		
Erg11p	Y132F and G307A	WT
Fur1p	WT	V58fs and G60K

WT: wild type; fs: frameshift mutation; ICU: intensive care unit.

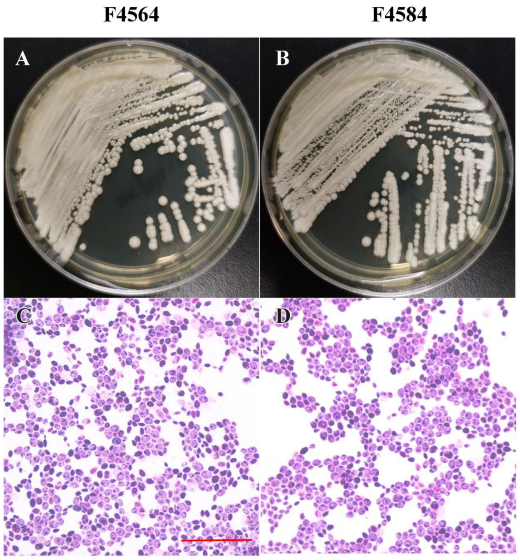

FIGURE 1
Phenotypic characteristics of two *C. haemulonii var. vulnera* isolates on Sabouraud dextrose agar. The plate contains colonies with typical appearance of circular, smooth, and moist **(A,B)**. Microscopic examination showed budding yeast cells with Gram's staining **(C,D)**. Scale bar = 10 μm **(C)**.

morphology of two strains is smooth, moist, and circular, which is the typical appearance of *Candida* species. Gram-stained microscopy showed budding yeast cells (**Figure 1**). The isolates were identified using Autof MS 1000 (Autobio, Zhengzhou, China), Smart MS (DL, Zhuhai, China), and Vitek MS (bioMérieux, Marcy l'Étoile, France) MALDI-TOF MS systems, in addition to Vitek 2 YST ID Card using VITEK 2 (9.02 version, bioMérieux, Marcy-l'Etoile, France) following the manufacturer's instructions. Primers ITS1 and ITS4 (Hou et al., 2016) were used for ITS amplification and sequencing, and Sanger sequencing was performed using ABI 3730XL DNA analyzer (Thermo Fisher Scientific, Cleveland, OH, USA). A phylogenetic tree of the ITS sequences was constructed using Mega X based on 1000 bootstrap replicates using the maximum likelihood method (Kumar et al., 2018).

DNA extraction and whole-genome sequencing

The whole genomic DNA of *C. haemulonii var. vulnera* was extracted as previously reported (Huang et al., 2022). The 350-bp DNA library was constructed using NEBNext® Ultra™, following the manufacturer's instructions. Library integrity was assessed using an Agilent 2100 Bioanalyzer (Agilent Technologies). Sequencing was performed on an Illumina NovaSeq using the PE150 strategy (Beijing Novogene Bioinformatics Technology Co., Ltd.). The Illumina reads generated in this study were obtained from the National Center for Biotechnology Information (NCBI) under BioProject PRJNA890168.

Genome analysis

The *C. haemulonii var. vulnera* K1 (GenBank accession number GCA_012184645.1) genome was concatenated and used as a reference genome for read mapping. BWA 0.5.9, SAMtools, and bcftools 0.1.19 (Li and Durbin, 2009; Li et al., 2009) were used for single-nucleotide polymorphism (SNP) and insertion/deletion (indel) analysis, and snpEff 4.3 was used for SNP and indel function annotations (Cingolani et al., 2012). Mutations on antifungal-resistant related genes, including *ERG11* and *TAC1*b for azoles, *FUR1* for 5-flucytosine, *FKS1* and *FKS2* for echinocandins, *ERG3* and *ERG6* for amphotericin B, and *ERG4* for other ergosterol pathway genes, were analyzed in detail (Arendrup and Patterson, 2017; Berkow and Lockhart, 2017).

Antifungal susceptibility testing

Antifungal susceptibility testing was performed using Sensititre YeastOne YO10 methodology (Thermo Scientific, Cleveland, OH, USA). *Candida krusei* ATCC 6258 and *Candida parapsilosis* ATCC 22019 were used as quality controls. As clinical breakpoints or epidemiological cutoff values against *C. haemulonii var. vulnera* have not been established, we used interpretation criteria for *Candida* species referring to CLSI M27-S3 guidelines (CLSI, 2008), including MIC value of ≥32 μg/mL as resistance to fluconazole ≥32 μg/mL as resistance to 5-flucytosine. In addition, MIC of ≥2 μg/mL was used for interpreting "resistance" to amphotericin B (Pfaller et al., 2012).

Review of *Candida haemulonii var. vulnera* cases reported

A literature review of previously reported *C. haemulonii var. vulnera* infections was done. A literature search was performed on 28 August 2022, using the following three databases: PubMed[1], Web of Science[2], and Embase[3]. The terms "*Candida haemulonii var. vulnera*" were entered in the category of "Title/Abstract" in the PubMed Advanced Search Builder, and "TS (*Candida haemulonii var. vulnera*)" was entered into the Web of Science database. The search in Embase was

1 https://pubmed.ncbi.nlm.nih.gov
2 https://webofknowledge.com
3 https://www.embase.com

conducted in the advanced search area, including the terms "*Candida haemulonii var. vulnera*': ab,ti.". All hits were further screened manually to find out all infection cases with antifungal susceptibility reports.

Results

Isolate information

The first case was an 88-year-old male patient who was admitted to the intensive care unit (ICU) with clinical diagnosis of pulmonary infection. F4564 was isolated from peripheral blood of this patient and initially misidentified as "*Candida krusei*" using CHROMagar chromogenic medium at local laboratory (Table 1). The second case was a 12-year-old boy who was admitted to the general surgical ward, and clinical diagnosis was abdominal infection. F4584 was isolated from peripheral blood of this patient and identified as "*Candida spp.*" using CHROMagar chromogenic medium initially (Table 1).

Identification of *Candida. haemulonii var. vulnera* using ITS sequencing, MALDI-TOF MS, and Vitek 2

The ITS sequences of the isolates exhibited 100% identity with the corresponding ITS sequences of the reference *C. haemulonii var. vulnera* CBS12439^T isolates (GenBank accession number: JX459686.1). Furthermore, both clinical isolates were identified as *C. haemulonii* by the Autof MS 1000 and Vitek MS, but with "no identification" results by Smart MS. While using the Vitek 2 Compact system, one strain was identified with low discrimination and the other was identified as *C. haemulonii* (score = 94%) (Table 1). In phylogenetic tree generated by *C. haemulonii* complex, *C. auris*,

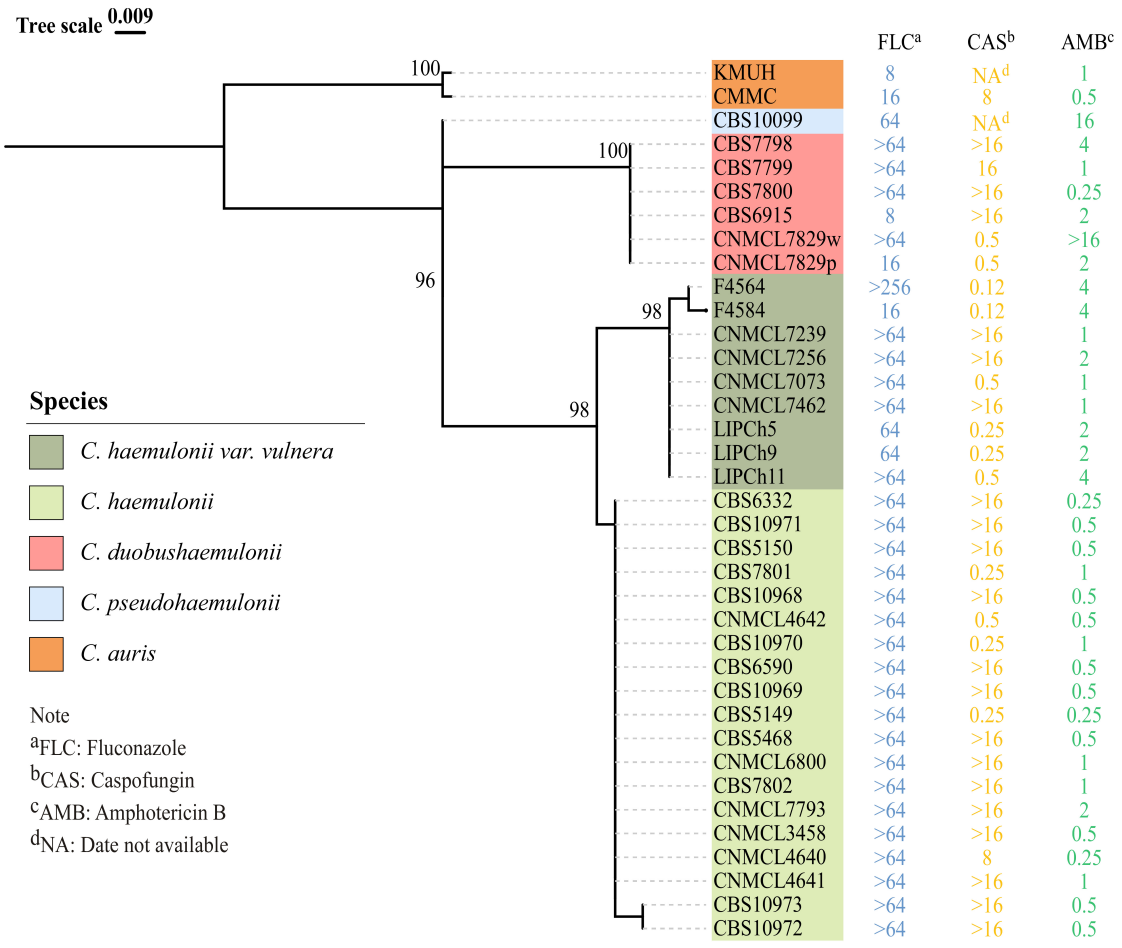

FIGURE 2
Phylogenetic tree for rDNA ITS region of previously reported *Candida haemulonii*, *C. duobushaemulonii*, *C. pseudohaemulonii*, *C. auris*, and *C. haemulonii var. vulnera*, including two *C. haemulonii var. vulnera* clinical strains identified in this study. Phylogenetic tree was constructed using Mega X with 1000 bootstrap replicates based on the maximum likelihood method.

and *C. pseudohaemulonii* ITS sequences, F4564 and F4584 were in the branch of *C. haemulonii var. vulnera* (Figure 2).

Genome analysis

We sequenced genomes of F4564 and F4584, and their total genome sizes were 13.51 Mb and 13.26 Mb, respectively, with an average GC content of 45% (N50 was 346,464 bp and 283,647 bp, and a number of assembled contigs were 270 and 262, comprising 95.7% and 95.6% of data according to BUSCO analysis, respectively).

Antifungal susceptibility

MIC values obtained for the nine antifungal agents against *C. haemulonii var. vulnera* isolates are shown in Table 1. F4564 was resistant to fluconazole with an MIC of >256 μg/ml. In addition, F4564 was classified as susceptible

TABLE 2 Overview of published reports on antifungal susceptibility profiles of *Candida haemulonii var. vulnera.*

No. isolates [Reference]	Strain or isolate	Antifungals (μg/ml)									Method
		FLU	VRC	ITC	POS	MCF	CAS	ANF	AMB	5FC	
***N* = 7 (Ramos et al., 2022)**											
MIC	LIPCh14	>64	>16	>16	>16	0.06	0.25	0.125	2	0.25	CLSI
	LIPCh18	>64	>16	>16	>16	0.125	1	0.125	4	0.25	
	LIPCh20	>64	>16	>16	>16	0.125	1	0.25	8	0.25	
	LIPCh21	>64	>16	>16	>16	0.125	1	0.06	4	0.25	
	LIPCh24	64	0.25	0.25	0.125	0.125	1	0.06	16	0.25	
	LIPCh25	>64	>16	>16	>16	0.06	0.5	0.06	4	0.25	
	LIPCh37	>64	>16	>16	>16	0.06	0.5	0.06	8	<0.125	
***N* = 3 (Ramos et al., 2015)**											
MIC	LIPCh5	64	0.5	0.5	ND	ND	0.25	ND	2	ND	CLSI
	LIPCh9	64	16	8	ND	ND	0.25	ND	2	ND	
	LIPCh11	>64	>16	16	ND	ND	0.5	ND	4	ND	
***N* = 2 (Rodrigues et al., 2020)**											
MIC	K1	8	0.25	0.5	0.25	0.12	0.25	0.06	8	< 0.06	YeastOne
	K2	16	0.25	0.5	0.25	0.12	0.25	0.06	2	< 0.06	
***N* = 4 (Cendejas-Bueno et al., 2012)**											
MIC	CNM-CL7239	>64	>8	>8	> 8	>16	> 16	>16	1	< 0.12	EUCAST
	CNM-CL7256	>64	>8	>8	> 8	0.12	> 16	0.06	2	0.5	
	CNM-CL7073	>64	>8	>8	> 8	0.12	0.5	0.06	1	0.25	
	CNM-CL7462	>64	>8	>8	> 8	0.06	> 16	< 0.03	1	0.5	
***N* = 1 (Pérez-Lazo et al., 2021)**											
MIC		>64	ND	ND	ND	ND	ND	0.06	1	ND	CLSI
***N* = 8 (de Almeida et al., 2016)**											
GM		17.4	11.53	ND	ND	ND	0.26	0.016	1	ND	CLSI
MIC_{90}		64	16	ND	ND	ND	0.5	0.03	2	ND	
MIC range		2- > 64	0.125 – > 16	ND	ND	ND	0.125-0.5	< 0.015-0.03	0.5-2	ND	
***N* = 5 (Isla et al., 2017)**											
Mode		2	0.03	0.5	0.06	0.12	0.12	ND	4	0.12	EUCAST
GM		8	0.24	0.33	0.07	0.14	0.12	ND	3.48	0.12	
MIC range		2-128	0.03-8	0.06-1	0.0-0.5	0.12-0.25	0.006-0.25	ND	2-8	0.12	
MIC_{50}		4	0.1	0.5	0.06	0.12	0.12	ND	4	0.12	
MIC_{90}		128	8	1	0.25	0.25	0.25	ND	8	0.12	
***N* = 3 (Rodrigues et al., 2021)**											
MIC range		16-32	0.06-0.12	ND	ND	0.06-0.12	0.06-0.12	0.015	ND	0.25-1	CLSI

FLC: Fluconazole; VRC: Voriconazole; ITC: Itraconazole; POS: Posaconazole; CAS: Caspofungin; ANF: Anidulafungin; MCF: Micafungin; AMB: Amphotericin B; 5FC: 5-flucytosine; MIC: minimum inhibitory concentration; GM: geometric mean; MIC_{50}: minimum inhibitory concentration able to inhibit 50% of all isolates tested; MIC_{90}: minimum inhibitory concentration able to inhibit 90% of all isolates tested.

dose-dependent to voriconazole (2 μg/ml) and itraconazole (0.25 μg/ml). F4684 was resistant to 5-flucytosine (>64 μg/ml) and susceptible dose-dependent to itraconazole. In addition, both isolates had high MIC values of 4 μg/ml for amphotericin B, while neither strain was non-susceptible to posaconazole, caspofungin, anidulafungin, and micafungin (**Table 1**).

Potential genomic variations contributed to antifungal resistance

Compared with the reference genome K1, which is from an isolate susceptible to all antifungals except for amphotericin B, we found that F4564 has two previously reported key amino acid substitutions (Y132F and G307A) in Erg11p. Interestingly, we discovered two novel mutations in Fur1p (V58fs and G60K) in strain F4584 with high 5-flucytosine MIC. However, we did not find any key variation in sterol metabolism-related genes like *ERG2*, *ERG3,* and *ERG6* that may result in amphotericin B resistance. In addition, all strains were susceptible to echinocandins and did not carry substitutions in Fks1p or Fks2p.

Literature review

We found eight articles in all reported antifungal susceptibility of *C. haemulonii var. vulnera* isolates. A number of strains exhibit high MICs to fluconazole or even all azoles (Cendejas-Bueno et al., 2012), but there was not any investigation on related resistance mechanisms. In addition, one study reported the emergence of pan-echinocandin-resistant *C. haemulonii var. vulnera* strains (Cendejas-Bueno et al., 2012). To date, there have not been any reports describing 5-flucytosine-resistant *C. haemulonii var. vulnera* strain (**Table 2**).

Discussion

Candida haemulonii var. vulnera was identified ever-first by ITS sequencing (Cendejas-Bueno et al., 2012). Although it has been involved in identification database of latest Vitek 2 YST ID system, the results from the current study and Rodrigues et al. (2020) still found YST ID card was not able to achieve a reliable identification between *C. haemulonii* sensu stricto and *C. haemulonii var. vulnera*. Furthermore, none of the current available MALDI-TOF MS systems could accurately identify *C. haemulonii var. vulnera* (Kathuria et al., 2015; Grenfell et al., 2016; Rodrigues et al., 2020), though Grenfell *et al.* described that some discriminatory protein peaks may be able to differentiate *C. haemulonii* sensu stricto and *C. haemulonii var. vulnera* in using FlexAnalysis and ClinProTools to analysis MALDI-TOF MS results (Grenfell et al., 2016). Therefore, DNA sequencing remained the only applicable methods for the identification of *C. haemulonii var. vulnera*. Interestingly, Cendejas-Bueno reported that *C. haemulonii* sensu stricto and *C. haemulonii var. vulnera* can be separated by ITS sequences, but these two species have identical *RPB1*, *RPB2,* and D1/D2 sequences. Therefore, these strategies could not be used for the identification of these two species (Cendejas-Bueno et al., 2012). To date, isolation of *C. haemulonii var. vulnera* has only been reported in Brazil, Argentina, and Peru. Due to the above-mentioned limitations of commercial identification systems, we reidentified all *C. haemulonii* complex isolates collected in CHIF-NET study by ITS sequencing and finally found two *C. haemulonii var. vulnera* strains among >80 cases.

Previously, fluconazole- and amphotericin B-resistant *C. haemulonii var. vulnera* have been discovered (Cendejas-Bueno et al., 2012; Ramos et al., 2015; de Almeida et al., 2016). Like findings in previous reports, one of the isolates we discovered was also resistant to fluconazole and amphotericin B. However, we also found a 5-flucytosine-resistant strain, and it is also cross-resistant to amphotericin B. Although 5-flucytosine resistance has been recognized in *C. haemulonii* sensu stricto and *C. duobushaemulonii* in China and other regions (Kathuria et al., 2015; Hou et al., 2016), this is the first 5-flucytosine-resistant *C. haemulonii var. vulnera* case characterized to date. Of note, both strains we discovered remained susceptible to all echinocandins.

Compared with *C. haemulonii* sensu stricto and *C. duobushaemulonii* that have been well characterized, there are very few studies on resistant mechanisms of *C. haemulonii var. vulnera*. Key amino acid substitutions in Erg11p and Fur1p have been noted as major reasons contributing to azole and 5-flucytosine resistance, respectively, in other *C. haemulonii* complex species (Gade et al., 2020) and Chen et al. (2022). In this study, it was found that the fluconazole-resistant *C. haemulonii var. vulnera* isolate carried Y132F and G307A mutations in Erg11p. Erg11p Y132F substitutions have been reported in a broad range of fluconazole-resistant *Candida* species including *C. albicans*, *C. tropicalis,* and *C. haemulonii* (Fan et al., 2019; Warrilow et al., 2019; Gade et al., 2020), while G307A has been reported in *C. parapsilosis* (Arastehfar et al., 2020; Binder et al., 2020). While in our 5-flucytosine-resistant *C. haemulonii var. vulnera* strain, a frameshift V58fs and a mutation G60K were found in Fur1p, which has not been recovered in any other *Candida* strains to our best knowledge. Literature review showed a high proportion of *C. haemulonii var. vulnera* isolates (13/17, 76.5%) were with reduced susceptibility to amphotericin B (≥2 μg/ml). However, resistant mechanisms to amphotericin B were not well understood, and in this study, we also failed to found any mutations in key genes may potentially contributed to amphotericin B resistance. As a major limitation, our study did not collect detailed medical records of these two cases; therefore, we were not able to further analyze the source of infections or assessing clinical risk factors of this species.

In conclusion, there is a potential threat posed by *C. haemulonii var. vulnera*, a highly antifungal-resistant fungal species. Resistance to fluconazole and 5-flucytosine in *C. haemulonii var. vulnera* was supposed to be resulted from variations in Erg11p and Fur1p, respectively. Although invasive infection with *C. haemulonii var. vulnera* remained rare, further monitoring of this specie is still warranted.

Data availability statement

The datasets presented in this study can be found in the online repositories. The names of the repository/repositories and accession numbers(s) can be found in the manuscript.

Author contributions

X-FC, XH, HZ, and X-MJ conceived and designed the experiments. L-PN and WC provided the isolates. X-FC, HZ, X-MJ, XF, XH, J-JH, W-HY, GZ, J-JZ, and WK performed experiments. X-FC and HZ analyzed the data and wrote the manuscript. MX, XH, and Y-CX revised the manuscript. All authors contributed to the manuscript and approved the submitted version.

Funding

This study was supported by the National Key Research and Development Program of China (2022YFC2300017), National Natural Science Foundation of China (82002178), National High Level Hospital Clinical Research Funding (2022-PUMCH-B-074), Tsinghua University-Peking Union Medical College Hospital Initiative Scientific Research Program (Grant No. 20191080604), Beijing Key Clinical Specialty for Laboratory Medicine-Excellent Project (No. ZK201000), and CAMS Innovation Fund for Medical Sciences (2021-I2M-1-038 and 2021-I2M-1-044).

Acknowledgments

The authors thank all Hospitals involved in the CHIF-NET study.

Conflict of interest

The authors declare that the research was conducted in the absence of any commercial or financial relationships that could be construed as a potential conflict of interest.

Publisher's note

All claims expressed in this article are solely those of the authors and do not necessarily represent those of their affiliated organizations, or those of the publisher, the editors and the reviewers. Any product that may be evaluated in this article, or claim that may be made by its manufacturer, is not guaranteed or endorsed by the publisher.

References

Arastehfar, A., Daneshnia, F., Hilmioglu-Polat, S., Fang, W., Yasar, M., Polat, F., et al. (2020). First report of candidemia clonal outbreak caused by emerging fluconazole-resistant *Candida parapsilosis* isolates harboring Y132F and/or Y132F+K143R in Turkey. *Antimicrob. Agents Chemother.* 64, e01001-20. doi: 10.1128/AAC.01001-20

Arendrup, M. C., and Patterson, T. F. (2017). Multidrug-resistant candida: Epidemiology, molecular mechanisms, and treatment. *J. Infect. Dis.* 216, S445–S451. doi: 10.1093/infdis/jix131

Berkow, E. L., and Lockhart, S. R. (2017). Fluconazole resistance in *Candida* species: A current perspective. *Infect. Drug Resist.* 10, 237–245. doi: 10.2147/IDR.S118892

Binder, U., Arastehfar, A., Schnegg, L., Hortnagl, C., Hilmioglu-Polat, S., Perlin, D. S., et al. (2020). Efficacy of LAMB against emerging azole- and multidrug-resistant *Candida parapsilosis* isolates in the *Galleria mellonella* model. *J. Fungi (Basel, Switzerland)* 6:377. doi: 10.3390/jof6040377

Cendejas-Bueno, E., Kolecka, A., Alastruey-Izquierdo, A., Theelen, B., Groenewald, M., Kostrzewa, M., et al. (2012). Reclassification of the *Candida haemulonii* complex as *Candida haemulonii* (*C. haemulonii* group I), *C. duobushaemulonii* sp. nov. (*C. haemulonii* group II), and *C. haemulonii* var. *vulnera* var. nov.: Three multiresistant human pathogenic yeasts. *J. Clin. Microbiol.* 50, 3641–3651. doi: 10.1128/jcm.02248-12

Chen, X.-F., Zhang, H., Jia, X.-M., Cao, J., Li, L., Hu, X.-L., et al. (2022). Antifungal susceptibility profiles and drug resistance mechanisms of clinical *Candida duobushaemulonii* isolates from China. *Front. Microbiol.* doi: 10.3389/fmicb.2022.1001845

Cingolani, P., Platts, A., Wang le, L., Coon, M., Nguyen, T., Wang, L., et al. (2012). A program for annotating and predicting the effects of single nucleotide polymorphisms, SnpEff: SNPs in the genome of *Drosophila melanogaster* strain w1118; iso-2; iso-3. *Fly (Austin)* 6, 80–92. doi: 10.4161/fly.19695

CLSI (2008). *Reference method for broth dilution anti fungal susceptibility testing of yeasts, third informational supplement. CLSI document M27-S3*, 3rd Edn. Wayne, PA: Clinical and Laboratory Standards Institute.

de Almeida, J. N. Jr., Assy, J. G., Levin, A. S., Del Negro, G. M., Giudice, M. C., Tringoni, M. P., et al. (2016). Candida haemulonii Complex Species, Brazil, January 2010-March 2015. *Emerg. Infect. Dis.* 22, 561–563. doi: 10.3201/eid2203.151610

Fan, X., Xiao, M., Zhang, D., Huang, J. J., Wang, H., Hou, X., et al. (2019). Molecular mechanisms of azole resistance in *Candida tropicalis* isolates causing invasive candidiasis in China. *Clin. Microbiol. Infect.* 25, 885–891. doi: 10.1016/j.cmi.2018.11.007

Gade, L., Munoz, J. F., Sheth, M., Wagner, D., Berkow, E. L., Forsberg, K., et al. (2020). Understanding the emergence of multidrug-resistant *Candida*: Using whole-genome sequencing to describe the population structure of *Candida haemulonii* species complex. *Front. Genet.* 11:554. doi: 10.3389/fgene.2020.00554

Grenfell, R. C., Da Silva Junior, A. R., Del Negro, G. M. B., Munhoz, R. B., Gimenes, V. M. F., Assis, D. M., et al. (2016). Identification of *Candida haemulonii* complex species: Use of ClinProToolsTM to overcome limitations of the bruker BiotyperTM, VITEK MSTM IVD, and VITEK MSTM RUO databases. *Front. Microbiol.* 7:940. doi: 10.3389/fmicb.2016.00940

Hou, X., Xiao, M., Chen, S. C., Wang, H., Cheng, J. W., Chen, X. X., et al. (2016). Identification and antifungal susceptibility profiles of *Candida haemulonii* species complex clinical isolates from a multicenter study in China. *J. Clin. Microbiol.* 54, 2676–2680. doi: 10.1128/JCM.01492-16

Huang, J. J., Chen, X. F., Tsui, C. K. M., Pang, C. J., Hu, Z. D., Shi, Y., et al. (2022). Persistence of an epidemic cluster of *Rhodotorula mucilaginosa* in multiple geographic regions in China and the emergence of a 5-flucytosine resistant clone. *Emerg. Microbes Infect.* 11, 1079–1089. doi: 10.1080/22221751.2022.2059402

Isla, G., Taverna, C. G., Szusz, W., Vivot, W., García-Effron, G., and Davel, G. (2017). *Candida haemulonii* sensu lato: Update of the determination of susceptibility profile in Argentina and literature review. *Curr. Fungal Infect. Rep.* 11, 203–208. doi: 10.1007/s12281-017-0300-y

Kathuria, S., Singh, P. K., Sharma, C., Prakash, A., Masih, A., Kumar, A., et al. (2015). Multidrug-resistant *Candida auris* misidentified as *Candida haemulonii*: Characterization by matrix-assisted laser desorption ionization-time of flight mass spectrometry and DNA sequencing and its antifungal susceptibility profile variability by Vitek 2, CLSI broth microdilution, and etest method. *J. Clin. Microbiol.* 53, 1823–1830. doi: 10.1128/jcm.00367-15

Kumar, A., Prakash, A., Singh, A., Kumar, H., Hagen, F., Meis, J. F., et al. (2016). *Candida haemulonii* species complex: An emerging species in India and its genetic diversity assessed with multilocus sequence and amplified fragment-length polymorphism analyses. *Emerg. Microbes Infect.* 5:e49. doi: 10.1038/emi.2016.49

Kumar, S., Stecher, G., Li, M., Knyaz, C., and Tamura, K. (2018). MEGA X: Molecular evolutionary genetics analysis across computing platforms. *Mol. Biol. Evol.* 35, 1547–1549. doi: 10.1093/molbev/msy096

Li, H., and Durbin, R. (2009). Fast and accurate short read alignment with Burrows-Wheeler transform. *Bioinformatics* 25, 1754–1760. doi: 10.1093/bioinformatics/btp324

Li, H., Handsaker, B., Wysoker, A., Fennell, T., Ruan, J., Homer, N., et al. (2009). The sequence alignment/map format and SAMtools. *Bioinformatics* 25, 2078–2079. doi: 10.1093/bioinformatics/btp352

Pérez-Lazo, G., Morales-Moreno, A., Soto-Febres, F., Hidalgo, J. A., Neyra, E., and Bustamante, B. (2021). Liver abscess caused by *Candida haemulonii* var. *vulnera*. First case report in Peru. *Rev. Iberoam Micol.* 38, 138–140. doi: 10.1016/j.riam.2020.12.001

Pfaller, M. A., Espinel-Ingroff, A., Canton, E., Castanheira, M., Cuenca-Estrella, M., Diekema, D. J., et al. (2012). Wild-type MIC distributions and epidemiological cutoff values for amphotericin B, flucytosine, and itraconazole and *Candida* spp. as determined by CLSI broth microdilution. *J. Clin. Microbiol.* 50, 2040–2046. doi: 10.1128/JCM.00248-12

Ramos, L. S., Figueiredo-Carvalho, M. H. G., Barbedo, L. S., Ziccardi, M., Chaves, A. L. S., Zancopé-Oliveira, R. M., et al. (2015). *Candida haemulonii* complex: Species identification and antifungal susceptibility profiles of clinical isolates from Brazil. *J. Antimicrob. Chemother.* 70, 111–115. doi: 10.1093/jac/dku321

Ramos, L. S., Figueiredo-Carvalho, M. H. G., Silva, L. N., Siqueira, N. L. M., Lima, J. C., Oliveira, S. S., et al. (2022). The threat called *Candida haemulonii* species complex in Rio de Janeiro State, Brazil: Focus on antifungal resistance and virulence attributes. *J. Fungi (Basel, Switzerland)* 8:574. doi: 10.3390/jof8060574

Rodrigues, D. K. B., Bonfietti, L. X., Garcia, R. A., Araujo, M. R., Rodrigues, J. S., Gimenes, V. M. F., et al. (2021). Antifungal susceptibility profile of *Candida* clinical isolates from 22 hospitals of São Paulo State, Brazil. *Braz. J. Med. Biol. Res.* 54:e10928. doi: 10.1590/1414-431X2020e10928

Rodrigues, L. S., Gazara, R. K., Passarelli-Araujo, H., Valengo, A. E., Pontes, P. V. M., Nunes-da-Fonseca, R., et al. (2020). First genome sequences of two multidrug-resistant *Candida haemulonii* var. *vulnera* isolates from pediatric patients with candidemia. *Front. Microbiol.* 11:1535. doi: 10.3389/fmicb.2020.01535

Warrilow, A. G., Nishimoto, A. T., Parker, J. E., Price, C. L., Flowers, S. A., Kelly, D. E., et al. (2019). The evolution of azole resistance in *Candida albicans* sterol 14alpha-demethylase (CYP51) through incremental amino acid substitutions. *Antimicrob. Agents Chemother.* 63:e02586-18. doi: 10.1128/AAC.02586-18

frontiers | Frontiers in Microbiology

TYPE Original Research
PUBLISHED 14 November 2022
DOI 10.3389/fmicb.2022.1033211

OPEN ACCESS

EDITED BY
Wenjie Fang,
Shanghai Changzheng Hospital,
China

REVIEWED BY
Somanon Bhattacharya,
Stony Brook University,
United States
Shuangjie Wang,
Nanning Maternal and Child Health Hospital, China

*CORRESPONDENCE
Cao Cun-wei
caocunwei@yeah.net
Jean-Paul Latgé
jplatge@pasteur.fr

†These authors have contributed equally to this work

SPECIALTY SECTION
This article was submitted to Antimicrobials, Resistance and Chemotherapy, a section of the journal Frontiers in Microbiology

RECEIVED 31 August 2022
ACCEPTED 31 October 2022
PUBLISHED 14 November 2022

CITATION
Kai-su P, Hong L, Dong-yan Z, Yan-qing Z, Andrianopoulos A, Latgé J-P and Cun-wei C (2022) Study on the mechanisms of action of berberine combined with fluconazole against fluconazole-resistant strains of *Talaromyces marneffei*. *Front. Microbiol.* 13:1033211. doi: 10.3389/fmicb.2022.1033211

Study on the mechanisms of action of berberine combined with fluconazole against fluconazole-resistant strains of *Talaromyces marneffei*

Pan Kai-su[1,2†], Luo Hong[3†], Zheng Dong-yan[1,2], Zheng Yan-qing[2,4], Alex Andrianopoulos[5], Jean-Paul Latgé[6]* and Cao Cun-wei[1,2]*

[1]Department of Dermatology and Venereology, The First Affiliated Hospital of Guangxi Medical University, Nanning, Guangxi, China, [2]Guangxi Key Laboratory of Mycosis Research and Prevention, Nanning, China, [3]Department of Dermatology, Changsha First Hospital, Changsha, China, [4]Fourth People's Hospital of Nanning, Nanning, China, [5]School of Biosciences, The University of Melbourne, Parkville, VIC, Australia, [6]Institute of Molecular Biology and Biotechnology, FORTH and School of Medicine, University of Crete, Crete, Greece

Talaromyces (Penicillium) marneffei (*T. marneffei*) is a thermally dimorphic fungus that can cause opportunistic systemic mycoses. Our previous study demonstrated that concomitant use of berberine (BBR) and fluconazole (FLC) showed a synergistic action against FLC-resistant *T. marneffei* (B4) *in vitro*. In this paper, we tried to figure out the antifungal mechanisms of BBR and FLC in *T. marneffei* FLC-resistant. In the microdilution test, the minimum inhibitory concentration (MIC) of FLC was 256μg/ml before FLC and BBR combination, and was 8μg/ml after combination, the partial inhibitory concentration index (FICI) of B4 was 0.28. After the treatments of BBR and FLC, the studies revealed that (i) increase reactive oxygen species (ROS), (ii) reduce ergosterol content, (iii) destroy the integrity of cell wall and membrane, (iv) decrease the expression of genes *AtrF*, *MDR1*, *PMFCZ*, and *Cyp51B* however *ABC1* and *MFS* change are not obvious. These results confirmed that BBR has antifungal effect on *T. marneffei*, and the combination with FLC can restore the susceptibility of FLC-resistant strains to FLC, and the reduction of ergosterol content and the down-regulation of gene expression of *AtrF, Mdr1, PMFCZ*, and *Cyp51B* are the mechanisms of the antifungal effect after the combination, which provides a theoretical basis for the application of BBR in the treatment of Talaromycosis and opens up new ideas for treatment of Talaromycosis.

KEYWORDS

***Talaromyces marneffei*, berberine, fluconazole, fluconazole-resistant, combination therapy**

Introduction

Talaromycosis is a characteristic opportunistic infection of HIV/AIDS patients in endemic areas. It is a serious disease with a mortality rate of up to 93% due to the insufficient efficacy of the drug used (Hu et al., 2013). Currently, this disease is treated according to the guidelines and is based on amphotericin B, or itraconazole or voriconazole, FLC as a low-cost and relatively safe drug, is not included in the guidelines because of its poor therapeutic effect in *Talaromyces marneffei* (Hoenigl et al., 2021). Traditional Chinese medicine used alone or in combination (Cao et al., 2009; Mo et al., 2014) may be useful to set up more effective therapy against this fungal infection. Most of the known fungal efflux pumps conferring azole resistance are ABC transporters(Leppert et al., 1990).The clarified target of FLC is the lanosterol 14α demethylase, a key enzyme responsible for the synthesis of ergosterol which is a pivotal component in cell membrane encoded by *ERG11* (Zavrel and White, 2015), respiration deficiency leading to decreased reactive oxygen species (ROS) and up-regulation of drug efflux pump mediated by ATP-binding cassette superfamily (APC transporter) and Mdr1p, a member of major facilitator superfamily (MFS) have also been recently documented to result in antifungal resistance to FLC (Patrick et al., 2005). *AtrF* and *Cyp51B* played an important role in the triazole resistance *Aspergillus fumigatus* strains (Yu et al., 2021). BBR is an alkaloid that has long been used to treat bacterial gastroenteritis and dysentery. In recent years, other pharmacological effects of BBR have been gradually discovered, of which the synergistic antifungal effects against FLC-resistant *Candida albicans*, *Candida tropicalis*, and *Cryptococcus* in combination with FLC are receiving increasing attention, *via* ROS increase, intracellular drug accumulation, ergosterol decrease and efflux inhibition (Xu et al., 2009; Bang et al., 2014; Dhamgaye et al., 2014; Shi et al., 2017). Previous combination drug sensitivity test of BBR against *T. marneffei* have suggested that BBR not only has potent antifungal effects against *T. marneffei* by itself, but also exhibits good synergistic effects in combination with FLC *in vitro*, especially for FLC-resistant strains showed synergistic effect (Luo et al., 2019). The aim of this study was to elucidate the synergistic mechanisms of the combined of BBR and FLC in FLC-resistant *T. marneffei*.

Materials and methods

Isolates, cultivation, and agent

The *T. marneffei* wide type strain FRR 2161 (WT) was kindly provided by Prof. Alex Andrianopoulos from the School of Biosciences, The University of Melbourne, Australia. The *T. marneffei* FLC-induced resistant strain B4 (point mutation G1587T, amino acid substitution G441V) was obtained in our laboratory by *in vitro* induction from the *T. marneffei* standard strain FRR 2161, and resistance was verified not to diminish or disappear over generations. *T. marneffei* strains were inoculated into brain-heart infusion (BHI) agar medium at 37°C and cultured for transmission. After microscopic observation, 95% or more of the cells were found to be in the yeast phase and then used for the experiment. The yeast cells were collected and the cell concentration was adjusted by turbidimetric method. The cell concentration was adjusted with the turbidimeter and diluted to $1–5 \times 10^3$ CFU/ml. Fluconazole (FLC, Pfizer Inc., Madrid, Spain) was obtained as pure powder and diluted in sterile distilled water, Berberine (BBR, Sigma–Aldrich, St Louis, MO, USA) was prepared in dimethyl sulfoxide (DMSO). Stock solutions were diluted in RPMI 1640 medium (Sigma Chemical Co., St. Louis, Mo.) and then serially diluted fourfold to achieve the final strength required for the test.

In vitro antifungal activity

Antifungal susceptibility testing was performed using the checkerboard broth microdilution method according to CLSI protocol M27-A3 (Clinical and Laboratory Standards Institute) with some modifications: The final concentration of FLC was set at 64 μg/ml in the range of 0.125–64 μg/ml for WT and 1,024 μg/ml in the range of 2–1024 μg/ml for B4 and BBR. Antifungal plates were incubated at 37°C and MIC assays were read 72 h after inoculation. The susceptibility test was repeated three times at different times using *Candida parapsilosis* ATCC 22019 and *Candida krusei* ATCC 6458 as quality control strains. The fractional inhibitory concentration index (FICI) was used to classify drug interaction. The FICI = MIC (A combo)/MIC (A alone) + MIC (B combo)/MIC (B alone). Synergy and antagonism were defined by FICI of ≤0.5 and>4, respectively. An FICI result of>0.5 but ≤4 was considered indifferent.

Growth curve assay

Exponentially growing yeast cells were harvested and resuspended in fresh yeast extract-peptone dextrose medium (YPD) to obtain a final concentration of 1×10^5 CFU/ml. Different concentrations of BBR and ergosterol (alone or mixed) were added to the cells. Cells were incubated under shaking 200 rpm at 37°C, and OD600 was measured at the indicated time points after incubation (0, 4, 8, 12, 24, 36, and 48 h). The same volumes of solvents (DMSO, Tween 80. and ethanol) were added to the untreated controls. Three independent experiments were performed at three different time points for optimal results.

Transmission electron microscopy

RPMI1640 medium was used to collect 2×10^6 CFU/ml of yeast cells. Then, 32 μg/ml BBR, 2 μg/ml FLC, 32 μg/ml + 2 μg/ml or 32 μg/ml + 256 μg/ml BBR/FLC and the same amount of DMSO

were added to the yeast cells and incubated at 37°C for 72 h. The suspension was washed three times with phosphate buffered saline (PBS). The cells were then fixed with 3% glutaraldehyde and 1% osmium acid solution. Cells were then dehydrated with a series of different grades of ethanol before embedding and ultrathin sections were prepared and observed in a transmission electron microscope (Japan, HTACHI company, type H-7650).

Measurement of intracellular reactive oxygen species

The cell suspension was treated with drugs as in the previous experiment and the same volume of DMSO was used as control. Incubate the cells for 24 h at 37°C, 7500 rpm for 5 min, resuspend them in sterile PBS, adjust the concentration to 6×10^6 CFU/ml, add DHR-123 (dihydrorhodamine) to increase the final concentration to 5 μg/ml, and place them at 37°C to avoid light. Incubate them for 30 min, measure the fluorescence intensity with a flow cytometer and determine the ROS content in the cells.

HPLC evaluation

As described in the literature (Shao et al., 2016) 5×10^6 CFU/ml cells were collected and treated with drugs, and the same amount of DMSO was used as control. After 24 h of shaking culture at 37°C, ergosterol was extracted: each group weighed 0.5 g, added saponifier-containing ethanol solution and was placed in a 90°C water bath for 120 min, shaken every 30 min, 2 ml of absolute ethanol was added and extracted, and finally the upper solution was filtered with a 0.22 μm microporous membrane. The ergosterol standard product was taken at a storage concentration of 20 mg/ml. Then a solution ranging from 0.0015–1.2 mg/ml was prepared with absolute ethanol and a standard curve was constructed by linear regression. The chromatographic column is an XTerraRMS C18 (4.6 mm × 250 mm 5 μm), the mobile phase is 100% methanol, the flow rate is 1.0 ml/min, and the detection wavelength is 284 nm. Injection volume: 20 μl; detection sensitivity: 0.01 AUFS. The upper solution of each group was detected by chromatography, and the content of ergosterol in each group of fungi treated with different drugs was calculated using the linear relationship.

Real-time PCR

One hundred milliliters of 5×10^3 cells were collected and 100 ml of different concentrations of drugs were added respectively, and the concentration of DMSO in the solution was not higher than 0.5%. The cells were then incubated for 48 h with shaking in a constant temperature shaker at 37°C. The cells were then collected to extract the RNA: 200 μl of pre-cooled chloroform was added, mixed gently and left at room temperature for 5 min and then was centrifuged for 15 min at 12000 rpm in a 4°C low temperature centrifuge. 400 μl of the upper water phase was then removed and placed in a clean microtube. Then 500 μl of pre-cooled isopropanol was added, mixed gently and allowed to left stand at room temperature for 10 min. Centrifuge at 12,000 rpm for 10 min in a low temperature centrifuge at 4°C. Used Nanodrop2000 (Thermo Scientific, Waltham, MA) to detect the RNA concentration and verify the stability by a gel running. Real-time quantitative PCR (qRT-PCR) measured the mRNA expression of *ABC1*, *AtrF*, *Mdr1*, *MFS*, *PMFCZ*, and *Cyp51B*. Primer primer5 was used to design primers, and the target fragment was amplified between 100–200 bp (Table 1). The feasibility of the primers was verified by PCR. In each group, 3 parallel wells were established. A fluorescent quantitative real-time PCR instrument (BIO -RADCFX96) was used for amplification, and the cDNA loading error was adjusted by the internal reference gene *β-actin*. The reaction system was performed according to the instructions of SYBR Premix Ex TaqTMII (TiiRNaseHPlus). And with thermal cycling as follows: initial step at 95°C for 60s, followed by 40 cycles at 95°C for 15 s, 55°C for 15 s, and 72°C for 45 s. Relative fold changes of the gene were calculated using the formula $2^{-\Delta\Delta Ct}$.

Statistical analysis

All experiments are performed in triplicate. Experimental results are all expressed as mean ± standard deviation, calculated using SPSS22.0 statistical software and statistically analyzed by one-way analysis of variance. $p < 0.05$ indicates that the difference is statistically significant.

TABLE 1 Primer sequences of gene *β-Actin*, *ABC1*, *AtrF*, *MFS*, *MDR1*, and *PMFCZ* and *Cyp51B*.

Primer name	Sequence
B-Actin	(F)5′- A C G C T C C T G C C T T C T A T G T C-3′
	(R)5′ - A A C A C G G G A G A T A G C G T G A G-′
ABC1	(F)5′ - G A T T C G C T C C G T T A C T T C T T T C G-3′
	(R)5′- C C T C C T T T G A C A T C C A C C T C G-3′
AtrF	(F)5′ - T G A T T T C C C A T T C C T C G C T A C-3′
	(R)5′ - G C C T G C G T C A A C A T C C A A-3′
MDR1	(F) 5′ - T G G C G A G C G A G G T T T C T T-3′
	(R) 5′ - A T G T G C C G T T T T G A T T G T G G-3′
MFS	(F) 5′ - A C T G G C T C T C A A A T C C C A A T C T A C-3′
	(R) 5′ - C A G A A C A A A C C A A A T C C A A C G A-3′
PMFCZ	(F) 5′ - T G G T T G C T A C G A A G T C C A A C T-3′
	(R)5′ - T C A C A A A G A A C C T T C C A A T G C-3′
Cyp51B	(F)5′ - G G T G T T C C A G C A A C T G A T T A C T C T T-3′
	(R)5′ - C G C A T C C C T T C T C T C G T A T T G - 3′

Results

In vitro antifungal activities

As already shown in a present study, our results confirmed that for WT, the MICs of FLC and BBR alone were 2 and 32 μg/ml, respectively, and the MICs of the combination were 0.5 μg/ml of FLC and 8 μg/ml of BBR, with a FICI of 0.5 (synergistic effect). For B4 strain, the MIC of BBR was also 32 μg/ml, while the MIC of FLC was 256 μg/ml. However, the MICs of both drugs decreased to 8 μg/ml after combination and reached a FICI of 0.28, indicating a synergistic effect (FICI ≤0.5; Table 2).

Growth curve

The growth of the WT strains treated with 32 μg/ml BBR alone with 2 μg/ml FLC was significantly slower than that of untreated strains, whereas growth of strains treated with the combination (8 μg/ml BBR and 0.5 μg/ml FLC) was the significantly inhibited ($p < 0.05$; Figure 1-WT). Similarly, BBR (32 μg/ml)/FLC (256 μg/ml) alone or in combination (8 μg/ml BBR and 8 μg/ml FLC) had a similar effect to B4 strain ($p < 0.05$; Figure 1-B4).

Transmission electron microscopy

Transmission electron microscopy showed that the WT and B4 cells showed a classical morpholohy. The unique difference between these two strains was that cell wall of B4 was thicker than that of WT. The cells of WT and B4 were most severely damaged by the combined effect of the two drugs, showing incomplete cell wall and cell membrane and lysis of organelles (Figure 2).

ROS

The ROS-specific dye DHR-123 could be oxidized to the fluorescent rhodamine 123 by the intracellular ROS that could be detected by fluorescent microscope. As shown, the intracellular ROS of WT and B4 strain increased compared with the control after BBR and FLC alone. The intracellular ROS of the WT and B4 increased were more obvious compared with the control after the combination of FLC and BBR ($p < 0.05$; Figure 3).

TABLE 2 Susceptibility activities of BBR and FLC alone and in combination against *T. marneffei.*

Isolates	Alone MIC(μg/ml)		Combination MIC(μg/ml)		FICI	Mode of interaction
	BBR	FLC	BBR	FLC		
WT	32	2	8	0.5	0.5	Synergism
B4	32	256	8	8	0.28	Synergism

FICI: fractional inhibitory concentration index; synergy, FICI ≤ 0.5; indifferent, FICI>0.5 and ≤ 4.0; antagonism, FICI>4.0.

HPLC

Compared with the control, ergosterol content in WT was reduced by 42% after using BBR, by 33% after FLC, and by 83% after BBR + FLC. Similarly, the ergocalciferol content of B4 was reduced by 69% after BBR, 63% after FLC, and 90% after BBR + FLC (Figures 4; $p < 0.05$).

RT-PCR

In absence of drug, the relative expression levels of the drug resistance genes *AtrF*, *MDR1*, and *PMFCZ* mRNA levels of B4 were 6.57, 5.4, and 3.76 times than that of the *T. marneffei* standard strain WT, respectively ($p < 0.05$); the expression of the B4 efflux pump genes *ABC1* and *MFS* was not significantly different from that of WT. The target enzyme gene *Cyp51B* mRNA level of FLC-resistant strain B4 is 16 times higher than the relative expression of the standard strain WT (Figures 5).

After FLC application alone, the genes *AtrF*, *MDR1*, and *PMFCZ* of WT were less expressed than in the blank control group ($p < 0.05$). The target enzyme gene *Cyp51B* was lower than in the control but showed no significant difference ($p > 0.05$). After exposure to BBR alone, the expression of the genes *AtrF*, *Mdr1*, *PMFCZ*, and the target enzyme gene *Cyp51B* were lower than in the control group ($p < 0.05$). While *ABC1* slightly decreased compared with the control ($p > 0.05$), MFS was slightly higher than in the blank group, but there was no significant difference ($p > 0.05$).

After the combination of FLC and BBR, the genes *AtrF, MDR1, PMFCZ* and the target enzyme gene *Cyp51B* were expressed less than with FLC alone ($p < 0.05$), while *ABC1* was expressed slightly more than with FLC alone, but there was no significant difference ($p > 0.05$); *MFS* was slightly lower than with FLC alone, but there was no significant difference ($p > 0.05$). This shows that BBR and FLC combination has a synergistic effect to reduce the relative expression of mRNA levels of WT genes *AtrF*, *MDR1*, *PMFCZ*, and *Cyp51B* (Figures 6, 7).

Discussion

Talaromyces marneffei often leads to systemic disseminated infection and high mortality. Amphotericin B is usually considered as a first choice for the treatment of *T. marneffei* infection, however, the majority of patients cannot tolerate the side effects associated to it (Zeng et al., 2015). Whereas the clinical efficacy of echinocandins in *T. marneffei* infections is poor (Nakai et al., 2003; Cao et al., 2009); the bioavailability of the oral itraconazole preparation is low (Le et al., 2017). Voriconazole, on the other

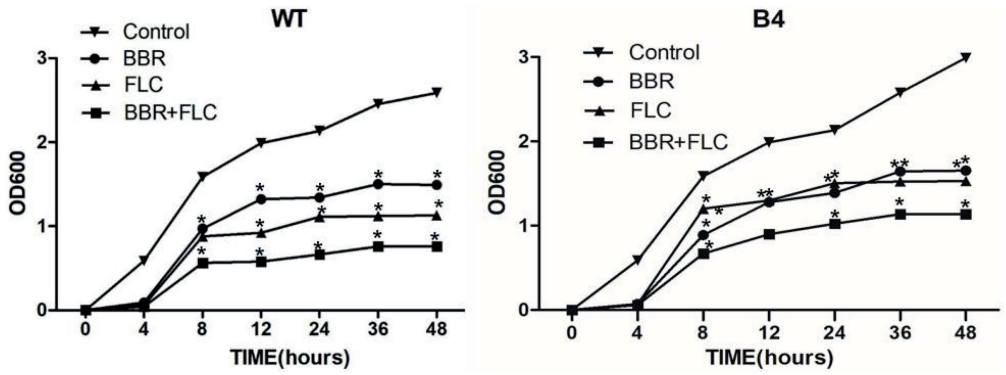

FIGURE 1
(**WT**). Growth curve of *T. marneffei* type strain FRR 2161 treated with BBR and/or FLC Growth curves of the synergism of BBR with FLC against *T. marneffei* type strain FRR 2161 that were obtained by using initial inoculums of 10^3CFU/ml. BBR (32μg/ml); FLC (2μg/ml); BBR (32μg/ml)+FLC (2μg/ml). (**B4**). Growth curve of (**B4**) treated with BBR and/or FLC. BBR (32μg/ml); FLC (256μg/ml); BBR (32μg/ml)+FLC (256μg/ml). *$p < 0.05$ compared with the control.

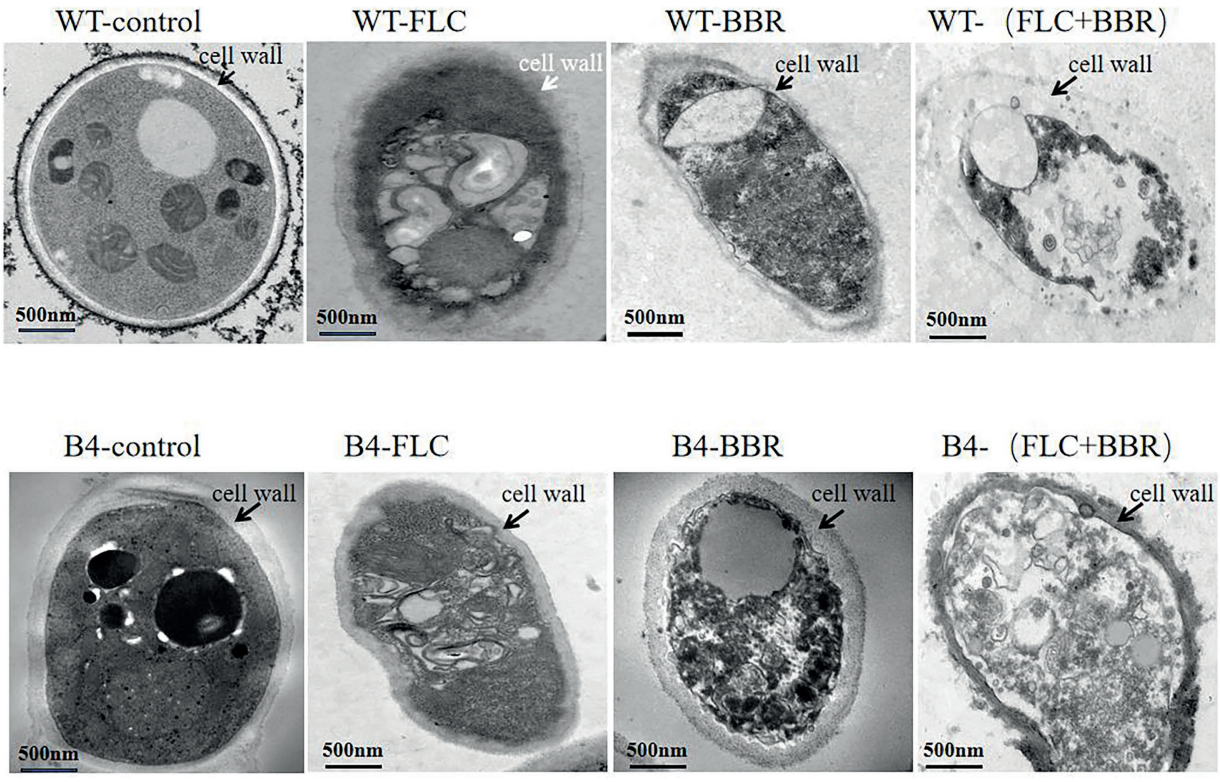

FIGURE 2
Transmission electron microscopy observation of cells (**WT,B4**) before and after using FLC or/and BBR. For (**WT**), add BBR 32μg/ml, FLC 2μg/ml, BBR/FLC 32μg/ml+2μg/ml; For (**B4**), add BBR 32μg/ml, FLC 256μg/ml, BBR/FLC 32μg/ml+ 256μg/ml.

hand, has good clinical efficacy and high safety in the treatment of *T. marneffei* infections, but the high cost of voriconazole is one of its disadvantages (Ouyang et al., 2017). FLC is an affordable antifungal agent with low toxicity and fewer side effects that has been used in the initial treatment of *T. marneffei* infections. However, FLC has poor clinical efficacy and a low cure rate (Supparatpinyo et al., 1993), and is not recommended in international guidelines for the treatment of *T. marneffei* infections (Masur et al., 2014).

According to the report, BBR has attracted much attention because it has very low toxicity in relatively high doses and reveals significant clinical benefits without major side effects

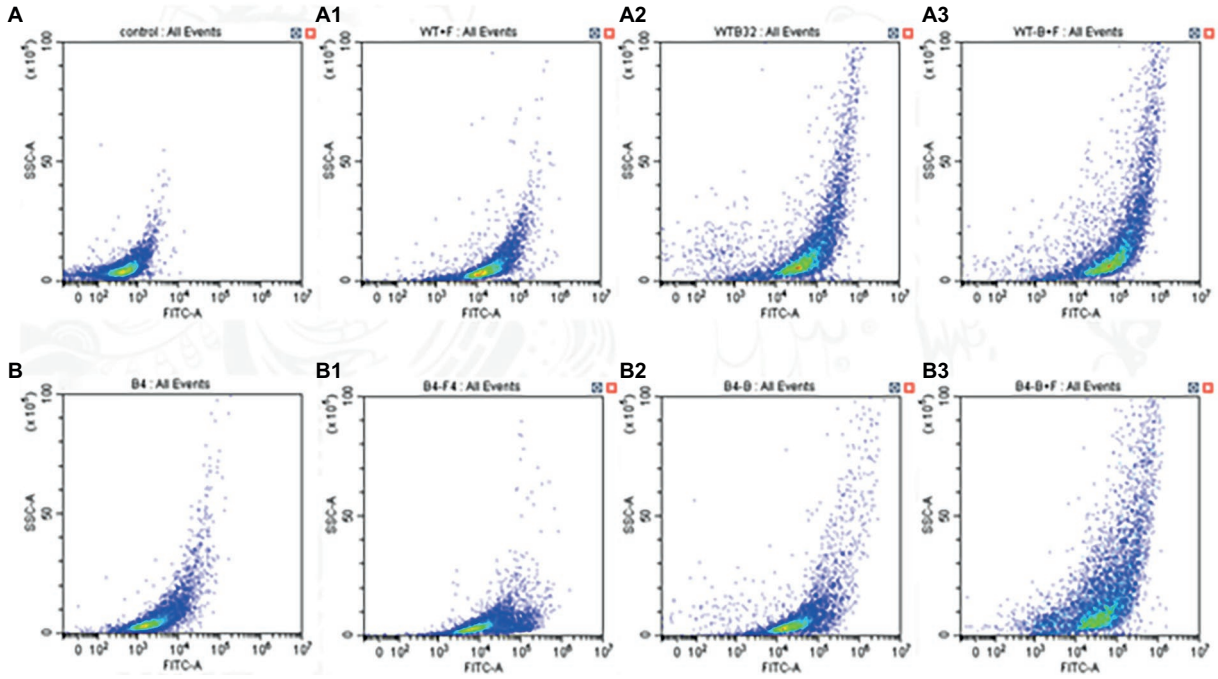

FIGURE 3
Effects of BBR and/or FLC on ROS production in (WT,B4). For (WT): Cells were treated with BBR (32μg/ml) and/or FLC (2μg/ml) 24h and incubated with DHR-123 for 30min. For (B4): Cells were treated with BBR (32μg/ml) and/or FLC (256μg/ml) 24h and incubated with DHR-123 for 30min.

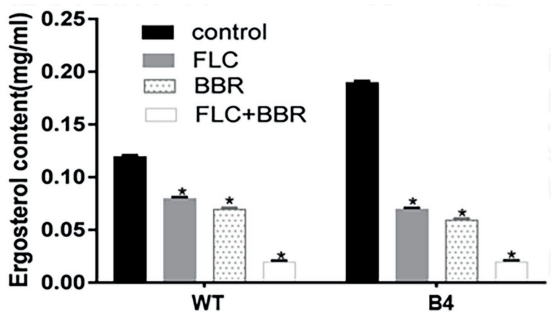

FIGURE 4
Ergosterol content surveyed by HPLC after the administrations of agents in WT and B4. *$p<0.05$ compared with the control.

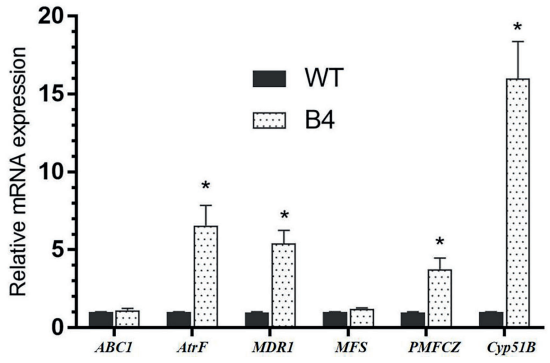

FIGURE 5
Gene expressions of important drug-related genes in WT and B4. *$p<0.05$ compared with the control.

(Chen et al., 2014), therefore, multiple functions have been explored such as anti-inflammatory, antidiabetic, antibacterial, hepatoprotective and neuroprotective effects (Chen et al., 2014; Mahmoudvand et al., 2014). In recent years, other pharmacological effects of BBR have been gradually discovered, including synergistic antibacterial effects on FLC-resistant *C. albicans*, *C. tropicalis*, and *Cryptococcus* spp, which have received increasing attention after combination with FLC (Bang et al., 2014; Chen et al., 2014; Dhamgaye et al., 2014; Shi et al., 2017). According to the literature, the mechanism of synergistic antibacterial effect of BBR in combination with FLC is mainly manifested in the following aspects: Bactericidal effect by promoting the production of intracellular reactive oxygen species (ROS; Xu et al., 2009); Acting on the expression of drug excretion pump genes, down-regulating the function of the main transposed subfamily (MFS) and ATP-binding box transporter family, and promoting intracellular drug accumulation to play a bactericidal role (Shao et al., 2016; Shi et al., 2017); Down-regulation of the expression of the gene encoding the azole drug target enzyme, wool sterol 14-α-demethylase (14DH), decreases cell membrane ergosterol

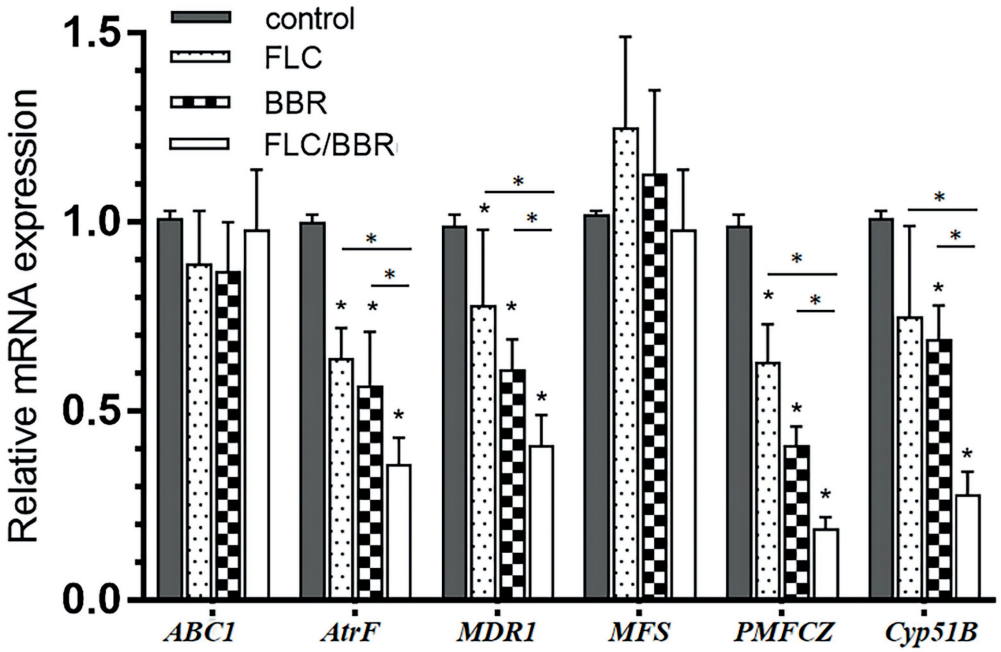

FIGURE 6
Gene expressions of *ABC1,AtrF, Mdr1,MFS, PMFCZ* and *Cyp51B* in WT under treatments. *$p<0.05$ compared with the control.

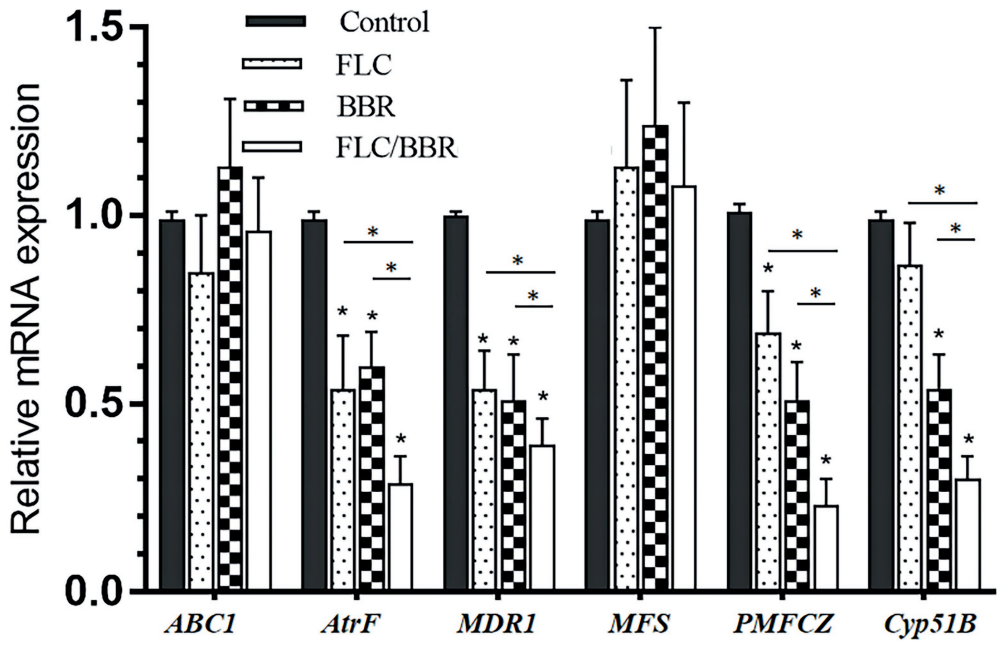

FIGURE 7
Gene expressions of *ABC1,AtrF, Mdr1,MFS, PMFCZ* and *Cyp51B* in TM (B4) under treatments. *$p<0.05$ compared with the control.

synthesis, and cell membrane integrity is destroyed and susceptible to killing (Li et al., 2013). This may lead to mitochondrial dysfunction and cell death by disrupting the integrity of the fungal cell wall (Shi et al., 2017).

Our previous study found that BBR in combination with FLC had a synergistic effect on the clinical isolates of *T. marneffei in vitro* (Luo et al., 2019). Therefore, this study further investigated the mechanisms after the combined application of BBR and

FLC. It was found that the combination caused significant growth inhibition and cell wall and cell membrane destruction in WT and drug-resistant strains.

BBR in combination with FLC can affect the integrity of the cell wall and cell membrane of *C. albicans* (Dhamgaye et al., 2014). It was also found that after combination, FLC-resistant *C. albicans* became sensitive to FLC by increasing the content of ROS in the cells (Xu et al., 2009; Li et al., 2013; Mahmoudvand et al., 2014). Computer aided research has revealed that BBR can embed DNA from its c5-c6-n + − C8 side (Mazzini et al., 2003). BBR can bind to double-stranded DNA and cause photooxidative DNA damage by producing ROS (Hirakawa et al., 2005), and changes its function by altering DNA structure and conformation to play an antibacterial role and induce cell apoptosis (Kumar et al., 1993), and also can be an excellent DNA intercalator rich in at sequence (Davidson et al., 1977; Iwazaki et al., 2010). In our study, in the strain WT, intracellular ROS increased after FLC/BBR alone and the combination of the two drugs. Similar results were obtained when B4 was examined. Electron microscopy examination revealed that the deformation of the nucleus and incompleteness of the cell membrane could be related to the insertion of BBR into DNA, resulting in damage to double-stranded DNA.

Up-regulation of the *Cyp51A* gene in *A. fumigatus* often leads to azole resistance (Camps et al., 2012). *Hagiwara* et al. (Hagiwara et al., 2016) recently investigated that mutations at different sites of the tandem repeats in the promoter region of the *Cyp51A* gene in *Aspergillus* can cause azole resistance. Whole genome sequencing of clinical and environmental azole-resistant strains of *A. fumigatus* in India, the Netherlands, and the United Kingdom showed that the environmental strains were mainly caused by the tr34/l98h mutation of the *Cyp51A* gene (Fan et al., 2015). In a previous study on *C. tropicalis*, significant down-regulation of *ERG11* gene expression is one of the mechanisms of the combination of BBR and FLC against *C. tropicalis* (Shi et al., 2017). However, our research found that *Cyp51B*, not *Cyp51A*, is an important gene associated with azoles in *T. marneffei* (unpublished). In this study, ergosterol synthesis from WT and B4 significantly decreased (83, 90%) and *Cyp51B* expression significantly decreased after the application of BBR in combination with FLC. It is suggested that *Cyp51B* plays an important role in the mechanism of FLC resistance.

Yuen et al. (2003) suggested that *T. marneffei* has a gene belonging to the *MFS* family (gene *PMFCZ*), which may be related to FLC resistance. When comparing the expression levels of the drug efflux transporter and ergosterol synthesis genes between the standard *T. marneffei* strain WT and B4, we found that the expression levels of the *AtrF*, *MDR1*, *PMFCZ*, and *Cyp51B* genes were higher in B4 than in WT, suggesting that the high expression of these genes may be related to the FLC resistance of the *T. marneffei*. Previous studies have shown (Shao et al., 2016) that FLC can promote the aggregation of BBR in cells and BBR impedes the normal function of *MDR1*. Fluconazole-promoted intracellular aggregation of BBR reached an effective concentration and further enhanced the antifungal activity of BBR. We speculate that BBR and FLC may promote each other, inhibit the efflux pump, and increase their concentration in cells to achieve a synergistic antifungal effect.

In conclusion, this study further investigated the mechanisms of BBR and FLC combination return to susceptibility of FLC-resistance of *T. marneffei*. Also, our study provides a new treatment option for talaromycosis. The combination could become a new efficient, safe and cost-effective regimen for the treatment of talaromycosis. However, the mechanisms of drug action is complex. In addition to the above possible mechanisms found in our study, further investigation is needed to determine whether there are other important mechanisms, and *in vivo* needs to be further verified by animal models and clinical research.

Data availability statement

The authors acknowledge that the data presented in this study must be deposited and made publicly available in an acceptable repository, prior to publication. Frontiers cannot accept a manuscript that does not adhere to our open data policies.

Author contributions

PK-s, LH, ZD-y, ZY-q, and AA contributed to the data collection. PK-s and LH contributed to the laboratory work. PK-S and LH wrote the manuscript. J-PL and CC-w supervised and evaluated the process of the study. All authors contributed to the article and approved the submitted version.

Acknowledgments

This study was supported by grants from the National Natural Science Foundation of China (81960567 and 82173433) and the Natural Science Foundation of Guangxi Province of China (2020GXNSFGA238001), and The First Affiliated Hospital of Guangxi Medical University Provincial and Ministerial Key Laboratory Cultivation Project: Guangxi Key Laboratory of Tropical Fungi and Mycosis Research (No. YYZS2020006).

Conflict of interest

The authors declare that the research was conducted in the absence of any commercial or financial relationships that could be construed as a potential conflict of interest.

Publisher's note

References

Bang, S., Kwon, H., Hwang, H. S., Park, K. D., Kim, S. U., and Bahn, Y. S. (2014). 9-O-butyl-13-(4-isopropylbenzyl)berberine, KR-72, is a potent antifungal agent that inhibits the growth of *Cryptococcus neoformans* by regulating gene expression. *PLoS One* 9:e109863. doi: 10.1371/journal.pone.0109863

Camps, S. M., Dutilh, B. E., Arendrup, M. C., Rijs, A. J. M. M., Snelders, E., Huynen, M. A., et al. (2012). Discovery of a hap E mutation that causes azole resistance in *aspergillus fumigatus* through whole genome sequencing and sexual crossing. *PLoS One* 7:e50034. doi: 10.1371/journal.pone.0050034

Cao, C., Liu, W., Li, R., Wan, Z., and Qiao, J. (2009). In vitro interactions of micafungin with amphotericin B, itraconazole or fluconazole against the pathogenic phase of *Penicillium marneffei*. *J. Antimicrob. Chemother.* 63, 340–342. doi: 10.1093/jac/dkn494

Chen, C., Yu, Z., Li, Y., Fichna, J., and Storr, M. (2014). Effects of berberine in the gastrointestinal tract - a review of actions and therapeutic implications. *Am. J. Chin. Med.* 42, 1053–1070. doi: 10.1142/S0192415X14500669

Davidson, M. W., Lopp, I., Alexander, S., and Wilson, W. D. (1977). The interaction of plant alkaloids with DNA II. Berberinium chloride. *Nucleic Acids Res* 4, 2697–2712. doi: 10.1093/nar/4.8.2697

Dhamgaye, S., Devaux, F., Vandeputte, P., Khandelwal, N. K., Sanglard, D., Mukhopadhyay, G., et al. (2014). Molecular mechanisms of action of herbal antifungal alkaloid berberine, in *Candida albicans*. *PLoS One* 9:e104554. doi: 10.1371/journal.pone.0104554

Fan, Z., et al. (2015). Csp A influences biofilm formation and drug resistance in pathogenic fungus *aspergillus fumigatus*. *Biomed Res Int.* 2015:960357. doi: 10.1155/2015/960357

Hagiwara, D., Watanabe, A., Kamei, K., and Goldman, G. H. (2016). Epidemiological and genomic landscape of azole resistance mechanisms in aspergillus fungi. *Front. Microbiol.* 7:1382. doi: 10.3389/fmicb.2016.01382

Hirakawa, K., Kawanishi, S., and Hirano, T. (2005). The mechanism of guanine specific photooxidation in the presence of berberine and palmatine: activation of photosensitized singlet oxygen generation through DNA-binding interaction. *Chem. Res. Toxicol.* 18, 1545–1552. doi: 10.1021/tx0501740

Hoenigl, M., Salmanton-García, J., Walsh, T. J., Nucci, M., Neoh, C. F., Jenks, J. D., et al. (2021). Global guideline for the diagnosis and management of rare mould infections: an initiative of the European Confederation of Medical Mycology in cooperation with the International Society for Human and Animal Mycology and the American Society for Microbiology. *Lancet Infect. Dis.* 21, e246–e257. doi: 10.1016/S1473-3099(20)30784-2

Hu, Y., Zhang, J., Li, X., Yang, Y., Zhang, Y., Ma, J., et al. (2013). *Penicillium marneffei* infection: an emerging disease in mainland China. *Mycopathologia* 175, 57–67. doi: 10.1007/s11046-012-9577-0

Iwazaki, R. S., Endo, E. H., Ueda-Nakamura, T., Nakamura, C. V., Garcia, L. B., and Filho, B. P. D. (2010). In vitro antifungal activity of the berberine and its synergism with fluconazole. *Antonie Van Leeuwenhoek* 97, 201–205. doi: 10.1007/s10482-009-9394-8

Kumar, G. S., Debnath, D., Sen, A., and Maiti, M. (1993). Thermodynamics of the interaction of berberine with DNA. *Biochem. Pharmacol.* 46, 1665–1667. doi: 10.1016/0006-2952(93)90337-V

Le, T., Kinh, N. V., Cuc, N. T. K., Tung, N. L. N., Lam, N. T., Thuy, P. T. T., et al. (2017). A trial of Itraconazole or amphotericin B for HIV-associated Talaromycosis. *N. Engl. J. Med.* 376, 2329–2340. doi: 10.1056/NEJMoa1613306

Leppert, G., McDevitt, R., Falco, S. C., van Dyk, T. K., Ficke, M. B., and Golin, J. (1990). Cloning by gene amplification of two loci conferring multiple drug resistance in saccharomyces. *Genetics* 125, 13–20. doi: 10.1093/genetics/125.1.13

Li, D. D., Xu, Y., Zhang, D. Z., Quan, H., Mylonakis, E., Hu, D. D., et al. (2013). Fluconazole assists berberine to kill fluconazole-resistant *Candida albicans*. *Antimicrob. Agents Chemother.* 57, 6016–6027. doi: 10.1128/AAC.00499-13

Luo, H., Pan, K. S., Luo, X. L., Zheng, D. Y., Andrianopoulos, A., Wen, L. M., et al. (2019). In vitro susceptibility of Berberine combined with antifungal agents against the yeast form of *Talaromyces marneffei*. *Mycopathologia* 184, 295–301. doi: 10.1007/s11046-019-00325-y

Mahmoudvand, H., et al. (2014). Antifungal, Antileishmanial, and Cytotoxicity Activities of Various Extracts of Berberis vulgaris (Berberidaceae) and Its Active Principle Berberine. *ISRN Pharmacol.* 2014: 602436. doi: 10.1155/2014/602436

Masur, H., Brooks, J. T., Benson, C. A., Holmes, K. K., Pau, A. K., Kaplan, J. E., et al. (2014). Prevention and treatment of opportunistic infections in HIV-infected adults and adolescents: updated guidelines from the Centers for Disease Control and Prevention, National Institutes of Health, and HIV medicine Association of the Infectious Diseases Society of America. *Clin. Infect. Dis.* 58, 1308–1311. doi: 10.1093/cid/ciu094

Mazzini, S., Bellucci, M. C., and Mondelli, R. (2003). Mode of binding of the cytotoxic alkaloid berberine with the double helix oligonucleotide d(AAGAATTCTT)(2). *Bioorg. Med. Chem.* 11, 505–514. doi: 10.1016/S0968-0896(02)00466-2

Mo, D., Li, X., Wei, L., Sun, C., Liang, H., and Cao, C. (2014). In vitro interactions of calcineurin inhibitors with conventional antifungal agents against the yeast form of *Penicillium marneffei*. *Mycopathologia* 178, 217–220. doi: 10.1007/s11046-014-9787-8

Nakai, T., Uno, J., Ikeda, F., Tawara, S., Nishimura, K., and Miyaji, M. (2003). In vitro antifungal activity of micafungin (FK463) against dimorphic fungi: comparison of yeast-like and mycelial forms. *Antimicrob. Agents Chemother.* 47, 1376–1381. doi: 10.1128/AAC.47.4.1376-1381.2003

Ouyang, Y., Cai, S., Liang, H., and Cao, C. (2017). Administration of voriconazole in disseminated *Talaromyces (Penicillium) Marneffei* infection: a retrospective study. *Mycopathologia* 182, 569–575. doi: 10.1007/s11046-016-0107-3

Patrick, V., et al (2005). Mechanisms of azole resistance in a clinical isolate of Candida tropicalis. *Biomed. Pharmacother.* 49, 4608–4615. doi: 10.1128/AAC.49.11.4608-4615.2005

Shao, J., Shi, G., Wang, T., Wu, D., and Wang, C. (2016). Antiproliferation of Berberine in combination with fluconazole from the perspectives of reactive oxygen species, Ergosterol and drug efflux in a fluconazole-resistant *Candida tropicalis* isolate. *Front. Microbiol.* 7:1516. doi: 10.3389/fmicb.2016.01516

Shi, G., Shao, J., Wang, T. M., Wu, D. Q., and Wang, C. Z. (2017). Mechanism of berberine-mediated fluconazole-susceptibility enhancement in clinical fluconazole-resistant *Candida tropicalis* isolates. *Biomed. Pharmacother.* 93, 709–712. doi: 10.1016/j.biopha.2017.06.106

Supparatpinyo, K., Nelson, K. E., Merz, W. G., Breslin, B. J., Cooper, C. R. Jr., Kamwan, C., et al. (1993). Response to antifungal therapy by human immunodeficiency virus-infected patients with disseminated *Penicillium marneffei* infections and in vitro susceptibilities of isolates from clinical specimens. *Antimicrob. Agents Chemother.* 37, 2407–2411. doi: 10.1128/AAC.37.11.2407

Xu, Y., Wang, Y., Yan, L., Liang, R. M., Dai, B. D., Tang, R. J., et al. (2009). Proteomic analysis reveals a synergistic mechanism of fluconazole and berberine against fluconazole-resistant *Candida albicans*: endogenous ROS augmentation. *J. Proteome Res.* 8, 5296–5304. doi: 10.1021/pr9005074

Yu, S., Wang, Y., Shen, F., Wu, R., Cao, D., and Yu, Y. (2021). Emergence of Triazole resistance in *aspergillus fumigatus* exposed to Paclobutrazol. *J. Agric. Food Chem.* 69, 15538–15543. doi: 10.1021/acs.jafc.1c05396

Yuen, K. Y., Pascal, G., Wong, S. S. Y., Glaser, P., Woo, P. C. Y., Kunst, F., et al. (2003). Exploring the *Penicillium marneffei* genome. *Arch. Microbiol.* 179, 339–353. doi: 10.1007/s00203-003-0533-8

Zavrel, M., and White, T. C. (2015). Medically important fungi respond to azole drugs: an update. *Future Microbiol.* 10, 1355–1373. doi: 10.2217/FMB.15.47

Zeng, W., Qiu, Y., Lu, D. C., Zhang, J., Zhong, X., and Liu, G. (2015). A retrospective analysis of 7 human immunodeficiency virus-negative infants infected by *Penicillium marneffei*. *Medicine (Baltimore)* 94:e1439. doi: 10.1097/MD.0000000000001439

frontiers | Frontiers in Microbiology

TYPE Original Research
PUBLISHED 18 November 2022
DOI 10.3389/fmicb.2022.1029966

OPEN ACCESS

EDITED BY
Wenjie Fang,
Shanghai Changzheng Hospital, China

REVIEWED BY
Wei Fang,
Shanghai Changzheng Hospital, China
Min Chen,
Shanghai Changzheng Hospital, China

*CORRESPONDENCE
Xin Huang
alida_huang@163.com

†These authors have contributed equally to this work

SPECIALTY SECTION
This article was submitted to Antimicrobials, Resistance and Chemotherapy, a section of the journal Frontiers in Microbiology

RECEIVED 28 August 2022
ACCEPTED 07 November 2022
PUBLISHED 18 November 2022

CITATION
Zhao S, Shang A, Guo M, Shen L, Han Y and Huang X (2022) The advances in the regulation of immune microenvironment by *Candida albicans* and macrophage cross-talk. *Front. Microbiol.* 13:1029966. doi: 10.3389/fmicb.2022.1029966

The advances in the regulation of immune microenvironment by *Candida albicans* and macrophage cross-talk

Shuo Zhao[1†], Anquan Shang[2†], Mengchen Guo[1], Liangliang Shen[1], Yu Han[1] and Xin Huang[1*]

[1]Department of Dermatology, School of Medicine, Tongji Hospital, Tongji University, Shanghai, China, [2]Department of Laboratory Medicine, The Second People's Hospital of Lianyungang, Lianyungang, China

Candida albicans (*C. albicans*) is the most common causative agent of invasive fungal infections in hospitals. The body defends against and eliminates *C. albicans* infection by various mechanisms of immune response, and the latter mechanism of immune evasion is a major challenge in the clinical management of *C. albicans* infection. The role of macrophages in combating *C. albicans* infection has only recently been recognized, but the mechanisms remain to be elucidated. This review focuses on the interaction between *C. albicans* and macrophages (macrophages), which causes the body to generate an immune response or *C. albicans* immune escape, and then regulates the body's immune microenvironment, to explore the effect of *C. albicans* virulence resistance vs. macrophage killing and clarify the role and mechanism of *C. albicans* pathogenesis. In general, a thorough understanding of the molecular principles driving antifungal drug resistance is essential for the development of innovative treatments that can counteract both existing and emerging fungal threats.

KEYWORDS

***Candida albicans*, macrophages, PRR, PAMP, morphological transition, immune escape**

Introduction

In recent decades, *Candida albicans* (*C. albicans*) has been the leading cause of life-threatening invasive fungal infections, and despite the low treatment difficulty, invasive candidiasis ranges from mild symptomatic bacteremia to fulminant sepsis with an associated mortality rate of more than 70% (Pappas et al., 2018). According to recent reports, there are approximately 750,000 cases worldwide IC and over 50,000 deaths per year (Gonzalez-Lara and Ostrosky-Zeichner, 2020). *C. albicans* infection is the second most common cause of vaginal candidiasis (VVC). Among women of reproductive age,

approximately 75% had at least one episode of VVC, and 40% had a second episode (Rolo et al., 2020). *C. albicans*, an important fungal pathogen in humans, exhibits different morphologies, such as yeast, pseudohyphae, and hyphae, which are recognized differently by the phagocytic cells of the innate immune response. Once *C. albicans* cells get into host tissues, immune cells like macrophages are drawn to the site of infection and activated to find, engulf, and kill the pathogen (Godoy et al., 2022). Understanding the virulence characteristics of *C. albicans*, the tissue-specific mechanisms of anti-Candida host defense, and its resistance mechanisms to existing antifungal agents should lead to better strategies to diagnose and treat affected individuals, which may help improve patient outcomes (Lopes and Lionakis, 2022). Cells of the innate immune system, including N eutrophils (N), macrophages (M), D endritic cells (DC), natural killer (NK) cells, and mast cells, play various roles in innate immune defense (**Figure 1**). Neutrophils can form neutrophil capture networks to kill pathogens (Jiang et al., 2019), but DC activates antigen-presenting cells and activates initial T cells to kill pathogens (de Albuquerque et al., 2018). Macrophages use surface pattern recognition receptor (PRRs) to recognize and phagocytose *C. albicans* by not only producing reactive oxygen species and reactive nitrogen species but also triggering the activation of signaling pathways such as MAPK and NF-kB, producing pro-inflammatory cytokines, and recruiting other immune cells to work together to eliminate pathogens (Gantner et al., 2005). A study found that *C. albicans* biofilm formation can destroy fine macrophages, and macrophages can also affect biofilm formation (Alonso et al., 2017; Arce Miranda et al., 2019). Candida-macrophage interactions are important immune defense responses associated with disseminated and deep-seated candidiasis in humans (Klotz et al., 2022). During *C. albicans* infection, macrophages can effectively detect, internalize, and kill invading pathogens, while *C. albicans* can escape macrophage killing by different pathways, and the interaction between the two leads to different diseases. And the mechanism by which *C. albicans* escapes lysosome digestion by macrophages remains to be investigated. In this paper, we describe how *C. albicans* identifies the cell wall components of *C. albicans* through the PRRs of macrophages, how macrophages engulf *C. albicans*, how they alter the phagocyte environment to induce hyphal formation, how *C. albicans* and macrophages interact, how *C. albicans* virulence factors, proteins, toxins and GPI proteins are responsible for its virulence on macrophages, etc. To provide a solid foundation for future research on *C. albicans* and macrophages. Understanding the mechanisms by which macrophages interact with *C. albicans* will facilitate more efficient killing of *C. albicans* by macrophages and reduced mortality from invasive *C. albicans* disease.

Candida albicans cell wall, structure and macrophages corresponding pattern recognition receptors

The cell wall of *C. albicans* is divided into an inner and an outer layer. The outer layer is mainly composed of mannose and proteins, with mainly O- and N-type mannose polymers (mannose) covalently linked to proteins to form glycoproteins. Among them, O-chain mannan, N-chain mannan and phosphorylated mannan are the main proinflammatory factors, and the inner layer is composed of skeletal polysaccharides, β-1,3-glucan, β-1,6-dextran and chitin, and its main components give shape and survival advantages to the cell (Silao et al., 2020). Compared with other pathogens, fungi can more easily activate the recognition mechanisms of the immune system, and almost all cell wall components belong to PAMP and interact with the corresponding PRRs to elicit an immune response in the host. Common PRRs where *C. albicans* interacts with macrophages mainly include type C lectin receptors (CLRs), Toll-like receptors (TLRs), and NOD -like receptors (NLRBs) (**Figure 2**).

Macrophages participate in the regulation of *Candida albicans* the formation of mycelium

There are four forms of *C. albicans*: yeast, hyphae, pseudomycelium, and chlamydial spores. The yeast is more resistant to macrophage killing and its virulence than the hyphal body. The ability of yeast to transform into hyphae is considered one of the most important pathogenic features of *C. albicans*. The transformation of yeast is often, but not always, influenced by environmental conditions such as pH, CO_2 levels, anaerobic conditions, and temperature. Among others, activation of the CAMP pathway plays an important role in the induction of certain genes. Expression during hyphal formation. Many previous studies have shown that environmental factors such as serum, CO2 concentration, glucosamine N-acetate (GlcNAc), and amino acids can activate the Ras- CAMP -signaling pathway under *in vitro* culture conditions (Salvatori et al., 2020). The CAMP -mediated signaling pathway is a protease. A (PKA) complex activates transcription factors that promote hyphal-specific gene expression and thus hyphal formation.

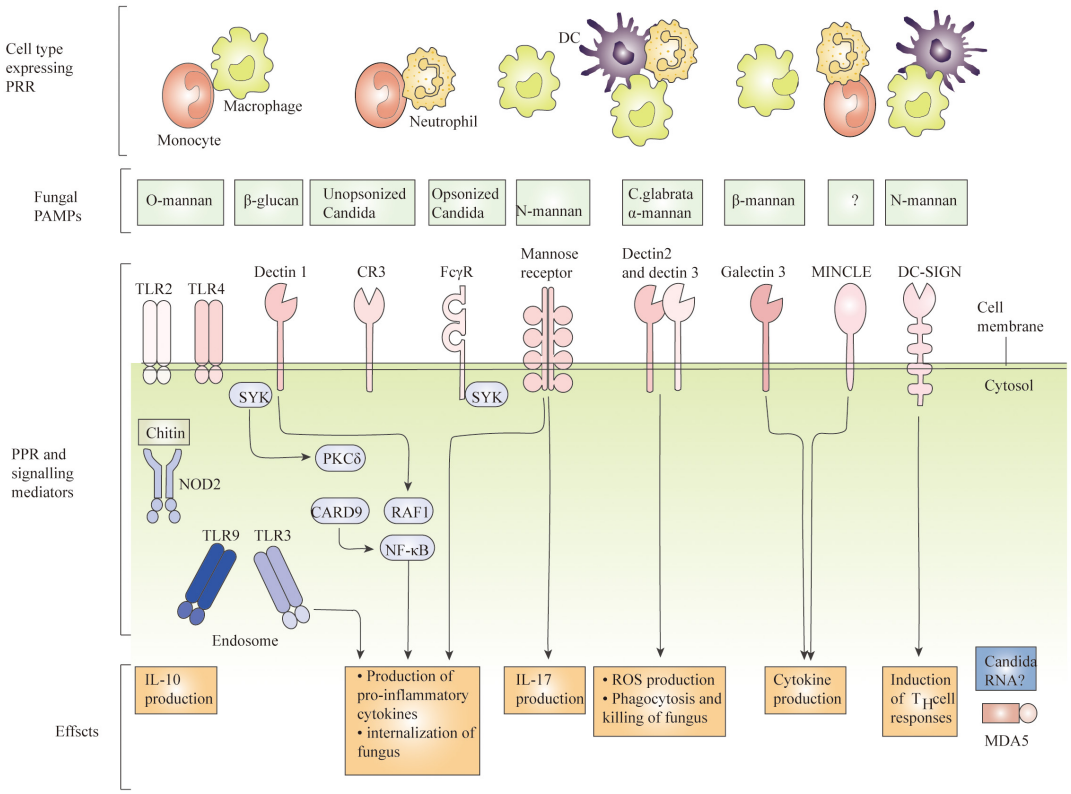

FIGURE 1
Recognition of *C. albicans* by immune cells.

Effect of macrophages on *Candida albicans* virulence

C. albicans is harmless as a commensal bacterium, but when the balance of normal flora is disturbed or immune defenses are compromised, these fungi can overgrow the mucosal flora and cause symptoms of disease. Two main types of infections have been observed after host immune status is compromised: superficial and invasive candidiasis. Superficial infection of the mucosal epithelium is common in immunocompromised patients, including chronic atrophic stomatitis, chronic cutaneous mucosal candidiasis, and vulvovaginal vaginitis. In more severe cases, *C. albicans* can enter the bloodstream and affect almost all organs of the body. Invasive candidiasis includes either acute or chronic hematogenous disseminated candidiasis and infection of a single or multiple deep organs, either by hematogenous seeding or by direct seeding. Although there is evidence that *C. albicans* can also disseminate in the lymphatic system, the major route of transmission is blood, and once Candida cells invade host tissues, the innate immune response is dominated by macrophages. Phagocytosis of these mononuclear phagocytes has been shown to slow the growth of *C. albicans* and leads to upregulation of genes involved in alternative carbon utilization and stress response. A study found that the importance of stress response pathways in drug resistance and tolerance is clear. These pathways directly affect the ability of the fungus to persist in its environment, and for fungal pathogens in humans, these signaling networks are critical factors in treatment failure (Henriques and Williams, 2020). In phagolysosomes, *C. albicans* is able to transform into a hyphal morphology that allows the pathogen to escape macrophages and thus continue to proliferate in the host. The hyphal-related aspartyl proteases Sap4, Sap5, and Sap6 have been shown to be required for macrophage survival. Proteases and phosphatomannose (PLM) on the surface of *C. albicans* can also promote macrophage survival by inducing apoptosis, for example by interacting with the ERK1/2 signal transduction pathway (Ibata-Ombetta et al., 2003). Some less pathogenic Candida species do not appear to respond in this way and are not viable (Mavor et al., 2005).

Candida albicans interacts with macrophages

As the first line of defense of the innate immune response, macrophages mediate the clearance of invading

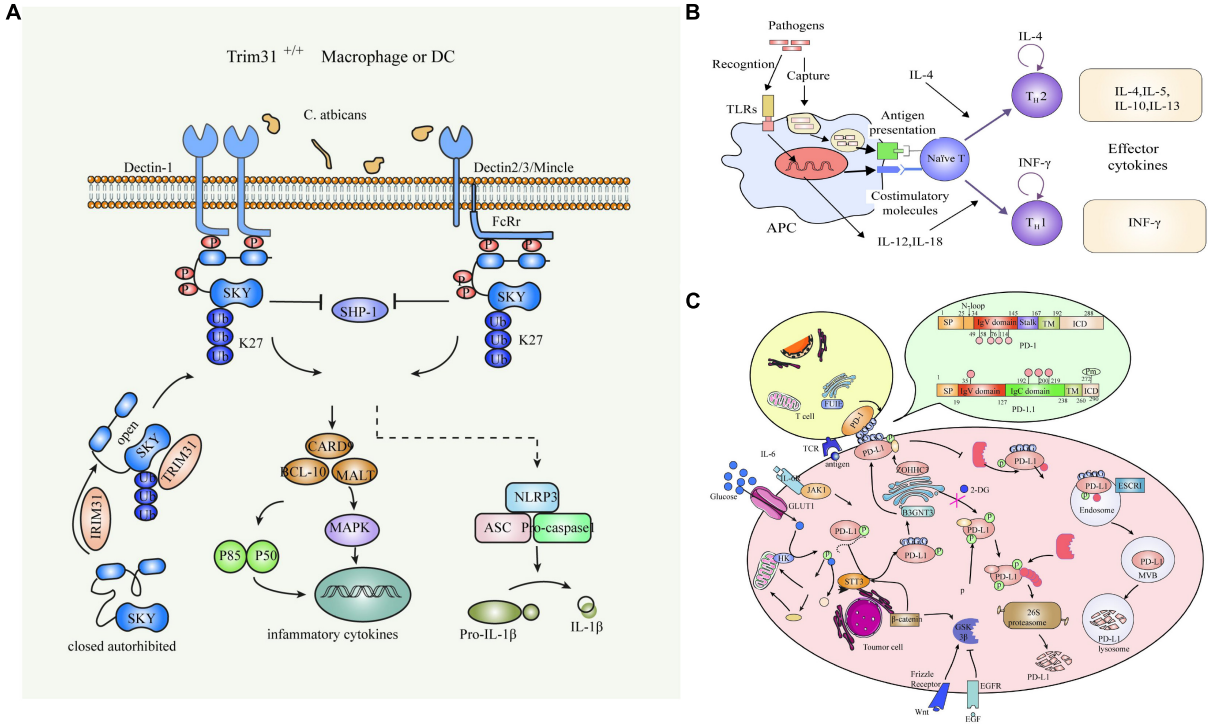

FIGURE 2
Common PRRs of *C. albicans* interacting with Macrophages. **(A)** Schematic diagram of the C-type lectin receptor. **(B)** Toll-like receptors. **(C)** NOD-like receptors.

C. albicans by intracellular killing. However, *C. albicans* has evolved sophisticated strategies for targeting macrophages to evade immune surveillance. The cytolytic peptide toxin, Candida lysine, promotes this fungal defense mechanism by disrupting immune cell membranes to escape the phagosomal environment. In the initial phase of interaction between *C. albicans* and macrophages, host cell lysis is mainly involved in mediating caspase-1-dependent cell pyroptosis through the activation of NOD -like receptor protein 3 (NLRP3) (Pietrella et al., 2013; Mao et al., 2020). The cytolytic peptide toxin Candida lysin contributes to macrophage lysis but also activates NLRP3, triggering secretion of pro-inflammatory cytokines that regulate macrophage defense against *C. albicans*. Candida bacteriolysin can be considered a microbial factor that has a dual function during its interaction with the host (König et al., 2020). It provides a mechanism for host cell lysis that contributes to escape from these immune cells. By activating NLRP3, it triggers a host proinflammatory protective response to eliminate *C. albicans*. This combination of beneficial and harmful effects on the host has also been proposed for the role of bacterial pore-forming toxin during its interaction with macrophages. The toxin causes host cell membrane damage associated with *C. albicans* invasion, translocation through the barrier, and escape from phagocytes. Macrophages are essential for the control of disseminated *C. albicans*. Elimination of *C. albicans* is mediated by a combination of antimicrobial activity during phagocytosis. *C. albicans* can counteract these attempts by producing hyphae that induce pyroptosis, mechanically stretching and eventually disrupting the phagosomal membrane, triggering immune cell death (Tucey et al., 2018; Li et al., 2022). However, Candida hemolysin also induces NLRP3 activation, leading to an enhanced host-protective proinflammatory response in mononuclear phagocytes (Kasper et al., 2018). Thus, Candida hemolysin promotes immune evasion by acting as a classical virulence factor but also contributes to the antifungal immune response (Case et al., 2021). Their differential effects in oral, vaginal and systemic infections highlight the dual function of this toxin in the interactions between *C. albicans* and macrophages as classical virulence factors and virulent toxic factors in mucosal and systemic infections (Patterson et al., 2013).

Candida albicans mediates the macrophages immune response

Different forms and different parts of *Candida albicans* cause different immune responses

The ability of *C. albicans* to rapidly and reversibly switch between yeast and filamentous morphology is critical

to pathogenesis, and the dextrans of the yeast cell wall are mainly protected by epithelial components. The normal mechanism of yeast germination and cell shedding is that adequate exposure *via* dectin-1 results in permanently scarred β-dextrans, including phagocytosis and activated production of reactive oxygen species. Pathogens are also unable to activate dectin-1 in the absence of β-dextran exposure without cell detachment or subsequent exposure during filamentous growth. It is believed that (Hasebe et al., 2018), The form of *C. albicans* directly affects the ability of phagocytes to recognize fungi. The migration of macrophages to *C. albicans* depends on the glycosylation state of the fungal cell wall, which significantly slows the phagocytosis rate of aberrant glycosylated mutants adhering to the macrophage surface, as it is related to the recognition of PAMP by the PRR. In addition, macrophage phagocytosis was significantly faster in hyphae than in yeast cells, and the phagocytosis rate of *C. albicans* hyphae was also affected by spatial arrangement. *C. albicans* contacts macrophages more readily than yeast, and different forms of *C. albicans* elicit different immune responses in macrophages.

The effect of macrophages from different sources on *Candida albicans*

Macrophages present in tissues play an important role in controlling disseminated fungal infections. Insufficient accumulation of macrophages in the kidney leads to renal failure and death due to deficiency of the chemokine receptor CX3CR 1. In addition, patients with CX3CR 1 function impaired by a polymorphism are more susceptible to diffuse candidiasis, suggesting an important role of macrophages in the kidney against disseminated Candida infection (Diez-Orejas et al., 2018a). Hematopoietic stem cells and macrophage progenitors differentiate into macrophages to engulf *C. albicans* and produce pro-inflammatory cytokines *via* the TLR2 and MyD 88-dependent pathways.

The extracellular sterilization and antibacterial methods of the macrophages

Macrophages not only activate a number of signaling pathways to secrete antimicrobial substances that kill *C. albicans* intracellularly, but also attempt to kill *C. albicans* and inhibit its survival by extracellular means. Macrophages are activated after contact with *C. albicans*. They intercept and kill *C. albicans* by releasing extracellular traps (METs) based on the etosis principle, which trap *C. albicans* at the site of infection and prevent systemic infection. Extracellular vesicles (Evs) act as messengers between macrophages infected with *C. albicans* and uninfected macrophages. When macrophages are infected with *C. albicans*, they secrete more Evs, migrate extracellularly, and activate peripheral or circulating monocyte ERK 2 and β 38 enzymes, which are inflammatory factors that enhance the ability to kill *C. albicans* (Liu et al., 2019).

Effect of the M1 and M2-type macrophages on *Candida albicans*

Macrophages can be divided into classically activated inflammatory macrophages (M1) and alternatively activated anti-inflammatory macrophages (M2). M1 is polarized in an inflammatory environment to produce proinflammatory cytokines, whereas M2 is anti-inflammatory and contributes to tissue repair during wound healing. Bacterial endotoxin (lipopolysaccharide; LPS) is an effective factor in infection that induces M1 to produce higher levels of iNOS, TNF α, and IL -12p70, thereby determining the inflammatory T cell response. M2 can be converted into M1 macrophages after LPS stimulation to promote inflammation. It has been shown that heat-killing *C. albicans* (HKC) strongly suppresses LPS-induced IL -12p70 production in M2 macrophages (Zheng et al., 2013). *C. albicans* induces the production of the anti-inflammatory cytokine IL -35 in M2 and blocks the LPS-induced conversion of M2 to the M1 phenotype. During the resolution phase of infection and wound healing, M1 can be polarized to M2 in tissues. M2 produces lower levels of inflammatory cytokines but higher levels of anti-inflammatory cytokines and growth factors after HKC stimulation. However, sustained production of inflammatory cytokines induced by M1 may lead to persistent inflammation caused by excessive Th1 and Th17 responses. Although the immigration of numerous Th1 and Th17 cells into the inflamed tissue contributes to increased killing by macrophages, they may also cause tissue damage. Combating pathogen invasion and initiating tissue repair by increasing concentrations of growth factors and releasing anti-inflammatory cytokines into tissues is associated with M2. M2 also exhibits phenotypic and functional plasticity, such as LPS, a potent bioactive factor that can cause macrophage phenotype transition from M2 to M1.

Candida albicans mediates macrophages immune tolerance

C. albicans is present on the moist mucosal surfaces of most healthy individuals and does not cause disease, and this symbiotic presence is associated with host immune tolerance. There are two basic morphological growth forms of *C. albicans*, hyphae and yeast. Mycelia on the mucosal surface elicit an immune response, whereas the primary presence of yeast is associated with symbiotic presence on the mucosal surface and may be more effective in inducing immune tolerance. IL-34 is able to promote the conversion of M1 to M2, which may benefit the skin in establishing immune tolerance and wound healing (Diez-Orejas et al., 2018b). *C. albicans* can inhibit host inflammatory responses in the skin mucosa by inhibiting LPS-induced IL-12p70 production, while lower IL-12p70 production can avoid unnecessary Th1 responses to maintain immune tolerance, which may be one of the mechanisms by which

C. albicans achieves a successful symbiotic lifestyle without compromising host health (Shao et al., 2022). IL-12p70 is an important proinflammatory cytokine that determines Th1 polarization, inhibits LPS-induced IL-12p70 production, and may be a key mechanism of *C. albicans*-induced immune tolerance. During the clearance of infection that promotes wound healing, proper conversion of macrophages from the M1 to the M2 phenotype is critical to limit tissue inflammation and promote tissue healing. Maintaining the M2 phenotype is key to maintaining immune tolerance. *C. albicans* induces the expression of EBI3 in M 2 and blocks the conversion of M2 to M1 phenotype induced by LPS, which may also be one of the mechanisms by which *C. albicans* induces immune tolerance (Patel, 2022).

Candida albicans mediates macrophages immune escape

Traditionally, masking of fungal antigenic ligands has been viewed as a strategy of fungal immune evasion in invasive infections (Pellon et al., 2022). However, In the process of interaction between *C. albicans* and macrophages, it avoids the killing effect of macrophages by blocking the recognition by macrophages, inhibiting the maturation of phagosome or neutralizing the pH of phagosome, changing the properties of macrophages and inhibiting the sterilization, lytic output or non-lytic export pathway to change its morphology or metabolic reprogramming.

Blocking of macrophages recognition

C. albicans is ability to form biofilms and hyphae, produce hydrolytic enzymes and candidiasis. Although mucosal immunity is activated, the combination of increased abundance and virulence of this pathogenic organism leads to infection, first through the formation of mycelial associated toxins by colonizing *Candida albicans* cells (Deng et al., 2019). Clinically refractory *C. albicans* infections suggest that the physical structure of the biofilm impedes macrophage migration, limiting macrophage antimicrobial activity and making the biofilm a host for persistent infection. The *C. albicans* surface amyloid and human binding serum amyloid β-component (SAP) impair recognition by macrophages and inhibit the macrophage immune response. Svoboda et al. (2015) found that *C. albicans* can produce secreted aspartyl proteinase 2 (Sap2)-cleaving complement inhibitor (FH), reduce the amount of FH recognized by CR3 and CR4, and impair recognition and killing by macrophages. In inducing oxidative stress, *C. albicans* promotes β-mannosylation of cell wall components, reduces hydrophobicity on the cell surface thereby decreasing ERK1/2P levels in macrophages, promotes oxidation and TNF-α production, and increases resistance of the fungus to macrophages (Ibata-Ombetta et al., 2003).

Inhibition of phagosomal maturation or neutralizing phagosomal pH

C. albicans is recognized, endocytosed by macrophages, and then trapped in phagosomes. These phagosomes are remodeled to obtain antimicrobial substances and lysis enzymes, e.g., by membrane fusion to acidify the phagosomal lumen. For *C. albicans*, which is engulfed by macrophages, to survive, it must destroy the powerful bactericidal machinery in the phagolysosomes.

(1) Inhibition of phagosome maturation.

Type O-mannose masks the p-glucan in the inner layer of the cell wall and suppresses the recognition of dectin-1, which is involved in promoting phagosome maturation. Strains lacking O-mannose in the cell wall increase the ability of mature phagosomes to bind RabGTPase and inhibit the growth of phagocyte filaments. *C. albicans* slows phagosome maturation by hyphal elongation.

(2) *C. albicans* neutralizes the pH of phagosomes by physical disruption or metabolic reprogramming.

The importance of metabolism and nutrient availability in fungus-host interactions has been highlighted in recent years. Upon activation, immune cells and other host cells reshape their metabolism to meet the energy-demanding processes that generate an immune response. These include up-regulation of glucose uptake by macrophages and treatment by aerobic glycolysis. Candida, on the other hand, ADAPTS its metabolic pathways to normally hostile environments in the host, such as the lumen of the phagosome. Further understanding of metabolic interactions between host and fungal cells may lead to new/enhanced antifungal therapies to combat these infections (Pellon et al., 2022). *C. albicans* disrupts the integrity of phagosomal membranes through hyphal growth, communicates phagosomes with the cytoplasm, neutralizes phagosome pH, causes morphological changes in hyphelias, and promotes survival within hyphal cells. After phagocytosis of *C. albicans* by macrophages, genes involved in arginine biosynthesis are upregulated, and arginine is converted to urea and degraded to produce CO2 and NH3, neutralizing acidic conditions and promoting hyphal growth. At the same time, *C. albicans* can utilize pyruvate, α-ketone, glutaric acid and lactic acid as the main carbon sources to neutralize the acidic environment rapidly.

Change the macrophages properties

Normally, *C. albicans* is a commensal bacterium that is harmless to the skin and mucous membranes. *C. albicans* modulates the antimicrobial activity of macrophages by altering their properties. During *C. albicans* infection, macrophages synthesize nitric oxide via nitric oxide synthase (iNOS) and

kill invading pathogens. *C. albicans* can produce extracellular DNA enzymes that are thought to degrade DNA, a structural component of METs, to prevent death of Macrophages and cause M1 to M2 type conversion, thereby increasing *C. albicans* survival.

Dissolution or non-dissolved output pathway

The dissolution-release pathway is the process by which *C. albicans* causes death and rupture of macrophages through morphological and metabolic changes, releasing phagocytosed *C. albicans* and causing disseminated infection. The febrile pathways caused by hyphal growth, nutrient starvation, and cell death are responsible for the lysis and release of macrophages (Deng et al., 2019). *C. albicans* can utilize multiple carbon sources in the phagocytosis of macrophages to increase its resistance in the presence of glucose. Carbon sources can induce drug resistance to fluconazole, and *C. albicans* undergoes a continuous transcriptional reprogramming process after phagocytosis by phagocytes. At an early stage, activation of the gluconeogenesis pathway and fatty acid depletion result in starvation of cells, and the glycolysis pathway is restored when *C. albicans* is engulfed. During the interaction between *C. albicans* and macrophages, metabolic changes are triggered between them that can enhance the glycolytic pathway and lead to glucose competition. *C. albicans* relies on various carbon sources for its intracellular growth, but infected macrophages can survive only with the help of glucose in glycolysis. *C. albicans* rapidly consumes glucose, and macrophages are killed due to lack of energy supply.

Effect of *Candida albicans* virulence on macrophages

The morphological transition between yeast and hyphal forms of *C. albicans*, expression of cell surface adhesins and invasins, tropism, biofilm formation, phenotypic turnover, and secretion of hydrotolytic enzymes are considered virulence factors. The pathogenic yeast *C. albicans* was found to be coated with phospholimannose (PLM) consisting of a β-1,2-oligomannose site and phytoceramide. PLM-induced externalization of membrane phosphatidylserine, loss of mitochondrial integrity, and DNA fragmentation suggest that PLM promotes yeast survival by inducing macrophage death (Ibata-Ombetta et al., 2003).

Summary and outlook

Interaction of *C. albicans* with macrophages is an important immune system defense response to Candida disease associated with deep dissemination of Candida cells in humans. Despite the obvious efficiency of killing pathogens, macrophages fail to effectively control the disease process of candidiasis in severely damaged patients. The patients with low immunity, prolonged use of antibiotics and immunosuppressants may develop severe *C. albicans* infection. The development of drugs against the transformation of the *C. albicans* form and virulence-related target drugs has become an effective means for the accurate diagnosis and treatment of *C. albicans*. On the other hand, macrophage remodeling promotes macrophage redifferentiation from M2 to M1 phenotype, which promotes macrophage phagocytosis and lysosomal digestion of *C. albicans*. In conclusion, our study investigated the mechanism behind the escape of *C. albicans* hyphae from macrophages. Inhibition of hyphal escape can reduce the inflammatory response of macrophages to *C. albicans* infection and provides an accurate prevention, diagnosis, and treatment basis for *C. albicans* infection.

Data availability statement

The original contributions presented in this study are included in the article/supplementary material, further inquiries can be directed to the corresponding author/s.

Author contributions

SZ, AS, and XH designed the research study. MG, LS, and YH carried out the data analysis and processing. SZ prepared the original manuscript. AS and XH revised the manuscript and edited the final version. All authors read and approved the final manuscript.

Funding

This work was supported by the National Natural Science Foundation of China (grant nos. 82073452 and 81772161), the Natural Foundation Project of Shanghai Science and Technology Commission (grant no. 17ZR1426300), the Shanghai Tongji Hospital Clinical Research and Cultivation Key Project (grant no. ITJ[ZD]1903), the Shanghai General Hospital Integrated Traditional Chinese and Western Medicine Special Project (grant no. ZHYY-ZXYJHZX-202002), and the Shanghai Outstanding Young Medical Talent Training Funding Program.

Conflict of interest

The authors declare that the research was conducted in the absence of any commercial or financial relationships that could be construed as a potential conflict of interest.

Publisher's note

References

Alonso, M. F., Gow, N., Erwig, L. P., and Bain, J. M. (2017). Macrophage migration is impaired within *Candida albicans* biofilms. *J. Fungi* 3:31. doi: 10.3390/jof3030031

Arce Miranda, J. E., Baronetti, J. L., Sotomayor, C. E., and Paraje, M. G. (2019). Oxidative and nitrosative stress responses during macrophage-*Candida albicans* biofilm interaction. *Med. Mycol.* 57, 101–113. doi: 10.1093/mmy/myx143

Case, N. T., Duah, K., Larsen, B., Wong, C. J., Gingras, A. C., O'Meara, T. R., et al. (2021). The macrophage-derived protein PTMA induces filamentation of the human fungal pathogen *Candida albicans*. *Cell Rep.* 36:109584. doi: 10.1016/j.celrep.2021.109584

de Albuquerque, J., Banerjee, P. P., Castoldi, A., Ma, R., Zurro, N. B., Ynoue, L. H., et al. (2018). The role of AIRE in the immunity against *Candida albicans* in a model of human macrophages. *Front. Immunol.* 9:567. doi: 10.3389/fimmu.2018.00567

Deng, L., Li, W., He, Y., Wu, J., Ren, B., and Zou, L. (2019). Cross-kingdom interaction of *Candida albicans* and *Actinomyces viscosus* elevated cariogenic virulence. *Arch. Oral Biol.* 100, 106–112. doi: 10.1016/j.archoralbio.2019.02.008

Diez-Orejas, R., Feito, M. J., Cicuéndez, M., Casarrubios, L., Rojo, J. M., and Portolés, M. T. (2018a). Graphene oxide nanosheets increase *Candida albicans* killing by pro-inflammatory and reparative peritoneal macrophages. *Colloids Surf. B Biointerfaces* 171, 250–259. doi: 10.1016/j.colsurfb.2018.07.027

Diez-Orejas, R., Feito, M. J., Cicuéndez, M., Rojo, J. M., and Portolés, M. T. (2018b). Differential effects of graphene oxide nanosheets on *Candida albicans* phagocytosis by murine peritoneal macrophages. *J. Colloid Interface Sci.* 512, 665–673. doi: 10.1016/j.jcis.2017.10.104

Gantner, B. N., Simmons, R. M., and Underhill, D. M. (2005). Dectin-1 mediates macrophage recognition of *Candida albicans* yeast but not filaments. *EMBO J.* 24, 1277–1286. doi: 10.1038/sj.emboj.7600594

Godoy, P., Darlington, P. J., and Whiteway, M. (2022). Genetic screening of *Candida albicans* inactivation mutants identifies new genes involved in macrophage-fungal cell interactions. *Front. Microbiol.* 13:833655. doi: 10.3389/fmicb.2022.833655

Gonzalez-Lara, M. F., and Ostrosky-Zeichner, L. (2020). Invasive Candidiasis. *Semin. Respir. Crit. Care Med.* 41, 3–12. doi: 10.1055/s-0040-1701215

Hasebe, A., Saeki, A., Yoshida, Y., and Shibata, K. I. (2018). Differences in interleukin-1β release-inducing activity of *Candida albicans* toward dendritic cells and macrophages. *Arch. Oral Biol.* 93, 115–125. doi: 10.1016/j.archoralbio.2018.06.004

Henriques, M., and Williams, D. (2020). Pathogenesis and Virulence of *Candida albicans* and *Candida glabrata*. *Pathogens* 9:752. doi: 10.3390/pathogens9090752

Ibata-Ombetta, S., Idziorek, T., Trinel, P. A., Poulain, D., and Jouault, T. (2003). *Candida albicans* phospholipomannan promotes survival of phagocytosed yeasts through modulation of bad phosphorylation and macrophage apoptosis. *J. Biol. Chem.* 278, 13086–13093. doi: 10.1074/jbc.M210680200

Jiang, H. H., Zhang, Y. J., Sun, Y. Z., Qi, R. Q., Chen, H. D., and Gao, X. H. (2019). Cell wall mannoprotein of *Candida albicans* polarizes macrophages and affects proliferation and apoptosis through activation of the Akt signal pathway. *Int. Immunopharmacol.* 72, 308–321. doi: 10.1016/j.intimp.2019.03.032

Kasper, L., König, A., Koenig, P. A., Gresnigt, M. S., Westman, J., Drummond, R. A., et al. (2018). The fungal peptide toxin Candidalysin activates the NLRP3 inflammasome and causes cytolysis in mononuclear phagocytes. *Nat. Commun.* 9:4260. doi: 10.1038/s41467-018-06607-1

Klotz, S. A., Bradley, N., and Lipke, P. N. (2022). Blocking serum amyloid-P component from binding to macrophages and augmenting fungal functional amyloid increases macrophage phagocytosis of *Candida albicans*. *Pathogens* 11:1000. doi: 10.3390/pathogens11091000

König, A., Hube, B., and Kasper, L. (2020). The dual function of the fungal toxin Candidalysin during *Candida albicans*-macrophage interaction and virulence. *Toxins* 12:469. doi: 10.3390/toxins12080469

Li, X. V., Leonardi, I., Putzel, G. G., Semon, A., Fiers, W. D., Kusakabe, T., et al. (2022). Immune regulation by fungal strain diversity in inflammatory bowel disease. *Nature* 603, 672–678. doi: 10.1038/s41586-022-04502-w

Liu, Y., Ou, Y., Sun, L., Li, W., Yang, J., Zhang, X., et al. (2019). Alcohol dehydrogenase of *Candida albicans* triggers differentiation of THP-1 cells into macrophages. *J. Adv. Res.* 18, 137–145. doi: 10.1016/j.jare.2019.02.005

Lopes, J. P., and Lionakis, M. S. (2022). Pathogenesis and virulence of *Candida albicans*. *Virulence* 13, 89–121. doi: 10.1080/21505594.2021.2019950

Mao, X., Qiu, X., Jiao, C., Lu, M., Zhao, X., Li, X., et al. (2020). *Candida albicans* SC5314 inhibits NLRP3/NLRP6 inflammasome expression and dampens human intestinal barrier activity in Caco-2 cell monolayer model. *Cytokine* 126:154882. doi: 10.1016/j.cyto.2019.154882

Mavor, A. L., Thewes, S., and Hube, B. (2005). Systemic fungal infections caused by *Candida* species: Epidemiology, infection process and virulence attributes. *Curr. Drug Targets* 6, 863–874. doi: 10.2174/138945005774912735

Pappas, P. G., Lionakis, M. S., Arendrup, M. C., Ostrosky-Zeichner, L., and Kullberg, B. J. (2018). Invasive candidiasis. *Nat. Rev. Dis. Primers* 4:18026. doi: 10.1038/nrdp.2018.26

Patel, M. (2022). Oral Cavity and *Candida albicans*: Colonisation to the Development of Infection. *Pathogens* 11:335. doi: 10.3390/pathogens11030335

Patterson, M. J., McKenzie, C. G., Smith, D. A., da Silva, Dantas, A., Sherston, S., et al. (2013). Ybp1 and Gpx3 signaling in *Candida albicans* govern hydrogen peroxide-induced oxidation of the Cap1 transcription factor and macrophage escape. *Antioxid. Redox Signal.* 19, 2244–2260. doi: 10.1089/ars.2013.5199

Pellon, A., Begum, N., Sadeghi Nasab, S. D., Harzandi, A., Shoaie, S., and Moyes, D. L. (2022). Role of cellular metabolism during *Candida*-Host Interactions. *Pathogens* 11:184. doi: 10.3390/pathogens11020184

Pietrella, D., Pandey, N., Gabrielli, E., Pericolini, E., Perito, S., Kasper, L., et al. (2013). Secreted aspartic proteases of *Candida albicans* activate the NLRP3 inflammasome. *Eur. J. Immunol.* 43, 679–692. doi: 10.1002/eji.201242691

Rolo, J., Caixeirinho, P., Gomes-Ruivo, P., Gaspar, C., Fernandes, I., Palmeira-de-Oliveira, R., et al. (2020). Semen supports growth of *Candida albicans*: A putative risk factor for recurrence of vulvovaginal infections. *J. Obstet. Gynaecol. Res.* 46, 1893–1899. doi: 10.1111/jog.14367

Salvatori, O., Kumar, R., Metcalfe, S., Vickerman, M., Kay, J. G., and Edgerton, M. (2020). Bacteria modify *Candida albicans* hypha formation, microcolony properties, and survival within macrophages. *mSphere* 5:e00689-20. doi: 10.1128/mSphere.00689-20

Shao, T. Y., Haslam, D. B., Bennett, R. J., and Way, S. S. (2022). Friendly fungi: Symbiosis with commensal *Candida albicans*. *Trends Immunol.* 43, 706–717. doi: 10.1016/j.it.2022.07.003

Silao, F., Ryman, K., Jiang, T., Ward, M., Hansmann, N., Molenaar, C., et al. (2020). Glutamate dehydrogenase (Gdh2)-dependent alkalization is dispensable for escape from macrophages and virulence of *Candida albicans*. *PLoS Pathog.* 16:e1008328. doi: 10.1371/journal.ppat.1008328

Svoboda, E., Schneider, A. E., Sándor, N., Lermann, U., Staib, P., Kremlitzka, M., et al. (2015). Secreted aspartic protease 2 of *Candida albicans* inactivates factor H and the macrophage factor H-receptors CR3 (CD11b/CD18) and CR4 (CD11c/CD18). *Immunol. Lett.* 168, 13–21. doi: 10.1016/j.imlet.2015.08.009

Tucey, T. M., Verma, J., Harrison, P. F., Snelgrove, S. L., Lo, T. L., Scherer, A. K., et al. (2018). Glucose homeostasis is important for immune cell viability during candida challenge and host survival of systemic fungal infection. *Cell Metab.* 27, 988–1006.e7. doi: 10.1016/j.cmet.2018.03.019

Zheng, X. F., Hong, Y. X., Feng, G. J., Zhang, G. F., Rogers, H., Lewis, M. A., et al. (2013). Lipopolysaccharide-induced M2 to M1 macrophage transformation for IL-12p70 production is blocked by *Candida albicans* mediated up-regulation of EBI3 expression. *PLoS One* 8:e63967. doi: 10.1371/journal.pone.0063967

frontiers | Frontiers in Microbiology

TYPE Original Research
PUBLISHED 05 December 2022
DOI 10.3389/fmicb.2022.1001845

OPEN ACCESS

EDITED BY
Weihua Pan,
Shanghai Changzheng Hospital, China

REVIEWED BY
Xiaofang Li,
Chinese Academy of Medical Sciences and Peking Union Medical College, China
Yinggai Song,
First Hospital, Peking University, China
Shallu Kathuria,
National Centre for Disease Control (NCDC), India
Mohammad Asadullah Asadzadeh,
Kuwait University,Kuwait
Lalitha Gade,
Centers for Disease Control and Prevention (CDC), United States

*CORRESPONDENCE
Ying-Chun Xu
xycpumch@139.com
Xin Hou
houxinyffs@163.com

†These authors have contributed equally to this work and share first authorship

SPECIALTY SECTION
This article was submitted to Antimicrobials, Resistance and Chemotherapy, a section of the journal Frontiers in Microbiology

RECEIVED 24 July 2022
ACCEPTED 22 August 2022
PUBLISHED 05 December 2022

CITATION
Chen X-F, Zhang H, Jia X-M, Cao J, Li L, Hu X-L, Li N, Xiao Y-L, Xia F, Ye L-Y, Hu Q-F, Wu X-L, Ning L-P, Hsueh P-R, Fan X, Yu S-Y, Huang J-J, Xie X-L, Yang W-H, Li Y-X, Zhang G, Zhang J-J, Duan S-M, Kang W, Wang T, Li J, Xiao M, Hou X and Xu Y-C (2022) Antifungal susceptibility profiles and drug resistance mechanisms of clinical *Candida duobushaemulonii* isolates from China.
Front. Microbiol. 13:1001845.
doi: 10.3389/fmicb.2022.1001845

Antifungal susceptibility profiles and drug resistance mechanisms of clinical *Candida duobushaemulonii* isolates from China

Xin-Fei Chen[1,2,3†], Han Zhang[1,3†], Xin-Miao Jia[3,4†], Jin Cao[5], Li Li[6], Xin-Lan Hu[7], Ning Li[7], Yu-Ling Xiao[8], Fei Xia[9], Li-Yan Ye[10], Qing-Feng Hu[11], Xiao-Li Wu[12], Li-Ping Ning[13], Po-Ren Hsueh[14,15], Xin Fan[16], Shu-Ying Yu[1,3], Jing-Jing Huang[1,2,3], Xiu-Li Xie[1,3], Wen-Hang Yang[1,2,3], Ying-Xing Li[3,4], Ge Zhang[1,3], Jing-Jia Zhang[1,3], Si-Meng Duan[1,3], Wei Kang[1,3], Tong Wang[1,3], Jin Li[1,3], Meng Xiao[1,3], Xin Hou[17]* and Ying-Chun Xu[1,3]*

[1]Department of Laboratory Medicine, State Key Laboratory of Complex Severe and Rare Diseases, Peking Union Medical College Hospital, Chinese Academy of Medical Science and Peking Union Medical College, Beijing, China, [2]Graduate School, Chinese Academy of Medical Science and Peking Union Medical College, Beijing, China, [3]Beijing Key Laboratory for Mechanisms Research and Precision Diagnosis of Invasive Fungal Diseases, Beijing, China, [4]Medical Research Center, Peking Union Medical College Hospital, Chinese Academy of Medical Science and Peking Union Medical College, Beijing, China, [5]Jinling Hospital Institute of Clinical Laboratory Science, School of Medicine, Nanjing University, Nanjing, Jiangsu, China, [6]Department of Dermatology, Hua Shan Hospital, Fudan University, Shanghai, China, [7]Department of Laboratory Medicine, Fujian Provincial Hospital, Fuzhou, China, [8]Department of Laboratory Medicine, West China Hospital, Sichuan University, Chengdu, China, [9]Department of Laboratory Medicine, Ruian People's Hospital, Wenzhou, China, [10]Department of Laboratory Medicine, The First Medicine Center, Chinese PLA General Hospital, Beijing, China, [11]Department of Laboratory Medicine, Zhejiang Provincial People's Hospital, Hangzhou, China, [12]Department of Laboratory Medicine, The People's Hospital of Liaoning Province, Shenyang, China, [13]Department of Laboratory Medicine, No.908 Hospital of Joint Logistics Support Force, Nanchang, China, [14]Department of Laboratory Medicine and Internal Medicine, National Taiwan University Hospital, National Taiwan University College of Medicine, Taipei, Taiwan, [15]Department of Laboratory Medicine and Internal Medicine, China Medical University Hospital, China Medical University, Taichung, Taiwan, [16]Department of Infectious Diseases and Clinical Microbiology, Beijing Institute of Respiratory Medicine and Beijing Chao-Yang Hospital, Capital Medical University, Beijing, China, [17]Department of Laboratory Medicine, Peking University Third Hospital, Beijing, China

Candida duobushaemulonii, type II *Candida haemulonii* complex, is closely related to *Candida auris* and capable of causing invasive and non-invasive infections in humans. Eleven strains of *C. duobushaemulonii* were collected from China Hospital Invasive Fungal Surveillance Net (CHIF-NET) and identified using matrix-assisted laser desorption/ionization time-of-flight mass spectrometry (MALDI-TOF), VITEK 2 Yeast Identification Card (YST), and internal transcribed spacer (ITS) sequencing. Whole genome sequencing of *C. duobushaemulonii* was done to determine their genotypes. Furthermore, *C. duobushaemulonii* strains were tested by Sensititre YeastOne™ and Clinical and Laboratory Institute (CLSI) broth microdilution panel for antifungal susceptibility. Three *C. duobushaemulonii* could not be identified by VITEK

2. All 11 isolates had high minimum inhibitory concentrations (MICs) to amphotericin B more than 2μg/ml. One isolate showed a high MIC value of ≥64μg/ml to 5-flucytosine. All isolates were wild type (WT) for triazoles and echinocandins. *FUR1* variation may result in *C. duobushaemulonii* with high MIC to 5-flucytosine. *Candida duobushaemulonii* mainly infects patients with weakened immunity, and the amphotericin B resistance of these isolates might represent a challenge to clinical treatment.

KEYWORDS

***Candida duobushaemulonii*, antifungal susceptibility, *FUR1*, whole genome sequence, drug resistance mechanisms**

Introduction

Candida duobushaemulonii belongs to the *Candida haemulonii* species complex, along with *Candida haemulonii* and *Candida haemulonii* var. *vulnera*. Yeasts belonging to this complex are closely related to the notorious *Candida auris*, which has attracted global attention with multi-drug resistant and widely disseminating (Du et al., 2020). *Candida duobushaemulonii* was initially classified as type II of *Candida haemulonii* complex. It was clearly identified as *C. duobushaemulonii* in 2012 (Cendejas-Bueno et al., 2012). The conventional panels used in routine microbiology laboratories often misidentify these species, making it hard to identify accurately (Fang et al., 2016; Ambaraghassi et al., 2019; Frias-De-Leon et al., 2019). Therefore, their actual incidence and global prevalence may be underestimated.

A retrospective study found that *C. duobushaemulonii* was first isolated in foot ulcers in 1996, where it was recovered from the toenail of a patient from Bizkaia, Spain (Jurado-Martin et al., 2020). The first isolate in China was collected under the China Hospital Invasive Fungal Surveillance Net (CHIF-NET) project in 2010 (Hou et al., 2016a). However, as an emerging species, it has been reported that fluconazole, amphotericin B, and echinocandins non-wild-type (non-WT) *C. duobushaemulonii* have been identified (Cendejas-Bueno et al., 2012), and the mechanism of *C. duobushaemulonii* with high MIC for antifungal drugs is still unclear.

Although currently reported cases of *C. duobushaemulonii* in China are few, hospital outbreaks of *C. duobushaemulonii* have been reported (Gade et al., 2020). Therefore, we conducted antifungal drug susceptibility testing and whole-genome sequencing of *C. duobushaemulonii* in China for 8 years. The aims were to confirm whether *C. duobushaemulonii* had broken out in China, and to discover the underlying mechanism of its resistance to antifungal drugs.

Materials and methods

Ethics statement

This study was approved by the Human Research Ethics Committee of Peking Union Medical College Hospital (No. S-263). Written informed consent was obtained from all the patients who participated in this study, aimed at culturing and studying the isolates obtained from them for scientific research.

Fungal isolates

During the period from 2010 to 2017 (Table 1), 11 *C. duobushaemulonii* isolates were collected from nine different hospitals in eight provinces under the CHIF-NET. These isolates were mainly of invasive fungal infection specimens. Strains isolated before 2015 were identified and their susceptibility tested in our previous article (Hou et al., 2016a).

Species identification

All *C. duobushaemulonii* were identified at the species level using Autof-MS 1000 (Autobio, Zhengzhou, China) and Vitek MS (bioMérieux, Marcy l'Étoile, France), and confirmed by sequencing the rDNA internal transcribed spacer region (ABI 3730XL, Thermo Fisher Scientific, Cleveland, OH, United States). PCR and sequencing of the amplicons were performed using the former primers (Zhang et al., 2014; Hou et al., 2016b). All 11 isolates were also re-identified using the Vitek 2 YST Card by VITEK 2 (9.02 version, bioMérieux, Marcy l'Etoile, France) following the manufacturer's instructions.

DNA extraction and whole-genome sequencing

The whole genomic DNA of *C. duobushaemulonii* was extracted by the sodium dodecyl sulfate (SDS) method (Lim et al., 2016). The DNA library was constructed using NEBNext® Ultra™, following the manufacturer's instructions. Agilent 2100 Bioanalyzer was used for quality confirmation. Whole genome of *C. duobushaemulonii* was sequenced using Illumina NovaSeq 6000 at Beijing Novogene Bioinformatics Technology Co., Ltd. Illumina reads from this study were deposited at National Center for Biotechnology Information (NCBI) under BioProject

TABLE 1 List of isolates included in the study.

Strain	Age/Gender	Year	Source of the isolate	Clinical diagnosis	Vitek 2 (Score)	Mating type
F4468	59/male	2010	Blood	Abdominal cavity infection	*Candida duobushaemulonii* (93%)	α
F4458	36/female	2012	Blood	Breast cancer	Low Discrimination	α
F4464	56/male	2012	Blood	Common bile duct	*Candida duobushaemulonii* (95%)	α
F4490	78/male	2014	Venous catheter	Lung infection	*Candida duobushaemulonii* (88%)	α
F4566	57/female	2015	Blood	moderately severe Acute pancreatitis	*Candida duobushaemulonii* (96%)	α
F4572	45/male	2015	Ascitic fluid	HBV-related liver cirrhosis	*Candida duobushaemulonii* (97%)	α
F4586	36/female	2016	Puncture fluid	Acute myeloid leukemia	*Candida haemulonii* (87%)	α
F4608	48/male	2016	BALF[a]	Lung infection	Unidentified	α
F4560	70/male	2016	Tissue	pyogenic Osteomyelitis	*Candida duobushaemulonii* (88%)	α
F4616	51/female	2017	Tissue	Granulomatous angiitis	*Candida duobushaemulonii* (95%)	α
F7396	57/male	2017	Catheter	Cerebral hemorrhage	*Candida duobushaemulonii* (97%)	α

[a]BALF, bronchoalveolar lavage fluid.

PRJNA883504. In addition, we downloaded the genome data of *C. duobushaemulonii* from the NCBI SRA database as described by Gade et al. (2020).

Genome variation, phylogenetic, and population genetic analyses

Paired-end sequences with greater than 100X coverage were used for Bioinformatics analysis. *Candida duobushaemulonii* B09383 (GenBank accession number PKFP00000000.1) was used as the reference genome for analysis (Chow et al., 2018). We used BWA 0.5.9 and SAMtools and bcftools 0.1.19 to analyze single nucleotide polymorphism (SNP) and insertion-deletion (indel) (Li and Durbin, 2009a; Li et al., 2009b). SNP and Indel function annotation analysis were used snpeff 4.3 (Cingolani et al., 2012). Phylogenetic tree was constructed using RAxML 8.2.12 based on 1,000 bootstrap replicates by maximum likelihood method to investigate the *C. duobushaemulonii* genetic relationships (Stamatakis, 2014). The genome-wide nucleotide diversity (Pi) and the average Tajima's D estimate were calculated by DNASP 6 (Rozas et al., 2017).

Chromosome structure analysis and mating type analysis

We used YMAP to perform Copy Number Variation (CNV) analysis of *C. duobushaemulonii* (Abbey et al., 2014). We checked the BAM (Binary Alignment Map) file of *C. duobushaemulonii* genome by SAMtools to determine the coverage depth of the region where the MTLα gene is located, and determine the mating type of *C. duobushaemulonii*.

Broth microdilution antifungal susceptibility testing

Candida duobushaemulonii strains were tested by Sensititre YeastOne (Thermo Scientific, Cleveland, OH, United States). In addition, the standard antifungal susceptibility testing was performed according to CLSI M27-A3. Essential agreement (EA) is defined as the percent of all Sensititre™ YeastOne™ MIC results within one 2-fold dilution of the CLSI MIC result. *Candida krusei* ATCC 6258 and *Candida parapsilosis* ATCC 22019 were selected for quality control. The epidemiological cutoff values (ECV) and clinical breakpoints of antifungals against *C. duobushaemulonii in vitro* have been established by the CLSI (CLSI, 2020). Among them, fluconazole MICs of greater than 32 μg/ml is considered as non-WT for *C. duobushaemulonii* and *C. auris*. Flucytosine MIC values (≥32 μg/ml) were interpreted according to the CLSI document M27-S3 (CLSI, 2008). In addition, MIC of ≥2 μg/ml was used for interpreting "resistance" of amphotericin B (Pfaller et al., 2012).

Identification of variations associated with high MICs for *Candida duobushaemulonii*

We analyzed the mutations in *ERG11*, *FUR1*, and other genes of interest in the pathways related to sterol metabolism and 5-flucytosine metabolism (Supplementary Table S1; Arendrup and Patterson, 2017; Berkow and Lockhart, 2017).

Review of *Candida duobushaemulonii* infections reported in PubMed

This literature review considered the available data regarding the susceptibility of the *C. duobushaemulonii* species to antifungals. The literature search was performed on June 26, 2022, using the following three databases: PubMed,[1] Web of Science,[2] and Embase.[3] The terms "*Candida duobushaemulonii*" were entered in the category of "Title/Abstract" in the PubMed Advanced Search Builder, and "TS = (*Candida duobushaemulonii*)" was entered in the Web of Science databases. The search in Embase was conducted in the advanced search area, including the terms "'*Candida duobushaemulonii*': ab,ti.."

Results

Isolates information

Of all 11 cases, seven were male and four were female, with an average age of 54 years. Among the specimens, blood specimens accounted for four patients, tissue culture specimens for two patients, bronchoalveolar lavage fluid (BALF) culture specimens, ascitic fluid, catheter, venous catheter, and puncture fluid specimens for one patient, respectively (Table 1). The patients belonged to the following departments: medicine department (45.5%; 5/11), surgery department (45.5%; 5/11), and emergency intensive care unit (9.1%; 1/11).

Species identification of *Candida duobushaemulonii* using MALDI-TOF, ITS sequencing and Vitek 2

All 11 clinical isolates were identified as *C. duobushaemulonii* by the Autof MS 1000 and Vitek MS. The ITS sequences of the study isolates exhibited over 99.5% identity to the corresponding ITS sequences of the reference *C. duobushaemulonii* CBS7798^T isolates. For Vitek 2 system, eight *C. duobushaemulonii* could be identified accurately, one could not be identified, one identified with low discrimination and the remaining one was misidentified as *C. haemulonii* (score = 87%; Table 1).

Phylogenetic relationships and genetic diversity among *Candida duobushaemulonii*

Candida duobushaemulonii isolated in China shows no clustering distribution, and its evaluation did not exhibit clustered outbreaks (Figure 1). Based on the number of SNPs that differ between the Chinese strains and the international strains with a very little difference, it can be seen that the evolution rate of *C. duobushaemulonii* is very slow. The average pairwise distance between *C. duobushaemulonii* isolates was 700 SNPs (range: 78–1,271). The average number of nucleotides is close to the previously reported average (Gade et al., 2020). All strains in the phylogenetic tree can be divided into two clades (Figure 1). The first clade includes strains isolated from China, the United States, Guatemala, Venezuela, and Panama. The second clade includes strains isolated from China, the United States, Guatemala, Colombia, and Panama. The strains around the world presented a scattered distribution. Genome-wide diversity estimates show reduced polymorphism in *C. duobushaemulonii* (Pi = 0.24013), but the average Tajima's D estimate was −0.89987 expected population expansion.

Chromosome variation and mating type

Analysis of large fragments of *C. duobushaemulonii* chromosomes showed neither copy number variation nor aneuploidy in genome (Supplementary Figure S1). All *C. duobushaemulonii* isolates were mating type alpha.

Antifungal susceptibility

The quality control strains (*Candida krusei* ATCC 6258 and *Candida parapsilosis* ATCC 22019) showed MICs within the expected ranges. Aggregated MIC distributions of nine antifungal agents of *C. duobushaemulonii* isolates by YeastOne™ are shown in Table 2. All strains were WT to fluconazole, voriconazole, itraconazole, posaconazole, caspofungin, anidulafungin, and micafungin. MIC of 5-flucytosine for one strain was >64 μg/ml, while that of the remaining strains were all less than 0.12 μg/ml. All the 11 isolates tested showed high amphotericin B MICs (MIC ≥4 μg/ml).

Agreement between the CLSI method and sensititre YeastOne™

The EA values of the MICs between the CLSI method and YeastOne™ for most of the antifungal drugs tested were > 90%. 100% EA values were obtained for amphotericin B and 5-flucytosine. EA values for anidulafungin and micafungin were 36.4 (4/11) and 27.3% (3/11), respectively (Supplementary Table S2).

Potential variation linked to 5-flucytosine and amphotericin B resistance

Compared with the reference genome of B09383, which is sensitive to azoles and echinocandins, we found that the

1 https://pubmed.ncbi.nlm.nih.gov
2 https://webofknowledge.com
3 https://www.embase.com

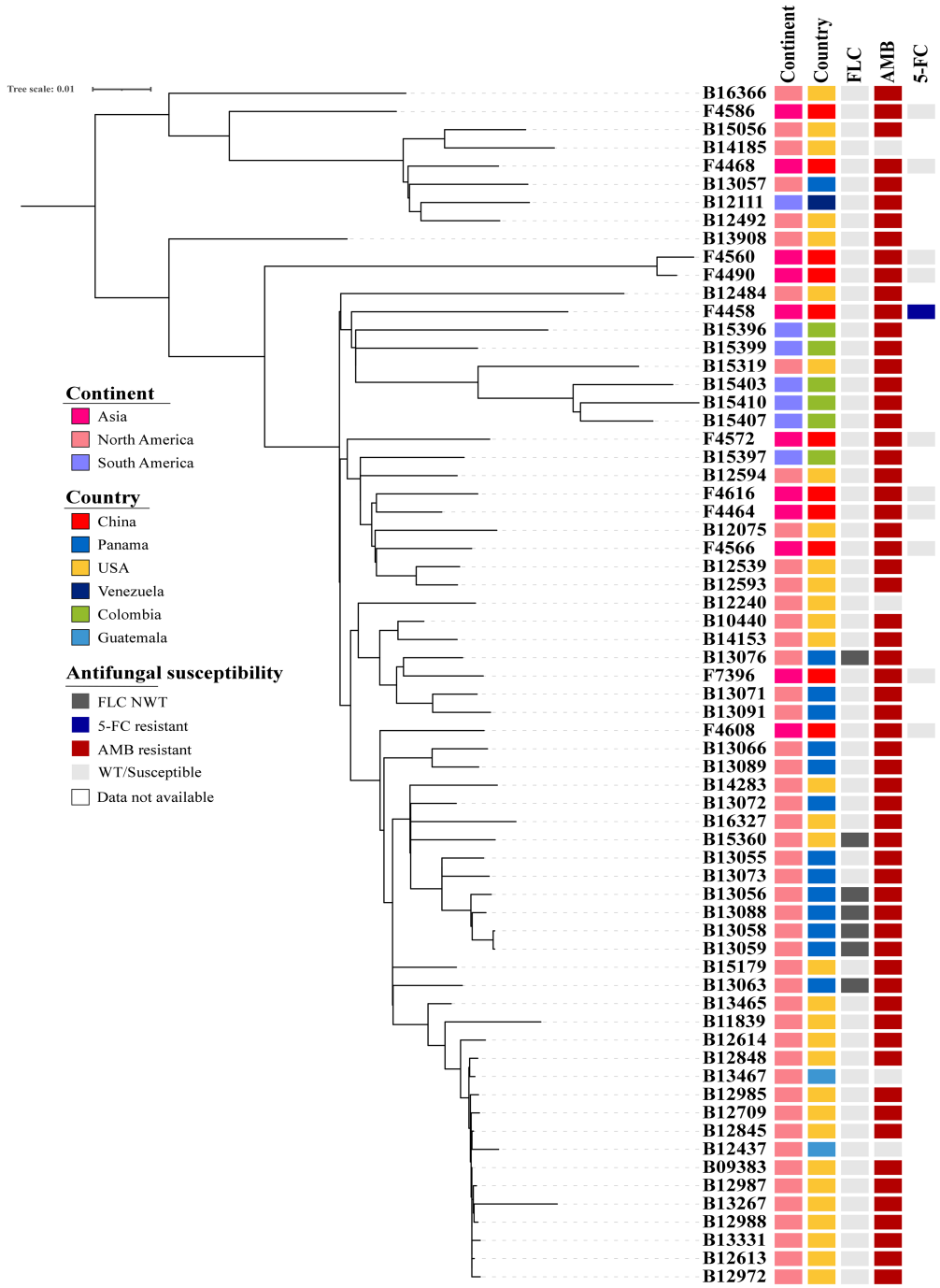

FIGURE 1
Phylogenetic tree of *Candida duobushaemulonii*. The phylogenetic tree was constructed with RAxML using the maximum likelihood method based on 8,117 SNPs. Phylogenetic tree detailing susceptibility to fluconazole (FLC), amphotericin B (AMB), and 5-flucytosine (5-FC).

amphotericin B-resistant *C. duobushaemulonii* isolated from China shows unique variation. We found that F4490 and F4560 have a novel mutation (V907A) in the *HMG1* gene and F4468 and F4586 has a previously reported mutation of S54N. In the *ERG20* gene, we found two novel mutations, K347N in F4468 and M101T in F4608. In the *UPC2* gene, both F4490 and F4608 possess A100T mutation. Interestingly, we discovered a novel mutation in the initiation codon (ATG-->ATA) of *FUR1* gene in a strain (F4458) with high MIC for 5-flucytosine (Table 2). In addition, it is interesting that we found that seven strains carried A626Y, T637I or P1042A substitutions in FKS1p and V30M，A485V and/or H352R in FKS2p. However, all strains were WT to echinocandins (Supplementary Table S1).

TABLE 2 Epidemiological cutoff values (ECV) of nine antifungal agents based on aggregated minimum inhibitory concentration distributions for *C. duobushaemulonii*.

	MIC (μg/ml)												MIC_{50}	MIC_{90}	Range	Mode[a]	ECV (μg/ml)[b]
	0.015	0.03	0.06	0.12	0.25	0.5	1	2	4	8	>8	>64					
Fluconazole						1	1	6	3				2	4	0.5–4	2	≥32
Voriconazole	3	4	2	2									0.03	0.12	0.015–0.12	0.03	≥0.5
Itraconazole		3	6	1	2								0.06	0.12	0.03–0.25	0.06	≥1
Posaconazole	8	1	2										0.015	0.06	0.015–0.06	0.015	≥1
Caspofungin	7	3	1										0.015	0.03	0.015–0.06	0.015	≥0.25
Micafungin	1	6	4										0.03	0.06	0.015–0.06	0.015	≥0.5
Anidulafungin	2	2	4	3									0.06	0.12	<0.015 to 0.12	0.06	≥1
5-flucytosine			10									1	<0.06	<0.06	<0.06 to >64	0.06	NA
Amphotericin B									3	5	3		8	>8	4 to >8	>8	NA

[a]Mode: Most frequent MIC.
[b]Calculated ECVs comprising ≥ 95% of the statistically modeled MIC population.

Literature review

Relatively limited data of 15 articles on antifungal susceptibility information for *C. duobushaemulonii* were reviewed. Some strains exhibited high MICs to fluconazole alone or to all azoles, and carried varation in Erg11p (Gade et al., 2020). In addition, there are three research reported emergence of echinocandin-resistant *C. duobushaemulonii*. To date there has been only one report on emergence of flucytosine-resistant *C. duobushaemulonii* strains (Supplementary Table S2).

Discussion

Candida duobushaemulonii, belongs to type II *Candida haeumlonii* complex, is relative of *C. auris* and *Candida pseudohaemulonii*. Literature reveals that *C. duobushaemulonii* was wrongly identified as *C. haemulonii, Candida intermedia*, and *Debaryomyces hansenii* (Desnos-Ollivier et al., 2008; Fang et al., 2016; Jurado-Martin et al., 2020). Previous studies have also shown that the identification ability of MALDI-TOF needs to be improved (Hou et al., 2016a). In the present study, although ITS sequencing, Autof MS 1000, and Vitek MS system have achieved good identification results, but three *C. duobushaemulonii* strains could not be identified by the Vitek 2 Compact system, which database includes *C. auris*, *C. duobushaemulonii*, and *C. haemulonii* var. *vulnera*. Considering, MALDI-TOF and ITS sequencing techniques are not all available in routine microbiology laboratories and *C. duobushaemulonii* actual incidence might be underestimated.

One case of hospital transmission of *C. duobushaemulonii* has been reported (Gade et al., 2020). Therefore, we conducted a genetic relationship analysis of *C. duobushaemulonii* isolated from China. We found that there was no obvious hospital infection transmission in China. However, considering the low isolation rate of *C. duobushaemulonii* in China, a large data sample is needed for analysis. In the overall genome evolution, the average SNP of *C. duobushaemulonii* is similar to that described by Gade et al. (2020).

In the drug susceptibility test, Gade *et al* reported that only 12.7% (7/55) strain as non-WT to fluconazole, and the MICs of these strains ranged from 64 to 256 μg/ml, with six isolates from Panama and one isolate from Texas, United States (Gade et al., 2020). De Almeida *et al* found that four *C. duobushaemulonii* isolated in Brazil has high MICs to azole and amphotericin B (de Almeida et al., 2016). Ramos *et al* has been reported echinocandins-resistance strains isolated in Brazil (Ramos et al., 2022). Regretfully, previous studies lacked 5-flucytosine antifungal drug sensitivity and only 18.2% (2/11) *C. duobushaemulonii* tested were 5-flucytosine-resistance (Cendejas-Bueno et al., 2012; de Almeida et al., 2016; Ramos et al., 2022). In the literature review, we can see that despite the low isolation rate of *C. duobushaemulonii*, strains resistant to azoles, echinocandins, amphotericin B, or 5-flucytosine have been emerging. However, our research found that all *C. duobushaemulonii* are WT to all azoles. Although there were seven isolates have missense mutations in the *FKS1* and *FKS2* genes, all strains were WT to echinocandins. In addition, our study might be the first to report the high MIC of 5-flucytosine for a strain isolated from China (MIC >64 μg/ml). All strains were with high MIC range to amphotericin B (4 to >8 μg/ml), which is consist with previous reports of *C. duobushaemulonii* high MIC to

amphotericin B (Ramos et al., 2022). Although 5-flucytosine and amphotericin B lack the interpretation breakpoint, *C. duobushaemulonii* is notable for the high MICs of 5-flucytosine and amphotericin B.

Compared with *C. auris*, *C. duobushaemulonii* fails to attract the attention of the whole world. *C. duobushaemulonii* is resistant to amphotericin B and 5-flucytosine, but the resistance mechanism is not well understood. In our study, there is no missense mutation in the common drug resistance gene *ERG11*, and aneuploidy and multiple copies were also not found in *C. duobushaemulonii*, which may be different from that in *C. auris* and *C. haemulonii*, with a quite different resistance mechanism as reported previously (Gade et al., 2020). *Candida duobushaemulonii* not only shows high MIC of 5-flucytosine, but also shows high MIC of amphotericin B. For 5-flucytosine, there is a missense mutation G3A (M1I) in the *FUR1* gene in the drug-resistant strains. This mutation is a completely new site and has not been reported. In addition, the resistance mechanism of amphotericin B is also worthy of attention. The mechanism of *C. duobushaemulonii* with high MIC to amphotericin B remains to be elusive. Although we found mutations involving sterol synthesis pathway genes in five strains, there were still six strains without mutations. In literature review, only 11.1% (11/99) *C. duobushaemulonii* had a lower amphotericin B MIC (<4 μg/ml). In addition, Carolus et al. founded the cell membrane sterols profile of *C. duobushaemulonii* was similar to amphotericin B-resistant species with mutations in *ERG2, ERG3*, *ERG6*, and *ERG11* (Silva et al., 2020). Thus, *C. duobushaemulonii* maybe possess high MIC to amphotericin B. Our study is similar to the previous studies in terms of shortcomings. Due to the lack of clinical treatment information, the correlation between the non-WT *C. duobushaemulonii* and the clinical treatment and prognosis needs further study.

In conclusion, the emergence of *C. duobushaemulonii*, a rare amphotericin B, and 5-flucytosine resistant fungus, is a potential threat. The phenotype of *C. duobushaemulonii* resistant to 5-flucytosine might be due to the variations in *FUR1*. Although the invasive infection of *C. duobushaemulonii* is very rare, it still needs our attention due to its drug resistance. Due to the lack of clear clinical treatment data, it is necessary to study *in vitro* the relationship between drug resistance and clinical treatment effect in the future.

Data availability statement

The whole genome sequence raw reads presented in the study are deposited in the NCBI, BioProject PRJNA883504.

Ethics statement

Written informed consent was not obtained from the individual(s) for the publication of any potentially identifiable images or data included in this article.

Author contributions

X-FC, HZ, and X-MJ conceived and designed the experiment. JC, LL, X-LH, NL, Y-LX, FX, L-YY, Q-FH, X-LW, L-PN provided isolates. X-FC, HZ, X-MJ, XF, XH, S-YY, J-JH, W-HY, X-LX, Y-XL, GZ, J-JZ, S-MD, WK, TW, and JL performed the experiments. X-FC, HZ, and X-MJ analyzed the data and wrote the manuscript. MX, Y-CX, XH, and P-RH revised the manuscript. All authors contributed to the article and approved the submitted version.

Funding

This work was supported by the National Natural Science Foundation of China (82002178), National High Level Hospital Clinical Research Funding (2022-PUMCH-B-074), CAMS Innovation Fund for Medical Sciences (2021-I2M-1-038 and 2021-I2M-1-044), and Beijing Key Clinical Specialty for Laboratory Medicine-Excellent Project (No. ZK201000).

Acknowledgments

The authors thank all the hospitals involved in the CHIF-NET study and Vladimir Gritsenko for his technical help in YMAP.

Conflict of interest

The authors declare that the research was conducted in the absence of any commercial or financial relationships that could be construed as a potential conflict of interest.

The reviewer XL declared a shared affiliation with the authors X-FC, HZ, X-MJ, S-YY, J-JH, X-LX, W-HY, Y-XL, GZ, J-JZ, S-MD, WK, TW, JL, MX, and Y-CX to the handling editor at the time of review.

Publisher's note

Supplementary material

The Supplementary material for this article can be found online at: https://www.frontiersin.org/articles/10.3389/fmicb.2022.1001845/full#supplementary-material

SUPPLEMENTARY FIGURE S1
No obvious copy number variation in *Candida duobushaemulonii*.

References

Abbey, D. A., Funt, J., Lurie-Weinberger, M. N., Thompson, D. A., Regev, A., Myers, C. L., et al. (2014). YMAP: a pipeline for visualization of copy number variation and loss of heterozygosity in eukaryotic pathogens. *Genome Med.* 6:100. doi: 10.1186/s13073-014-0100-8

Ambaraghassi, G., Dufresne, P. J., Dufresne, S. F., Vallieres, E., Munoz, J. F., Cuomo, C. A., et al. (2019). Identification of *Candida auris* by use of the updated Vitek 2 yeast identification system, version 8.01: a multilaboratory evaluation study. *J. Clin. Microbiol.* 57:e00884-19. doi: 10.1128/JCM.00884-19

Arendrup, M. C., and Patterson, T. F. (2017). Multidrug-resistant *Candida*: epidemiology, molecular mechanisms, and treatment. *J. Infect. Dis.* 216, S445–S451. doi: 10.1093/infdis/jix131

Berkow, E. L., and Lockhart, S. R. (2017). Fluconazole resistance in *Candida* species: a current perspective. *Infect. Drug Resist.* 10, 237–245. doi: 10.2147/IDR.S118892

Cendejas-Bueno, E., Kolecka, A., Alastruey-Izquierdo, A., Theelen, B., Groenewald, M., Kostrzewa, M., et al. (2012). Reclassification of the *Candida haemulonii* complex as *Candida haemulonii* (*C. haemulonii* group I), *C. duobushaemulonii* sp. nov. (*C. haemulonii* group II), and *C. haemulonii var. vulnera* var. nov.: three multiresistant human pathogenic yeasts. *J. Clin. Microbiol.* 50, 3641–3651. doi: 10.1128/JCM.02248-12

Chow, N. A., Gade, L., Batra, D., Rowe, L. A., Juieng, P., Loparev, V. N., et al. (2018). Genome sequence of the amphotericin B-resistant *Candida duobushaemulonii* strain B09383. *Genome Announc.* 6:e00204-18. doi: 10.1128/genomeA.00204-18

Cingolani, P., Platts, A., Wang le, L., Coon, M., Nguyen, T., Wang, L., et al. (2012). A program for annotating and predicting the effects of single nucleotide polymorphisms, SnpEff: SNPs in the genome of Drosophila melanogaster strain w1118; iso-2; iso-3. *Flying* 6, 80–92. doi: 10.4161/fly.19695

CLSI (2008). *Reference method for broth dilution anti fungal susceptibility testing of yeasts, third informational supplement. CLSI document M27-S3. 3rd Edn.* Wayne, PA: Clinical and Laboratory Standards Institute.

CLSI (2020). *Epidemiological Cutoff Values for Antifungal Susceptibility Testing. CLSI document M59. 3rd Edn.* Wayne, PA: Clinical and Laboratory Standards Institute.

de Almeida, J. N., Assy, J. G. P. L., Levin, A. S., del Negro, G. M. B., Giudice, M. C., Tringoni, M. P., et al. (2016). *Candida haemulonii* complex species, Brazil, January 2010-march 2015. *Emerg. Infect. Dis.* 22, 561–563. doi: 10.3201/eid2203.151610

Desnos-Ollivier, M., Ragon, M., Robert, V., Raoux, D., Gantier, J. C., and Dromer, F. (2008). *Debaryomyces hansenii* (*Candida famata*), a rare human fungal pathogen often misidentified as *Pichia guilliermondii* (*Candida guilliermondii*). *J. Clin. Microbiol.* 46, 3237–3242. doi: 10.1128/JCM.01451-08

Du, H., Bing, J., Hu, T., Ennis, C. L., Nobile, C. J., and Huang, G. (2020). *Candida auris*: epidemiology, biology, antifungal resistance, and virulence. *PLoS Pathog.* 16:e1008921. doi: 10.1371/journal.ppat.1008921

Fang, S. Y., Wei, K. C., Chen, W. C., Lee, S. J., Yang, K. C., Wu, C. S., et al. (2016). Primary deep cutaneous candidiasis caused by *Candida duobushaemulonii* in a 68-year-old man: the first case report and literature review. *Mycoses* 59, 818–821. doi: 10.1111/myc.12540

Frias-De-Leon, M. G., Martinez-Herrera, E., Acosta-Altamirano, G., Arenas, R., and Rodriguez-Cerdeira, C. (2019). Superficial candidosis by *Candida duobushaemulonii*: an emerging microorganism. *Infect. Genet. Evol.* 75:103960. doi: 10.1016/j.meegid.2019.103960

Gade, L., Munoz, J. F., Sheth, M., Wagner, D., Berkow, E. L., Forsberg, K., et al. (2020). Understanding the emergence of multidrug-resistant candida: using whole-genome sequencing to describe the population structure of *Candida haemulonii* species complex. *Front. Genet.* 11:554. doi: 10.3389/fgene.2020.00554

Hou, X., Xiao, M., Chen, S. C., Wang, H., Cheng, J. W., Chen, X. X., et al. (2016a). Identification and antifungal susceptibility profiles of *Candida haemulonii* species complex clinical isolates from a multicenter study in China. *J. Clin. Microbiol.* 54, 2676–2680. doi: 10.1128/JCM.01492-16

Hou, X., Xiao, M., Chen, S. C., Wang, H., Zhang, L., Fan, X., et al. (2016b). Sequencer-based capillary gel electrophoresis (SCGE) targeting the rDNA internal transcribed spacer (ITS) regions for accurate identification of clinically important yeast species. *PLoS One* 11:e0154385. doi: 10.1371/journal.pone.0154385

Jurado-Martin, I., Marcos-Arias, C., Tamayo, E., Guridi, A., de Groot, P. W. J., Quindos, G., et al. (2020). *Candida duobushaemulonii*: an old but unreported pathogen. *J. Fungi* 6, 374–384. doi: 10.3390/jof6040374

Li, H., and Durbin, R. (2009a). Fast and accurate short read alignment with burrows-wheeler transform. *Bioinformatics* 25, 1754–1760. doi: 10.1093/bioinformatics/btp324

Li, H., Handsaker, B., Wysoker, A., Fennell, T., Ruan, J., Homer, N., et al. (2009b). The sequence alignment/map format and SAMtools. *Bioinformatics* 25, 2078–2079. doi: 10.1093/bioinformatics/btp352

Lim, H. J., Lee, E. H., Yoon, Y., Chua, B., and Son, A. (2016). Portable lysis apparatus for rapid single-step DNA extraction of *Bacillus subtilis*. *J. Appl. Microbiol.* 120, 379–387. doi: 10.1111/jam.13011

Pfaller, M. A., Espinel-Ingroff, A., Canton, E., Castanheira, M., Cuenca-Estrella, M., Diekema, D. J., et al. (2012). Wild-type MIC distributions and epidemiological cutoff values for amphotericin B, flucytosine, and itraconazole and *Candida* spp. as determined by CLSI broth microdilution. *J. Clin. Microbiol.* 50, 2040–2046. doi: 10.1128/JCM.00248-12

Ramos, L. S., Figueiredo-Carvalho, M. H. G., Silva, L. N., Siqueira, N. L. M., Lima, J. C., Oliveira, S. S., et al. (2022). The threat called *Candida haemulonii* species complex in Rio de Janeiro state, Brazil: focus on antifungal resistance and virulence attributes. *J. Fungi* 8, 574–593. doi: 10.3390/jof8060574

Rozas, J., Ferrer-Mata, A., Sanchez-DelBarrio, J. C., Guirao-Rico, S., Librado, P., Ramos-Onsins, S. E., et al. (2017). DnaSP 6: DNA sequence polymorphism analysis of large data sets. *Mol. Biol. Evol.* 34, 3299–3302. doi: 10.1093/molbev/msx248

Silva, L. N., Oliveira, S. S. C., Magalhães, L. B., Neto, V. V. A., Torres-Santos, E. C., Carvalho, M. D. C., et al. (2020). Unmasking the mmphotericin B resistance mechanisms in *candida haemulonii* species complex. *ACS Infect Dis.* 6, 1273–1282. doi: 10.1021/acsinfecdis.0c00117

Stamatakis, A. (2014). RAxML version 8: a tool for phylogenetic analysis and post-analysis of large phylogenies. *Bioinformatics* 30, 1312–1313. doi: 10.1093/bioinformatics/btu033

Zhang, L., Xiao, M., Wang, H., Gao, R., Fan, X., Brown, M., et al. (2014). Yeast identification algorithm based on use of the Vitek MS system selectively supplemented with ribosomal DNA sequencing: proposal of a reference assay for invasive fungal surveillance programs in China. *J. Clin. Microbiol.* 52, 572–577. doi: 10.1128/JCM.02543-13

Frontiers in Microbiology

Explores the habitable world and the potential of microbial life

The largest and most cited microbiology journal which advances our understanding of the role microbes play in addressing global challenges such as healthcare, food security, and climate change.

Discover the latest Research Topics

See more →

Frontiers

Avenue du Tribunal-Fédéral 34
1005 Lausanne, Switzerland
frontiersin.org

Contact us

+41 (0)21 510 17 00
frontiersin.org/about/contact